

Die approbierte Originalversion dieser
Dissertation ist in der Hauptbibliothek der
Technischen Universität Wien aufgestellt und
zugänglich.

<http://www.ub.tuwien.ac.at>



The approved original version of this thesis is
available at the main library of the Vienna
University of Technology.

<http://www.ub.tuwien.ac.at/eng>



TECHNISCHE
UNIVERSITÄT
WIEN

Vienna University of Technology

PhD Thesis

Dissertation

NOVEL CONCEPTS FOR PHOTOINITIATING MOIETIES

ausgeführt zum Zwecke der Erlangung des akademischen Grades eines Doktors der
Naturwissenschaften unter der Leitung von

Ao. Univ. Prof. Dr. Robert Liska

E163 - Institut für Angewandte Synthesechemie

eingereicht an der Technischen Universität Wien

Fakultät für Technische Chemie

von

Mag. Claudia Dworak

9901396

Anton Baumgartnerstrasse 44

1230 Wien

Wien, am 1. Oktober 2009

„The whole is more than the sum of its parts.”

- Aristotle

Diese Stelle ist allen Menschen gewidmet, die zum Gelingen dieser Arbeit beigetragen haben.

Mein besonderer Dank gilt Herrn Prof. Robert Liska für die herzliche Aufnahme in seine Arbeitsgruppe, die interessante Aufgabenstellung mit viel Freiraum zur Mitgestaltung, die immerwährende Diskussionsbereitschaft und die stete, engagierte Betreuung.

Herrn Prof. Gruber möchte ich für die Möglichkeit danken, diese Dissertation am Institut für Angewandte Synthesechemie durchzuführen.

Für die Übernahme des Zweitgutachtens danke ich Herrn Prof. Jürgen Stampfl vom Institut für Werkstoffwissenschaften.

Ich möchte mich weiters bei DI Niki Pucher für die Aufnahme zahlreicher GC-MS und NMR-Spektren bedanken, bei DI Sabine Unger für die Einschulung am GPC Gerät, bei DI Christian Heller und Dr. Thomas Koch von Institut für Werkstoffwissenschaften für die Durchführung der Mechanikmessungen, bei DI Markus Griesser von der TU Graz für die photo-CIDNP Untersuchungen und die großartige Hilfe bei deren Auswertung, bei Prof. Franz Varga vom Hanusch Krankenhaus Wien für die Durchführung der Zytotoxizitätstests, bei Isolde Hisch und Franz Kreiml, die für den reibungslosen Ablauf des Laboralltags gesorgt haben, bei Walter Dazinger für die Hilfe bei allen technischen Belangen, schließlich bei Frau Inge Rohrer für ihren Einsatz bei allen organisatorischen Problemen und natürlich für ihre tollen, selbstgebastelten Adventkalender.

Mein Dank gilt ebenfalls allen Kollegen aus der Arbeitsgruppe „Makromolekulare Chemie“ für ihre Hilfsbereitschaft und das gute Arbeitsklima - hier ganz besonders meinen ehemaligen und gegenwärtigen Zimmerkollegen, DI Stefan Krivec und Josef „Seppi“ Kumpfmüller. Ein wesentlicher Beitrag zum raschen Fortgang dieser Arbeit wurde durch meine Wahlpraktikanten Andreas Schröder, Josef Kumpfmüller, DI Dzanana Dautefendic und Therese Johansson geleistet.

Ein großer Dank geht an meine Eltern und meine Schwester, die mich in allen Belangen unterstützt haben und mir immer mit Rat und Tat zur Seite gestanden sind.

Meinem Mann Christian danke ich für die praktische Hilfe in Form von unzähligen Phosphor-NMR Messungen, für seinen unerschütterlichen Glauben an mich, für seinen ansteckenden Humor, der mich aus dem tiefsten Loch herausreißen kann, und für seine bedingungslose Liebe.

ABSTRACT

Among the bimolecular Type II photoinitiators (PIs) for radical photopolymerization e.g. of coatings, chromophores like benzophenone with tertiary amines as coinitiators find a broad application spectrum. However, the efficiency of this system is usually decreased by a back electron transfer (BET) and limited diffusion capability in highly viscous formulations. Therefore, *N*-phenylglycine was used as coinitiator, which prevents a BET by spontaneous decarboxylation. It was connected covalently to the benzophenone unit, thus keeping the coinitiator in close vicinity of the chromophore and delivering a novel class of Type II PIs with excellent reactivity. Moreover, it was discovered, that the very good performance of such PIs originated not only from the spontaneous decarboxylation, but also from a second mechanism – a β -phenylogous cleavage.

With respect to the impact of this cleavage mechanism on the reactivity of such PI systems, it was the aim of this PhD thesis to design and characterize similar PI structures with sulfur and N-O heteroatom moieties, which are also able to induce the photoscission of the β -phenylogous bond. Extraordinary good results with the UV-cleavable N-O moiety led to the development of a new class of migrationstable PIs based on di- and triacrylated hydroxylamines, which displayed a reactivity comparable to industrially employed Type II PI systems like benzophenone/amine. The need for “safe” PIs, which do not contaminate the material in contact with the cured polymer by migration effects, is high. To fulfil such demands for applications in food packaging or biomedical applications, the concept of the self-initiating acrylates with the N-O bond was extended to monomers bearing less toxic vinyl ester and vinylcarbamate moieties, as well as UV-cleavable acylphosphine groups. The properties of the new PIs and monomers were determined by UV-Vis spectroscopy, photo-DSC experiments and ATR-IR spectroscopy. A method to derive the double bond conversion from the ATR-IR spectra of the monomers and the cured polymers was employed, that permitted the accurate calculation of the so far unknown theoretical polymerization heats of the investigated monomers. With respect to further applications in the biomedical field, also cytotoxicity hydrolytic degradation behaviour and mechanical properties of the most promising phosphomonomers were investigated, thus revealing good to excellent biocompatibility and mechanical strength almost resembling human bone.

ZUSAMMENFASSUNG

Unter den bimolekularen Typ-II-Photoinitiatoren (PI) für die radikalische Photopolymerisation z.B. von Beschichtungen, finden Chromophore wie beispielsweise Benzophenon in Kombination mit tertiären Aminen als Coinitiatoren ein breites Anwendungsspektrum. Die Effizienz dieses Systems wird für gewöhnlich durch eine Elektronenrückübertragung vom angeregten Keton auf das Amin, sowie einem eingeschränkten Diffusionsvermögen in hochviskosen Formulierungen limitiert. Folglich wurde *N*-Phenylglycin als Coinitiator eingesetzt, welches durch spontane CO₂-Freisetzung diese Rückübertragungsreaktion verhindert. Durch kovalente Anbindung von *N*-Phenylglycin an den Benzophenonchromophor konnte die Reaktivität dieses neuen Photoinitiatorstyps deutlich gesteigert werden. Darüberhinaus wurde neben der Decarboxylierungsreaktion ein zusätzlicher β -phenyloger Spaltungsmechanismus festgestellt, der für die enorme Leistungsfähigkeit dieses Systems verantwortlich ist.

Hinsichtlich des beträchtlichen Einflusses, den dieser Spaltungsmechanismus auf die Reaktivität solcher PI-Systeme ausübt, war es das Ziel dieser Arbeit, ähnliche Photoinitiatorstrukturen mit Schwefel- oder N-O-Gruppen herzustellen und zu charakterisieren. Hier sollte ebenfalls eine UV-Licht induzierte Spaltung in der β -phenyloger Position erfolgen. Außergewöhnlich gute Ergebnisse bei Strukturen mit einer N-O-Heteroatomeinheit führten zur Entwicklung von neuartigen, migrationsstabilen Photoinitiatoren, basierend auf di- und triacrylierten Hydroxylaminderivaten, deren Reaktivität sich mit den industriell eingesetzten Typ II Photoinitiatoren, wie beispielsweise Benzophenon/Amin, messen kann. Für Anwendungen in der Verpackungstechnik und Biotechnologie werden dringend neue Ideen hinsichtlich migrationsstabiler Photoinitiatoren benötigt, da es bei Verwendung herkömmlicher PIs zur Kontamination der Materialien, die direkten Kontakt mit dem Polymer aufweisen, kommen kann. Daher wurde das Konzept der selbstinitiiierenden Acrylate mit der UV-spaltbaren N-O Einheit weiterentwickelt, hinzu Monomeren mit geringer Toxizität, basierend auf Vinylestern, Vinylcarbamaten und UV-sensitiven Acylphosphingruppen. Die neuen Substanzen wurden mittels UV-Spektroskopie, Photo-DSC und ATR-IR Spektroskopie untersucht. Aus dem Vergleich der ATR-IR Spektren der Harze vor und nach der Polymerisation wurde eine Methode entwickelt, um den Doppelbindungsumsatz und hieraus die bislang unbekanntenen Werte für die theoretische Polymerisationswärmen der untersuchten Monomere zu bestimmen. Im Hinblick auf spätere Anwendung im Bereich der Medizin wurden die besten phosphorhaltigen Monomere auch auf ihre Zelltoxizität, ihren hydrolytischen Abbau und ihr mechanisches Verhalten untersucht. Hierbei konnten für diese Substanzen teilweise ausgezeichnete Biokompatibilität und mechanische Eigenschaften fast schon im Bereich von menschlichem Knochenmaterial nachgewiesen werden.

TABLE OF CONTENTS

INTRODUCTION	1		
OBJECTIVE TARGETS	20		
GENERAL PART	22		
EXPERIMENTAL PART	136		
MATERIALS, TECHNICAL EQUIPMENT AND CHARACTERIZATION.....	183		
SUMMARY	192		
ABBREVIATIONS	198		
REFERENCES	202		
		GP	EP
1. Novel Photoinitiators bearing the Benzophenone Moiety	22.....		136
1.1. Synthesis.....	28.....		136
1.1.1. Bis-[(4-methyl)-benzophenone] disulfane (4)	28.....		136
1.1.2. Attempted synthesis of 4,4'-(dibenzoyl)-bis (thiocarbonylphenyl) disulfide (5)	30.....		137
1.1.2.1. 2-Phenyl-2-(4-bromophenyl)-1,3-dioxalane (9)			137
1.1.3. Synthesis of dithiocarbonates 6 and 7	32.....		138
1.1.3.1. Potassium dithiocarbonyl-O-ethanoate (11).....			138
1.1.3.2. S-(4-Benzoyl)-benzyl O-ethyl dithiocarbonate (6)			139
1.1.3.3. 4-Benzoyl benzoic acid chloride (12)			141
1.1.3.4. S-(4-Benzoyl)-benzoyl O-ethyl dithiocarbonate (7)			142
1.1.4. Attempted synthesis of <i>N</i> -(benzoyloxy)-(4-benzoyl)- benzenemethanamine (8).....	34.....		143
1.1.4.1. 2-Phenyl-2-(4-formylphenyl)-1,3-dioxalane (13).....			143

TABLE OF CONTENTS

1.1.4.2.	(4-[[1,3]-Dioxalan-2-yl-2-phenyl])benzamidoxime (14).....	144
1.1.4.3.	Benzaldoxime (17).....	146
1.1.4.4.	(4-Phenyl)-O-phenylacetyl benzamidoxime (20).....	147
1.1.4.4.1.	(4-[[1,3]-Dioxalan-2-yl-2-phenyl])-O-phenylacetyl benzamidoxime (19).....	147
1.1.4.5.2.	(4-Phenyl)-benzamidoxime (21).....	148
1.1.4.5.3.	(4-Phenyl)-O-phenylacetyl benzamidoxime (20).....	149
1.1.5.	Reference compounds 2 and 3	40..... 151
1.2.	Analyses.....	41
1.2.1.	UV-Vis spectroscopy	42
1.2.1.1.	Bis-[(4-methyl)-benzophenone] disulfane (4)	42
1.2.1.2.	Dithiocarbonates 6 and 7	43
1.2.1.3.	(4-Phenyl)-O-phenylacetyl benzamidoxime (20).....	44
1.2.2.	Photo-DSC	45
1.2.2.1.	Comparison of 4 and 20 with reference PIs	46
1.2.2.2.	Variation of PI concentration.....	48
1.2.2.3.	Addition of amine co-initiators and photosensitizers	49
1.2.2.4.	PI reactivity and control of molecular weight distribution	50
1.2.3.	GPC analysis.....	53
1.2.4.	Photo-CIDNP experiments	55
1.2.4.1.	Benzophenone-N-phenyl glycine ethyl ester (2)	55
1.2.4.2.	(4-Phenyl)-O-phenylacetyl benzamidoxime (20).....	56
1.2.4.3.	Bis-[(4-methyl)-benzophenone] disulfane (4)	58
2.	Alternative Co-Initiators for Bimolecular PI Systems	59..... 152
2.1.	Synthesis.....	61..... 152
2.1.1.	Synthesis of benzaldoxime esters 22 , 23 and 24	61..... 152
2.1.1.1.	O-Benzoyl benzaldoxime ester (22).....	153
2.1.1.2.	O-Methyl benzaldoxime ester (23).....	153

TABLE OF CONTENTS

2.1.1.3.	O-Methacryloyl benzaldoxime ester (24)	154
2.1.2.	S-Benzyl-O-ethyl dithiocarbonate (25)	62..... 154
2.2.	Analyses.....	62
2.2.1.	UV-Vis spectroscopy	62
2.2.1.1.	Benzaldoxime esters 22 , 23 and 24	63
2.2.1.2.	S-Benzyl-O-ethyl dithiocarbonate (25)	64
2.2.2.	Photo-DSC	65
2.2.2.1.	Benzaldoxime esters 22 , 23 , 24	66
2.2.2.2.	S-Benzyl-O-ethyl dithiocarbonate (25)	68
2.2.3.	GPC analysis.....	69
3.	Photoinitiating Monomers based on Di- and Triacylated Hydroxylamine Derivatives	72..... 156
3.1.	Synthesis.....	72..... 156
3.1.1.	O,N-Bis(1-oxo-2-propen-1-yl)-hydroxylamine (26)	156
3.1.2.	O,N-Bis(1-oxo-2-propen-1-yl)-N-(alkyl)-hydroxylamines	74..... 157
3.1.2.1.	O,N-Bis(1-oxo-2-propen-1-yl) N-(methyl)-hydroxylamine (27).....	158
3.1.2.2.	O,N-Bis(1-oxo-2-propen-1-yl)-N-(isopropyl)-hydroxylamine (28).....	158
3.1.2.3.	O,N-Bis(1-oxo-2-propen-1-yl)-N-(t-butyl)-hydroxylamine (29)	159
3.1.2.4.	O,N-Bis(1-oxo-2-propen-1-yl)-N-(cyclohexyl)-hydroxylamine (30).....	160
3.1.2.5.	O,N-Bis(1-oxo-2-propen-1-yl)-N-(benzyl)-hydroxylamine (31).....	160
3.1.3.	O,N,N-Tris(1-oxo-2-propen-1-yl)-hydroxylamine (32).....	161
3.2.	Analyses.....	74
3.2.1.	UV-Vis spectroscopy	74
3.2.2.	ATR-IR analysis.....	75
3.2.3.	Photo-DSC	79
3.2.3.1.	PI activity in HDDA	79
3.2.3.2.	Monomer reactivity with a Type I PI	82
3.2.3.3.	PI-free photopolymerization.....	84

TABLE OF CONTENTS

3.2.4.	Steady state photolysis experiments with TEMPO and t-BAM	85	163
3.2.4.1.	Compound 27 with TEMPO		163
3.2.4.2.	Compound 27 with t-BAM		163
4.	Monomers for Biomedical Applications	90	164
4.1.	Hydroxylamine-based monomers	92	164
4.1.1.	Synthesis	92	164
4.1.1.1.	<i>N</i> -(1-Oxo-2-propen-1-yl)- <i>N</i> -(vinylloxycarbonyl)- <i>O</i> -methyl-hydroxylamine (34)	92	164
4.1.1.1.1.	<i>N</i> -(1-Oxo-2-propen-1-yl)- <i>O</i> -methyl-hydroxylamine (37)		164
4.1.1.1.2.	<i>N</i> -(Vinylloxycarbonyl)- <i>O</i> -methyl-hydroxylamine (38)		165
4.1.1.1.3.	<i>N</i> -(1-Oxo-2-propen-1-yl)- <i>N</i> -(vinylloxycarbonyl)- <i>O</i> -methyl hydroxylamine (34)		166
4.1.1.2.	Attempted synthesis of <i>N,N</i> -bis(vinylloxycarbonyl)- <i>N</i> -methoxy hydroxylamine (35)		95
4.1.1.3.	<i>O,N</i> -Bis(vinylloxycarbonyl)- <i>N</i> -(methyl)-hydroxylamine (36)	96	169
4.1.2.	Analyses		96
4.1.2.1.	UV-Vis spectroscopy		97
4.1.2.2.	ATR-IR analysis		98
4.1.2.3.	Photo-DSC		98
4.1.2.3.1.	PI-free photopolymerization		99
4.1.2.3.2.	Monomer reactivity with a Type I PI		100
4.1.2.4.	Toxicology tests		102
4.2.	Phosphorus-containing vinyl esters and vinyl carbamates	103	171
4.2.1.	Synthesis of phosphonates and phosphoformates	106	171
4.2.1.1.	Diphenyl vinylloxycarbonyl phosphineoxide (40)	107	171
4.2.1.2.	Diethyl vinyl phosphoformate (41)	108	172
4.2.1.3.	Attempted synthesis of ethyl divinyl phosphobisformate (44)		108
4.1.2.4.	Diphenyl methacryloyl phosphineoxide (42)	109	173
4.2.1.5.	Diethyl methacryloyl phosphonate (43)	110	174

TABLE OF CONTENTS

4.2.2.	Synthesis of vinyl esters of phosphoric acid	111	175
4.2.2.1.	Ethyl dichlorophosphate (52)		175
4.2.2.2.	Vinyl esters of phosphoric acid 45 , 46 and 47		176
4.2.2.2.1.	Diethyl vinyl phosphate (45)		176
4.2.2.2.2.	Ethyl divinyl phosphate (46).....		177
4.2.2.2.3.	Trivinyl phosphate (47)		178
4.2.3.	Synthesis of phosphovinyl carbamates.....	114	179
4.2.3.1.	2-Hydroxyethyl vinyl carbamate (54)		179
4.2.3.2.	2-(Diethyl phospholoyloxy) ethyl vinyl carbamate (48).....		180
4.2.3.3.	Bis-(2,2'-(ethoxyphospholoyloxy)) ethyl vinyl carbamate (49).....		181
4.2.4.	Analyses		116
4.2.4.1.	UV-Vis spectroscopy		116
4.2.4.2.	ATR-IR analysis.....		118
4.2.4.2.1.	Monovinylated phosphorus containing monomers		118
4.2.4.2.2.	Divinylated phosphorus containing monomers.....		120
4.2.4.2.3.	Trivinylated phosphorus containing monomers.....		122
4.2.4.3.	Photo-DSC		123
4.2.4.3.1.	Monovinylated phosphorus containing monomers		124
4.2.4.3.2.	PI-activity of monoacyl phosphineoxides 40 , 41 and 43		125
4.2.4.3.3.	Divinylated phosphorus containing monomers.....		127
4.2.4.3.4.	Trivinylated phosphorus containing monomers.....		128
4.2.4.4.	GPC analysis.....		129
4.2.4.5.	Toxicology and cell compatibility tests.....		130
4.2.4.6.	Mechanical properties		131
4.2.4.7.	Degradation behaviour		132
4.2.4.7.1.	Alkaline hydrolysis.....		134
4.2.4.7.2.	Acidic hydrolysis.....		134

INTRODUCTION

The first assignment of paint as decorative and protective coating has already been used by people for thousands of years. The first evidence, that people utilized mixtures of colored earth, grease, soot and other natural compounds to decorate their homes, places of worship and also their own bodies, can be found on numerous cave paintings in Spain or France, which are over 30000 years old (Figure 1).



Figure 1. Image of a horse from the Lascaux Cave (France, Stone Age)¹

Also high civilized cultures like Egyptians, Romans and Greek developed painting techniques for their buildings, statues, textiles from natural raw products like vegetable gums, beeswax, charcoal, and natural dyes indigo, purple and madder.

The first decorative and protective layers were developed by ancient Chinese people around 2000 BC. They used balsams and resins from India to create lacquerwork for smooth and glossy surfaces on goods of their daily life. The word “Lacquer” is related to the Indian “laksha” from the pre-Christian Sanskrit language and refers to shellac, a resin produced by insects.

Not before the Industrial Revolution in the 18th century the coating technology was boosted up by the need for protection of all the buildings and goods from iron. Especially seafaring was dependent on the development of proper protection paints for their ships. With the starting 20th century the first entirely synthetic resins, the phenol-formaldehyde condensates (“Bakelit”), were developed, followed by vinyl-, urea-, alkyd-, and acrylic resins, polyurethanes and also melamine resins. Together with the coating material also the coating technologies advanced. Finally, also the automation of coating was employed due to demand for increased production rates by driving forces like automotive industry or warfare.

Nowadays, a countless amount of compounds designed to meet the different requirements of our daily life are available. The item “paint” covers a broad range from environmentally-sound latex paints, that decorate and protect our homes, over translucent coatings in the inner part of food containers, up to complex finishes used by automobile manufacturers.^{2,3,4} Summarizing, coatings and paints developed slowly but steadily from an Early Man art form over an empirical craft into the modern, versatile and highly intricate coating technologies of today.

Requirements for new products in the field of paints and resins are low cost, excellent performance and low adverse impact on the environment. Especially coating technologies are constantly in flux for better optimization concerning the above mentioned features. In Figure 2 the most common curing procedures are presented.

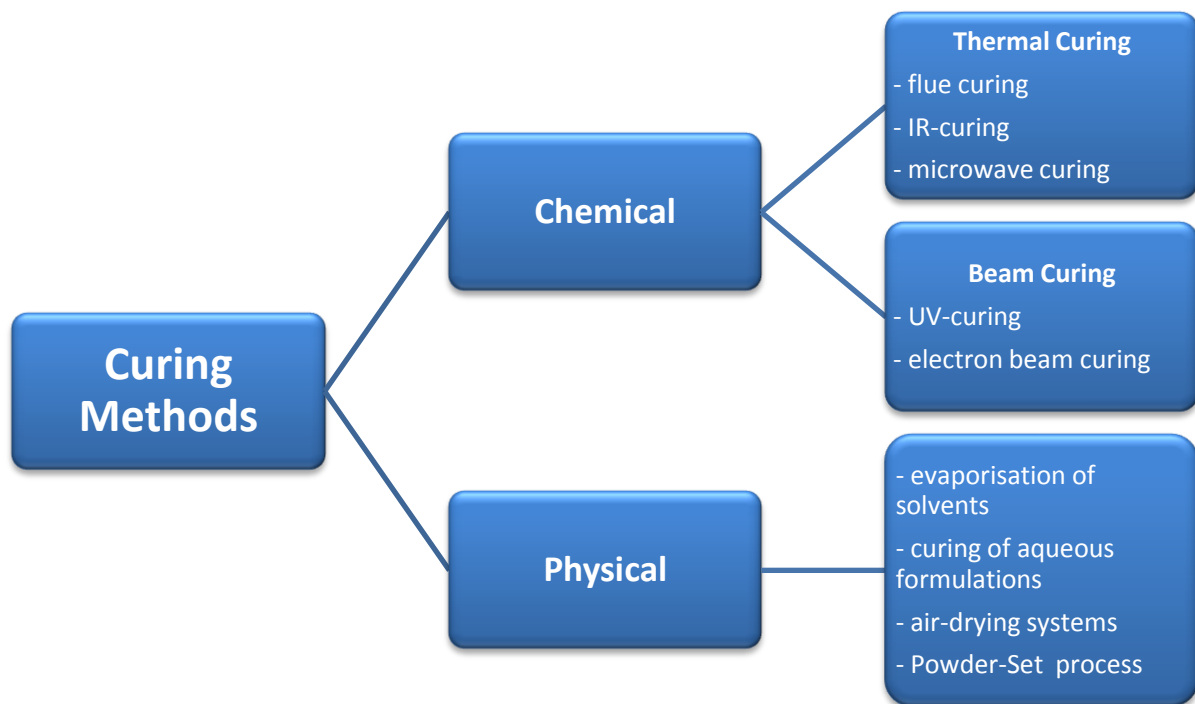


Figure 2. Procedures for surface coating

Nowadays physical methods are more and more abandoned due to reasons of environment pollution, limited availability of resources and saving of energy costs. Therefore, conventional curing, which is performed by evaporation of organic solvents is more and more replaced by curing of aqueous formulations and the Powder Set process.⁵

Besides thermal curing based on polycondensation, chemical methods like radical

polymerization are of significant importance. Such formulations contain multi-functional monomers with polymerizable groups, as e.g. double bonds. Herein belong the oxidative curing methods (for example catalyzed by peroxides) as well as thermal and beam induced polymerizations.⁶

Electron Beam Curing (EBC)^{7,8,9} displays few advantages compared to UV-induced curing, as e.g. better in-depth curing, higher curing speed, and initiator-free formulations. However, major drawbacks like high energy input and operative expense turned it less attractive than the UV-induced curing for industrial applications.

For all these reasons, photocuring is still the most rapid growing polymerization method as it offers a broad application spectrum in industry. It allows solvent-free working, high productivity, high curing speed and better mechanical properties of the polymer, combined with low energy costs and spatial requirements. These advantages still outbalance the higher acquisition costs for UV-curing systems, which occur due to lamp equipment, safety devices for eyes and skin as well as ozone removing aspirators.¹⁰ The following part will outline the most common applications of this method:¹¹

- **Decorative Coatings:** book covers, album covers, poster, coatings for wood panels, artificial fingernails...
- **Protective Coatings:** abrasion-resistant coatings, for polycarbonate sheets, protective coatings for plastic lenses, heat-resistant coatings, corrosion protection...
- **Printing Industry:** printing-ink manufacture, water-based printing inks for posters, decals for noble metal decoration of ceramics; braille printing ink for raised characters...
- **Optics:** optical fibre coating, optical fibre cables, protective coatings for compact discs, holographic relief image protection, waveguides and lenses for integrated optics, contact lenses...
- **Electronics:** adhesion primers, etch resists, solder resists, insulation layers for printed circuits, conductive and insulating inks...

- **Primers, Adhesives, Release Coatings:** primers for metal and glass coating, coating for reinforced fibres, adhesive layers for laminated safety glass, adhesive layers, release coatings...
- **Miscellaneous:** dental filling compounds, sealing compounds, traffic markings, stereolithography, polymer-dispersed liquid crystal films, water repellent porous membranes for all-weather garments...

In contrast to the traditional mercury lamps, nowadays a large variety of lamps and lasers is available for the irradiation process in the UV, UV/visible and visible light range.

The photosensitive formulation is always a mixture of the components, which will be discussed in the following part. They are always adapted to the actual requirements.¹⁰

The demand for polymerizable monomers, which form network structures with defined properties *via* a photoinduced free-radical process, is high. Monomers and oligomers for radical and cationic polymerization determine the final properties of the cured polymer. Therefore great efforts have been made to enhance their photochemical properties. Research focuses on the following items: to improve the performance level, such as cure speed, high conversion rate, scratch resistance etc., to design new properties, such as lower toxicity, low shrinkage, low odour, suitable rheology etc., to limit the oxygen inhibition and to increase the photostability of the cured materials.¹² These requirements can be met by unsaturated polyesters, acrylated polyesters, polyethers, epoxy resins and polyurethanes (Figure 3).

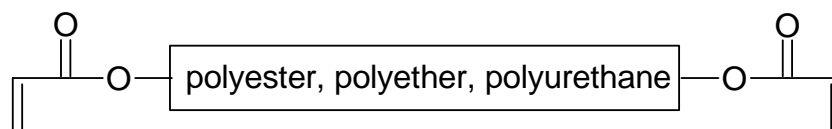


Figure 3. Example for acrylated monomers for radical polymerization

Using reactive diluents, the viscosity of a given formulation can be manipulated. Diluents also obtain a function as cross-linkers, thus influencing flexibility and elasticity of the cured material. For example, butane-1,4 diacrylate (**BDDA**), hexane-

1,6-diol diacrylate (**HDDA**), trimethylolpropane triacrylate (**TMPTA**) and pentaerythritoltri- and -tetra acrylate are commonly used reactive diluents (Figure 4).^{10,13}

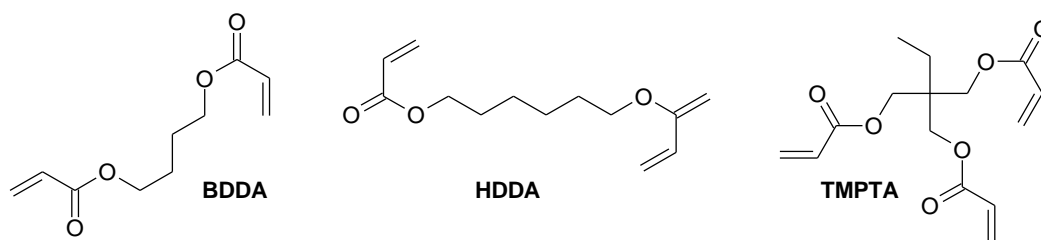


Figure 4. Examples for reactive diluents in radical photopolymerization

Furthermore, numerous additives are required in amounts typically less than 1 wt%. Frequently used examples are stabilizers, inhibitors, filling material, plasticizers, antioxidants, surfactants, matting agents, pigments, *etc.*

Besides the monomers, photoinitiators (PIs) play a key role in the development of optimum formulations. The PI absorbs energy from a photon either in a direct or an indirect process and transfers it into chemical energy. By formation of a reactive radical, polymerization can be induced.

The properties of an ideal PI are:¹⁴

- Easy synthetic access and low price
- Lack of toxicity and odour (this is also applicable for the photoproducts)
- Good solubility
- Appropriate shelf-life in ready-to-use formulations with monomers
- High initiation efficiency
- Non-yellowing

In some cases also photosensitizers are required. Photosensitizing is based on two distinct processes, these are energy transfer and /or electron transfer. By radiationless electronic energy transfer, energy is passed from an excited donor molecule (sensitizer) to the ground state acceptor, which then becomes excited. An exothermic sensitizing reaction proved to be significantly more efficient than an endothermic one. Besides, the photosensitizer should absorb light in a higher wavelength range than the acceptor molecule. Classical photosensitizers are benzophenone, 2-isopropyl thioxanthone and dibutyl anthracene.

Basically, the process of radical photopolymerization is divided into 5 steps:¹⁰

- 1) Absorption of light or energy transfer from a photochemically excited photosensitizer
- 2) Formation of initiating radicals from the excited state by
 - Photofragmentation (α - or β -cleavage)¹⁵
 - Hydrogen abstraction from a H-donor¹⁶
 - Electron transfer followed by proton transfer¹⁷
- 3) Start of the chain reaction
- 4) Propagation
- 5) Termination by recombination or disproportionation

There are two possibilities for a photoinitiator to absorb energy, either by direct uptake or indirectly transmitted by a photosensitizer (triplet-triplet transfer). Crucially for the efficiency of this process is the match of emission bands of the UV lamp with the absorption maxima of the initiators, or of the sensitizer, respectively. The absorption of light occurs through chromophores with conjugated double or triple bonds (Table 1). They are often in combination with carbonyl groups, which cause electronic transitions of π - π^* or n - π^* orbitals.¹⁸

Table 1. Absorption maxima of common chromophores

Chromophores	λ_{\max} [nm]	λ_{\max} [nm]
	π - π^*	n - π^*
C=C	170	-
C=O	166	280
C=N	190	300
N=N	-	350
C=S	-	500

The first step involves the excitation of one electron from the ground state (S_0) to the excited singlet state (S_1^*) by absorption of light with the energy $h\nu$ (

Figure 5). The energy can be dissipated by fluorescence or radiationless deactivation. By “intersystem crossing” (ISC) the transition into an excited triplet state (T_1^*) is possible. Thus the molecule can relaxate to T_1 .

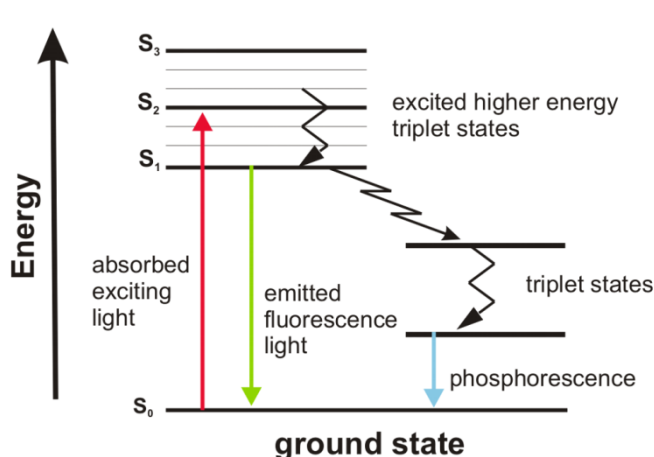


Figure 5. Simplified Jablonski diagram¹⁹

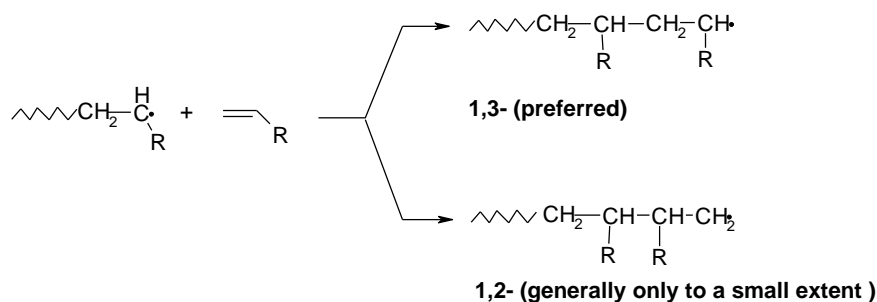
The triplet states are characterized by longer lifetime ($\sim 10^{-6}$ s vs. 10^{-9} s for the singlet state). The electrons are of the same spin direction, thus exhibiting the characteristics of a biradical. From this state radical formation can be induced, but this action is concurring with radiationless deactivation, phosphorescence or bimolecular extinction processes. The more stable a triplet state is, the more prone it is for extinction.

According to their stability, radicals can start a chain reaction, recombine or provoke chain terminations as well as chain transfer reactions.²⁰ A chain reaction is started by the addition of an initiator radical to a monomer (Scheme 1).



Scheme 1. Start of chain reaction by initiator radical

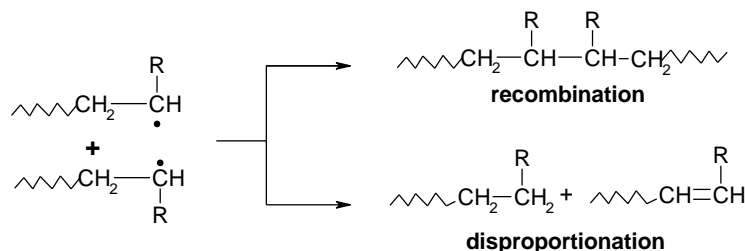
Propagation is defined by the addition of monomers to a growing polymer chain radical (Scheme 2).



Scheme 2. Propagation mechanisms

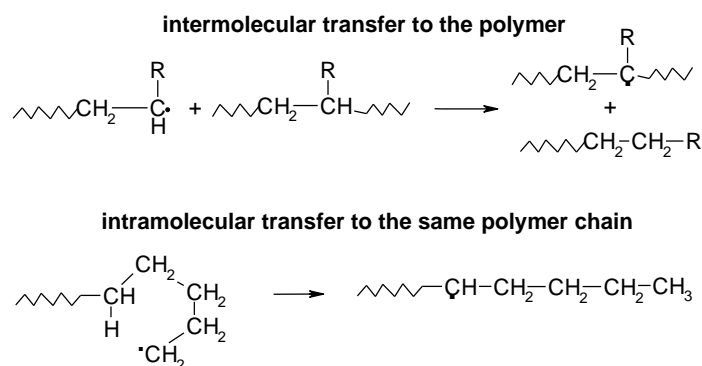
Two ways of addition are possible, but for most monomers the 1,3-position (head to tail addition) is the preferred one (anti-Markownikoff addition).

The type of chain termination depends on the monomer and the reaction temperature. Lower temperature favors recombination (higher molecular weight) whereas higher temperature results in disproportionation (molecular weight unchanged). The two processes are outlined in Scheme 3.



Scheme 3. Chain termination mechanisms

Chain transfer reactions to the polymers cause branching. Transfer to another macromolecule results in long chain branching, whereas intramolecular transfer causes short-chain branches as shown in Scheme 4.



Scheme 4. Chain transfer mechanisms

Most radical generating PIs contain the benzoyl chromophore, because it displays an appropriate absorption in the UV-range (200-400 nm) and also good photoreactivity. They are divided into cleavable Type I or hydrogen abstracting Type II systems. Type I refers to a monomolecular, Type II to a bimolecular reactivity. The modes of operation for radical photoinitiators are cleavage – normally at the α - or β -position of a carbonyl group (Type I), abstraction of a hydrogen atom with a hydrogen donor, or last but not least electron transfer *via* an amine (Type II).¹²

The principle of the α -cleavage is the homolytic scission of the bond next to the carbonyl group. Important PIs of this type are presented in Figure 6.²¹ Herein belong benzoin ethers (a), dialkoxyacetophenones (b), hydroxyalkylphenones (c),

aminoketones (d), benzoylphosphineoxides (e) and benzoyloxime esters (f).

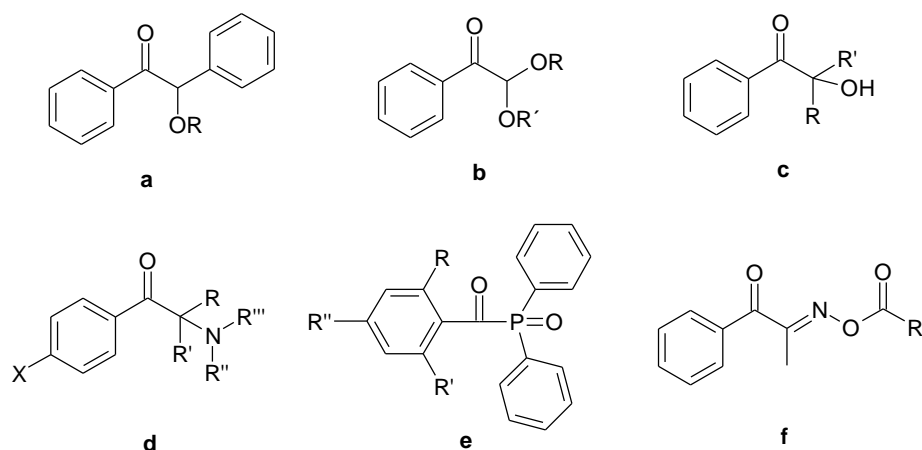


Figure 6. Type I photoinitiators

α -Cleavage is based on the presence of a C-X (X = heteroatom), as for example in acylated phosphineoxides and thioacid esters (Figure 7).²¹

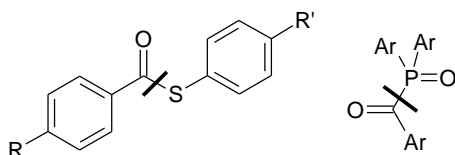


Figure 7. C-X bond of an α -cleaving PI

It can also take place at an activated C-C bond, as for example next to a keto group. By stabilization of the ion pair, that is generated by a heteroatom like oxygen or nitrogen at the α -carbon atom the efficiency can be enhanced (Figure 8).²¹

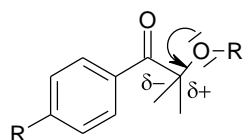
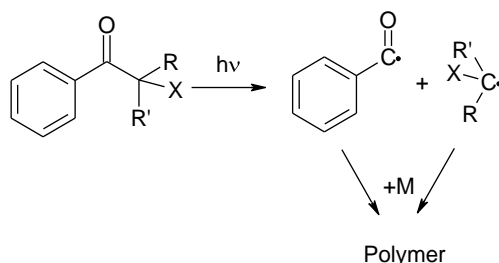


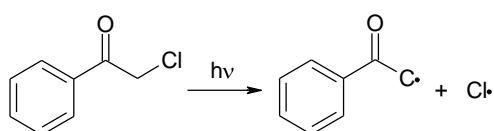
Figure 8. C-C bond in a photoinitiator with α -cleavage

Scheme 5 displays the decomposition of a Type I photoinitiator, that undergoes α -cleavage (Darocur 1173 ©Ciba; R = R' = CH₃, X = OH).



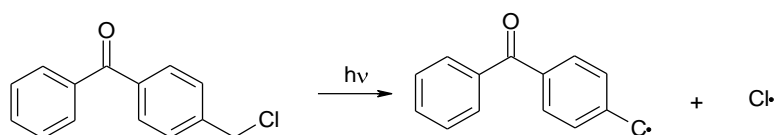
Scheme 5. α -Cleavage of a Type I PI (Darocur 1173 ©Ciba; R = R' = CH₃, X = OH)

Photoinitiators with β -cleavage contain α -haloketones (e.g. α -chlorinated acetophenone) and ketosulfides. In Scheme 6 the decomposition of α -chloroacetophenone is shown.



Scheme 6. α -Chloro acetophenone, a Type I PI with β -cleavage

Besides, among the PIs with β -cleavage also belong PIs with “ β -phenylogous cleavage” mechanism. Photofragmentation takes place in a defined distance from the carbonyl moiety, which is determined by specific functionalities, as for example the phenyl group. In Scheme 7 the decomposition of 4-chloromethyl benzophenone is shown.



Scheme 7. 4-Chloromethyl benzophenone, a Type I PI with β -phenylogous cleavage

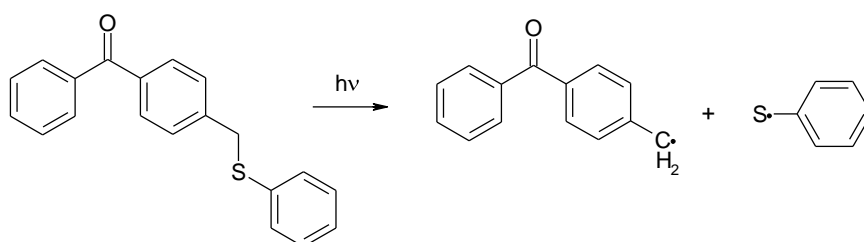
For such cleavage mechanisms it is essential, that the binding enthalpy is smaller than the energy of the excited state (Table 2).²² The triplet energy of benzophenone-derivatives accounts for 289 kJ mol⁻¹.

Table 2. Enthalpies for the $\Delta_{(C-X)}$ of BP-CH₂-X²²

X	$\Delta_{(C-X)}$ [kJ mol ⁻¹]
Br	222
SH	255
SC ₆ H ₅	229 ²³
Si	234 ²⁴
Cl	275
N	292 ²⁵
OH	309

Referring to the binding enthalpies from Table 2, 4-hydroxymethyl benzophenone displays no photolytical cleavage of the C-O bond. This could only be achieved for hydroxyl- phenoxy and methoxy derivatives with two-photon excitation.²⁶ This technique is also suitable for the cleavage of p-acetophenone-C-Si(CH₃)₃.²⁴ The analogous benzophenone-Si derivative could be decomposed with common UV-light sources.²⁷

The cleavage of the corresponding 4-methylbenzophenone thiophenol derivative has been investigated by Yamaji et al.²⁷ A β -phenylogous cleavage mechanism from the excited triplet state as shown in Scheme 8 was identified by ESR experiments.

**Scheme 8.** β -Phenylogous cleavage of phenyl-(4-phenylsulfanylmethyl-phenyl)-methanone

Type II PIs operate by hydrogen abstraction in a bimolecular process. General PIs of this type are presented in Figure 9.²¹ They consist primarily of benzophenone (g), thioxanthone (h), anthraquinone (i), xanthone (j), fluorenone (k), benzil (l), ketocoumarine (m) and camphorquinone (n), as well as their derivatives. Diketones as for example camphorquinone,²⁸ can also be used for applications in the visible light range due to their absorption behaviour.

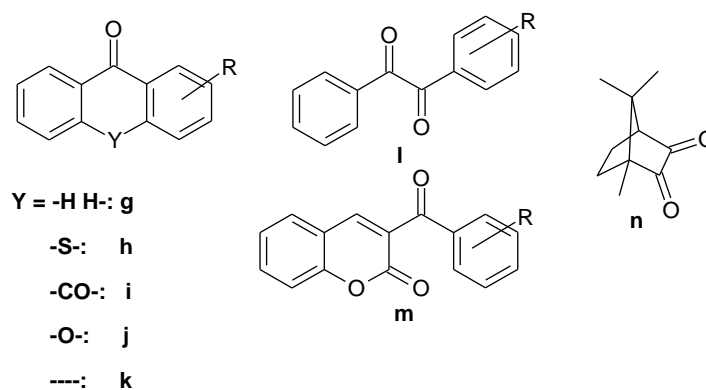
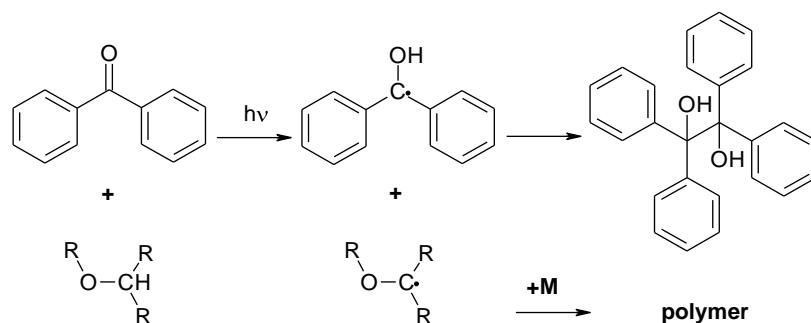


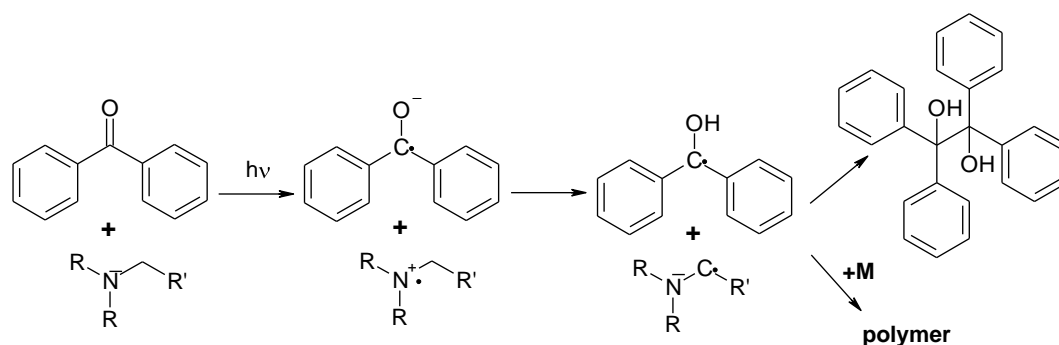
Figure 9. Type II photoinitiators

Basically, alcohols and ethers can generate radicals by direct hydrogen abstraction (Scheme 9), which can only occur from the $n-\pi^*$ triplet. In contrast to that, electron and proton transfer might originate either from the $n-\pi^*$ triplet or the more intensive $\pi-\pi^*$ transition.



Scheme 9. Proton transfer on ether to benzophenone

More commonly, electron-donors like secondary or tertiary amines as well as thiols²⁹ are in use, which are able to transfer an electron to the excited PI, generating two radical ions at the same time. In a second step, radicals are formed by proton transfer.^{30,31} Scheme 10 shows the mechanism for benzophenone and amine.



Scheme 10. Electron and proton transfer by tertiary amines to benzophenone

The oxidation of the tertiary amine by benzophenone proceeds via an electron transfer from the amine to the **BP**-triplet.^{31,32} An ionpair is generated, then a deprotonation takes place in the α -position of the amino radical cation. This electron/proton transfer can be induced by excitation of the $n-\pi^*$ as well as by excitation of the more intensive $\pi-\pi^*$ transition. The kinetic constant of the proton transfer depends on the structure of the amine and is located in the range of 2×10^9 to $7 \times 10^9 \text{ s}^{-1}$.³³ A drawback presents the quenching reaction by the back electron transfer (BET), because the BET reduces strongly the initiation reactivity of the PI.³⁴

As a general rule, not the excited ketone, but the co-initiator intrinsically starts the polymerization reaction. The influencing factors for the performance of a formulation are sterical hindrance, which plays a role for recombination reactions, as well as the radical reactivity related to the monomer and the radical generating rate.^{35,36}

A comparison of Type I and II initiators shows, that later need a longer lifetime of the excited state, as the coincidence with the co-initiator is essential for the radical forming process. These limitations result in a lower excitation rate and lower curing speed.³⁷

As already discussed before, photoinitiators play a key role for the performance of a given formulation. They are responsible for the curing speed, the double bond conversion and the final properties of a polymer. Unfortunately, a major part of the PI amount stays unreacted in the cured material, which results in difficulties, mostly caused by the formation of photoproducts.^{38,39,40,41,42}

- decomposition under thermal or sun-light exposure of the cured material
- toxicity of PIs or their photoproducts
- migration effects of PI or photoproducts out of the polymer
- odour
- yellowing
- additional cost factor

Being aware of the growing application field of photopolymerization in the rather delicate field of food packaging or health – whenever the partly unreacted and still active products of photopolymerization might present a hazard for living organisms,

research has to break new ground.

There has been a great uproar in Europe some years ago concerning contamination of baby-milk products by 2-isopropyl thioxanthone (**ITX**) and its photo products. **ITX** is in common use as fixative for printing inks on milk cartons. Although no harmful effects of the contaminating compounds could be identified up to now, it triggered a lot of rethinking in the UV-curing industry, as people and politics became more sensitive to the topic of proper regulation and control in the use of chemicals for food packaging. More recently, also 4-methyl-benzophenone and its photoproducts, which are components of printing inks for breakfast cereal boxes came under scrutiny. In this case also the possibility of health risks was debated, if large amounts of the cereals were consumed.^{43,44}

From these experiences it's understandable, that the demand for migration stability of photoinitiators presents a fundamental aspect. There were two possible pathways investigated during the last decades. On the one hand, common PIs were attached to co-polymerizable acrylate groups, thus embedding the PI into the polymer network. Unfortunately, these systems often exhibit low stability and a short shelf-life.^{45,46} Another approach was the preparation of oligomer-based PIs, which displayed better migration stability due to their high molecular weight, but suffered from less reactivity due to impaired diffusion ability.^{47,48,49}

A totally new concept was the development of monomers, which have the ability of self-initiate polymerization upon irradiation with UV-light. With respect to these considerations it was the aim of recent studies⁴² to create monomer systems with the ability to induce free-radical polymerization upon exposure to UV light. Examples are maleimide/vinyl ether,^{50,51,52,53} acrylate/vinyl ester,⁵⁴ divinyl fumarate,³⁹ and also monomers containing thiol groups as presented by Jonsson and Hoyle.^{42,50,55} Very recently, it was shown, that also diacrylamides are able to self-initiate photopolymerization.⁵⁶ Besides high monomer reactivity, the ability to be sensitized is one of their key features.

Maleimides, which are excited by absorption of UV-light react by electron transfer with unsaturated monomers followed by hydrogen abstraction to deliver initiating radicals (Scheme 11).



Scheme 11. Structures of maleimide/vinyl ester system and schematical initiation process

Also *N*-substituted maleimide monomers have been discovered, that undergo homopolymerization under irradiation with UV-light, under the condition, that easily abstractable hydrogens are present in the monomer. A mixture of *N*-substituted difunctional maleimides and difunctional vinyl ethers leads to an alternating copolymer network by the formation of a donor-acceptor complex. The chain reaction is started by the abstraction of a hydrogen atom from either the maleimide or the vinyl monomer. The drawback of this system is again the bimolecularity of the reaction, and often poor reactivity due to low absorptivity of UV-light.⁵⁷

Very recently, the self-initiating behaviour of diacrylamides as outlined in Figure 10 was discovered.⁵⁶

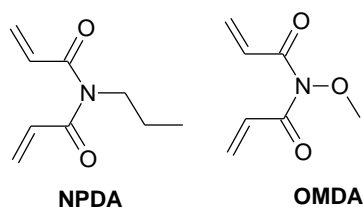
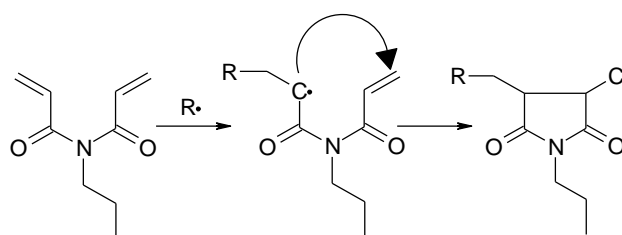


Figure 10. Structures of the self-initiating diacrylamides, *N*-propyl-*N,N*-diacrylamide (**NPDA**) and *O*-methoxy-*N,N*-diacrylamide (**OMDA**)

They exhibited high polymerization reactivity, although only a fraction of light could be consumed compared to wide-spread used Type II PI system benzophenone – amine. A cyclopolymerization process (Scheme 12), which leads to some extent to the formation of linear polymer chains, might contribute to the high efficiency of these self-initiating monomers.



Scheme 12. Cyclopolymerization process for diacrylamides (example **NPDA**)

Furthermore, the remarkable initiation reactivity could be sensitized efficiently in homopolymerization experiments as well as when it was used as co-polymerizable PI in acrylates.

The self-initiating ability of vinyl acrylate (**VA**) and divinyl fumarate (**DVF**) under irradiation with UV-light has been reported recently (Figure 11).^{58,59}

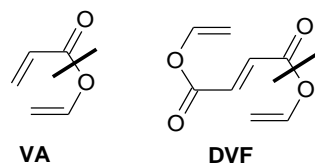
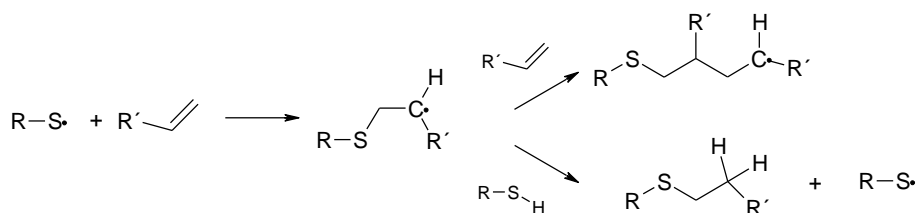


Figure 11. Structures of self-initiating monomers, vinyl acrylate (**VA**) and divinyl fumarate (**DVF**)

The radical reaction can either lead to intramolecular cyclization or to linear free-radical polymerization by cleavage of the C-O bond next to the carbonyl group. The vicinity of the acrylate and the vinyl group provokes special features of this molecule, for example the conjugation results in a significant red-shift of the UV-Vis absorption behaviour.⁵⁸ Unfortunately, the boiling point of **VA** is very low, thus limiting its application in UV-curable formulations significantly.

Therefore, similar molecules to vinyl acrylate with higher molecular weight and amplified double bond conjugation were synthesized. Among them **DVF** turned out to be a highly reactive self-initiating monomer with a strong UV absorption greater than 300 nm, which is essential for efficient PIs. It could initiate even acrylate polymerization under irradiation with UV-light, but as it is rapidly consumed by co-polymerization with the acrylate, only low conversions could be achieved.³⁹

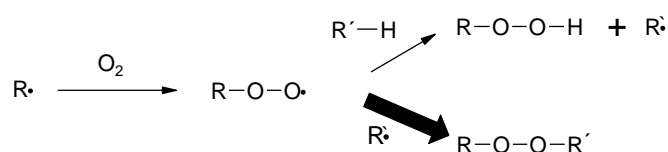
Sulfur-centered radicals find already wide-spread use as initiators for classical radical photopolymerization techniques, e.g. for thiol-ene systems (Scheme 13).^{60,61} Thiols are also used as chain transfer agents in many industrial applications.⁶²



Scheme 13. The thiol-ene polymerization mechanism

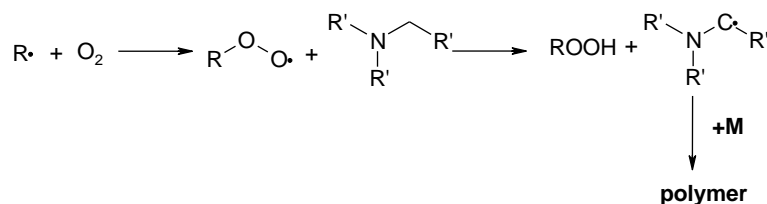
By irradiation with UV-light some thiols can be cleaved to give highly reactive thiyl radicals, which initiate a radical polymerization. Thiol-ene additions work by a free radical chain reaction of a thiol to an “ene”, proceeding by a step-growth process. The advantage of these systems is their low affinity for oxygen inhibition, high curing speed, low shrinkage and great diversability.⁵⁵

Oxygen inhibition constitutes a general problem for radical polymerization processes, as molecular oxygen shows a high affinity for radicals (kinetic constant for reaction of oxygen with carbon radicals $> 10^9 \text{ mol}^{-1} \text{ s}^{-1}$). It binds to the radicals of the growing polymer chain and leads to the termination of chain growth by formation of peroxides (Scheme 14).^{63,64} Besides, oxygen – being in a biradical triplet state itself, quenches the excited triplet state of PIs efficiently, thus suppressing the formation of further radicals.⁶⁵



Scheme 14. Formation of hydrogenperoxides and peroxides (preferred) in the presence of molecular oxygen

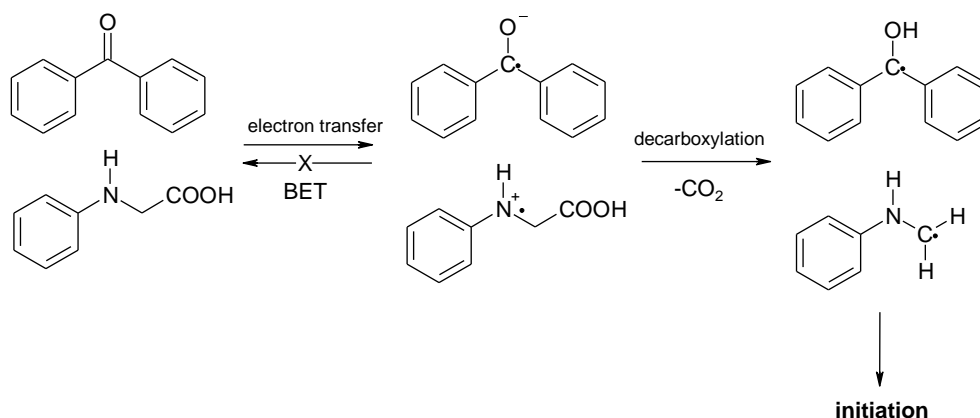
This is crucial, especially in the case of Type II photoinitiators, which have a much longer triplet lifetime than Type I PIs. Also for the polymerization of thin films a drawback is given by the oxygen inhibition due to reduced polymerization rates and longer irradiation times as well as degradation of optical and superficial properties. Remedy to this problem is on the one hand a nitrogen atmosphere during the polymerization process. On the other hand, addition of alkylamines helps to reduce the oxygen inhibition to some extent as presented in Scheme 15.⁶⁶



Scheme 15. Reduction of oxygen inhibition by alkylamines

Another possibility to avoid oxygen inhibition is the in-situ formation of oxygen

barriers. If glycine or its derivatives are used as co-initiating amines, they can undergo photo-induced decarboxylation. The mechanism of radical formation is shown in Scheme 16.⁶⁷



Scheme 16. Electron transfer, proton transfer and decarboxylation in *N*-phenyl glycine coiniciators

By electron transfer an extremely short-lived radical ion is formed, which further reacts by decarboxylation, thus generating the α -aminoalkylradical.⁶⁸ The photosensitized oxidation occurs at the tertiary amine and not at the carboxy moiety, as studies on *N*-phenyl glycine have shown.^{69,70}

This decarboxylation process in combination with the transformation of the amino radical cation to the amino radical avoids the BET efficiently.

Another disadvantage of Type II PIs is the bimolecularity. With increasing viscosity of the formulation also the initiation activity decreases due to hindered diffusion of the PI to the co-initiator. Furthermore, there is almost no migration stability, which presents an issue for applications in the food packaging and medical sector. By the covalent linkage of the PI and the co-initiating amine the migration stability can be increased by the extension of the molecular weight of the PI although this leads to less reactivity due to limited diffusion.

Recently, a new generation of covalently bound PIs and co-initiators has been investigated. It was shown, that benzophenone, covalently bound to *N*-phenyl glycine in the para-position and derivatives thereof, were more efficient PIs than their physical mixtures of benzophenone and the corresponding amine. A further enhancement of the reactivity was given by a β -phenylogous cleavage mechanism of the H₂C-N bond near the benzophenone chromophore (Figure 12).^{71,72}

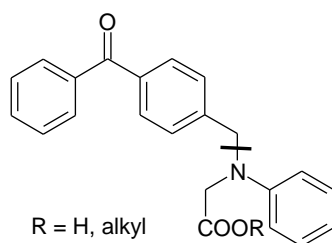
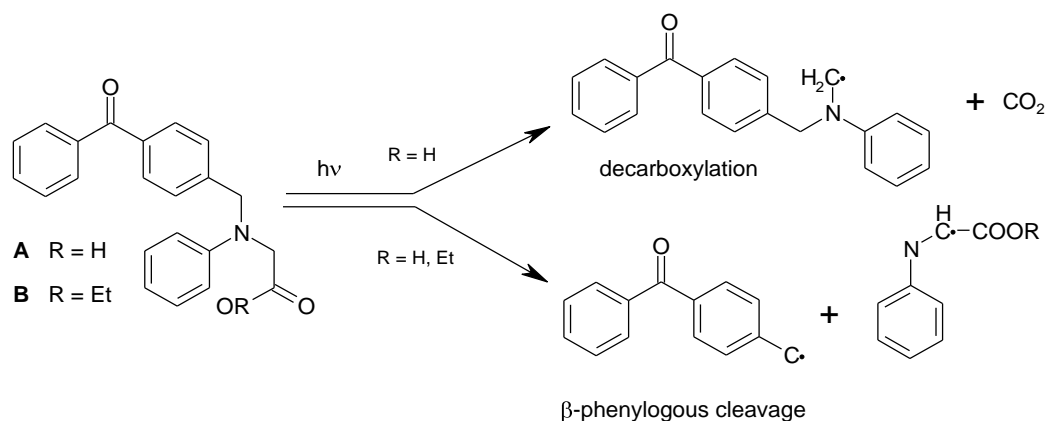


Figure 12. β -Phenylogous cleavage of benzophenone-*N*-phenyl glycine derivatives

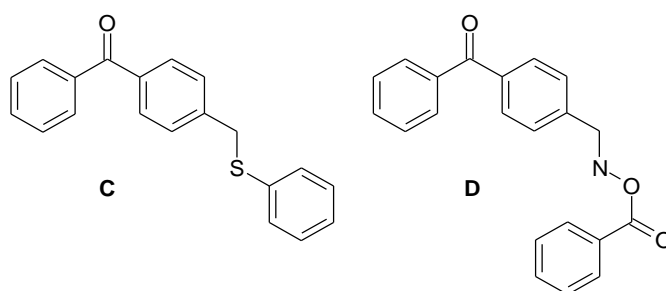
OBJECTIVE TARGETS

Recently, a highly efficient benzophenone-containing Type II photoinitiator (PI), **A**, has been developed. The key step is the spontaneous decarboxylation of the *N*-phenyl glycine residue, thus avoiding the efficiency-limiting back electron transfer. As also the ester **B** has shown unusually good photo-reactivity, high efficiency has been explained by a β -phenylogous cleavage mechanism.

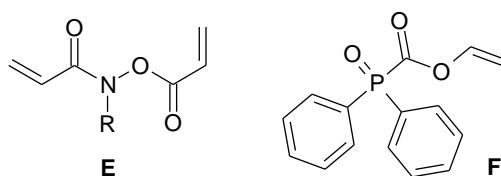


Encouraged by these results, it was the aim to introduce new photocleavable moieties to the benzophenone group, which might provoke the very efficient β -phenylogous cleavage mechanism upon irradiation with UV-light.

As phenyl-(4-phenylsulfanylmethyl-phenyl)-methanone (**C**) exhibited such a cleavage reaction, the *N*-phenyl glycine ethyl ester group in **B** should be substituted by other sulfur containing moieties. Furthermore, also the integration of a labile N-O bond in position of the glycine-nitrogen atom might induce weakening of the β -phenylogous position as in compound **D**.



Furthermore, the concept of the labile N-O bond, which tends to undergo homolytic cleavage under irradiation with UV-light, should be employed to synthesize monomers, which are able to self-initiate photopolymerization upon irradiation with UV-light. Acrylate-based hydroxylamines (**E**) constitute an ideal tool to gain high speed curing polymers. By avoiding the use of PIs and their possible toxic photoproducts, also the application of these self-initiating monomers in the bio-medical field could be considered. Referring to the known toxicity of acrylate-based monomers, also monomers containing low-toxic vinyl ester functionalities should be prepared.



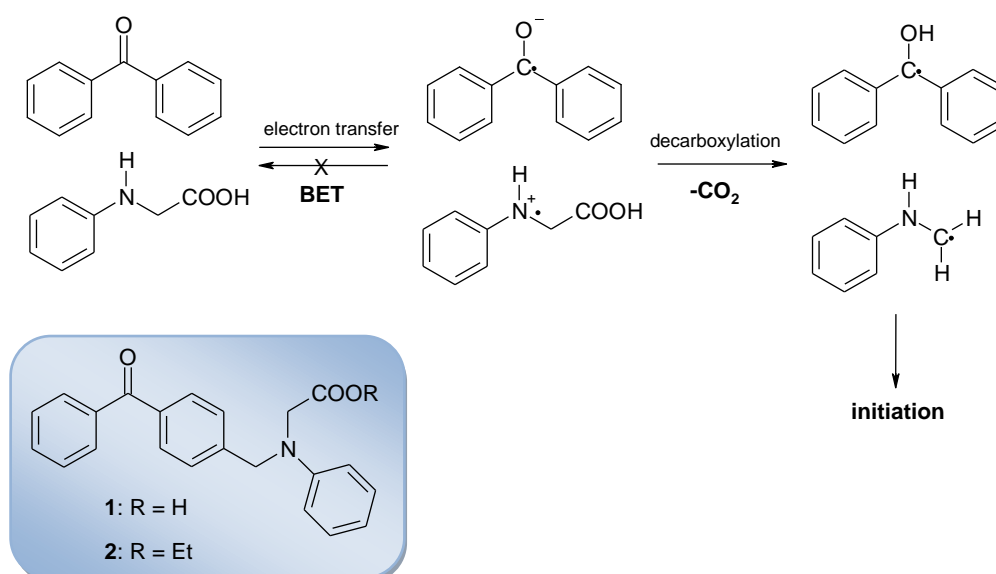
To extend this promising idea of photoinitiating monomers, further investigations on polymerizable compounds based on highly efficient acylphosphine oxides such as **F** can be considered. As phosphorus-containing compounds gained increasing interest as biomaterials during the last years several monomers containing a phosphorus moiety as well as a vinyl ester group leading to a non-toxic poly(vinyl alcohol) backbone should be synthesized. Besides studies on the photoreactivity also biocompatibility and biodegradability of these compounds should be examined.

GENERAL PART

1. Novel Photoinitiators bearing the Benzophenone Moiety

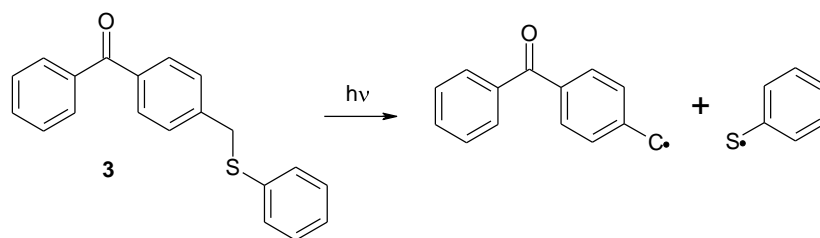
Aromatic carbonyl compounds are well known as chromophores for Type II photoinitiators. Especially the benzophenone moiety was studied intensively to understand the photochemical and photophysical processes in detail.^{73,74}

Tertiary amines find general application as coinitiators, but also have their limitations due to diffusion control. The most recent approach to circumvent this problem was to bind the coinitiator covalently to the benzophenone-moiety as in **A**. If *N*-phenyl glycine is used as coinitiator, it is possible by spontaneous decarboxylation to avoid the back-electron transfer, which leads to deactivation of the radical species (Scheme 17).^{71,72}



Scheme 17. Initiation mechanism of benzophenone-*N*-phenyl glycine and inhibition of BET

However, not only the acid, but also the ethyl ester **2** of benzophenone-*N*-phenyl glycine showed remarkable photoinitiator reactivity. Thus, the spontaneous decarboxylation could not be the only reason for this excellent performance, but additionally a β -phenylogous cleavage mechanism was identified by radical trapping experiments.⁷⁵ Lately, this β -phenylogous cleavage mechanism had also been demonstrated by Yamaji *et al.*²⁷ in ESR experiments of a PI, **3**, with related structure to benzophenone-*N*-phenyl glycine as presented in Scheme 18.



Scheme 18. β -Phenylogous cleavage mechanism for phenyl-(4-phenylsulfanylmethyl-phenyl)-methanone (**3**)

Due to these promising results, displaying the extraordinary reactivity of PIs, which undergo a β -phenylogous cleavage upon irradiation with UV-light, it was the aim of this work to develop new benzophenone-based derivatives, exhibiting an analogous radical forming mechanism. Possible target molecules are illustrated in Figure 13.

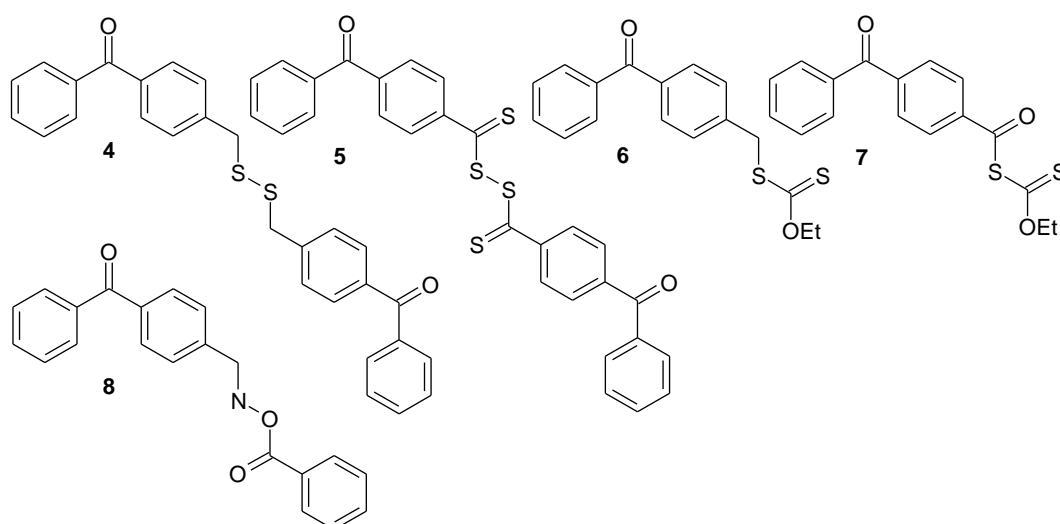


Figure 13. Structures of the new benzophenone-based photoinitiators and reference PIs

To enhance the PI activity of the covalent bound benzophenone-*N*-phenyl glycine model, it should be possible to exchange the amino moiety by other functional groups, that could weaken the β -position under irradiation with UV-light, as it had already been shown for compound **3**. This might be achieved by introduction of a disulfide bridge between two benzophenone-4-methylene moieties as for **4**.

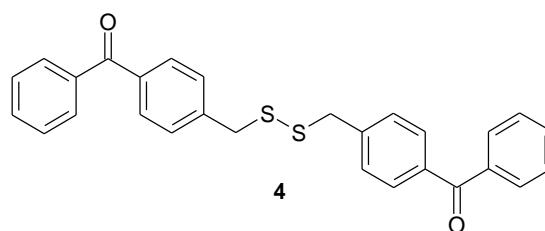


Figure 14. Structure of disulfide target molecule **4**

The choice of disulfide **4** is supported by several experiences from literature. The radical forming mechanism could evolve on the one hand from β -phenylogous cleavage, delivering a dithiyl radical and a benzophenone-methyl radical. This also seems to be the preferred photo-induced dissociation mechanism for disulfides according to literature.^{76,77} On the other hand also two symmetric thiyl radicals, if the scission appeared at the disulfide bridge, might be generated by direct cleavage at 254 nm.⁷⁶ Furthermore, the presence of the covalent bound benzophenone-moiety might have positive effects on the PI efficiency through photosensitization of the C-S, respectively S-S bond. Lalevée *et al.*⁷⁸ investigated the photoinitiating properties of different disulfides alone and also in combination with sensitizing agents as for example 2-isopropylthioxanthone (**ITX**), benzophenone (**BP**), or camphorquinone (**CQ**). They demonstrated, that the use of a photosensitizing agent improved the photo-initiating efficiency of the disulfides to some extent.

According to literature, thiyl radicals from disulfides present a quite useful tool for polymerizations. They show a high reactivity for different monomer double bond species and they exhibit only a low sensitivity to oxygen inhibition.⁷⁹ One of their great drawbacks is the intensive odour of sulfur-containing compounds, especially of mercaptanes.

Developing the concept of the photoactive disulfide bonds further, it was of interest to introduce a trithiocarbonate disulfide bond to the benzophenone-chromophore as shown for compound **5** in Figure 15.

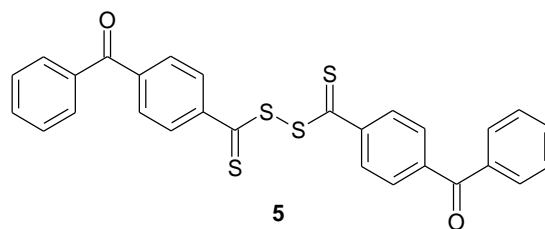
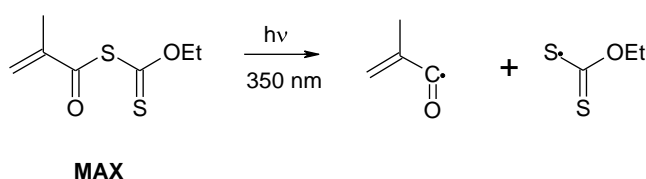


Figure 15. Structure of possible **BP** derivatives containing a photo-cleavable dithio-moiety

Also in case of **5** a β -phenylogous cleavage mechanism could be expected, as well as a scission of the disulfide bond. Not many citations on the photochemistry and use in photopolymerization of trithiocarbonate disulfides could be found in literature. Otsu *et al.* and Niwa and co-workers described the use of dithiocarbonate disulfides as photoinitiators for radical photopolymerization.^{80,81} Niwa *et al.*⁸⁰ reported, that the investigated PI, bis(isopropylxanthogen) disulfide, was found to act as initiator, chain terminator and chain transfer agent. A compound which combines the functions of a PI, a transfer agent and a chain terminator is called a photoiniferter.⁸² The iniferters, which are already in use for thermal radical polymerization reactions often contain a dithioester or trithiocarbonate moiety.⁸³ More recently, Lalevée and co-workers^{78,84} performed studies on dithiocarbonate disulfides as photoiniferters. These pioneer studies might indicate interesting new features of target compound **5**, thus being able to regulate molecular weight dispersity of photopolymers.

Another type of photoiniferters is based on the dithiocarbonate structure. Xanthates are important representatives of transfer agents for living radical polymerization (LRP) under thermal conditions^{83,85} or for photopolymerization. For example Ajayaghosh and Francis^{86,87} described the use of *S*-methacryloyl *O*-ethyl xanthate (**MAX**) as PI for controlled living radical photopolymerization of styrene and methyl methacrylate. The cleavage mechanism of **MAX** occurred according to literature by scission of the (C=O)-S bond of the xanthate at irradiation with monochromatic UV-light at 350 nm (Scheme 19).



Scheme 19. Photochemical cleavage of *S*-methacryloyl *O*-ethyl xanthate as described by Ajayaghosh and Francis

Also Lalev e *et al.*⁸⁸ reported the use of S-benzoyl O-ethyl xanthate as photoiniferter with a high polymerization rate (Figure 16).

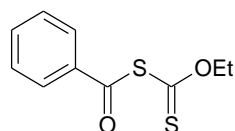


Figure 16. Structure of S-benzoyl O-ethyl xanthate

Therefore, by introduction of a **BP**-moiety covalently linked to a xanthate via a methylene or a carbonyl group as shown in Figure 17, it should be possible to obtain a PI with β -phenylogous cleavage mechanism and the ability to perform controlled radical polymerization.

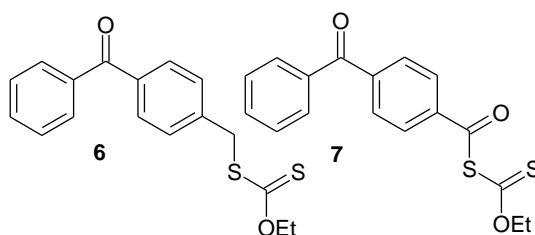
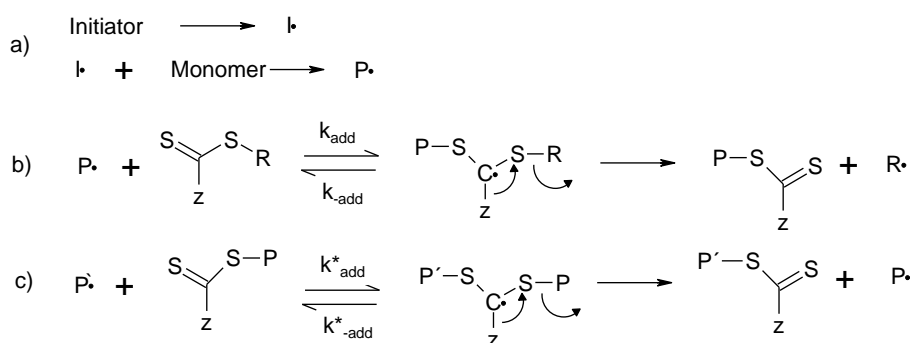


Figure 17. Xanthate based photoinitiators for living free radical polymerization

For better understanding, the core features, as well as the mechanism of living radical polymerization will be explained in the following part. The advantage of LRP is the controlled and reversible formation of radicals, hence leading to a smaller molecular weight dispersity and influencing the polymer properties. The most common techniques for living free radical polymerization are nitroxide mediated polymerizations (NMP),⁸⁹ atom transfer radical polymerization (ATRP),^{90,91} and reversible addition-fragmentation chain transfer polymerization (RAFT).⁸⁵ From these three, RAFT presents the method with the broadest application spectrum concerning monomer diversity. The addition-fragmentation transfer process is outlined in Scheme 20.



Scheme 20. Mechanism for addition-fragmentation chain transfer

The control of polymerization activity by a transfer agent is determined by the two characteristic groups, Z and R. Z should provide the appropriate reactivity for the propagating radicals and is also responsible for the stability of the intermediate radicals. R presents a homolytic leaving group with sufficient capability to reinitiate a polymerization step. The first step, (a) is a common initiation process, delivering free radicals for starting the polymerization. (b) is the transfer reaction, which releases R as new initiating radical. (c) presents finally the core-step of the RAFT process, determining the bimolecular reaction between free polymeric radicals and the macroRAFT radical. Besides these three steps highlighted above, also propagation, re-initiation and termination steps occur as in classic radical polymerizations.⁸³

Apart from the sulfur containing target molecules already discussed, it could also be interesting to introduce a hydroxylamine group via a methylene linker to the benzophenone-chromophore. There are several examples in literature, that the N-O bond in acylated hydroxylamine derivatives can be broken by irradiation with UV-light.⁹²

In this context, three possible PI structures were defined as shown in Figure 18.

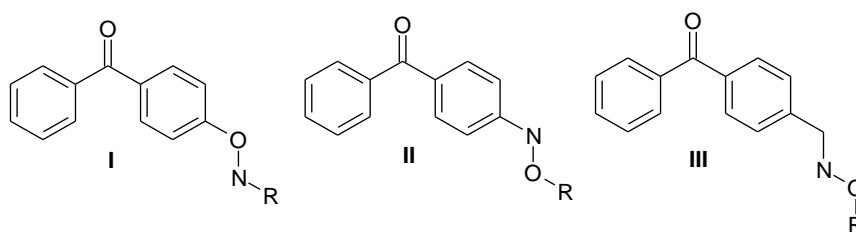


Figure 18. Target structures of hydroxylamine-based PIs with possible β -phenylogous cleavage

In case of **I** a β -phenylogous cleavage mechanism could be expected, but then an unreactive phenol-radical would be generated as well. Structure **II** might also undergo cleavage at the N-O-bond, but the direct attachment of the nitrogen atom to the benzophenone moiety might change the photochemistry of this PI completely. The direct relationship to the model of benzophenone-*N*-phenyl glycine (**1**) would be given by compound **III**, displaying a methylene spacer between the nitrogen atom and the benzophenone-chromophore. For the residue R a benzoyl group was chosen, as the N-O bond scission would lead to the formation of the highly reactive benzoyloxy radical. Although no β -phenylogous cleavage could be expected in target compound **8** presented in Figure 19 – however, it might not be totally excluded – it was considered as a compound, which might develop interesting photochemical features upon irradiation with UV-light.

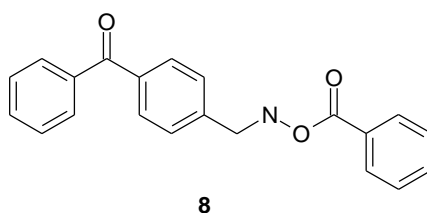


Figure 19. Structure of covalent **BP**-co-initiator system **8**

The novel PIs should be characterized by UV-Vis spectroscopy and photo-Differential Scanning Calorimetry (photo-DSC). Their reactivity should be compared to industrially applied PIs, Darocur 1173 and benzophenone/triethanolamine (**BP/TEA**). Besides also PIs with a covalent bound co-initiator, like in benzophenone-*N*-phenyl glycine ethyl ester (**2**), or thiophenyl PI **3** should be used as reference materials. Further investigations were planned to examine the cleavage mechanism by photochemically induced dynamic nuclear polarization (photo-CIDNP) experiments. Also the possible regulation of molecular weight by the sulfur-containing compounds should be examined by gel permeation chromatography (GPC) of the cured samples from the photo-DSC experiments.

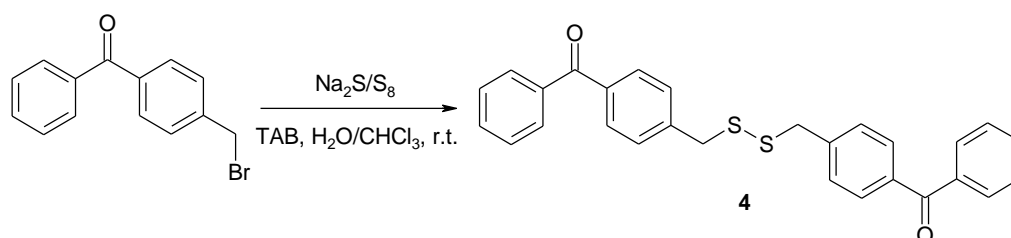
1.1. Synthesis

1.1.1. Bis-[(4-methyl)-benzophenone]-disulfane (**4**)

In literature several ways to obtain disulfides are described. For example, sulfur-

containing precursors like thiols can be oxidized by several methods, e.g. by oxygen,⁹³ dihydrogen peroxide,⁹⁴ halogens,⁹⁵ or hypiodites.⁹⁶ By reaction of arylalkyl bromides with sulfur under base catalysis symmetric disulfides can be obtained in good yields,⁹⁷ but to avoid the formation of toxic dihydrogen sulfide, another method was taken into account. By reaction of alkyl halogenides with a mixture of sodium sulfide and sulfur under phase transfer conditions also symmetric disulfides were prepared. Sonavane and co-workers⁹⁸ used tetrabutylammonium bromide as phase transfer catalyst in water/chloroform as solvent for the formation of symmetric disulfides.

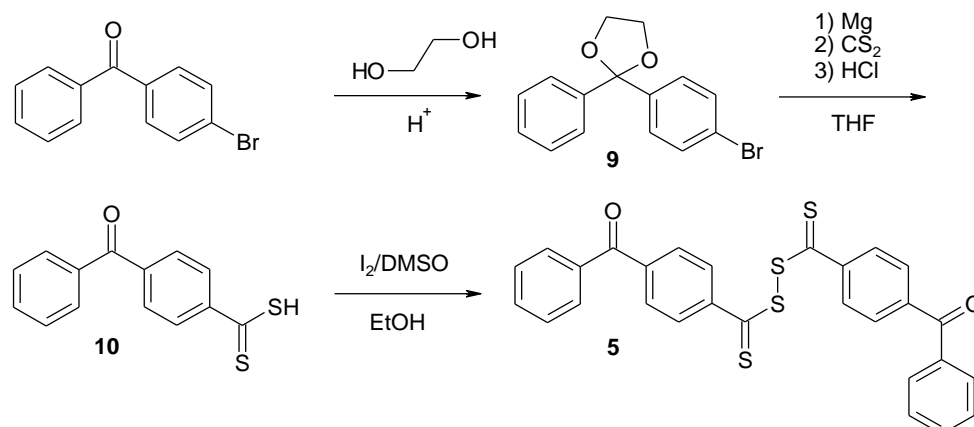
In the current study, 4-bromomethyl benzophenone was used as starting material for the synthesis of disulfane **4**, as it was easily accessible by bromination of 4-methyl benzophenone with *N*-bromosuccinimide in tetrachloromethane.⁹⁹ Unfortunately, also the dibromo derivative was obtained as by-product, which could not be removed by recrystallization or column chromatography.



For the preparation of **4**, 4-methyl benzophenone was reacted with mixture of sulfur and sodium sulfide under phase transfer conditions (PTC). As phase transfer catalyst tetrabutyl ammonium bromide (**TAB**) was used. The raw product was purified by column chromatography. Nevertheless the pink-orange product was still impure to about 18% due to the dibromo substrate, as could be seen from $^1\text{H-NMR}$ analysis (peak of the methylene- CH_2 at 6.69 ppm). Also the integration of the aromatic protons showed a too high amount, possibly due to the formation of sulfides or trisulfides as described in literature,⁹⁸ which could not be removed by column chromatography or recrystallization. Nevertheless, disulfide **4** was tested on its photoreactivity, as it was assumed, that the impurities would not show significant influence on the photochemistry of this compound.

1.1.2. Attempted synthesis of 4,4'-(dibenzoyl)-bis(thiocarbonylphenyl) disulfide (**5**)

The formation of dithiocarbonate disulfide **5** should be carried out according to Scheme 21.

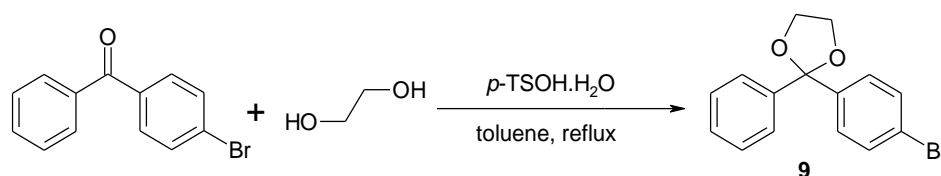


Scheme 21. Planned synthesis pathway for dithiocarbonate disulfide **5**

In the first step it would be necessary to protect the keto group of 4-bromobenzophenone by a dioxalane group before in the second step the magnesium bromide could be obtained by a Grignard reaction. The formation of the dithiocarbonyl acid would occur by the addition of carbon disulfide, followed by acidification with hydrochloric acid. Under acidic conditions, also the dioxalane protecting group should be removed. In the final step the dithiocarbonate disulfide should be generated by the oxidation of the dithiocarbonyl acid with iodine/DMSO.

Therefore, the synthesis of disulfide **5**, started with the protection of the keto group in 4-bromobenzophenone.

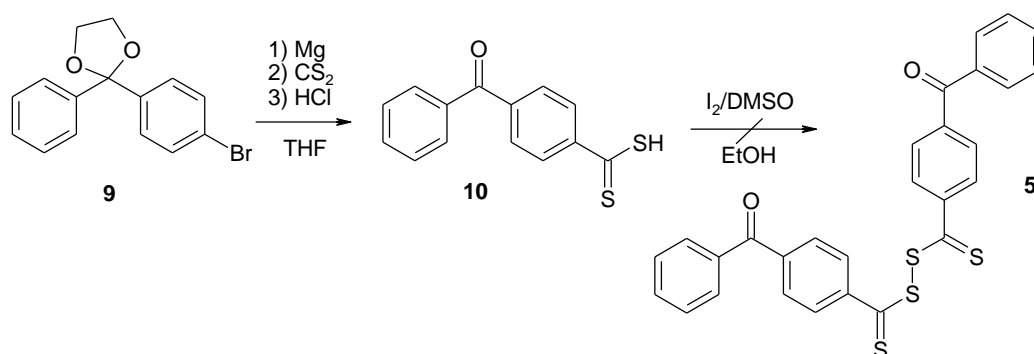
Suitable protecting groups for ketones are several kinds of acetals (*O,O*-, *S,S*-, *O,S*-, *N,O*-), cyanhydrins or oxazolines.¹⁰⁰ For this reaction pathway the *O,O*-acetal group was chosen as dioxalane **9** had already been described in literature.^{101,102}



Hence, 4-bromobenzophenone was heated to reflux with a twofold excess of ethylene glycol and a catalytic amount of *p*-toluene sulfonic acid monohydrate. Toluene was used as solvent instead of benzene, which was employed in literature,

due to toxicology reasons. According to $^1\text{H-NMR}$ analysis of the raw product it contained still traces of starting material. Purification was carried out by column chromatography and finally yielded 75% of product **9**. In a second run the purification was also carried out by recrystallization from ethanol. By this way only 51% yield were obtained.

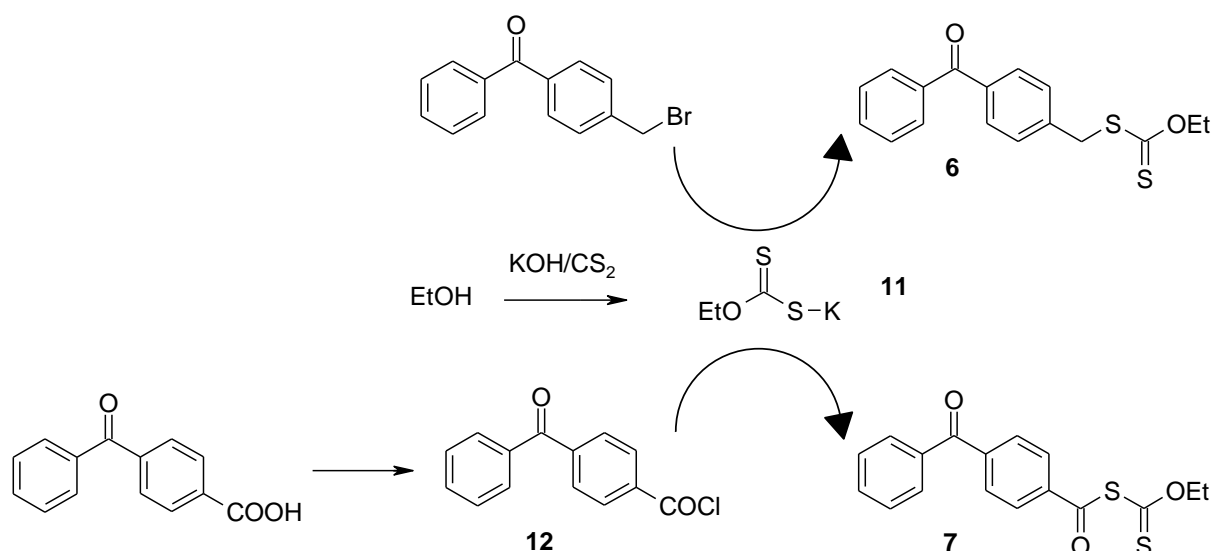
Dioxalane **9** was converted to disulfide **5** by a Grignard reaction with magnesium turnings, followed by thiolation with carbon disulfide and formation of the disulfide **5** by oxidation with iodine/DMSO, as it was described by Sprong *et al* for the synthesis of dithiobenzoyl disulfide.¹⁰³ This preparation was performed in a one-pot reaction, as there were indications in literature,^{104,105} that the generated dithiobenzoic acid was highly instable towards any isolation method.



Unfortunately, the desired product **5** could not be obtained by this reaction pathway, probably due to even higher instability of the intermediate (4-benzoyl)-dithiobenzoic acid (**10**) compared to dithiobenzoic acid.

1.1.3. Synthesis of dithiocarbonates **6** and **7**

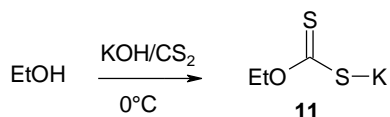
Possible reaction pathways for the synthesis of the dithiocarbonates **6** and **7** are displayed in Scheme 22.



Scheme 22. Planned syntheses of dithiocarbonates **6** and **7**

Dithiocarbonates **6** and **7** contain the *O*-ethyl ester moiety. Therefore, potassium *O*-ethyl dithiocarbonate (**11**) can be used as the starting materials for both compounds. It should be converted to the desired benzyl dithiocarbonate **6** by reaction with 4-bromomethyl benzophenone. For the synthesis of **7**, the acid chloride of 4-benzoylbenzoic acid (**12**) should be prepared first, which could deliver benzoyl dithiocarbonate **7** after reaction with the potassium dithiocarbonate salt **11**.

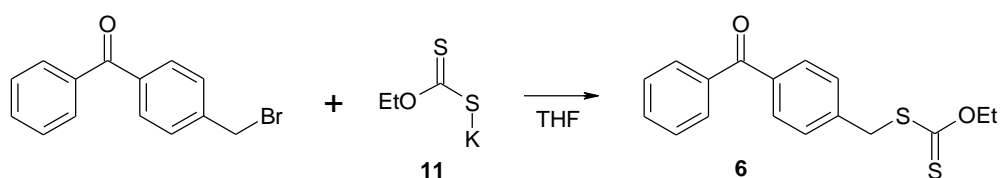
According to literature,¹⁰⁶ salts of xanthogenates are easily accessible by reaction of an alcohol with carbon disulfide in the presence of an alkali metal hydroxide. Therefore, potassium dithiocarbonate **11** was used as starting material for compounds **6** and **7**.



Potassium ethanolate was mixed with an equimolar amount of carbon disulfide at low temperature. During the addition of CS₂ the potassium xanthogenate salt already precipitated as brown solid. Finally, the precipitate was filtered off and dried in vacuum. From ¹H-NMR and ¹³C-NMR analysis no by-products were seen, therefore this precursor was used without further purification in the following syntheses.

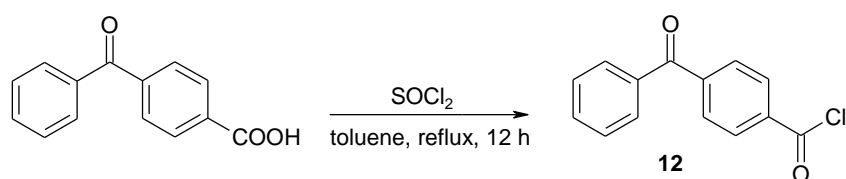
The synthesis of *S*-(4-benzoyl)-benzyl *O*-ethyl dithiocarbonate (**6**) was performed

according to methods described in literature.^{83,107,108}



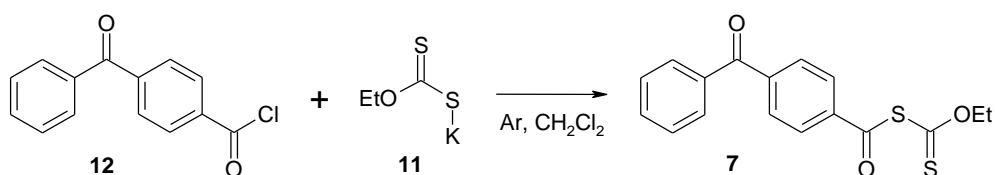
Thus, an equimolar amount of 4-bromomethyl benzophenone was added to potassium O-ethyl dithiocarbonate (**11**) in tetrahydrofurane and stirred for 20 h at room temperature. The raw product was purified by column chromatography to deliver 32% highly viscous, slightly yellow oil **6**.

The formation of the (4-benzoyl)-benzoyl chloride (**12**) as precursor for benzoyl dithiocarbonate **7** was performed according to the method described by Wheeler.¹⁰⁹



Therefore, (4-benzoyl) benzoic acid was heated to reflux with 5 mole equivalents of thionyl chloride under Ar-atmosphere. To remove remaining thionyl chloride, the white residue was re-dissolved in toluene and placed onto the rotary evaporator. This procedure was repeated three times. Product **12** was obtained as brownish solid in 98% yield of adequate purity for further reactions. An analytical sample for the determination of the melting point was recrystallized from a mixture of toluene and petrolether (1:4) to deliver white needles of **12**.

Synthesis of S-(4-benzoyl)-benzoyl O-ethyl dithiocarbonate (**7**) was carried out according to the method described by Ajayaghosh and co-workers,¹¹⁰ who prepared S-benzoyl O-ethyl xanthate in a similar way.

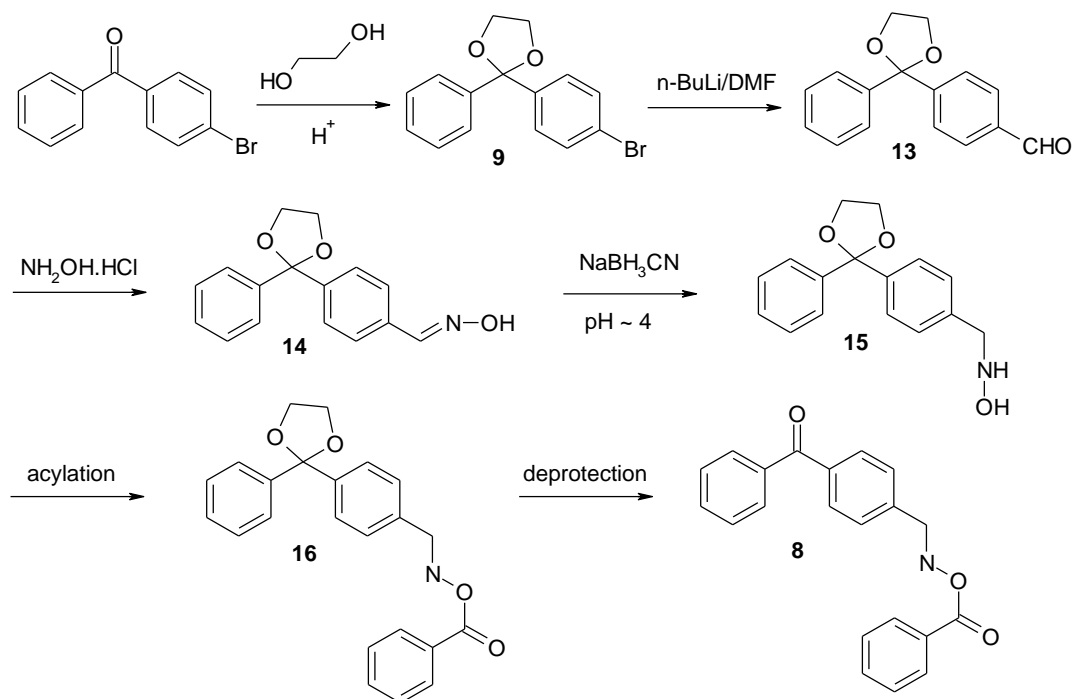


Hence, the acyl chloride **12** was added to a suspension of O-ethyl dithiocarbonate **11** in dichloromethane under Ar-atmosphere at 0°C. The reaction mixture was stirred then for 2 h at room temperature. The raw product was obtained as orange-brown

solid. It was purified by recrystallization from ethanol, which delivered 49% of light yellow solid **7**.

1.1.4. Attempted synthesis of *N*-(benzoyloxy)-(4-benzoyl)-benzene-methanamine (**8**)

The following Scheme 23 shows a possible reaction pathway for the synthesis of hydroxylamine **8**.



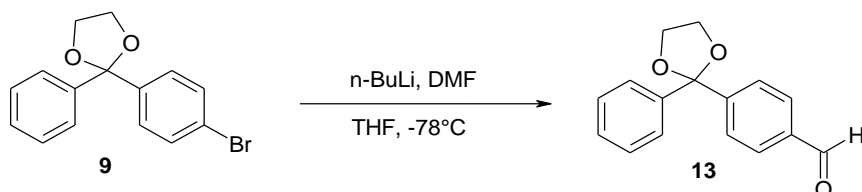
Scheme 23. Synthesis strategy for *O*-benzoylated hydroxylamine **8**

Obviously, to gain target molecule **8**, a multistep reaction pathway would be necessary, considering also the lability of the benzophenone-ketogroup towards hydroxylamine and reducing agents. Hence, in the first step the keto group of the starting material, 4-bromobenzophenone, should be protected as acetal in **9** by reaction with ethylene glycol under acid catalysis. In the next step the bromo group should be converted to an aldehyde moiety as in **13** by formylation with *N,N*-dimethylformamide after bromine-lithium exchange. The aldehyde group could then be transformed into the corresponding oxime **14** using hydroxylamine. Consequently, the oxime moiety should be reduced to the corresponding hydroxylamine **15**. Target compound **8** could then be obtained by acylation of **15** with benzoyl chloride, thus delivering **16** followed by deprotection of the keto group.

Therefore, in the first step 2-phenyl-2-(4-bromophenyl)-1,3-dioxalane (**9**) was

synthesized. The preparation of **9** has already been described in chapter 1.1.2., as it was a precursor for the synthesis of bis(thiocarbonylphenyl) disulfide **5**.

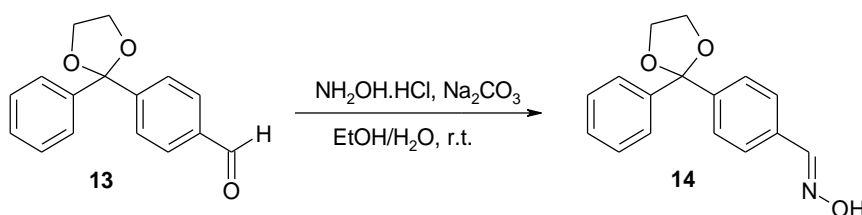
The next step was the preparation of 2-phenyl-2-(4-formylphenyl)-1,3-dioxalane (**13**). The synthesis of **13** had already been described in a paper by Matsuda and co-workers.¹⁰¹



Accordingly, the preparation of **12** was performed by lithiation of compound **9** with an equimolar amount of n-butyllithium in THF at -78°C, followed by formylation with 1.1 eq. *N,N*-dimethylformamide. It is necessary to keep the temperature of the reaction mixture below -50°C due to the formation of undesired by-products by cycloreversion of THF at elevated temperatures.¹¹¹ Purification of was carried out by column chromatography and delivered product **13** in 60% yield as white solid.

The third reaction step was the preparation of (4-[[1,3]-dioxalan-2-yl-2-phenyl]) benzamidoxime (**14**). Generally, the conversion of aromatic aldehydes or ketones to oximes is well documented.^{112,113,114} The reaction with hydroxylamine hydrochloride is carried out in a mixture of water and a water-miscible organic solvent, e.g ethanol. It is catalyzed by a base, which also serves as acceptor for the evolving hydrogen chloride. As base several examples were found in literature, for example sodiumbicarbonate,¹¹² sodium acetate,¹¹³ or pyridine.¹¹⁴ Generally, a mixture of (*E*)- and (*Z*)-oximes is obtained.

Thus, the protected aldehyde **13** was converted to the oxime **14** in aqueous ethanol, using sodium carbonate as acid scavenger.



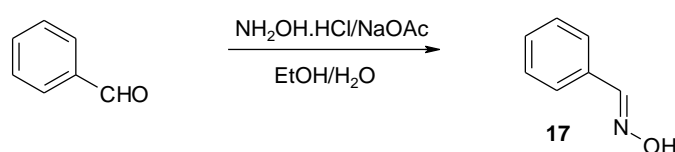
Monitoring of the reaction progress by TLC was difficult, as the product decomposed on the silica gel TLC plates to the starting product **13** and ammonia. Aluminium oxide

TLC plates could not be used neither, as the product was smeared broadly over the trace. Therefore it was not possible to determine the end of the conversion to the desired oxime **14**, so it was worked up after 8 days reaction time. $^1\text{H-NMR}$ analysis of the raw product showed still impurities of starting material **13**. For purification the impure compound was dissolved in diethylether and then ice-cold petrolether was added. The precipitate was collected and finally 46% of oxime **14** could be isolated as white solid. In case of **14** only the (*E*)-isomers were obtained according to $^1\text{H-NMR}$, possibly due to sterical hindrance by the bulky benzophenone residue.

According to literature, there are only a few possibilities to obtain hydroxylamines by selective reduction of oximes, as many common reduction agents lead directly to the corresponding amines. Nevertheless, there was found some evidence, that oximes could be reduced selectively to the stage of the hydroxylamine by the use of sodium cyanoborohydride at pH 3-4.^{115,116,117}

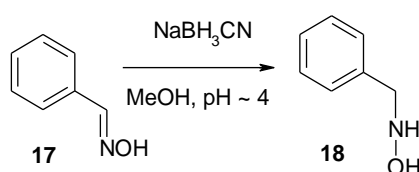
Being aware of the challenges of this reaction, the reduction should first be tested on a far simpler model compound, benzaldoxime (**17**), which was available in much larger amounts than the benzophenone-derived oxime **14**, as it was obtained easily by hydroxylation from benzaldehyde.

The synthesis of oxime **17** was performed in accordance with methods from literature.^{118,119,120}



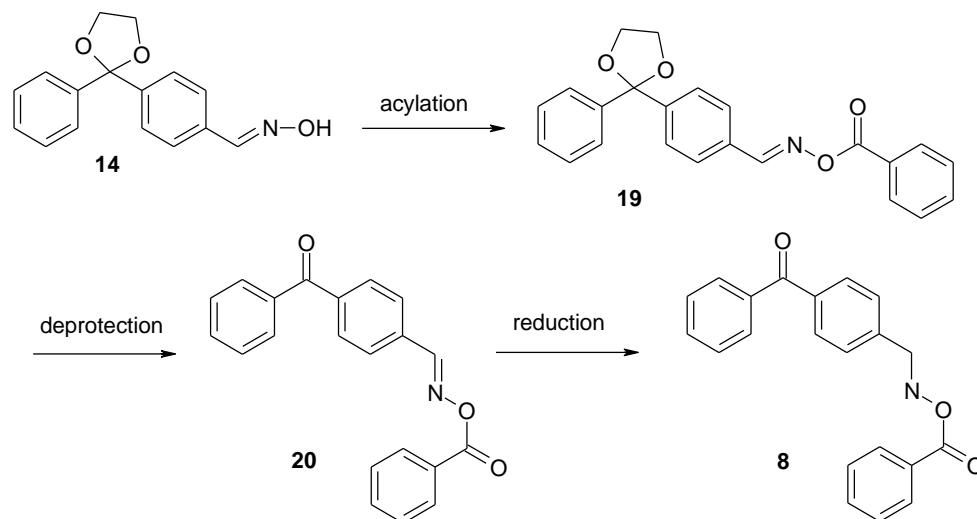
Acetaldehyde was converted to benzaldoxime (**17**) with hydroxylamine hydrochloride and sodium acetate. By this reaction pathway the (*Z*)-isomer of **17** was obtained as white solid in 91% yield.

For the synthesis of *N*-benzylhydroxylamine (**18**), sodium cyanoborohydride was added to a solution of oxime **17** and methylorange as indicator in methanol.



Finally, the pH of the mixture was adjusted to 3-4 by dropwise addition of methanolic

HCl until no further color change could be seen. After isolation of the raw product $^1\text{H-NMR}$ analysis and GC-MS analysis showed only 50% conversion of the oxime and also a remarkable amount of benzylamine. Due to the low conversion and the high danger potential of this reaction (development of HCN during the reduction with sodium cyanoborohydride), another synthesis pathway was chosen as shown in Scheme 24.

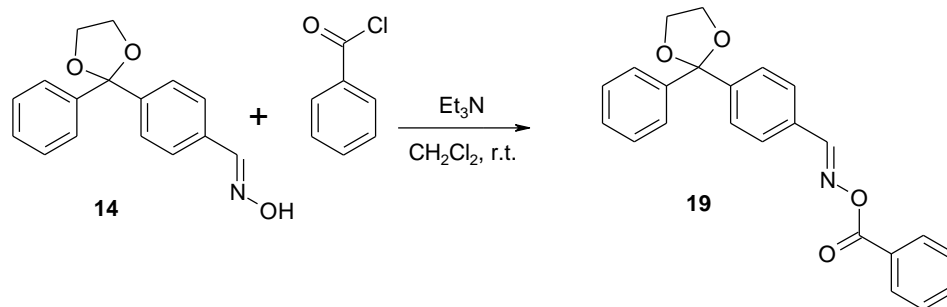


Scheme 24. Second synthesis route to hydroxylamine **8**

In the alternative synthesis plan for **8** the reduction should take place from the *O*-benzoyl oxime ester **20**, which could be obtained by acylation of the protected oxime **14** followed by deprotection of the keto group in **19**, as the ester **20** was considered more stable against overreduction to the amine compared to the free oxime.

Therefore, the first step of the alternative pathway leading to compound **8**, consisted of the oxime benzylation. According to literature, an easy method for the formation of oxime esters is the base catalyzed acylation.^{120,121}

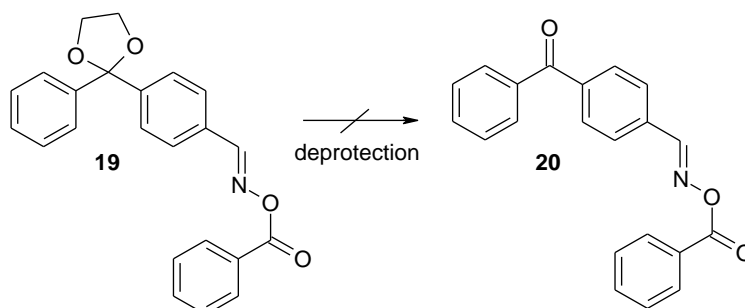
Hence, for the synthesis of (4-[[1,3]-dioxolan-2-yl-2-phenyl])-*O*-phenylacetyl benzamidoxime (**19**), benzamidoxime **14** was converted with 1.2 equ. of benzoylchloride and 1.2 equ of triethylamine.



Purification was performed by column chromatography to give **19** as white solid in 35% yield.

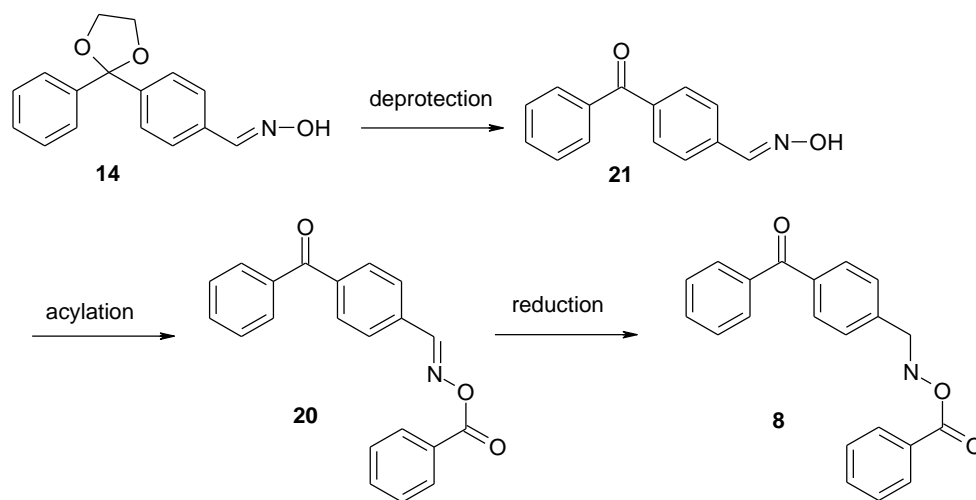
The next step to obtain the (4-benzoyl)-*O*-phenylacetyl benzamidoxime (**20**) was the cleavage of the protecting group from the keto-moiety.

Several attempts were made to remove the acetal group from **19** by mild methods, e.g. by using *p*-toluene sulfonic acid in acetone¹²² at room temperature or transacetalization with iodine in acetone¹²³ at room temperature, or with pyridinium *p*-toluene sulfonate in acetone/water¹²⁴ at room temperature.



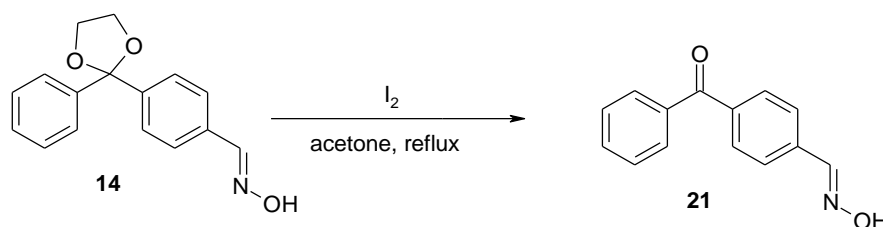
Unfortunately, all deprotection methods presented here led to the decomposition of the substrate **19**.

Therefore, another pathway was chosen as shown in Scheme 25: deprotection should be already performed at the stage of the free oxime **14**, followed by the acylation with benzoyl chloride and finally reduction to hydroxylamine **8**.



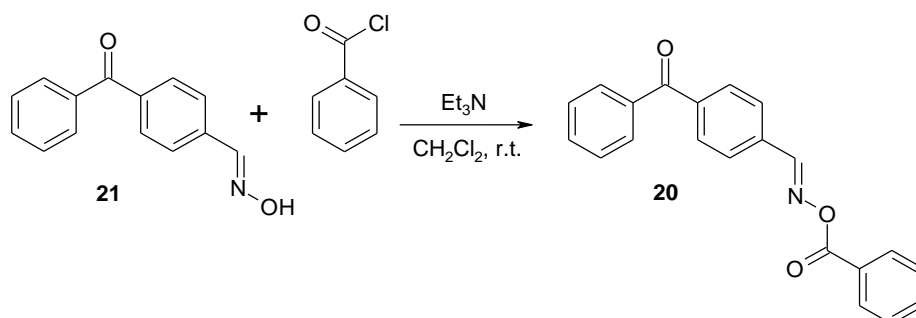
Scheme 25. Third synthesis route to hydroxylamine **8**

For the deprotection of oxime **14** the mild transacetalization with iodine in acetone¹²⁴ was chosen due to the acid lability of the oxime moiety.



Thus, a $1/10$ molar equivalent of iodine and oxime **14** were heated to reflux. To finalize the reaction an excess of iodine was necessary. Without further purification, **21** was obtained as yellow oil in 72%. The raw product of **21** was directly used for the benzoylation step due to instability towards any purification method.

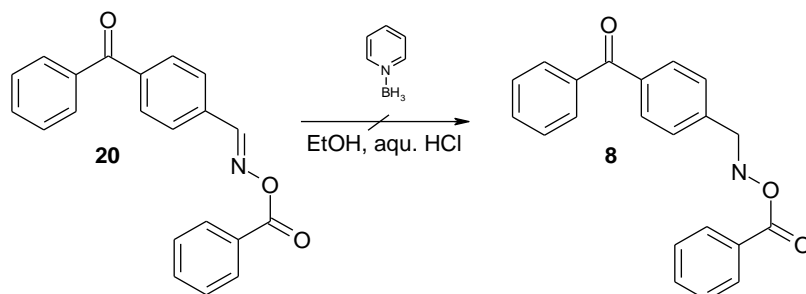
The acylation of deprotected benzamidoxime **21** to generate (4-benzoyl)-*O*-phenylacetyl benzamidoxime (**20**) was carried out with 1.2 equ. of benzoyl chloride and 1.2 equ. of triethyl amine as acid scavenger.



The yellow-brown oily raw product was purified by column chromatography. By this

method 34% of product **20** were yielded as white solid.

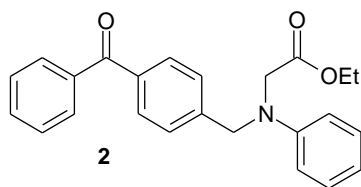
The final step, the reduction of the oxime ester **20** to the hydroxylamine **8** should be performed according to the method described by Kawase and Kikugawa¹²⁵ with pyridine-borane under acidic conditions, as the use of sodium cyanoborohydride had not been successful in case of the free oxime.



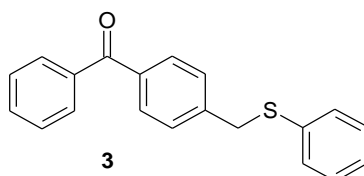
Therefore, *O*-benzoyl oxime **20** was mixed with 3.3 equ. of pyridine borane complex in ethanol and an aqueous solution of 10% HCl at 0°C. The raw product consisted of an oily residue, which was obtained after alkaline work up. However, from ¹H-NMR analysis of the raw product a huge signal of the benzophenone carbaldehyde could be found, indicating, that the oxime had been hydrolyzed to a large extend during the reaction. Also TLC analysis showed at least 7 by-products which could not be separated by column chromatography. Therefore, it was not possible to prepare hydroxylamine **8** by this method. As oxime **20** seemed to have interesting photochemical properties as well, similar to *O*-acyl oximino ketones and *O*-acyl oximes, that were already described in literature as photoinitiators,^{126,127} it was included in the following analysis series.

1.1.5. Reference compounds **2** and **3**

The preparation of **2** has already been described in literature¹²⁸ and was synthesized recently at the institution, where the work on this thesis has been performed, by a coupling reaction of *N*-phenyl glycine ethyl ester and 4-bromomethyl benzophenone.⁷¹ As the compound was susceptible to oxidation under air and also impurities from the synthesis were still present, several attempts for further purification were done. After column chromatography and three times of recrystallization from diethylether/hexane compound **2** could be obtained in sufficient purity for the photo-DSC and photo-CIDNP experiments.



Synthesis of compound **3** was described by Yamaji *et al.*²⁷ and it was also prepared by Jauk, converting 4-bromomethyl benzophenone with thiophenol using sodium hydroxide as catalyst.¹²⁹ By two times recrystallization from petrolether **3** could be obtained in ample purity for photo-DSC and photo-CIDNP measurements.



1.2. Analyses

The photochemical properties of the new photoinitiating compounds **4**, **6**, **7** and the references **2**, **3** were investigated by UV-Vis analysis and photo-differential scanning calorimetry (photo-DSC). Also intermediate **20** was subjected to all analyses, as photoreactivity could be assumed from the acylated oxime moiety.^{126,130} Besides, special investigations were made on the cleavage mechanism for the covalently bound PIs by photo-chemically-induced-dynamic-nuclear-polarisation (photo-CIDNP) experiments and on the use of the sulfur-containing compounds as control agents for molecular weight distribution by GPC analysis.

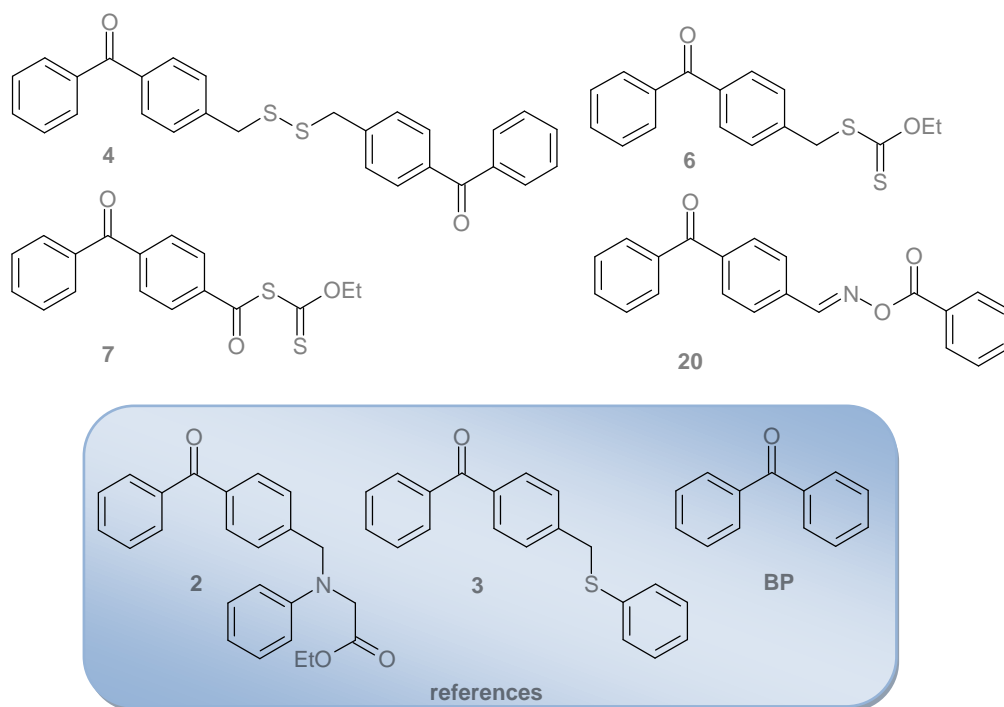


Figure 20. Structures of investigated PIs **4**, **6**, **7**, **20** and reference compounds **2**, **3**, **BP**

1.2.1. UV-Vis spectroscopy

First, the UV-Vis absorption behavior of the newly synthesized oxime **20**, the disulfane **4** and the two dithiocarbonates **6** and **7** should be investigated in comparison to well known photoinitiator benzophenone (**BP**), and the references **2** and **3**. The UV-Vis analyses were conducted in acetonitrile solutions of 1×10^{-2} M to 1×10^{-5} M concentration.

1.2.1.1. Bis-[(4-methyl-benzophenone) disulfane (**4**)]

Generally, transitions of **BP** in the region of 250 nm are known to have a $\pi-\pi^*$ character. The $n-\pi^*$ transition, which plays an important role in the photochemistry of **BP**, is usually located in the range of 300 and 350 nm. It is characterized by a low extinction coefficient (ϵ), caused by this spin forbidden transition.^{130,131}

The results of the UV-Vis analysis of **4** are presented in Figure 21 and Table 3.

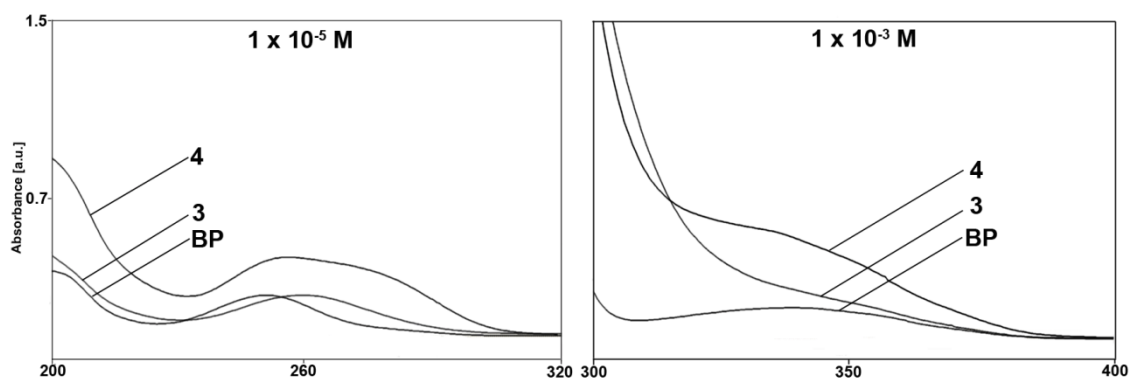


Figure 21. UV/Vis spectra of disulfane **4** in comparison to references **BP** and **3**

Table 3. UV-Vis data for disulfane **4** and the references, **BP** and **3**

PI	$\pi-\pi^*$ transition		$n-\pi^*$ transition	
	λ_{\max} [nm]	$\epsilon_{\max} \times 10^{-3}$ [L mol ⁻¹ cm ⁻¹]	λ_{\max} [nm]	$\epsilon_{\max} \times 10^{-3}$ [L mol ⁻¹ cm ⁻¹]
4	256	37.1	-	-
3	256	17.1	-	-
BP	250	19.7	339	0.14

Disulfane **4** showed different absorption behaviour than the thiophenyl reference **3**, with higher absorbance for the $\pi-\pi^*$ transition at 256 nm, probably due to the presence of two benzophenone moieties, overlapping with the shoulder of a second maximum, which might be caused by the excitation of the S-S bond, that is usually found at ~250 nm for alkyldisulfides.¹³² The maximum of the intensive $\pi-\pi^*$ transition of the keto group was only red-shifted for 6 nm in case of **4** and **3** compared to simple benzophenone due to the presence of the alkyl substituent. At higher concentrations (1×10^{-3} M) an absorption shoulder from the symmetry-forbidden $n-\pi^*$ transition, tailing out at 400 nm was identified with a significantly increased ϵ than for the reference compounds. Basically, as stated in literature, disulfides present only weak absorption in the range between 300 and 400 nm, which can be activated by the use of photosensitizers like **ITX**.⁷⁸

1.2.1.2. Dithiocarbonates **6** and **7**

The $\pi-\pi^*$ transitions of dithiocarbonates **6** and **7** were found to be in the same wavelength range as for **BP** and reference **3**. In case of **6** it forms no clear maximum, but only a shoulder (Figure 22 and Table 4).

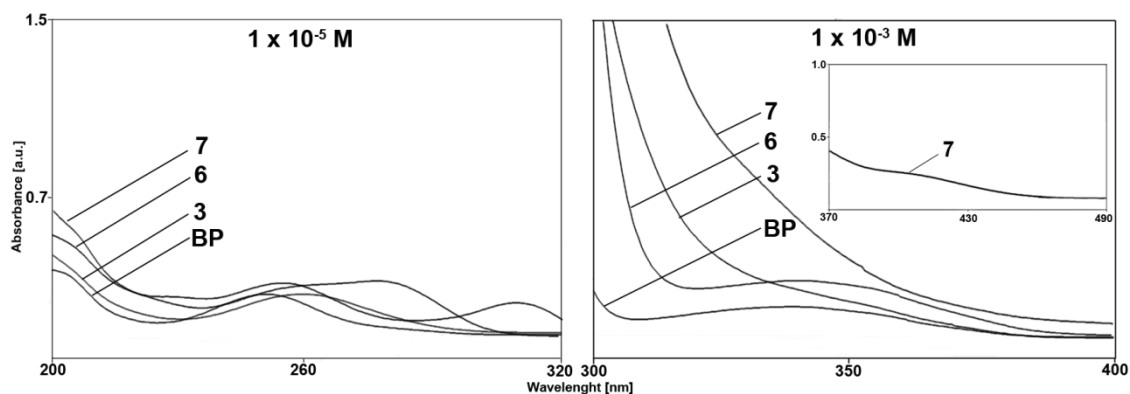


Figure 22. UV/Vis spectra of dithiocarbonates **6**, **7** in comparison to references **BP** and **3**

Table 4. UV-Vis data for dithiocarbonates **6** and **7** compared to the references, **BP** and **3**

PI	$\pi-\pi^*$ transition		$n-\pi^*$ transition	
	λ_{\max} [nm]	$\epsilon_{\max} \times 10^{-3}$ [L mol ⁻¹ cm ⁻¹]	λ_{\max} [nm]	$\epsilon_{\max} \times 10^{-3}$ [L mol ⁻¹ cm ⁻¹]
6	276	26.8	342	0.26
7	254	26.9	-	-
	309	17.8	-	-
3	256	17.1	-	-
BP	225	19.7	339	0.14

A second $\pi-\pi^*$ transition of the dithiocarbonate moiety of **6** might be indicated by the maximum at 276 nm. Another absorption maximum was found for **7** at 309 nm, which probably belonged to the $\pi-\pi^*$ transition of the benzoyl dithiocarbonate functionality, which is strongly red-shifted by the presence of the additional carbonyl chromophore and thus extended conjugated system. Furthermore, compound **6** displayed also a maximum at 342 nm, congruent with the maximum for the $n-\pi^*$ transition of **BP**. Dithiocarbonate **7** exhibited here only a shoulder like reference **3**, which passed into another absorption shoulder already in the visible part of the spectrum at 400 nm, tailing out at 450 nm, which is shown in the insert of Figure 22.

1.2.1.3. (4-Phenyl)-O-phenylacetyl benzamidoxime (**20**)

The presence of the oxime group in **20** led to a strong red-shifted $\pi-\pi^*$ transition absorption maximum with significantly higher extinction coefficient (ϵ), compared to **BP** and the two reference PIs, **2** and **3**.

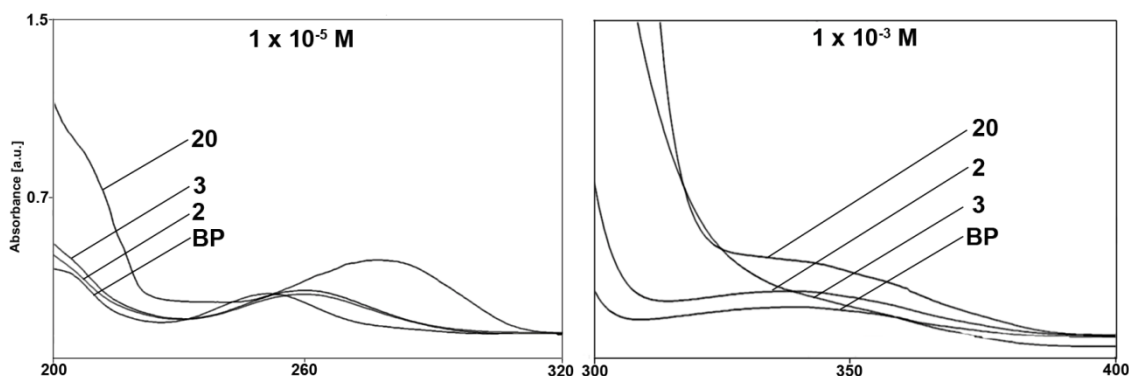


Figure 23. UV/Vis spectra of oxime **20** in comparison to references **BP**, **2** and **3**

Table 5. UV-Vis data for oxime **19** and the references, **BP**, **2** and **3**

PI	$\pi-\pi^*$ transition		$n-\pi^*$ transition	
	λ_{\max} [nm]	$\epsilon_{\max} \times 10^{-3}$ [L mol ⁻¹ cm ⁻¹]	λ_{\max} [nm]	$\epsilon_{\max} \times 10^{-3}$ [L mol ⁻¹ cm ⁻¹]
20	276	35.6	-	-
2	259	21.2	338	0.21
3	256	17.1	-	-
BP	225	19.7	339	0.14

The shift added up between 17 and 26 nm as presented in Table 5 and might be caused by the longer conjugated system due to the oxime group adjacent to the benzophenone chromophore. The ethyl ester of benzophenone-*N*-phenyl glycine, **2**, and the phenylsulfide **3** displayed similar absorption behavior concerning the $\pi-\pi^*$ transition maximum at 256 nm and 269 nm, respectively. Interestingly, also an intensive shoulder at 339 nm, clearly visible at higher concentrations, could be detected for the *O*-benzoyl oxime **20**, although recent studies by Lalevée *et. al* did not report any absorption for related *O*-acyl oximes in this region of the UV-Vis spectrum.¹³⁰ This might indicate a $n-\pi^*$ transition, comparable to the known known photochemistry of **BP**.¹³³

1.2.2. Photo-DSC

By photo-DSC experiments, the performance of a given formulation can be determined in a simple and accurate way. The reactivity is evaluated by the time t_{\max} (s), that is needed to reach the maximum polymerization heat. Additional information on the efficiency of a system can be obtained from the rate of polymerization ($R_{P_{\max}}$; mol L⁻¹ s⁻¹) and the double bond conversion (DBC; %). Apart from the photoreactivity

of the sulfur-containing PIs also their ability to regulate molecular weight dispersity should be examined in a second experimental set.

Measurements were carried out in hexane-1,6-diol diacrylate (**HDDA**) for analyses of PIs **4** and **20** with a PI concentration of 12.1 mmol L^{-1} . For the second series concerning molecular weight regulation studies with PIs **4**, **6** and **7**, *N*-acryloyl morpholine (**NAM**) was used as monomer, with a PI concentration of 12.1 mmol L^{-1} . UV-light in the range of 280 – 450nm with an intensity of 3000 mW cm^{-2} at the tip of the light guide was applied. All experiments were performed under nitrogen atmosphere (20 mL min^{-1}).

1.2.2.1. Comparison of **4** and **20** with reference PIs

The reactivity of the new photoinitiating compounds **4** and **20** should be compared to industrially applied Type I PI Darocur 1173 and well known equimolar physical mixtures of 4-methyl benzophenone (**MBP**) with amines like triethanolamine (**TEA**) and *N,N*-dimethyl aminobenzoic acid ethyl ester (**DMAB**) as shown in Figure 24. Additionally, the PIs should be compared to other covalently bound PIs, like benzophenone-*N*-phenyl glycine ethyl ester (**2**) and the phenylsulfide **3**.

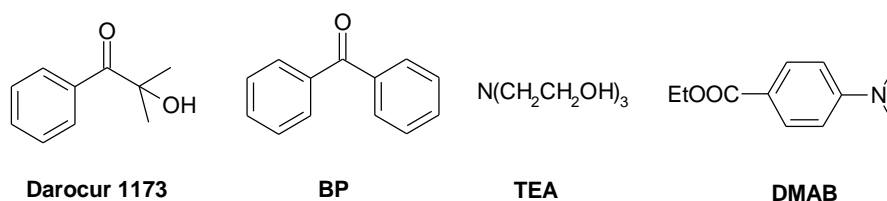


Figure 24. Structures of the commercial reference PIs for the photo-DSC experiments

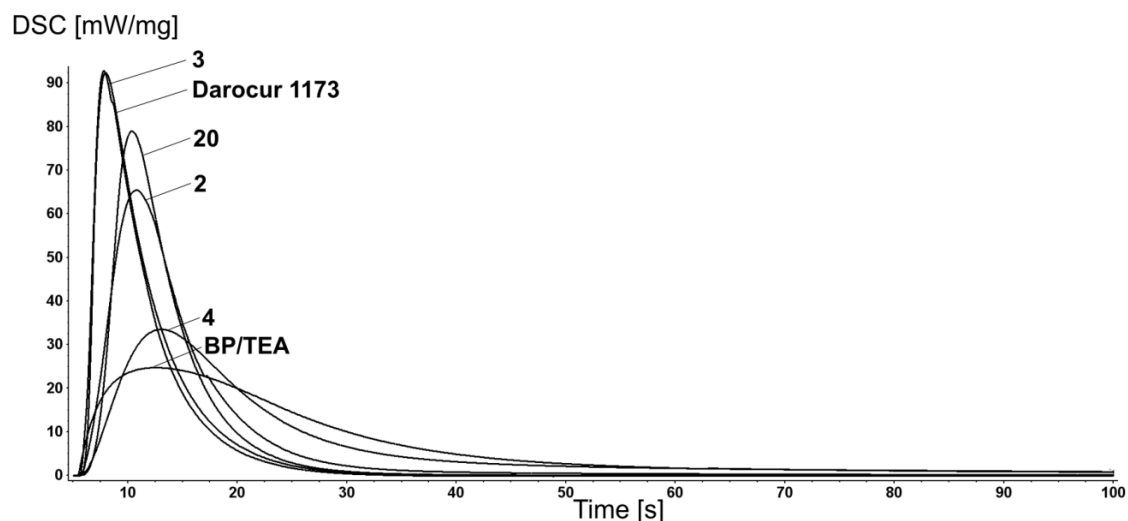


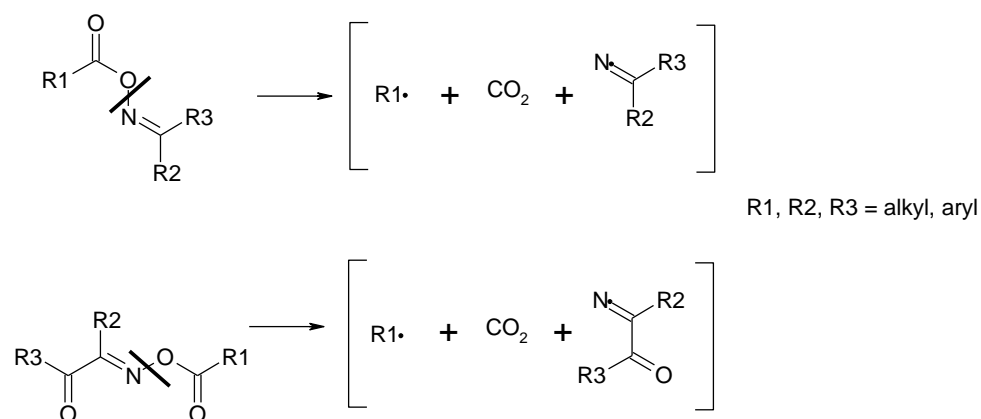
Figure 25. Photo-DSC plots for PIs **4** and **20** in comparison to references **2**, **3**, **BP/TEA** and Darocur 1173

Table 6. Photo-DSC data of **HDDA** with PIs **4**, **20** and references (12.1 mmol L⁻¹)

PI	t _{max} [s]	DBC [%]	R _{Pmax} x 10 ³ [mol L ⁻¹ s ⁻¹]
4	7.5	81	218
20	4.6	86	540
2	5.0	87	444
3	2.0	82	636
BP/TEA	7.1	89	165
BP/DMAB	7.4	93	170
Darocur 1173	2.0	87	632

The reactivity of the novel disulfide PI **4** without any coinitiator was in the range of well-known mixtures based on benzophenone/amine. Nevertheless, the initiator reactivity of disulfane **4** was much lower than of oxime PI **20**, which surprisingly displayed an excellent efficiency. The reactivity of **20** without any coinitiator even surpassed reference PI **2**, which assumedly undergoes a β-phenylogous cleavage mechanism. The performance of **20**, expressed by a low t_{max} and high R_{Pmax}, is only slightly smaller than of industrially used Type I PI, Darocur 1173, and the phenylsulfide reference **3**, which is known to undergo β-phenylogous cleavage upon irradiation with UV-light.²⁷

The excellent reactivity of **20** might be derived from the efficient UV-induced cleavage of the N-O bond. Also several types of acylated oximes have demonstrated good PI properties.^{126,130} Very recently, they found attention also as photobase generators, having more advantages compared to photoradical and photoacid generators, which suffer from oxygen inhibition and corrosion of metal substrates, respectively.¹²⁷

**Figure 26.** N-O bond cleavage of O-acyl oximes and of O-acyl oximino ketones

1.2.2.2. Variation of PI concentration

Industrially applied PI concentrations are in the range of 1-7 wt%. Therefore, it was of interest to examine the influence of PI concentration in a given monomer. The **HDDA** formulation with a PI concentration of 12.1 mmol L⁻¹ was diluted, delivering 6.0 mmol L⁻¹, 3.0 mmol L⁻¹ and 0.6 mmol L⁻¹ solutions. The results for the PI-concentration dependent photo-DSC experiments are shown in Figure 27.

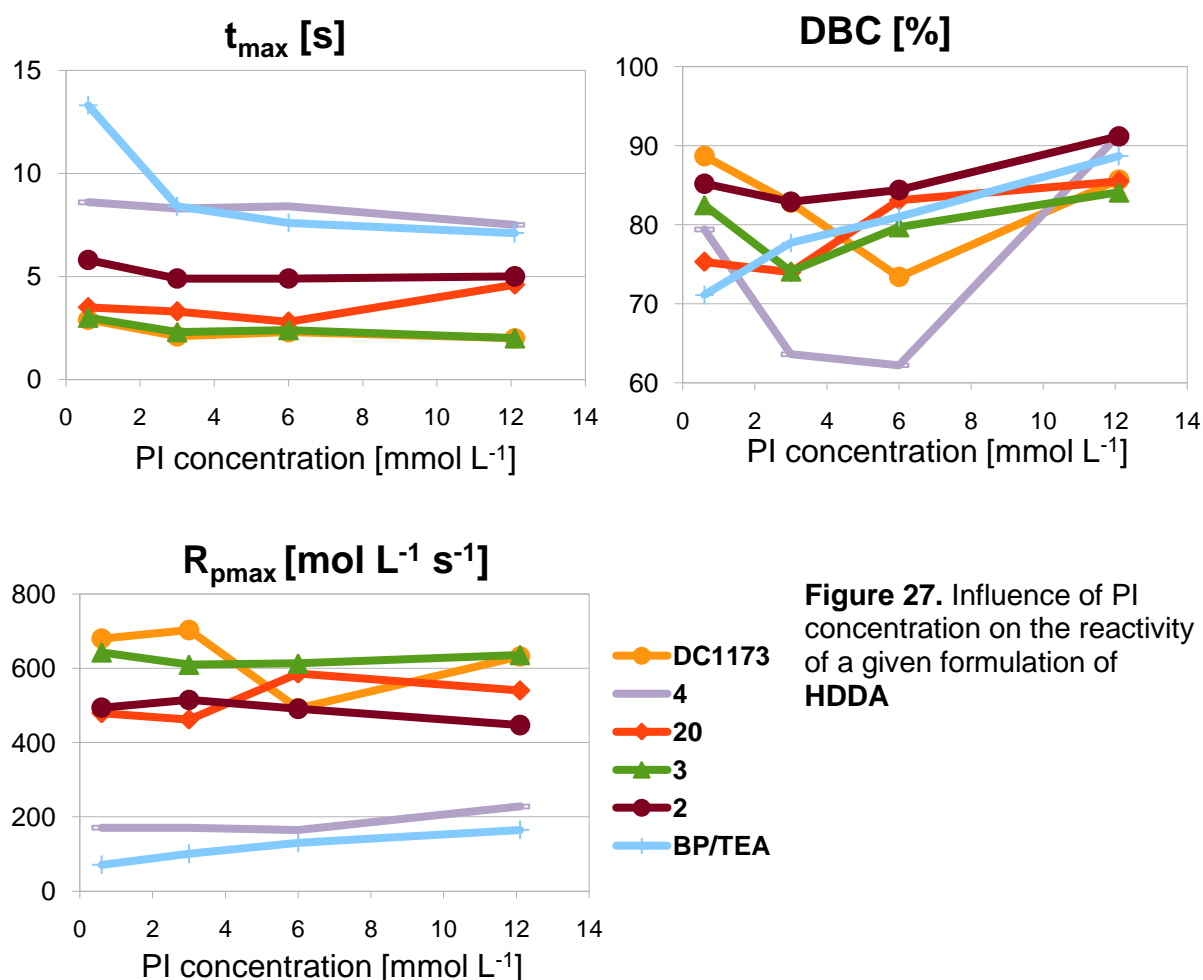


Figure 27. Influence of PI concentration on the reactivity of a given formulation of HDDA

As expected, t_{\max} was continuously rising with decreasing concentration of the PIs. Only **BP/TEA** displayed a sudden loss of reactivity at the lowest concentration value, which might originate from diffusion control of the bimolecular radical forming process. Obviously, the amount of amine close to the excited ketone was then too low for an efficient co-initiation. The DBC was falling constantly with lower PI concentration in the case of bimolecular system **BP/TEA**. The other PIs displayed a slight minimum of the DBC at mediocre concentrations, with a very distinctive drop to 62% for disulfane **4**. A reason for this surprising result could not be discovered yet. The polymerization rate, $R_{p\max}$, basically was not changed significantly, but showed a

decrease for **4** and the physical mixture of **BP/TEA** with lower PI concentration, in accordance with the trend for t_{\max} . The other PIs displayed a slight rise for $R_{P_{\max}}$ with decreasing amount of PI in the formulation. This might be explained by light screening effects¹³⁴ at lower PI concentration, dependent also on the sample thickness.

1.2.2.3. Addition of amine co-initiators and photosensitizers

Experiments with **TEA** as co-initiator for the PIs **4**, **20**, **2** and **3** were performed to see, if the presence of a hydrogen donating amine could improve the PI reactivity. Equimolar solutions of PI and **TEA** in **HDDA** with a concentration of 6.0 mmol L^{-1} of PI were measured under nitrogen atmosphere.

In a second series, also the use of a photosensitizer like 2-isopropylthioxanthone (**ITX**), which acts as an energy transfer agent,¹³⁵ was examined. **ITX** was added in 0.2 mol% to the formulations containing 6.0 mmol L^{-1} of PI.

The data of these photo-DSC experiments is presented in Figure 28.

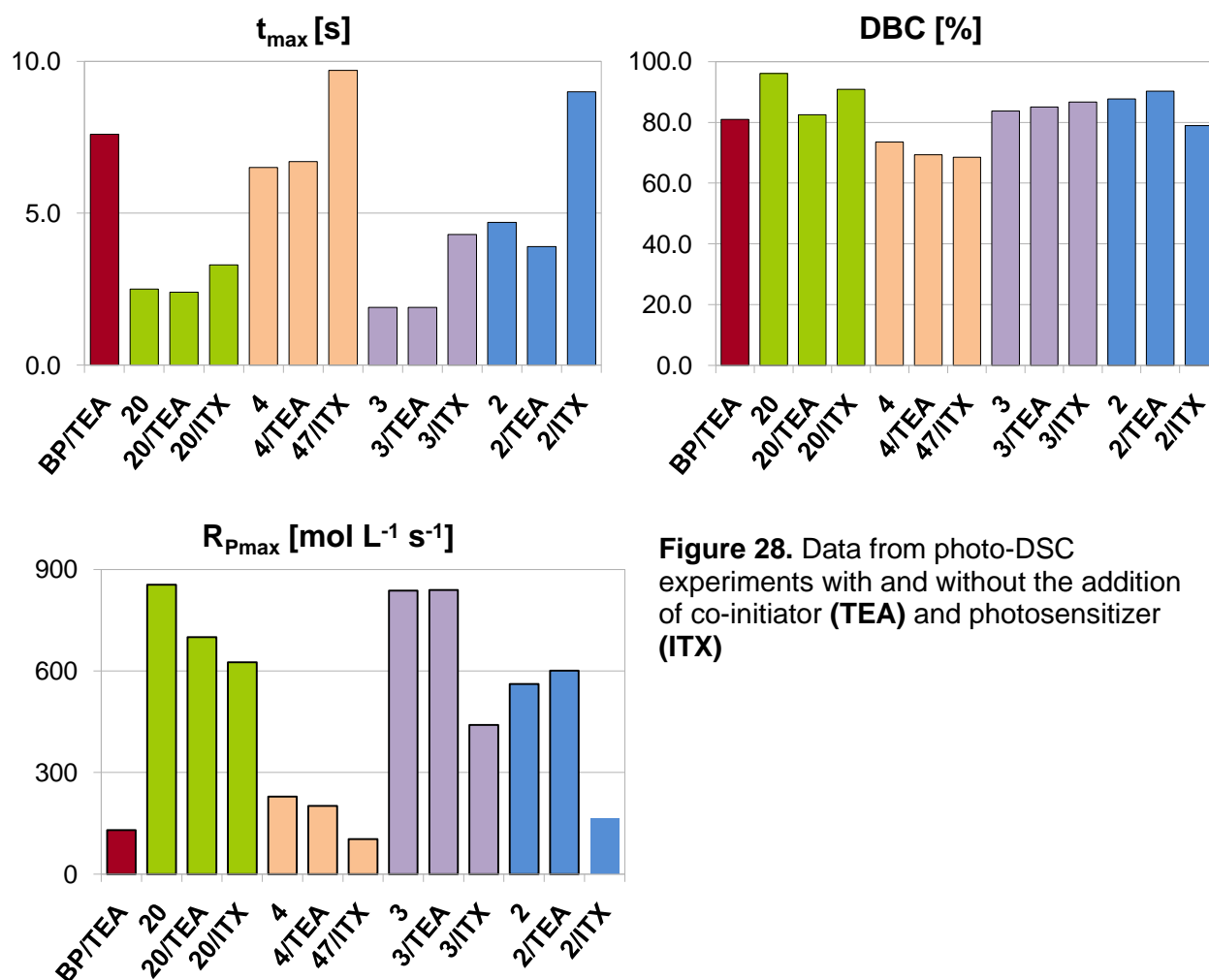


Figure 28. Data from photo-DSC experiments with and without the addition of co-initiator (**TEA**) and photosensitizer (**ITX**)

Generally, reactivity, expressed by t_{\max} , was marginally influenced by addition of the amine. This might indicate, that the intramolecular photo-reaction was at least as efficient as the bimolecular reaction involving the amine. For **2** and **3** the addition of the amine even entailed a slight improvement of reactivity. In contrast to that, the presence of the PS led to higher t_{\max} values and therefore lesser reactivity of the formulations, probably due to a light screening effect, quenching or mismatch of the excited state energy levels. The same trend could be seen for the DBC values, although to much weaker extend, and more drastically in the case of the polymerization rates, $R_{P\max}$. Here addition of the PS led to diminished reactivity.

1.2.2.4. PI reactivity and control of molecular weight distribution

Generally, controlled or living radical polymerization is a process for the reversible formation of radicals and finds wide-spread use in thermal polymerization techniques. Only few approaches were ventured towards the use of this method in photopolymerization due to the lack of suitable initiators, so-called photoiniferters.⁸⁴ Such structures are mainly based on a photoinitiating moiety, e.g. a benzyl group, and a dithiocarbonate or dithiocarbamate functionality as the terminating species. Lalevée and co-workers carried out photoiniferter studies on *O,O*-diethyl xanthogene disulfide (**DEXDS**) and phenylacetyl disulfide (**PADS**),⁸² which were used as reference compounds in the present work.

For a first evaluation, the newly synthesized dithiocarbanoates **6** and **7** were tested for their ability to initiate photopolymerization efficiently. Their reactivity was compared to physical mixtures of a Type I PI, Darocur 1173 containing 20 mol% (referred to the PI concentration) of control agent (CA, Figure 29), Darocur 1173 alone and disulfide **4**, which was also considered to display influence on the molecular weight distribution of a given formulation. As control agents part from above mentioned **DEXDS** and **PADS** also *N,N,N',N'*-tetrabutyl dithiocarbamate disulfide (**TBDTS**) and dibenzoyl disulfide (**DBODS**) were used. A suitable monomer for this kind of experiments was mono-functional *N*-acryloyl morpholine (**NAM**), which delivered water soluble polymers, appropriate for the subsequent GPC analysis of the cured photo-DSC samples. The PI concentration was 12.1 mmol L⁻¹ for the photo-DSC experiments. Sample weight was 12 ± 0.6 mg. The analyses were done under nitrogen atmosphere, using a UV filter of 280-450 nm and light intensity of 3000 mW cm⁻² at the tip of the light guide.

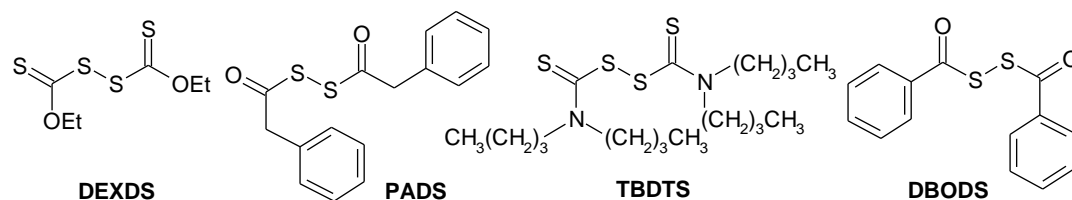


Figure 29. Structures of the investigated molecular weight control agents

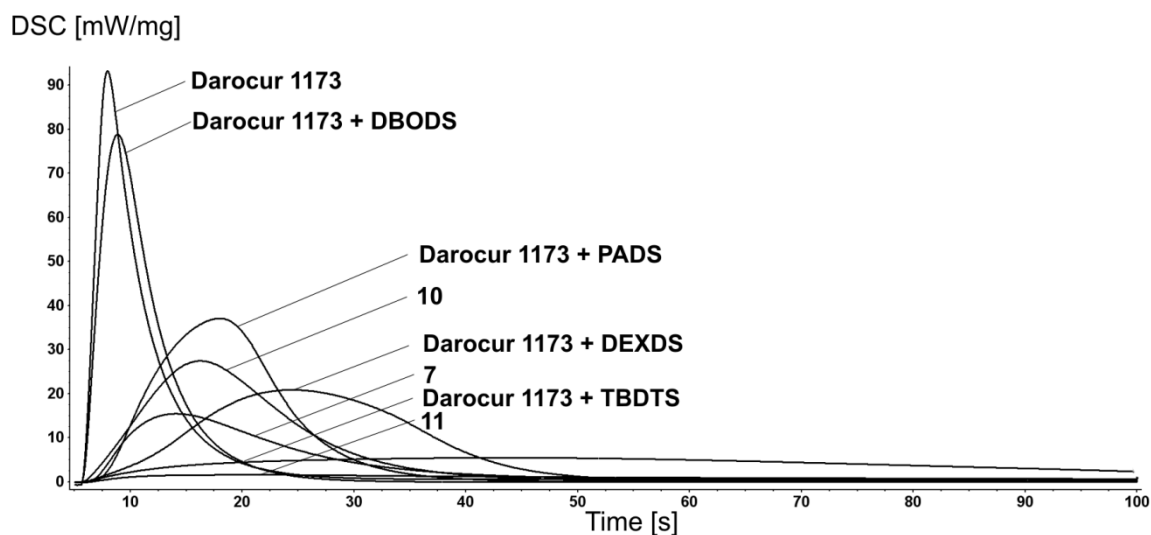


Figure 30. Photo-DSC plots of PIs 4, 6 and 7 compared to Darocur 1173 with/without molecular weight control agent in **NAM**

Table 7. Photo-DSC data for analysis of PIs 4, 6 and 7 compared to Darocur 1173 with/without CA

PI	CA	t_{\max} [s]	DBC [%]	$R_{P_{\max}} \times 10^2$ [mol L ⁻¹ s ⁻¹]
Darocur 1173	-	2.0	91	142
Darocur 1173	DEXDS	18.8	94	31.9
Darocur 1173	PADS	12.6	98	57.0
Darocur 1173	TBDS	41.5	88	8.2
Darocur 1173	DBODS	3.2	95	121
4	-	8.2	55	23.6
6	-	10.5	85	42.0
7	-	15.7	26	2.25
MBP/TEA ¹	-	10.8	91	45.0

¹ Graph not shown in Figure 21 for better optical clarity

A clear trend was identified from the data presented in Figure 30 and Table 7 for the mixtures of Darocur 1173 with the CAs, where the reactivity decreased from the most reactive control agent, **DBODS** to the least reactive **TBDTS** CA according to **DBODS>PADS>DEXDS>TBDTS**. Reactivity of the covalently bound PI/CA compounds **4** and **7** were far below industrially applied PIs Darocur 1173 and **MBP/TEA**. Also DBC and R_{Pmax} values were only moderate. In case of **7** presumably radical formation was poor, explaining the very low DBC of 26%.

Astonishingly, dithiocarbonate **6** without any coinitiator showed better DBC and R_{Pmax} values, already in the range of the reference CAs and also **MBP/TEA**.

It was also investigated, if the reactivity of the PIs can be improved by the use of an equimolar amount of **TEA** as co-initiator.

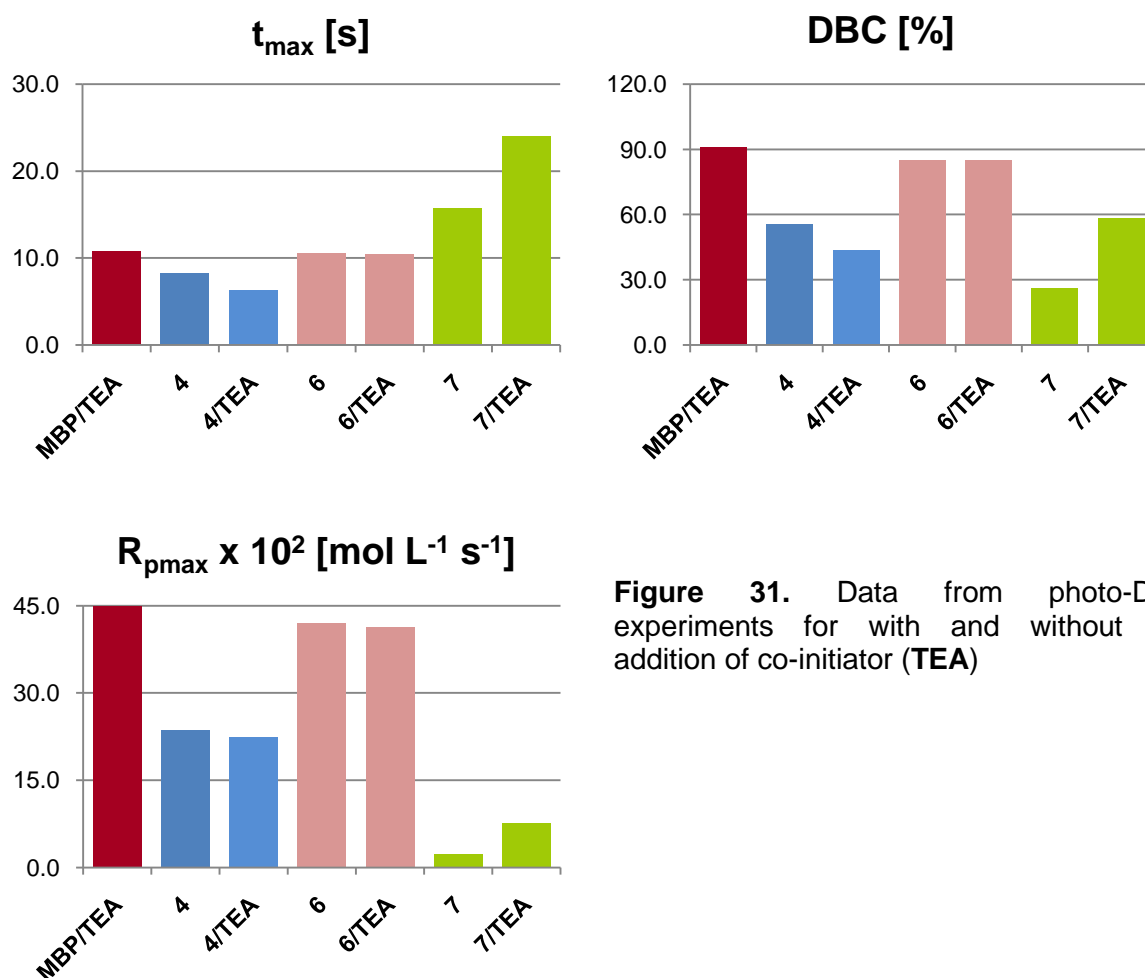


Figure 31. Data from photo-DSC experiments for with and without the addition of co-initiator (**TEA**)

The photo-DSC data presented in Figure 31 show, that addition of an amine as co-initiator had no influence on the performance of PI **6**, as the intramolecular photo-reaction might be faster than the reaction with the co-initiating amine. It led to lower DBC and rate of polymerization in the case of disulfane **4**. Only for benzoyl dithiocarbonate **7** the DBC and R_{Pmax} could be enhanced significantly by twice the amount as without co-initiator. Unfortunately, this improvement was obtained at the cost of curing speed.

1.2.3. GPC analysis

To evaluate the efficiency of the CAs and the photoinitiating CAs, **4**, **6** and **7** the samples from the photo-DSC experiments should directly be submitted to GPC analysis. The polymer disks were dissolved in 1.5 mL of eluent and filtered through a polyamide filter. As eluent an aqueous Na_2SO_4 solution (0.05 M) containing 20 v% of acetonitrile, was used. The GPC analyses were performed with a flow rate of 0.6 mL min^{-1} at 40°C , using two Ultrahydrogel columns (250 and 1000), a Viscotek VE3580 RI detector and polyvinylalcohol standards for calibration.

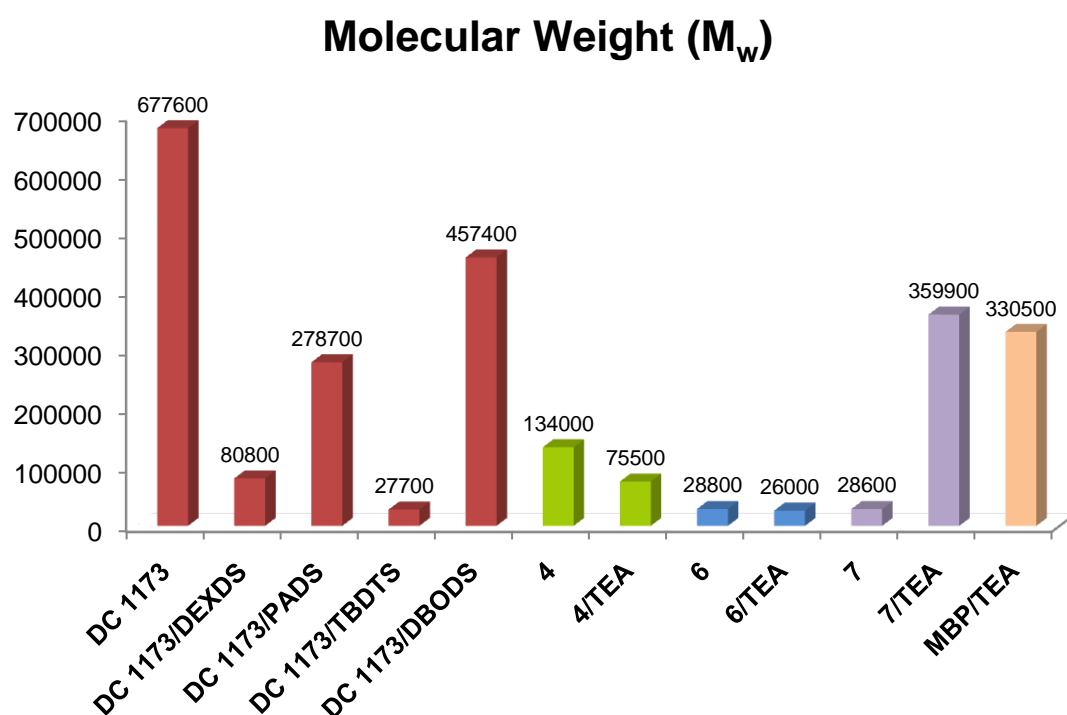


Figure 32. Comparison of molecular weight reduction by the use of CAs (**DEXDS**, **PADS**, **TBDTS**, **DBODS**) with a PI (Darocur 1173) and covalently bound PI/CA systems **4**, **6** and **7** with /without co-initiator (**TEA**)

As can be seen from Figure 32, a strong reduction of molecular weight could be found for **TBDTS**, when used as CA in combination with Darocur 1173 (DC 1173) as photoinitiator. This reflects also the results from the photo-DSC experiments, where a strongly reduced reactivity was found, although a high DBC of 88% was reached. Also the molecular weight dispersity (M_w/M_n) was reduced from 6.5 (Darocur 1173 without CA) to 2.8 (Figure 33). Like **TBDTS**, **DEXDS** showed remarkable reduction of the molecular weight. Of the covalently bound PI/CA systems the benzyl dithiocarbonate **6** exhibited the best results, with a MW reduction in the range of the DC 1173/**TBDTS** system and also a similar molecular weight dispersity of 2.8. The use of **TEA** as co-initiator did not lead to a significant change of the performance of **6**. In the case of **4** also a molecular weight reduction was found, nevertheless from photo-DSC experiments a poor DBC of only 55% had been detected, which indicated diminished efficiency of this PI. Nevertheless, use of **TEA** as co-initiator enhanced not only photoreactivity, but also the molecular weight reduction properties of **4**. Poorest performance was displayed by the benzoyl dithiocarbonate **7**, which suffered from low photoreactivity and low MW controlling ability. As DBC was only 26% in the GPC analysis also only low weight oligomers could be detected, simulating a reduction, which could be unmasked by the high molecular weight dispersity of 15.4. Although the initiation reactivity could be enhanced by the addition of **TEA** as co-initiator, this had no positive effects on the CA properties. Molecular weight and polydispersity displayed values in the range of common **MBP/TEA** PI system.

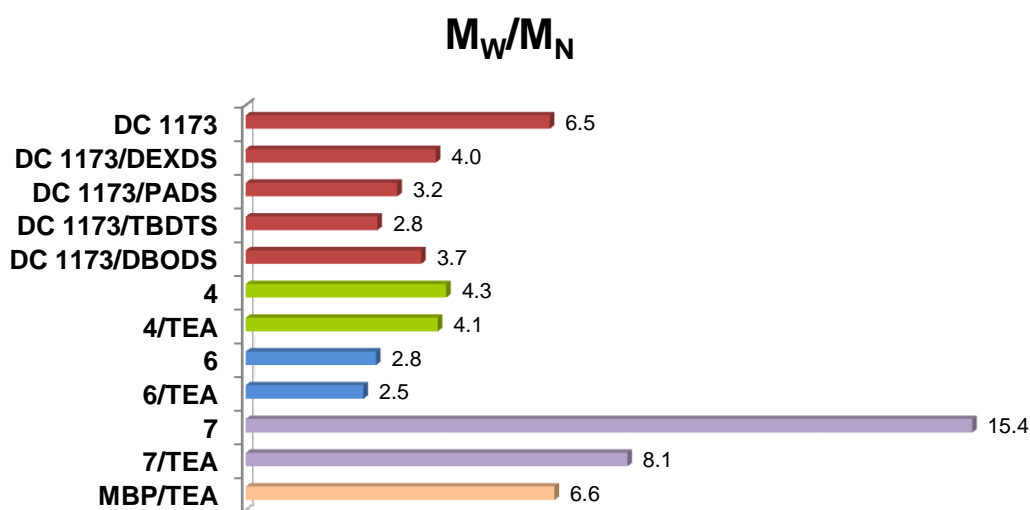


Figure 33. Molecular weight dispersity obtained by GPC analysis of the samples from photo-DSC experiments

1.2.4. Photo-CIDNP experiments

Chemically-induced-dynamic-nuclear-polarisation (CIDNP) is an ideal tool to follow radical pair reactions, as for example electron/proton transfer and bond cleavage.

The CIDNP effect can be detected by NMR spectroscopy as emission and not absorption – as usually – of radio waves. It occurs if radicals, that are produced during the NMR experiment, for example by irradiation with UV-light of the sample, recombine. Thus polarization of the nuclear spin is provoked, which is responsible for the CIDNP effect.

To identify UV-induced cleavage mechanisms of the newly synthesized oxime PI **20** and the disulfane **4** in comparison to the reference PIs with a proposed β -phenylogous cleavage mechanism, *N*-phenyl glycine derivative **2** and phenylsulfide **3**, photo-CIDNP analyses should be carried out.

The measurements and analyses were performed at the Institute of Physical and Theoretical Chemistry, Graz University of Technology (Austria) by Dipl. Ing. Markus Griesser.

1.2.4.1. Benzophenone-*N*-phenyl glycine ethyl ester (**2**)

The CIDNP spectrum of the ethyl ester **2** showed formation of the expected cage and escape products after β -phenylogous cleavage, which could be identified as 4-methyl benzophenone (**MBP**), the imine (**I**) and the dimers (**D1 and D2**).

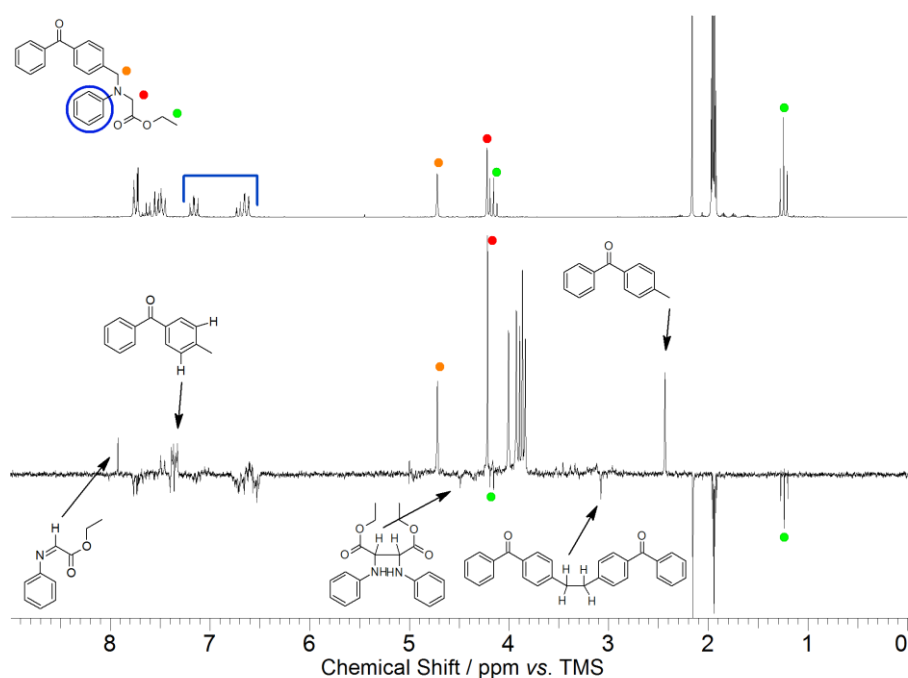
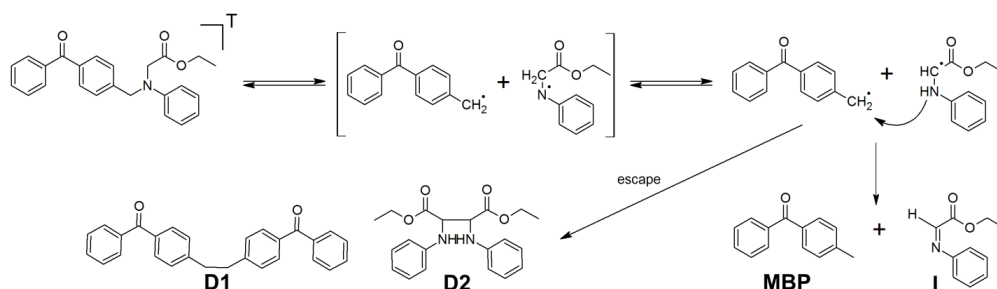


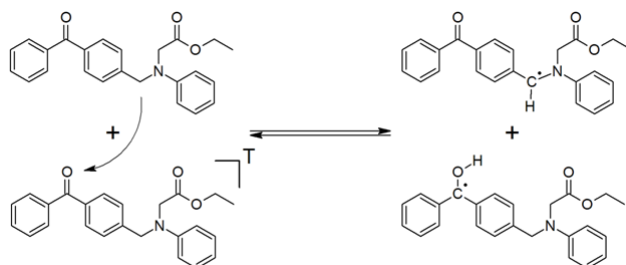
Figure 34. Photo-CIDNP spectrum of ethyl ester **2**

They resulted from the β -scission in the excited triplet state (Scheme 26). By this method the proposed β -phenylogous cleavage mechanism of **2** could be confirmed, analogous to phenylsulfide **3**, which had already been investigated by Yamaji *et al.*²⁷



Scheme 26. Cleavage mechanism for **2** from the excited triplet energy state

A general reaction of **2**, which had also been detected in the CIDNP spectra of **3** and **20**, is the reversible H-transfer between the excited triplet state and a second initiator molecule, that leads to strongly polarized parent signals (Scheme 27).



Scheme 27. Mechanism of the reversible H-transfer from the excited triplet state of **2**, that leads to stronger polarization of the protons attached to the benzophenone rings

Compound **3** reacted according to the same mechanism as the ethyl ester **2**. The corresponding photoproducts could be identified with one single difference: no disproportionation products could be identified due to the unavailability of easily abstractable hydrogen atoms.

1.2.4.2. (4-Phenyl)-O-phenylacetyl benzamidoxime (**20**)

As expected, no β -phenylogous cleavage mechanism could be detected by photo-CIDNP experiments of oxime **20**.

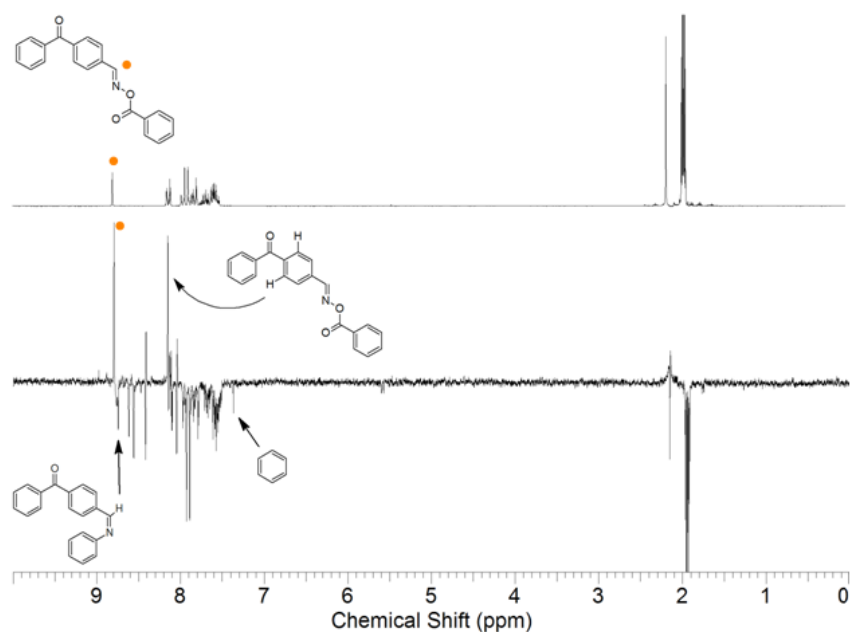
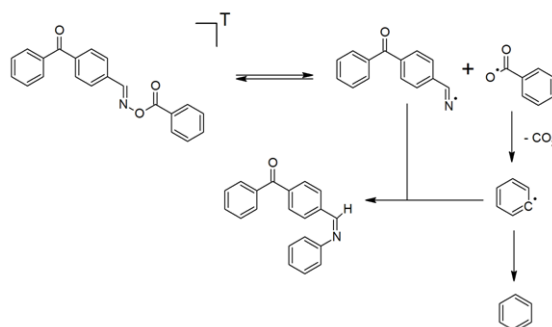


Figure 35. Photo-CIDNP spectrum of oxime **20**

Analysis of the photoproducts showed, that the cleavage occurs at the N-O bond of the oxime, followed by a decarboxylation step. Like for ethyl ester **2** and phenylsulfide **3**, polarizations originate from the reversible H-abstraction mechanism (Scheme 28).



Scheme 28. Products identified after UV-induced cleavage and decarboxylation of **20**

Photoproducts formed after cleavage and decarboxylation could be identified, as presented in Scheme 28. Probably, this decarboxylation reaction is partly responsible for the high reactivity of PI **20**. Furthermore, the iminyl radical has been found to be a very stable species and almost insensitive to oxygen.¹³⁰ Through the cleavage of the N-O bond a fast deactivation of the triplet state might occur, thus leading to a high amount of radicals in a very short time.¹³⁶ Lalevée and co-workers also proposed the participation of the singlet state besides the triplet state in the photodissociation process of O-acyl oximes, which might set an additional boost on radical generation.¹³⁰

1.2.4.3. Bis-[(4-methyl)-benzophenone] disulfane (**4**)

It was up to now not possible to identify all products in the CIDNP-spectrum (Figure 36), except a thio aldehyde, that is formed by H-transfer after scission of the disulfide bond.

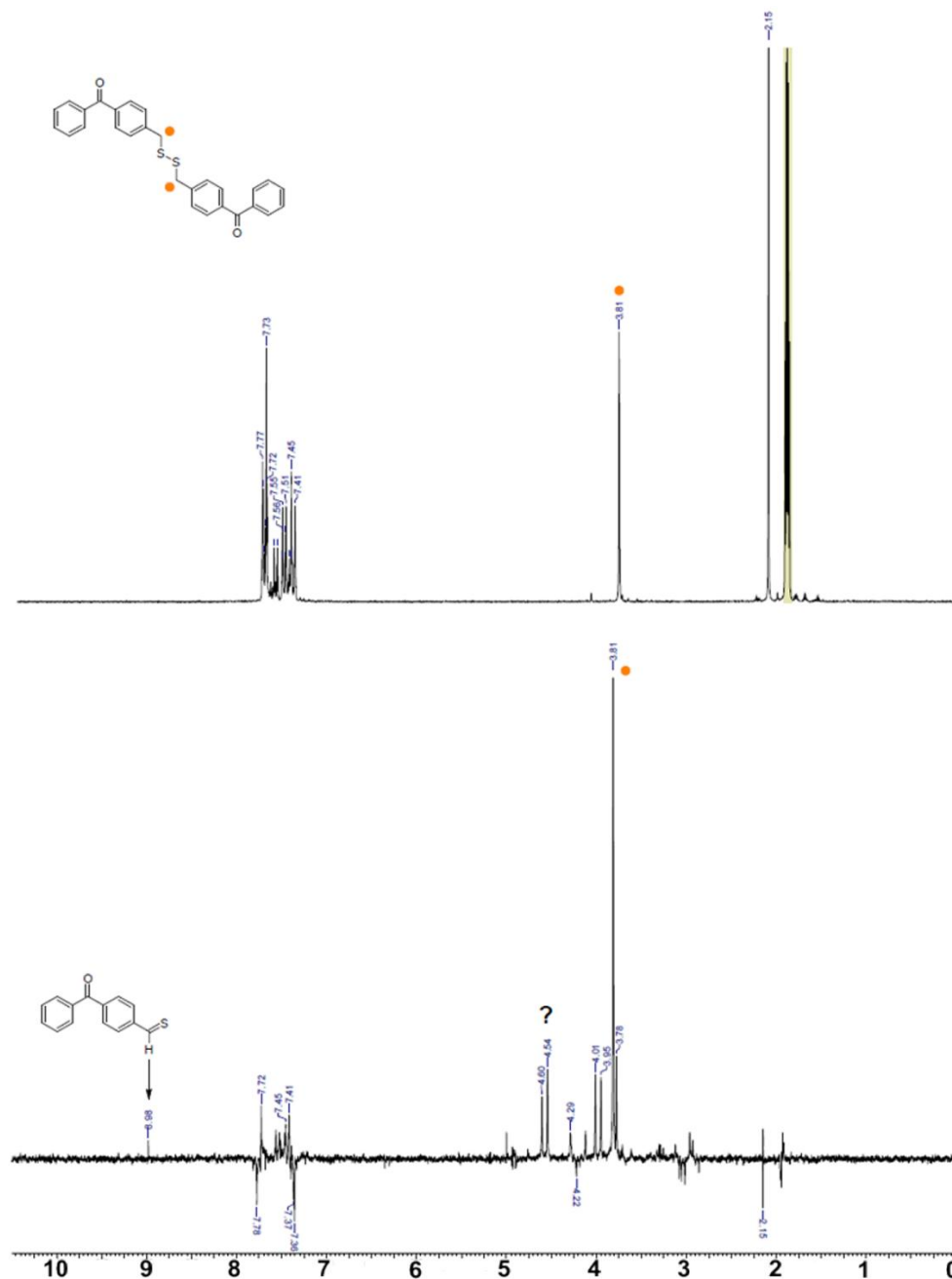


Figure 36. Photo-CIDNP spectrum of disulfane **4**

Besides, 4-methyl benzophenone and the benzophenone-dimer could be found in the product ¹H-NMR spectrum, but not in the CIDNP spectrum, which leads to the assumption, that these products were formed by a secondary, yet unknown, reaction.

2. Alternative Co-Initiators for Bimolecular PI Systems

Photoinitiator systems with a bimolecular radical generation process typically consist of an excitable chromophore and a tertiary amine as co-initiator.¹³⁷ Ketone-amine interactions proved to be highly efficient concerning radical formation by an electron transfer process. However, the yield of the primary photochemical process depends on more than the rate constant of electron transfer. Important parameters include ability for proton transfer, reactivity of the α -amino alkyl radical and quenching by side reactions.¹³⁸ Furthermore, the structure of the electron donating species (amine) turned out to play a crucial role as well. Aliphatic tertiary amines are more efficient co-initiators than secondary amines. Alkyl amines tended to be less efficient than the corresponding hydroxyalkyl amines. Besides, also studies on the use of anilines were performed by Valderas *et. al.*¹³⁹

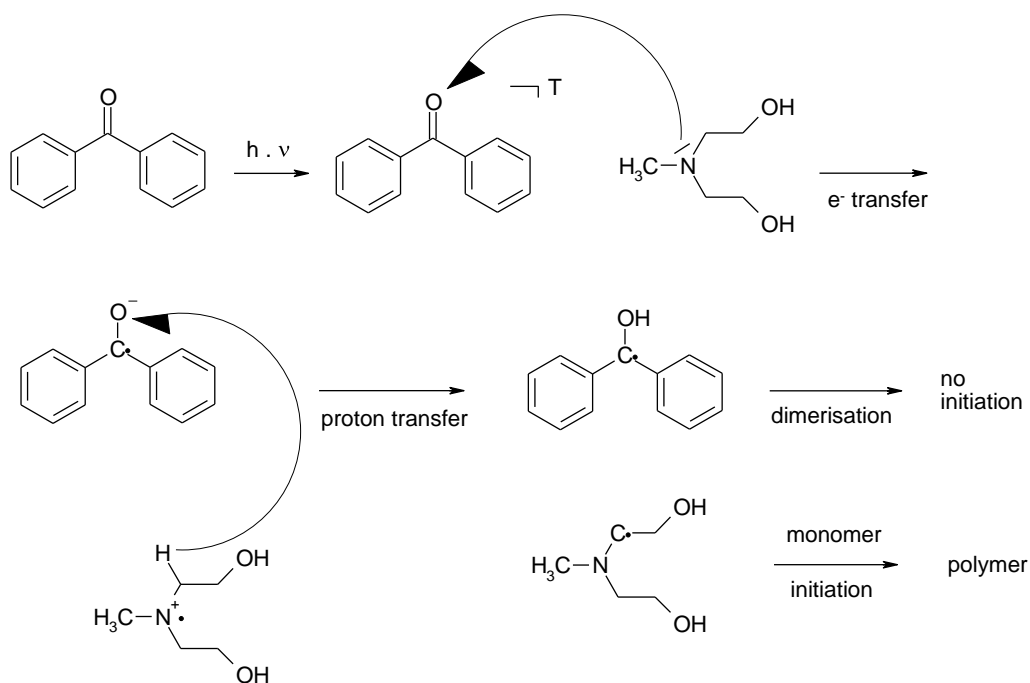


Figure 37. Photochemistry of BP based on hydrogen abstraction from e^- -rich alkyl amines¹³⁵

As one can see, the options for suitable co-initiators of aromatic ketones are rare. Apart from high reactivity, they should also display features like easy synthetic accessibility, storage stability, low volatility and they should not provoke undesired properties in the cured material like yellowing or bad odour.

Based on the high reactivity of the novel **BP**-derived *O*-benzoyl oxime PI **20**, which

was described in detail in chapter 1, an alternative concept for appropriate co-initiators of aromatic ketones should be investigated. Several reports on the use of different photosensitizers for *O*-acyl oximes, leading to high polymerization rates, were found in literature.^{140,141} Yoshida *et al.*¹⁴² described the nature of the triplet states for aromatic *O*-acyl oximes as presented in Figure 38.

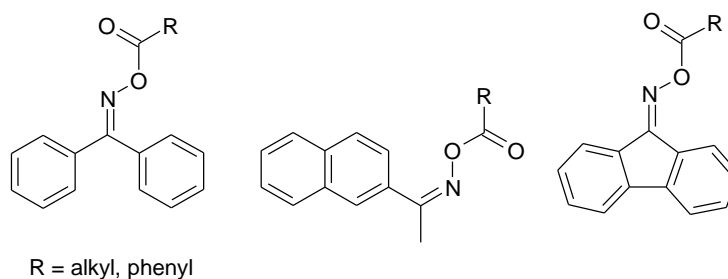
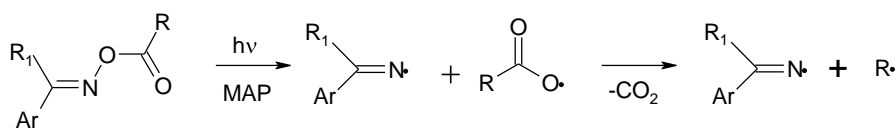


Figure 38. *O*-acyloximes examined by Yoshida *et al.*

The triplet state energies of the oximes ($E_T = 289\text{-}305 \text{ kJ mol}^{-1}$) are close to their parent ketones, displaying a $\pi\text{-}\pi^*$ character. Excitation energies are dissipated by cleavage of the N-O bond. Obviously, the triplet energy of the sensitizing compound plays a key role for the efficiency of the radical forming process. The efficiency of the energy transfer is lowered with lower triplet energy of the sensitizer. Better decomposition of the oxime can only be achieved for sensitizers with a higher triplet energy than the oxime itself.¹²⁷ Also McCarroll and Walton described the effective photolysis of aldoxime esters in presence of a sensitizer like 4-methoxyacetophenone (**MAP**) by ESR measurements and radical trapping experiments, thus presenting a new class of radical precursors for spectroscopic studies (Scheme 29).¹⁴¹



Scheme 29. UV-induced **MAP** sensitized decomposition of aldoximes

Therefore, to characterize possible co-initiating features of the oxime moiety with the adjacent benzophenone as in compound **20** and to compare its surprisingly high reactivity with a physical mixture of 4-methyl benzophenone and a corresponding benzaldoxime, *O*-benzoyl benzaldoxime ester (**22**) should be synthesized. Photo-DSC experiments should help to characterize the nature of the excellent efficiency of

20. To determine influence of the *O*-acyl group, also the acetyl and the methacryloyl derivatives, **23** and **24** should be prepared.

With respect to the good results of dithiocarbonate **6** as combined PI and molecular weight control agent, also a physical mixture of 4-methyl benzophenone with benzyl thiocarbonate **25** was examined by photo-DSC experiments and GPC analysis, which was of interest due to possible reduction of molecular weight.

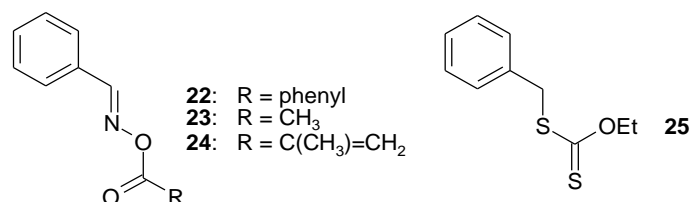


Figure 39. Structures of the investigated coin initiators for **MBP**

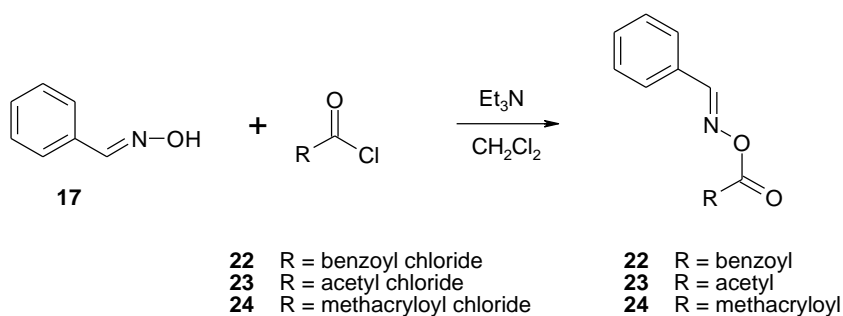
2.1. Synthesis

2.1.1. Syntheses of benzaloxime esters **22**, **23** and **24**

For the preparation of the benzaloxime esters **22**, **23** and **24** benzaloxime (**17**) should serve as starting material.

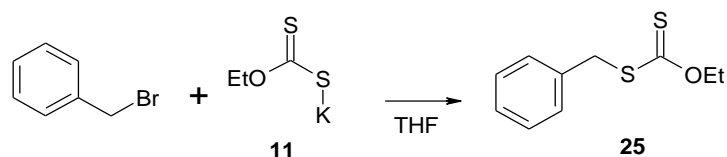
Oxime **17** was prepared according to the procedure already described in chapter 1.1.3.

Formation of oxime esters was performed as already described in chapter 1.1.1.6. for compound **20**, using benzaloxime as starting material and 1.5 equ. of benzoyl chloride for **22**, 1.5 equ. of acetyl chloride for **23** and 1.5 equ. of methacryloyl chloride for the formation of **24**. The pure products could be isolated after column chromatography in 33-58% yield.



2.1.2. S-Benzyl-O-ethyl dithiocarbonate (25)

The synthesis of S-benzyl-O-ethyl dithiocarbonate (**25**) has already been described in literature.^{107,108}



It was performed similar to the preparation of compound **6**, starting from benzyl bromide. Benzyl bromide was preferred as reagent to benzyl chloride, due to less toxicity. The product **25** could be obtained in 57% yield after vacuum distillation as slightly yellow liquid.

2.2. Analyses

The investigation on the photochemical properties of the synthesized co-initiators should be carried out as measurements with single components and as physical mixtures with 4-methyl benzophenone by UV-Vis analysis and photo-differential scanning calorimetry (photo-DSC). Besides, special investigations would be necessary on the use of the thiocompound **25** as control agent for molecular weight distribution by GPC analysis.

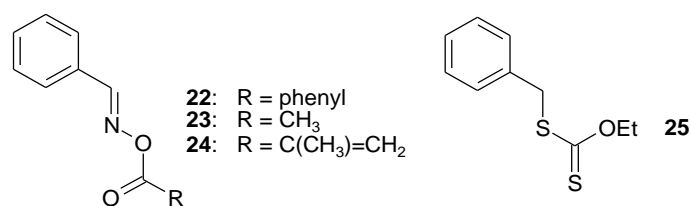


Figure 40. Structures of the investigated co-initiators

2.2.1. UV-Vis spectroscopy

The UV-Vis absorption behavior of the oximes **22-24** should be investigated in comparison to their physical mixtures with **MBP**, **BP** alone and the covalently bound oxime **20**. The UV-Vis absorption behavior of dithiocarbonate **25** should be examined in comparison to its physical mixture with **MBP**, **BP** alone and the covalently **BP**-bound dithiocarbonate **6**. The analyses were conducted in acetonitrile solutions of 1×10^{-2} M to 1×10^{-5} M concentration.

2.2.1.1. Benzaldoxime esters **22**, **23** and **24**

The results from the UV-Vis analyses of the oximes **22**, **23** and **24** and the references are presented in Figure 41 and Table 8.

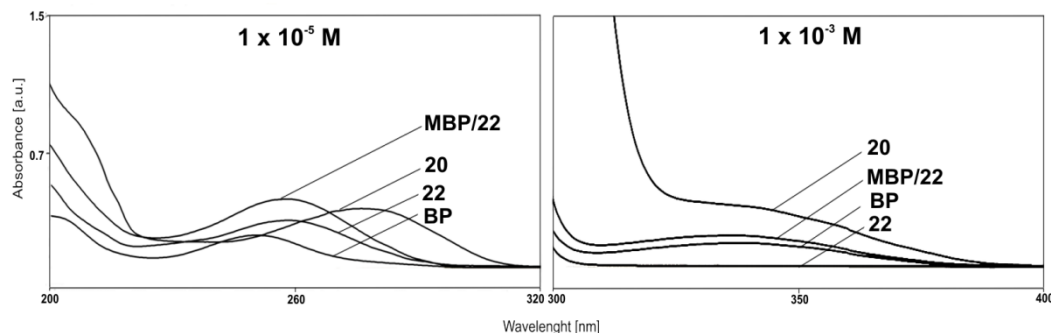


Figure 41. UV-Vis spectra of oxime **22** with/without **MBP** in comparison to references **BP** and **20**

Table 8. UV-Vis data for oximes **22**, **23**, **24**, the mixture **22/MBP** and the references, **20** and **BP**

PI	$\pi-\pi^*$ transition		$n-\pi^*$ transition	
	λ_{\max} [nm]	$\epsilon_{\max} \times 10^{-3}$ [L mol ⁻¹ cm ⁻¹]	λ_{\max} [nm]	$\epsilon_{\max} \times 10^{-3}$ [L mol ⁻¹ cm ⁻¹]
22	259	28.6	-	-
23	253	19.2	-	-
24	256	16.4	-	-
MBP/22	258	41.3	336	0.19
20	276	35.6	339	0.37
BP	250	19.7	339	0.14

Comparison of the UV-Vis spectra of the physical mixture of oxime **22** with **MBP** and BP-oxime **20** displayed a strong bathochromic shift of the wavelength of about 17 nm for the covalently bound system due to a larger conjugated system of **20**. The extinction coefficient (ϵ) was higher in the physical mixture, probably caused by the presence of the additional chromophore (benzophenone and the conjugated system of benzaldoxime). For the O-benzoyl oxime **22** alone the maximum of the $\pi-\pi^*$ transition was located at the same wavelength as for the physical mixture, ϵ was about a third lower in absence of **MBP**. The other two oximes, **23** and **24**, showed almost the same absorption behavior as **22**, only the extinction coefficient for the

$\pi-\pi^*$ transition was a little bit decreased due to the absence of one phenyl group. The contribution to the $n-\pi^*$ transition in **20** seemed to evolve almost exclusively from the **MBP** part, as there were no indications for a absorption maximum in the range of 300 to 400 nm for the single oximes **22**, **23** and **24**. In the physical mixture of **22** and **MBP** the $n-\pi^*$ transition showed almost the same trend as in **BP** alone.

2.2.1.2. *S*-Benzyl-*O*-ethyl dithiocarbonate (**25**)

The results from the UV-Vis analyses of **25**, a physical mixture of **25** and **MBP** and the reference materials are shown in Figure 42 and Table 9.

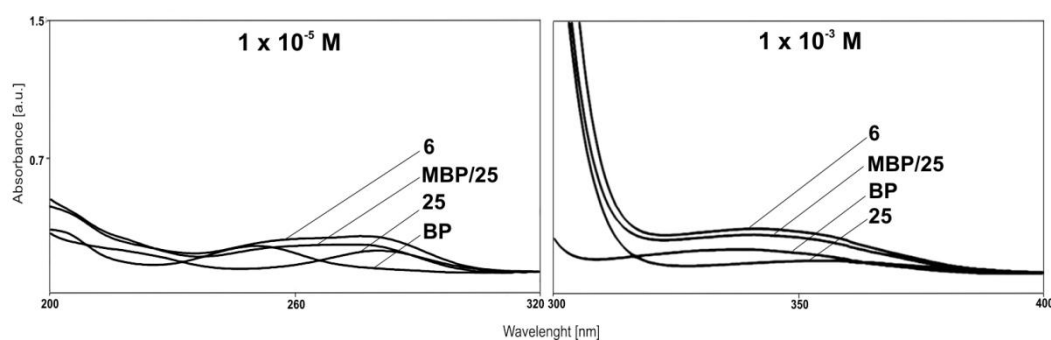


Figure 42. UV/Vis spectra of dithiocarbonate **25** with/without **MBP** in comparison to references **BP** and **6**

Table 9. UV-Vis data for dithiocarbonate **25**, its mixture with **MBP** and the references, **6** and **BP**

PI	$\pi-\pi^*$ transition		$n-\pi^*$ transition	
	λ_{\max} [nm]	$\epsilon_{\max} \times 10^{-3}$ [L mol ⁻¹ cm ⁻¹]	λ_{\max} [nm]	$\epsilon_{\max} \times 10^{-3}$ [L mol ⁻¹ cm ⁻¹]
25	280	16.3	355	0.07
MBP/24	275	20.7	341	0.23
6	276	26.8	342	0.26
BP	250	19.7	339	0.14

The physical mixture of **25** with **MBP** displayed a similar absorption behavior as the corresponding covalently bound compound **6** with almost identical ϵ values. From the UV-Vis spectra in Figure 42 it is obvious, that both $\pi-\pi^*$ transitions of **6** and the physical mixture of **25** with **MBP** result from an addition of the absorption maxima from the single components. In the region of the $n-\pi^*$ transitions only a weak absorption maximum at 355 nm was found for dithiocarbonate **25**.

2.2.2. Photo-DSC

The photoreactivity of the novel co-initiating oximes **22**, **23** and **24** in equimolar mixtures with **MBP** should be compared to the covalent bound **BP**-oxime **20**, as well as industrially applied mixture **BP/TEA** and Type I PI, Darocur 1173. Additionally, two commercially available oximes, acetoxime benzoate (**AB**) and *p*-dibenzoylquinone dioxime (**DBQD**) would be tested as single component PIs and in their physical mixtures as co-initiators with **MBP** to gain information on possible structural preferences for highly efficient co-initiating oximes. Photoinitiation behaviour of **AB** had already been investigated by Hong and co-workers,¹⁴³ but they reported no photoinitiating activity of this compound. However, they did not use any mixtures with photosensitizers as e.g. benzophenone. **DBQD** finds industrial application as crosslinking additive in rubber vulcanization technology.¹⁴⁴ No indications on its use in photopolymerization had been found in literature up to now. For *O*-benzoyl oxime **22** additional experiments with another common Type II PI, **CQ**, aimed at the evaluation of different ketones as suitable initiators for oximes.

Measurements were carried out in hexane-1,6-diol diacrylate (**HDDA**) under nitrogen atmosphere with a PI concentration of 12.1 mmol L⁻¹. UV-light in the range of 280 – 450 nm with an intensity of 3000 mW cm⁻² at the tip of the light guide was applied.

In a second series it was intended to test the ability of co-initiator **25** for molecular weight control in radical photopolymerization. Experiments with **25** alone and **25** with **MBP** should be carried out and compared with measurements of covalently bound **BP**-dithiocarbonate **6** and industrially applied PI system **BP/TEA**.

As monomer *N*-acryloyl morpholine (**NAM**) was used, which delivered a water soluble polymer, suitable for subsequent GPC analysis of the photo-DSC samples. PI concentration in the equimolar formulations was 12.1 mmol L⁻¹.

2.2.2.1. Benzaldoxime esters **22**, **23** and **24**

The structures of the investigated PIs and references are shown in Figure 43.

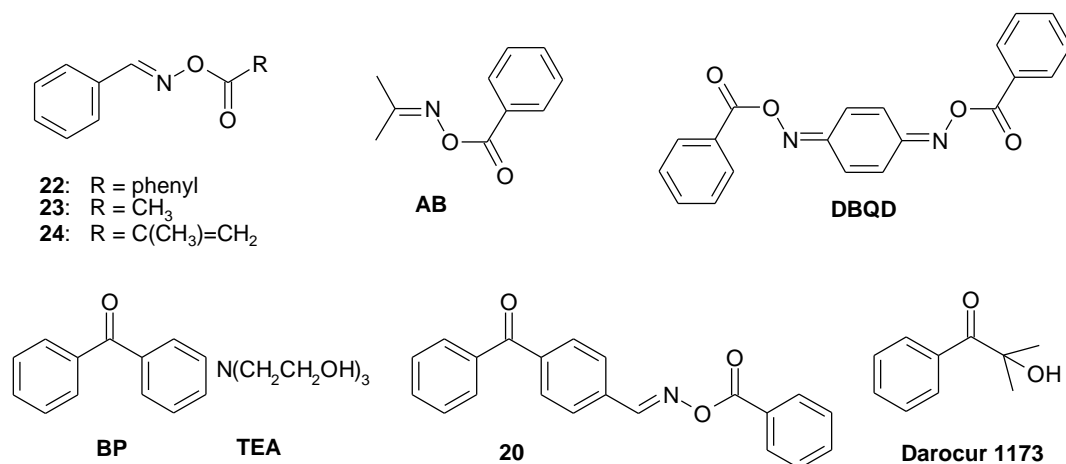


Figure 43. Structures of the investigated PIs

First, the coinitiators **22**, **23** and **24** as well as the reference oximes, **AB** and **DBQD** were tested for PI activity as single components. Unfortunately, the performance of these formulations was very poor. The measurements were characterized by very high t_{\max} (38-204 s), low polymerization rates and low conversions of 40-67%. Reference **DBQD** could not be analysed due to poor solubility in **HDDA**.

Additionally to the experiments without co-initiator, also formulations containing each an oxime (**22**, **23** or **24**) and equimolar amounts of **MBP** were tested. Photo-DSC plots in Figure 44 and the data in Table 10 show the results of these measurements.

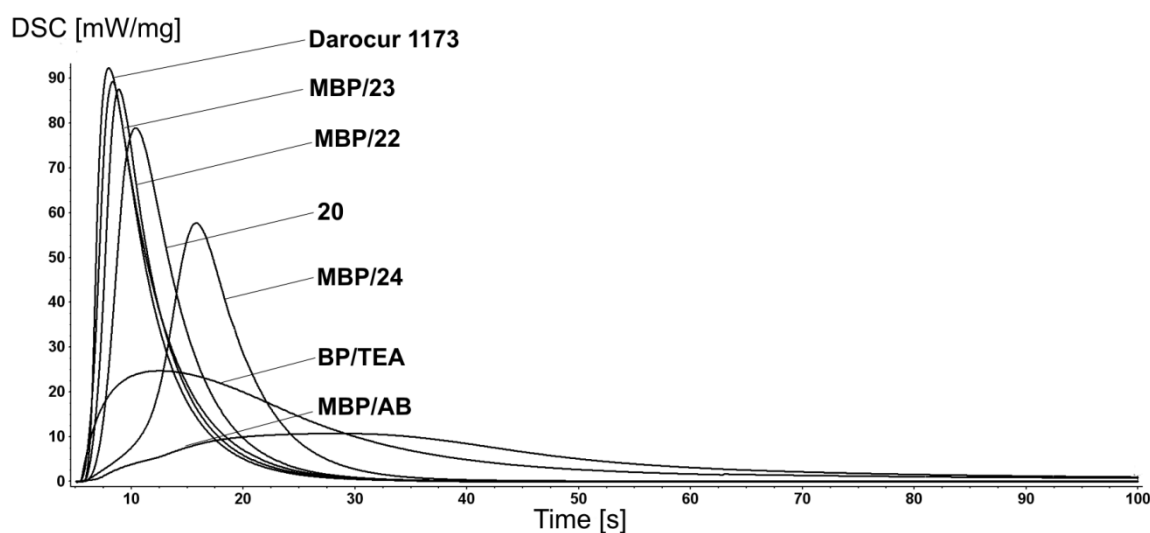


Figure 44. Photo-DSC plots for the oximes **22**, **23**, **24** and **AB** as co-initiators for **MBP** and reference PIs Darocur 1173, **BP/TEA** and oxime **20**

Table 10. Photo-DSC data for **HDDA** with oximes **22, 23, 24, AB, DBQD** as co-initiators of **MBP** compared to oxime **20** and industrially applied PIs **BP/TEA** and Darocur 1173

PI	t_{\max} [s]	DBC [%]	$R_{P\max} \times 10^3$ [mol L ⁻¹ s ⁻¹]
MBP/22	3.0	77	599
MBP/23	2.4	78	610
MBP/24	10.1	76	394
MBP/AB	22.7	66	70.4
MBP/DBQD	25.4	66	77.8
20	4.6	86	540
BP/TEA	7.1	89	165
Darocur 1173	2.0	87	632

Surprisingly, the mixtures of oximes **22** and **23** with **MBP** superseded the industrially applied benzophenone-amine system **BP/TEA** by far and were in the same order of reactivity as highly reactive Type I PI, Darocur 1173. Interestingly, the physical mixture of **22** and **MBP** was even better than the covalently bound corresponding **BP**-oxime **20**. The spatial arrangement of **MBP** and its co-initiator seems to play a minor role in the radical forming process, as the smaller radical of **22** could move much faster through the growing polymer than the comparably huge covalent bound **BP**-oxime **20**. The mixture of **24** with **MBP** was less reactive than the other two, probably due to co-polymerization of the methacrylate moiety and the increased stability of the methacryloyl radical with its larger conjugated system. The mixtures of the commercially available oximes acetoxime benzoate and p-dibenzoylquinone dioxime, were the least reactive, even less than **BP/TEA**. As their photo-DSC plots are almost similar, only the plot of **MBP/AB** is shown. Their poor efficiency led to the conclusion, that for highly reactive co-initiating oximes a benzaldoxime related structure is necessary, as in oximes **22-24**. The nature of the acyl residue played a minor part. The only limitation seemed to be a co-polymerizable group, which led to delayed t_{\max} values due to co-polymerization effects.

For comparison camphorquinone as another ketone was used. Equimolar mixtures of **22** and **CQ** were compared to industrially applied mixture **CQ/DMAB** and **CQ** alone. Unfortunately, using **CQ** as PI, **22** showed only very low co-initiating reactivity with high t_{\max} values of 40 s and low polymerization rates, two times lower than for **CQ/DMAB** as PI system. This favored the results from Yoshida's study,¹⁴² that the

triplet of the ketone played a key role for the decomposition of the *O*-acyl oxime ($E_T \sim 289\text{-}305 \text{ kJ mol}^{-1}$). If the triplet energy of the ketone was lower than that of the oxime, almost no radicals were formed. This would be the case for **CQ** with a $E_T(p)$ of 216 kJ mol^{-1} , whereas **BP** has a much higher $E_T(p)$ of 289 kJ mol^{-1} .¹⁴⁵

2.2.2.2. *S*-Benzyl-*O*-ethyl dithiocarbonate (**25**)

The photoreactivity of dithiocarbonate **6** was compared to its physical mixture of benzyl dithiocarbonate **25** and **MBP**. For comparison **25** was also measured as single component, as it was already known from literature, that it can act as a photoinitiator alone.¹⁴⁶ Another reference was the industrially applied PI system **BP/TEA** and also an equimolar mixture of dibenzyl disulfide (**DBDS**), which might also own molecular weight controlling properties as the covalent bound disulfane **4**.

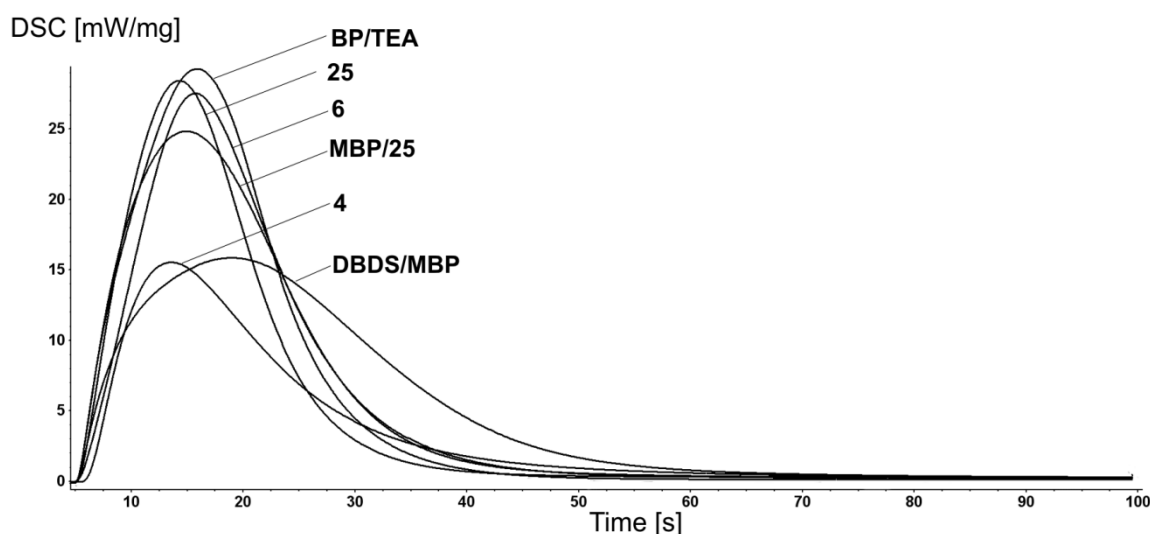


Figure 45. Photo-DSC plots for the dithiocarbonate **25** as single component and in equimolar mixture with **MBP**, compared to covalent bound corresponding compound **6**, **BP/TEA**, disulfane **4** and mixture of **DBDS** with **MBP**

Table 11. Photo-DSC data for **NAM** containing dithiocarbonate **25**, with/without **MBP** in comparison to **6**, disulfane **4** and **DBDS/MBP** as PI

PI	t_{\max} [s]	DBC [%]	$R_{P\max} \times 10^3$ [mol L ⁻¹ s ⁻¹]
MBP/24	9.9	87	379
MBP/DBDS	13.9	84	241
25	9.2	81	437
6	10.5	85	420
4	8.2	55	236
BP/TEA	10.8	91	450

Surprisingly, the results of the photo-DSC measurements as outlined in Figure 45 and Table 11 showed for dithiocarbonate **25** alone already very good photoinitiator performance, comparable to industrial applied Type II PI, **BP/TEA**. It turned out, that the use of **MBP** as co-initiator for **25** was not favourable, independent if it was a physical mixture or covalently bound as in **6**. Assumably, the presence of the aromatic keton provoked some quenching effect on the dithiocarbonate. Nevertheless, all three models are in the same order of reactivity as the industrial used mixture, **BP/TEA**. The physical mixture of **DBDS** and **MBP** displayed the least reactivity, although a good DBC of 83% was reached. The samples from the photo-DSC experiments were directly used for GPC analysis.

2.2.3. GPC analysis

To evaluate the efficiency of the co-initiating CAs **25** and **DBDS** in comparison to the photoinitiating CAs, **4** and **6**, the samples from the photo-DSC experiments were directly used for GPC analysis. The polymer disks were dissolved in 1.5 mL of eluent and filtered through a polyamide filter. As eluent an aqueous Na_2SO_4 solution (0.05 M) containing 20 v% of acetonitrile, was used. The GPC analyses were performed with a flow rate of 0.6 mL min^{-1} at 40°C , using two Ultrahydrogel columns (250 and 1000), a Viscotek VE3580 RI detector and polyvinylalcohol standards for calibration. The results from the GPC measurements, displaying M_n and the polymer dispersity M_w/M_n are displayed in Figures 46 and 47.

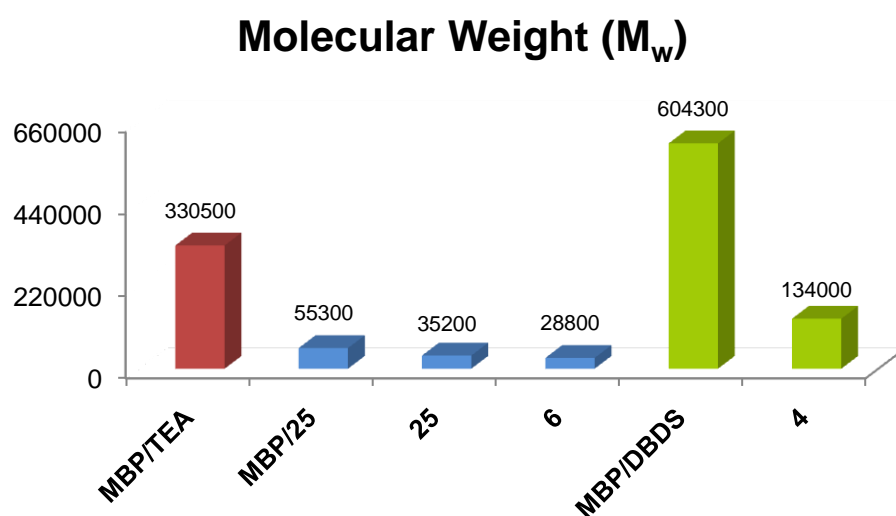


Figure 46. Comparison of molecular weight reduction by the use of **25** as CA for **MBP**, **25** alone and covalently bound PI/CA systems **4**, **6** to industrially applied PI system **BP/TEA**

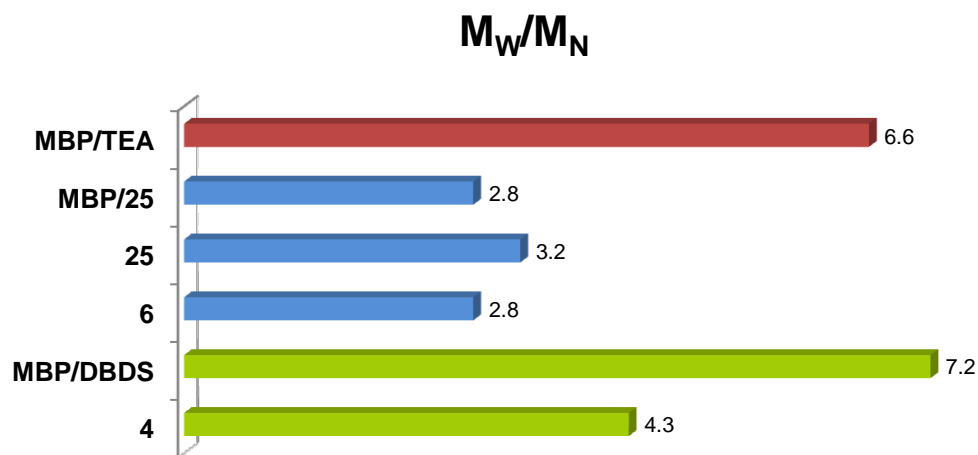
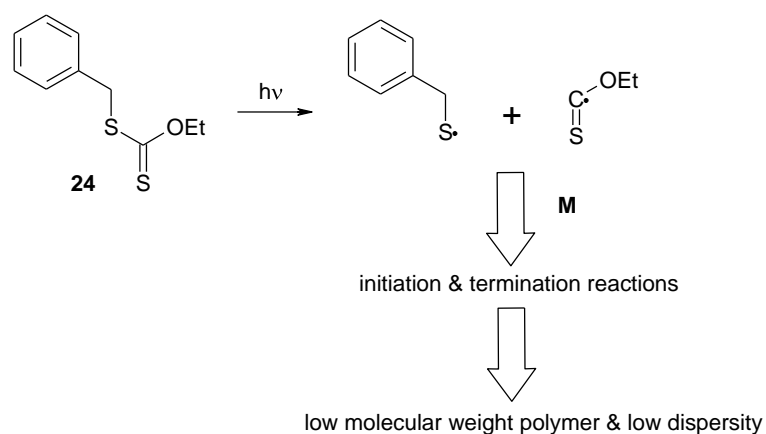


Figure 47. Molecular weight dispersity obtained by GPC analysis of the samples from photo-DSC experiments for **MBP/TEA**, **MBP/25**, **25**, **4**, **6**, **MBP/DBDS**

The results from the GPC analysis of the photo-DSC samples presented in Figure 46 show, that the physical mixture of **MBP/25** was also able to reduce molecular weight during radical photopolymerization. However, the PI reactivity of **BP/TEA** and **MBP/25** was in the same order of magnitude, as could be derived from the photo-DSC experiments. **25** as single PI reduced the molecular weight stronger than the physical mixture with **MBP**, although molecular weight dispersity (Figure 47) was higher by 0.4 units. The strongest reduction could be seen in the covalent bound **BP**-thiocarbonate **6**. The regulation of molecular weight assumedly was caused by the *O*-ethyl-dithiyl radical, which was formed by homolytic scission of the S-C=S bond, that had already been reported by Okawara *et al.* (Scheme 30).¹⁴⁶



Scheme 30. Proposed photodissociation mechanism of dithiocarbonate **25**

Their studies revealed, that the chain transfer mechanism is based on the reaction of a growing polymer radical and a molecule of **25** in the excited state. If **25** was not in the excited state, then no chain transfer could take place. This could be confirmed by photo-DSC experiments of **25** with filtered UV light of 400-500 nm wavelength using camphorquinone as chromophore. In this range of the UV-Vis spectrum no excitation of dithiocarbonate **25** was possible and therefore almost no molecular weight regulating effect had been detected.

Interestingly, Ajayaghosh and co-workers proposed, that **25** could not be decomposed at monochromatic UV-light of 350 nm and therefore could not be used as photoiniferter,¹⁴⁷ although during this work a weak absorption maximum at 355 nm had been identified in the UV-Vis spectrum of **25** (see chapter 2.2.1.2.). However, under irradiation with broad UV-light (280-450 nm) **25** exhibited good reactivity as PI and as co-initiator. Also a good molecular weight regulating efficiency was detected. No molecular weight regulation could be detected in the physical mixture of **MBP** with **DBDS**, only for the covalent bound **BP** analogous disulfane **4** a slight reducing effect was visible compared to well-known PI mixture **BP/TEA**.

3. Photoinitiating Monomers based on Di- and Triacylated Hydroxylamine Derivatives¹⁴⁸

The photochemically labile N–O group in hydroxylamine⁹² seemed a powerful functional tool, that would start the free radical process after the photochemical cleavage. Searching for an appropriate monomer part of the molecule, the choice was made for acrylates, as methacrylates had proven to give poor results in initial photo-differential scanning calorimetry (photo-DSC) experiments.¹⁴⁹ Another point of interest was the influence of variable substituents to the nitrogen atom on the polymerization performance. In previous studies, the *N*-methyl hydroxylamine compound **27** showed good performance with 2wt % of photoinitiator (Darocur 1173).¹⁴⁹ Therefore derivatives with different *N*-alkyl-residues R and finally also a triacylated hydroxylamine compound as shown in Figure 48 should be prepared.

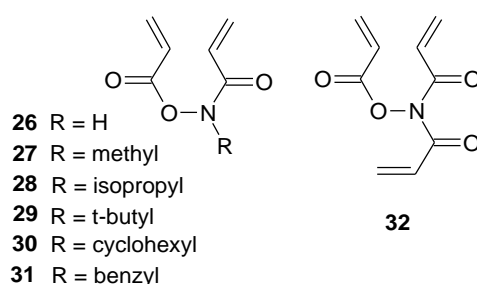


Figure 48. Chemical structures of the photoinitiating monomers **26-32**

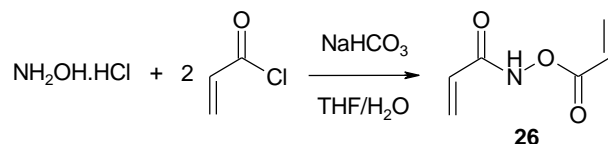
UV-Vis spectroscopy should be applied for the characterization of the compounds. The evaluation of the photochemical properties can be carried out by photo-differential scanning calorimetry (photo-DSC) and ATR-IR spectroscopy. A method to derive the double bond conversion from the IR spectra of the monomers and the cured polymers¹⁵⁰ should be adapted to calculate approximate values of the theoretical polymerization heats of the hydroxylamine compounds.

3.1. Synthesis

According to literature^{151,152} there are several ways to obtain di- and triacylated hydroxylamines. For example, by adding an excess of aliphatic acid anhydrides to hydroxylamine¹⁵³, or by using acyl chlorides and a base (alkali hydroxide, -carbonate, or -acetate) as per Schotten-Baumann conditions^{154,155,156} Preparation of benzylated

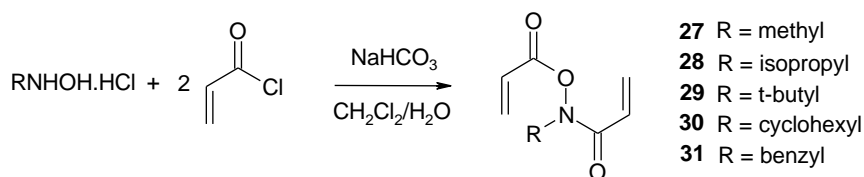
compound **31** had already been mentioned by Miyata *et al.*¹⁵⁷ as intermediate in amino acid synthesis.

In the current study, the diacylated hydroxylamine **26**¹⁵⁸ was prepared from hydroxylamine hydrochloride salt and 2 mol equivalents of acryloyl chloride in an aqueous THF solution at 0°C, using sodium hydrogencarbonate as base.



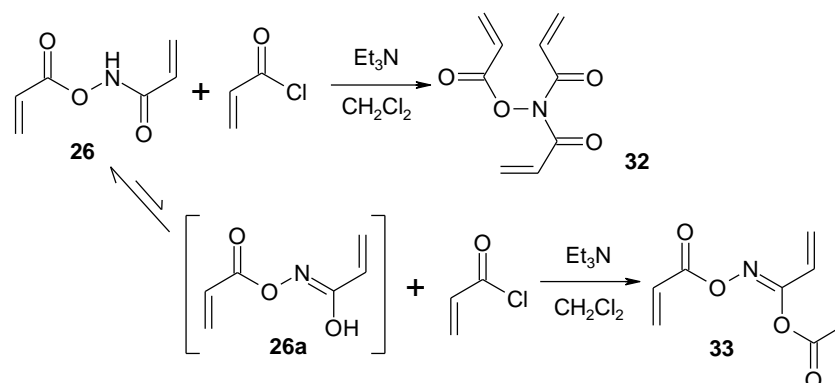
For this reaction THF was the preferred solvent due to its good miscibility with water. Other, not water miscible solvents, gave lower yield of product due to enhanced formation of the triacylated hydroxylamine **32**. The reason for this solvent effect might be the hydrophilicity of the hydroxylamine molecule, that leaves it preferably in the aqueous layer, whereas the acyl chloride and the diacylated product remain in the organic layer. After purification by column chromatography, **26** was obtained in 82% yield.

For the diacylated hydroxylamines **27-31** the corresponding alkylated hydroxylamine hydrochloride salts, were used as starting materials.



They were treated in aqueous CH₂Cl₂ with 2.2 equivalents of acryloyl chloride at 0°C, using sodium bicarbonate as base. CH₂Cl₂ proved to be the preferred solvent, as in case of the alkylated hydroxylamines no triacylation could take place. The first step, which is the acylation on the nitrogen atom¹⁵⁹ occurred according to TLC monitoring quite fast, whereas the second step, the acylation on the O-atom, determined the length of the reaction time. For the sterically hindered derivatives **29**, **30** and **31** one more equivalent of acryloyl chloride were added in the course of the reaction to ensure full conversion of the starting material. The products were obtained in yields of 60-80% after purification by column chromatography.

For preparation of the triacylated hydroxylamine **32**, diacrylate **26** served as precursor.



Again under Schotten-Baumann conditions, **26** was converted with 1.5 equ of acryloyl chloride in the presence of 1.5 equ of triethylamine in dry CH₂Cl₂ to give **32** in 28% yield. Henecka *et al.*¹⁵¹ described also the formation of the tautomer (1Z)-N-(acryloyloxy) prop-2-enimidic acid (**26a**). The tautomers could not be separated, but several derivatives of the oxime tautomer were identified in literature.^{160,161} Nevertheless, in the preparation of the triacylated hydroxylamine **32**, where **26** was used as a precursor, the corresponding O-acylated oxime **33** was obtained as a by-product in 16% yield. Unfortunately it exhibited no remarkable photochemical activity and therefore will not be discussed any further.

The purity of all new synthesized compounds was confirmed by reversed phase HPLC and GC/MS analysis.

3.2. Analyses

3.2.1. UV-Vis spectroscopy

UV-Vis spectroscopy (1×10^{-4} mol L⁻¹ in MeOH) was carried out to investigate the absorption behaviour of the hydroxylamine based acrylates **26-32**, each one containing an acrylamide and an acrylic ester group. Therefore, typical representatives for each functionality were used for comparison. For the acryl group, laurylacrylate (**LA**) was used as a reference; the model compounds for the amide group were *N,N*-dimethyl acrylamide (**DMAA**) and *N*-propylacrylamide (**PAA**). **DMAA** and **PAA** exhibited a clear maximum at 238 nm, respectively 226 nm, with extinction coefficients (ϵ) of 4.53×10^{-3} L mol⁻¹·cm⁻¹ and 5.25×10^{-3} L mol⁻¹·cm⁻¹, whereas

detectable absorption for the reference acrylate, **LA**, started not till a concentration of $10^{-2} \text{ mol L}^{-1}$, as presented in the inserted window of Figure 49.

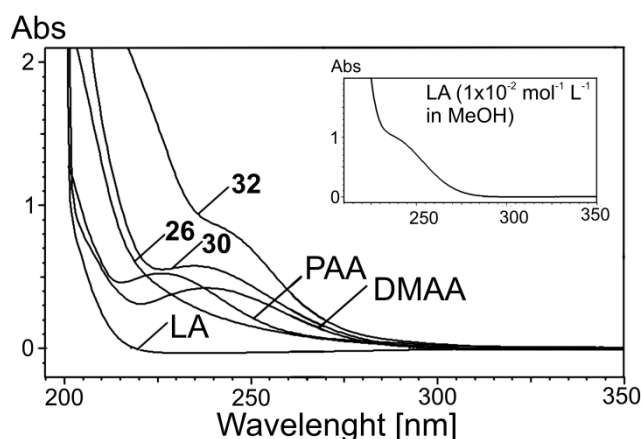


Figure 49. UV spectra of **26**, **30**, **32**, **DMAA** and **LA** at 10^{-4} M L^{-1} ; insert of the UV-spectrum of **LA** at a concentration of 10^{-2} M L^{-1}

All alkylated hydroxylamine derivatives showed very similar absorption patterns. Therefore, Figure 49 compares non-alkylated diacyl-hydroxylamine **26**, alkylated diacyl-hydroxylamine **30** and triacylated hydroxylamine **32**. The spectra of the hydroxylamine based acrylates had shoulders with no clear absorption maximum in the range of 330 nm to 220 nm. Obviously, stronger red-shifted UV absorption was favoured by the presence of an alkyl or a third acyl group on the nitrogen atom in contrast to the non-alkylated diacyl-hydroxylamine, which exhibited only a very weak absorption. **PAA** exhibited a similar red-shift compared to **DMAA**, which might be explained by the formation of hydrogen bridges. Surprisingly, no significant influence of the benzyl group in the UV spectrum of compound **30** was detected in comparison with the other hydroxylamine derivatives. The stronger absorption of compound **32** resulted from the presence of one additional acrylate group on the nitrogen atom. All UV-Vis absorption spectra were also measured in MeCN. No significant wavelength shift from the protic to the aprotic solvent could be identified. Therefore, in agreement with the literature¹⁶² and due to the high extinction coefficient of $\sim 5 \cdot 10^3 \text{ L mol}^{-1} \text{ cm}^{-1}$, the shoulders should be assigned to a $\pi\text{-}\pi^*$ transition.

3.2.2. ATR-IR analysis

For the evaluation of the photoreactivity of the new compounds as a monomer it is essential to know the theoretical heat of polymerization ($\Delta H_{0,p}$). A well established method⁵⁰ to determine this value is to cure monomer formulations by photo-DSC that

gives the actual heat of polymerization (H_P) evolved under these conditions. In combination with the DBC obtained from ATR-IR analysis of this sample it is possible to calculate the $\Delta H_{0,P}$ following equation 1, where M_M (g mol^{-1}) is the molecular weight of the monomer.

$$\Delta H_{0,P} = \frac{H_P \times M_M}{DBC} \quad \text{Equation 1}$$

For all hydroxylamine based acrylates **26-32** ATR-IR spectra of the monomers and of the UV-cured polymer specimen from photo-DSC experiments were measured (example given in Figure 50). The liquid monomer samples were placed directly onto the crystal layer of the ATR-IR instrument. The solid polymer lenses were pressed onto the crystal by the “Golden Gate” attachment. Both sides of the polymer lenses were measured and as photocuring was performed under a nitrogen atmosphere only negligible differences were observed. Compounds **26-32** showed similar absorption patterns and no major change of wavenumbers for the characteristic bonds, C=O (1775 cm^{-1} , 1750 cm^{-1}) and C=C (1665 cm^{-1} , 1625 cm^{-1} and 800 cm^{-1} , 780 cm^{-1}), could be detected.

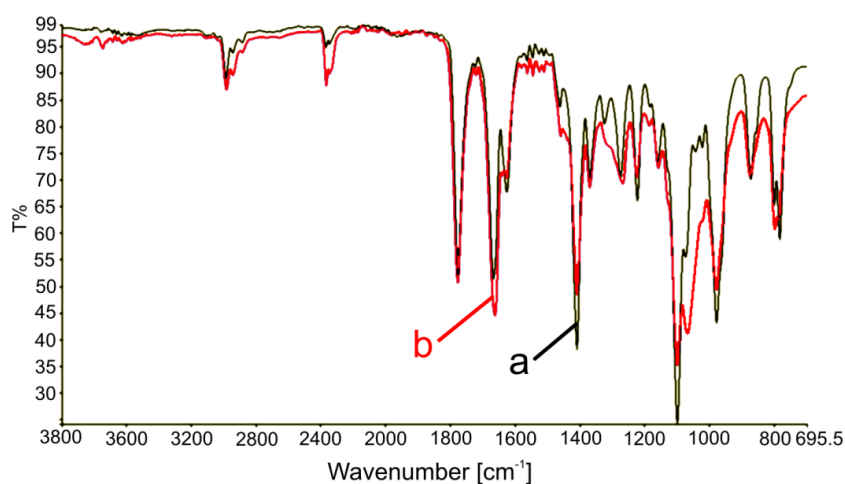


Figure 50. ATR-IR spectra of compound **28** as monomer (a) and UV cured polymer (b)

To evaluate the reactivity of the hydroxylamine-based acrylates **26-32** and in terms of calculating the $\Delta H_{0,P}$ of our new monomers, we had to use an accurate way to determine the DBC. This was done by comparison of the peak areas for the C=C bonds in the monomer and the polymer ATR-IR spectra using peak deconvolution (PeakFit V4.12, SSI). For the data fit the “Residuals method” was chosen together with a “Loess smoothing” algorithm. The fitting procedure was repeated until the

square of the correlation coefficient, r^2 , exceeded 0.99. Figure 51 and Figure 52 present an example for the fitted data of monomer and polymer IR spectra for the alkylated compounds. The C=O bond at 1775 cm^{-1} was considered as the internal reference, whereas the C=C bonds at 1665 cm^{-1} and 800 cm^{-1} varied according to the double bond conversion. After peak deconvolution a splitting up for all investigated bonds was detected, presumably caused by formation of hydrogen bridges in case of the carbonyl group, in case of the olifinic groups due to differences between acrylamide and acrylate double bond. For the calculation of the DBC, the area from the fitted data for each peak was used. The areas of both C=O peaks (with and without hydrogen bridges) were summarized due to their additive behaviour. From the relation of the monomer (DBC = 0%) to the polymer, the actual DBC could be derived according to equation 2, where x_m and x_p are the area of the C=C double bonds in the monomer, respectively the polymer, $(y_1+y_2)_m$ and $(y_1+y_2)_p$ belong to the summarized area of the corresponding C=O double bonds. Good correlation between the DBC values for both C=C bonds at 1665 cm^{-1} and 800 cm^{-1} could be seen (data shown in Table 12).

$$DBC = \left[1 - \frac{x_m}{(y_1 + y_2)_m} \times \frac{y_p}{x_p} \right] \times 100 \quad \text{Equation 2}$$

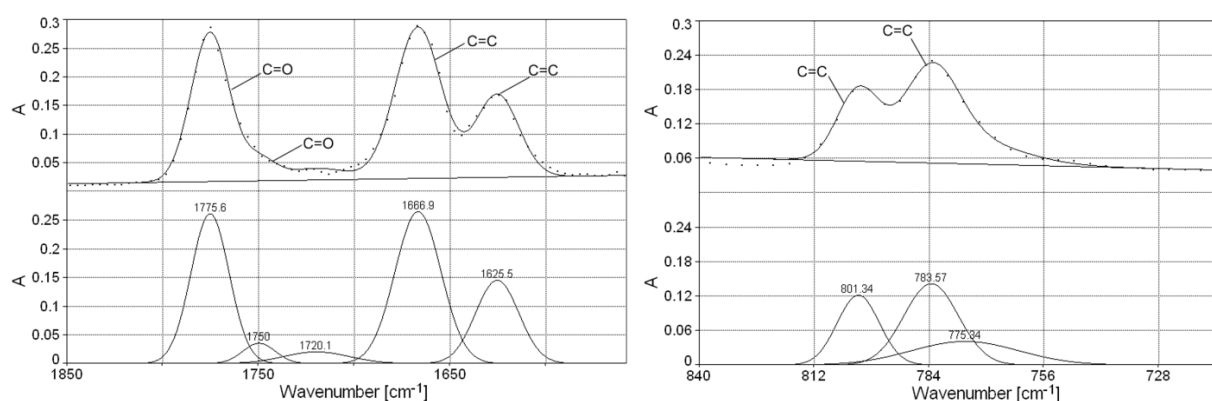


Figure 51. Peak deconvolution for compound **28** as monomer

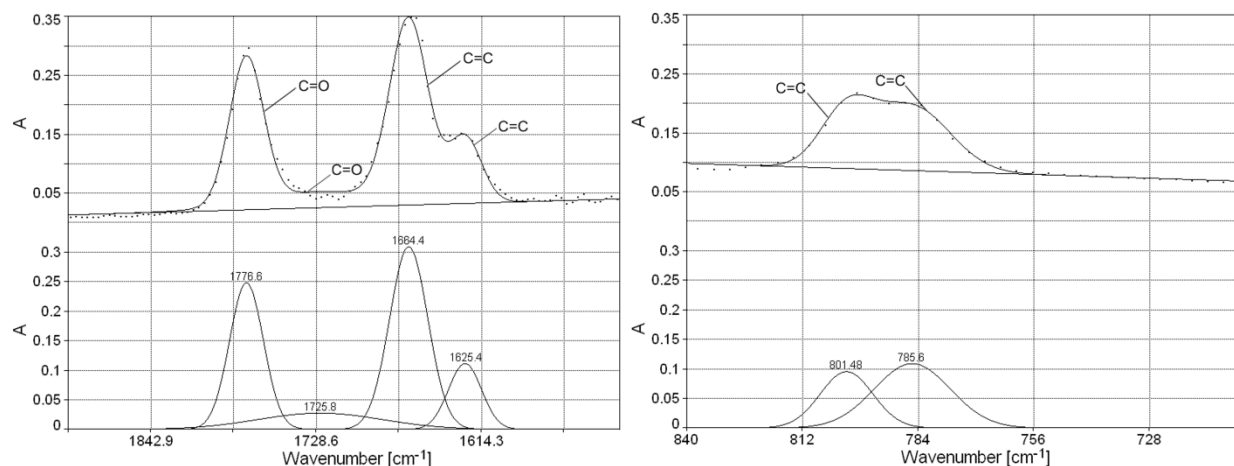


Figure 52. Peak deconvolution for compound **28** as polymer

Table 12. Comparison of DBC values for compounds **26-32** and **HDDA** obtained from ATR-IR C=C vibrations at $\sim 1600\text{ cm}^{-1}$ and $\sim 800\text{ cm}^{-1}$

Compound	R	DBC [%] at	
		$\sim 1600\text{ cm}^{-1}$	$\sim 800\text{ cm}^{-1}$
26	H	31	29
27	methyl	28	24
28	isopropyl	34	30
29	t-butyl	25	25
30	cyclohexyl	40	40
31	benzyl	31	34
32	acryl	50	43
HDDA	-	90	83

Generally, DBC values were derived from the 1665 cm^{-1} double bond, as this was the vibration with the more intensive transmittance. However, in case of compounds **27**, **32** and **HDDA** the DBC of the 800 cm^{-1} was considered more accurate due to a better correlation coefficient ($r^2 \rightarrow 1$) in the peak fit calculations. Especially in case of triacrylate **32** the 1665 cm^{-1} vibration showed a lot of other overlapping peaks in this region of the IR-spectrum.

Thus obtained values for the DBC and the overall heat evolved (H_P), determined in the photo-DSC experiments of PI-free formulations, discussed in the following part of this chapter, made it possible to calculate the theoretical heat, $\Delta H_{0,P}$ of the unknown polymers obtained for 100% conversion of the double bonds, according to equation 1 (Table 13). As there are different functionalities (acrylate, acrylamide) present in the

new monomers it makes only sense to give the $\Delta H_{0,P}$ of the monomer and not for each double bond. Additionally it was not possible to distinguish between both types of double bonds in the IR spectra, which was confirmed from simple acrylates (**LA**) and acrylamides (**DMAA**, **PAA**) that were studied as reference. The $\Delta H_{0,P}$ determined in bulk and PI (2wt% Darocur 1173) containing photo-DSC experiments for the monomers, were in scope with the values for a standard diacrylate as e.g. hexane-1,6-diole diacrylate (**HDDA**; $\Delta H_{0,P} = 148 \text{ kJ mol}^{-1}$), which was evaluated during this study using 2 wt% Darocur 1173 as PI. Consistency was also given with $\Delta H_{0,P}$ values for **HDDA** described by Scoconi *et al.*¹⁶³

Table 13. Calculated DBC and theoretical polymerization heat values for compounds **26-32** (PI free) and **HDDA** (2wt% Darocur 1173)

Compound	R	DBC [%] by ATR-IR	H _p [J g ⁻¹] by Photo-DSC	$\Delta H_{0,P}$ [J mol ⁻¹]
26	H	31	313	142700
27	methyl	24	204	132000
28	isopropyl	34	252	135600
29	t-butyl	25	152	120200
30	cyclohexyl	40	209	116700
31	benzyl	31	171	127500
32	acryl	43	441	200500
HDDA	-	83	543	148000

3.2.3. Photo-DSC

This study was carried out to investigate the so far unknown photoreactivity of the newly prepared di- and triacrylated hydroxylamine systems. Interest focused on the following characteristics: PI activity (100 $\mu\text{mol g}^{-1}$) in an well-established acrylate-based monomer like **HDDA**, reactivity as a monomer in the presence of a Type I PI (Darocur 1173, 2 wt%) and ability to undergo self-initiation in absence of any PI. Generally, irradiation (EFOS Novacure, 250-450 nm filter) was carried out under nitrogen atmosphere.

3.2.3.1. PI activity in **HDDA**

The PI activity of the hydroxylamine-based compounds **26-32** (100 $\mu\text{mol g}^{-1}$) was compared with an equimolar mixture of **BP/TEA** (100 $\mu\text{mol g}^{-1}$), an established Type II PI system (Table 14). All alkylated derivatives, except compound **21**, and also the

non-alkylated compound **26** had almost similar performance with slightly lower activity than the reference PIs. With PI **31** decreased performance was expected due to the light screening effect of the aromatic moiety, nonetheless, this seemed to have no influence. Poor results of *N*-methyl diacrylate **26** could not be clarified yet. Selected plots of exotherms are shown in Figure 53. Surprisingly, the triacylated hydroxylamine **32** showed similar performance to well-known **BP/TEA** system. The good photoinitiating activity of these compounds was quite unexpected as only a fraction of the light can be absorbed by them compared to **BP**.

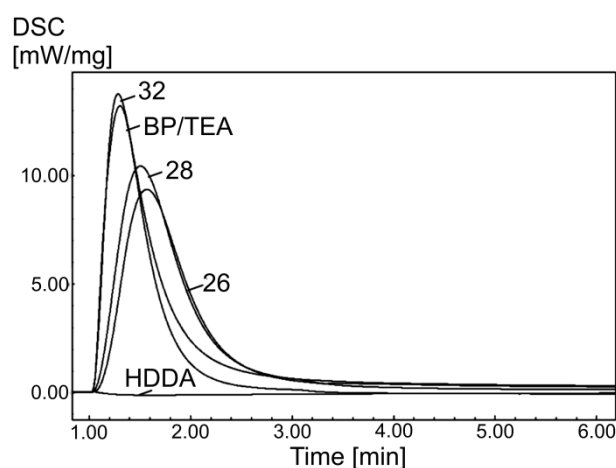


Figure 53. Photo-DSC plots of **HDDA** with compounds **26**, **28**, **32**, and **BP/TEA** as PI in comparison to PI-free **HDDA**

Table 14. Photo-DSC data of **HDDA** with compounds **26-32**, and **BP/TEA** as PI

Compound	R	t_{\max} [s]	h [W g ⁻¹]	H _p [J g ⁻¹]	DBC [%]	R _{Pmax} × 10 ³ [mol L ⁻¹ s ⁻¹]
26	H	34	9.23	448	72	65.9
27	methyl	46	5.62	431	69	40.1
28	isopropyl	31	10.25	464	74	73.1
29	t-butyl	31	8.81	484	77	62.9
30	cyclohexyl	32	9.61	451	72	68.6
31	benzyl	31	10.48	467	75	74.8
32	acryl	17	13.77	450	72	98.3
BP/TEA	-	19	13.23	416	67	94.4

To enhance the PI reactivity (99 mmol L⁻¹) of the new compounds, also their performance in **HDDA** after addition of different photosensitizers to extend the spectral range of sensitivity was investigated. As there is nothing known on the

photochemistry and photophysics of this compounds, a set of typical sensitizers that react by energy transfer and/or electron transfer were selected. Therefore 11 mmol L⁻¹ **BP**, dibutylanthracene (**DBA**) and isopropylthioxanthone (**ITX**) were used as sensitizers. However, no significant improvement was seen. The reactivity was even decreased by addition of 0.2 wt% **DBA**, respectively **ITX**. Only the addition of **BP** resulted in some increase of the peak height.

Furthermore, to determine the influence of the concentration from the new hydroxylamine-based acrylate compounds on their photoinitiating performance, a series of photo-DSC experiments was performed, varying the concentration of the photoinitiating hydroxylamine compounds in the range from 1 wt% to 100 wt% in **HDDA** as monomer. As model system for all alkylated hydroxylamines, the methyl compound **27** with the lowest reactivity is presented in Figure 54. A clear dependence could be seen, as the peak height increased from 1 wt% up to the maximum at 5 wt% and then drops down to the level of pure **27**. t_{\max} was reduced nearly linear with increasing amount of **27**. No information on the accurate value of the DBC could be derived from the photo-DSC experiments as the $\Delta H_{0,P}$ of the monomers differ and it was also not possible to distinguish between the different type of reactive groups in ATR-IR spectroscopy. Nevertheless, for a qualitative overview the DBC was calculated using a mean value for the heat of polymerization as shown in Figure 55. The same photo-DSC experiment was repeated with the trifunctional acrylate **32**. In contrast to the difunctional acrylates, the peak height (h ; mW mg⁻¹) decreased even at PI concentrations higher than 2 wt%, while t_{\max} is slightly reduced with increasing amount of **32**. Unfortunately, also in this case only qualitative considerations were possible due to the different $\Delta H_{0,P}$ but also due to the different numbers of reactive groups.

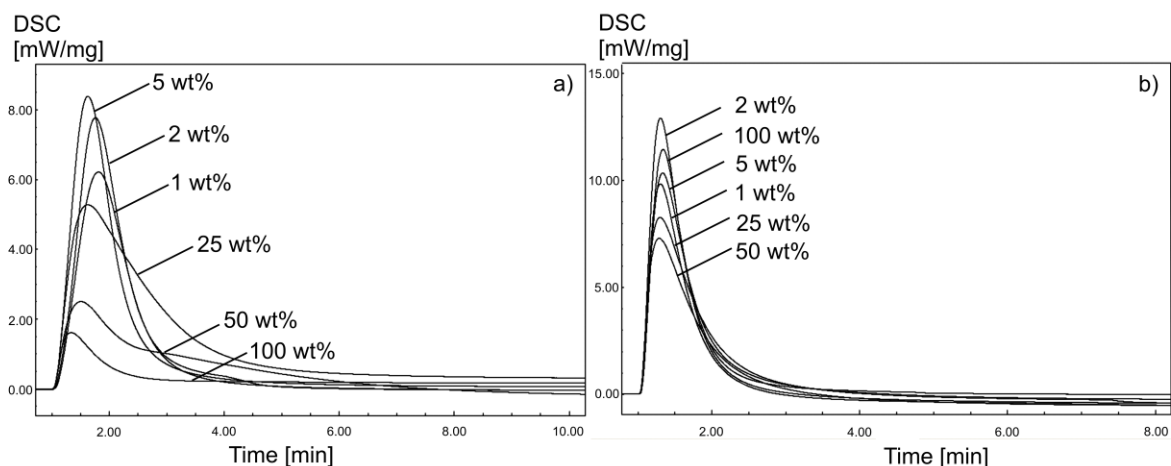


Figure 54 Photo-DSC plots for **HDDA** with compound **27** (a) (1, 2, 5, 25, 50 and 100 wt%) as PI and with compound **32** (b) (1, 2, 5, 25, 50 and 100 wt%) as PI

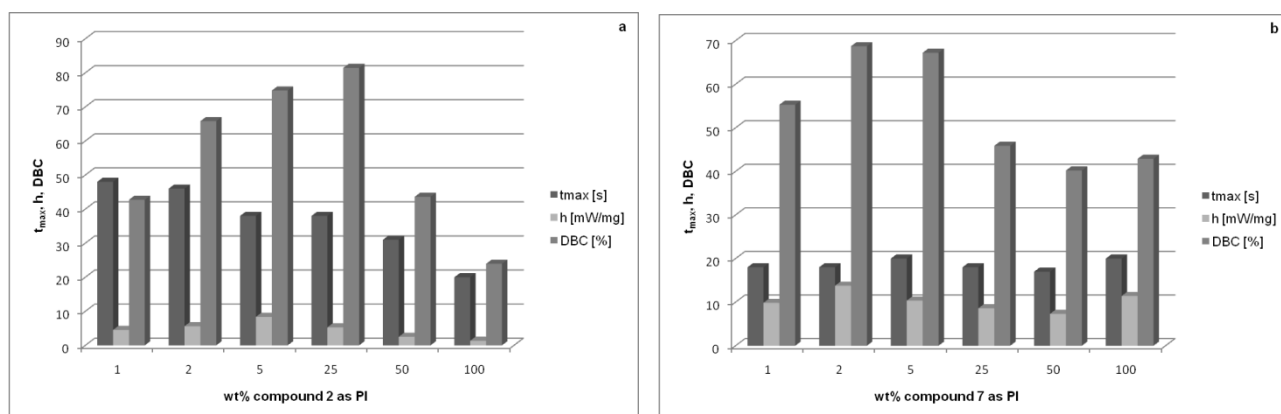


Figure 55. Photo-DSC data for compound **27** (a) and **32** (b)

3.2.3.2. Monomer reactivity with a Type I PI

Photo-DSC measurements with a Type I PI, Darocur 1173, were carried out, to investigate the monomer reactivity of the newly developed hydroxylamine compounds. As reference monomer systems **HDDA**, **LA** and 2-(2-ethoxy-ethoxy) ethyl acrylate (**EEEA**) were used. The PI concentration was 99 mmol L⁻¹. Some representative plots in Figure 56 demonstrate, that the reactivity expressed by t_{max} of the new compounds is placed between **HDDA** and **EEEA**. With increasing bulkiness of the alkyl residue R the polymerization performance also decreased due to sterical hindrance. As expected, highest DBC was observed with monoacrylates like **LA** and **EEEA** (Table 15).

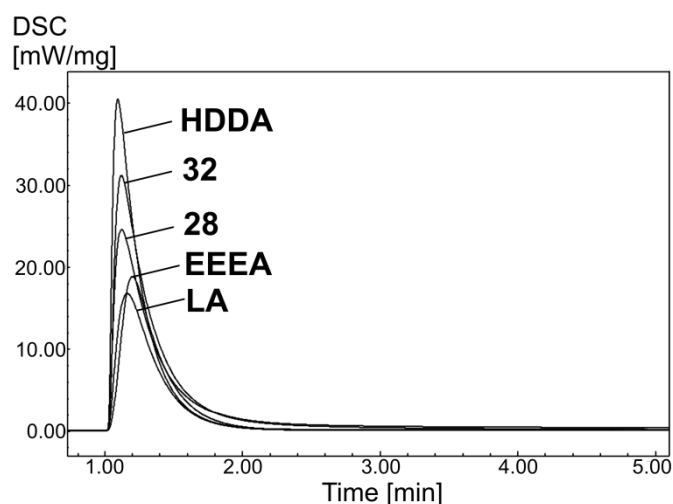


Figure 56. Photo-DSC plots for compounds **28** and **32** in comparison with **HDDA**, **LA** and **EEEA** (2wt % PI Darocur 1173)

Table 15. Photo-DSC data for monomers **26-32** with Darocur 1173 as PI (2 wt%)

Compound	R	t_{\max} [s]	DBC [%]	$R_{P_{\max}} \times 10^3$ [mol L ⁻¹ s ⁻¹]
26	H	7.2	66	225
27	methyl	6.6	62	269
28	isopropyl	7.2	61	169
29	t-butyl	7.2	67	116
30	cyclohexyl	7.2	71	101
31	benzyl	12.0	66	81
32	acryl	7.2	79	176
HDDA	-	5.2	83	288
EEEA	-	12.0	89	237
LA	-	9.6	98	182

The performance of the diacrylates was significantly poorer than of **HDDA**. The reason for the low DBC values of our compounds might be the high cross-linking ability of the monomers and the resulting inhibition of the polymerization progress by microgelation and trapping of monomer.¹⁶⁴ Triacrylate **32** showed quite good results for a monomer with such a high number of reactive groups incorporated in a low molecular weight monomer. The reason for that might be on the one hand some kind of cyclopolymerization of the diacrylamide unit as described by McCormick *et al.*,¹⁶⁵ although this could not be proved by ATR-IR analysis. On the other hand, N-O bond cleavage might be expected leading to less cross-linked networks.

3.2.3.3. PI-free photopolymerization

After evaluation of our hydroxylamine-based acrylates concerning their ability to initiate photopolymerization in **HDDA** as acrylate-based monomer and their ability to act as monomer with a Type I PI, the combined PI and monomer properties of the new compounds in PI-free, self-initiating formulations was investigated.

DMAA and **LA** were used as reference systems, presenting the properties of the acryl amide and the acrylic ester residue. Selected photo-DSC plots are presented in Figure 57 and all analysed data are outlined in Table 16. As expected, both reference systems displayed no activity. The alkylated hydroxylamine compounds **27-31** showed comparable reactivity, almost independent of the alkyl residue R. Although t_{\max} was reached quite fast, exothermic polymerization reaction occurred for nearly 5 min under these conditions. They were superseded by the non-alkylated derivative **26** concerning monomer activity expressed by $R_{p\max}$ but by far the highest photoinitiating activity was observed with the triacrylate **32**.

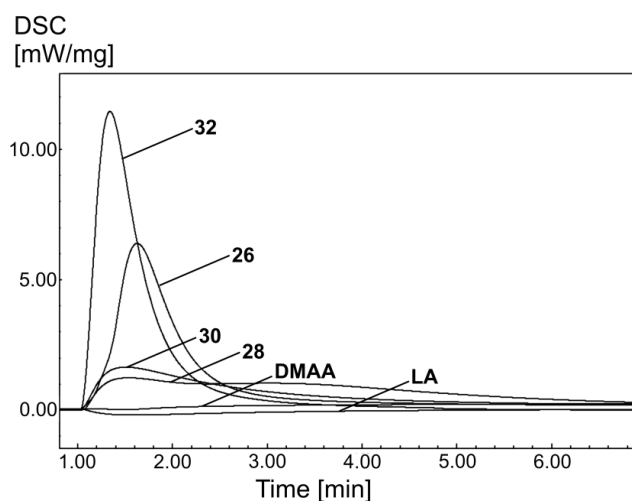


Figure 57. Photo-DSC plots for compounds **26**, **28**, **30** and **32**, **DMAA** and **LA** (PI-free)

Table 16. Photo-DSC data for compounds **26-32**, **DMAA** and **LA** (PI-free)

Compound	R	t_{\max} [s]	h [W g ⁻¹]	H_P [J g ⁻¹]	$\Delta H_{0,P}$ [J mol ⁻¹]	DBC [%]	$R_{P\max} \times 10^3$ [mol L ⁻¹ s ⁻¹]
26	H	38	6.28	313	142700	31	440
27	methyl	30	1.36	204	132000	24	111
28	isopropyl	32	1.18	252	135600	34	81.2
29	t-butyl	34	0.76	152	120200	25	61.3
30	cyclohexyl	31	1.53	209	116700	40	89.2
31	benzyl	22	1.08	171	127500	31	67.1
32	acryl	20	11.42	441	200500	43	629
DMAA	-	-	-	-	-	-	-
LA	-	-	-	-	-	-	-

The DBC values of compounds **26-32** were only moderate (24% to 43%), compared to the experiments with Darocur 1173 as PI (60%-79%). The reason for the lower DBC might be the limited absorption behaviour up to 320 nm and the high chromophore density.

3.2.4. Steady state photolysis experiments with TEMPO and t-BAM

Formation of radicals during radiation curing is the most crucial step in the photolysis of photoinitiators. The following mechanisms are responsible for the generation of radicals:

- 1) Photodissociation: α -cleavage (Norrish Type I process) or β -cleavage
- 2) Intramolecular γ -proton abstraction (Norrish Type II process)
- 3) Intermolecular proton abstraction
- 4) Electron transfer followed by proton transfer

Radicals can be identified by various spectroscopic methods, e.g. Electron Spin Resonance Spectroscopy (ESR), Laser Flash Photolysis (LFP), or chemically induced dynamic nuclear polarization (CIDNP).

Furthermore, it is possible to react the primary radicals with other stable radicals or with molecules that contain a non-polymerizable double bond, as for example **TEMPO**¹⁶⁶ and **t-BAM**,¹⁶⁷ which were already described in literature. The photolysis adducts of the radicals with those compounds can be detected by HPLC or GC-MS.

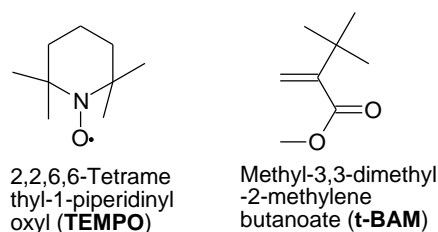
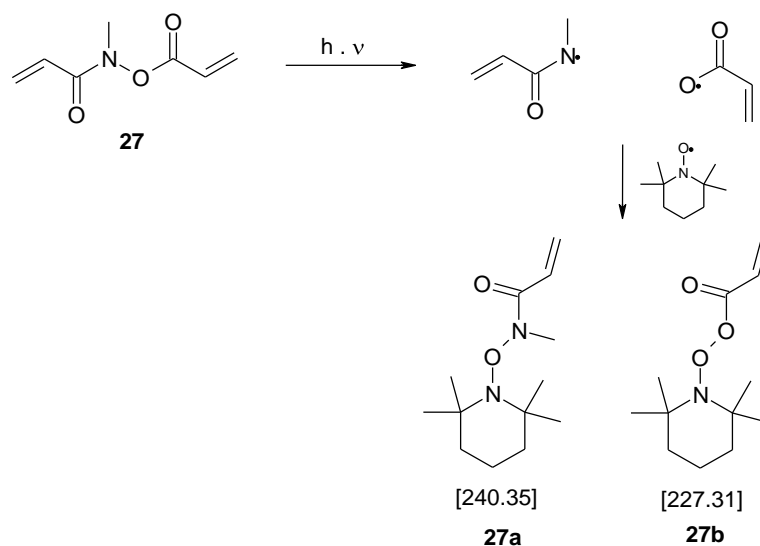


Figure 58. Radical Quenchers

To investigate the photochemistry, in particular the presumed mechanism of cleavage between the N-O bond at irradiation with UV light, of the newly synthesized di- and trifunctional acrylates, photolysis experiments of compound **27** with the stable radical **TEMPO** and the non-polymerizable monomer **t-BAM** were performed. The methyl hydroxylamine based diacrylate **27** was chosen as representative monomer for compounds **26-32** because of its simple structure. As internal standard for GC-MS experiments, eicosane was used in a concentration of 10 wt% relating to the amount of PI. This method allows a first evaluation of quantification for the detected photo-adducts.

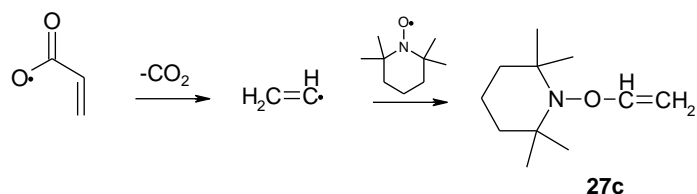
TEMPO is known to be a very stable radical and was therefore chosen for the diffusion-controlled quenching of the generated radicals. In literature¹⁶⁸ the existence of the proposed adduct structure was confirmed, namely for the -OCOON- bond as in **27b**, whereas formation of **27a** could not be proved by citation of structure analogues in literature (Scheme 31). The photolysis experiments were carried out in MeCN under nitrogen atmosphere with 4 equivalents of **TEMPO**. 4 mL of photolysis solution containing 0.516 mmol of **27** and 2.07 mmol of **TEMPO** were irradiated at 250-450 nm for 30 min. At different times samples for GC-MS and HPLC analysis were drawn. During the photolysis experiments a precipitate occurred in the reaction vessel, insoluble in MeCN. For GC-MS analysis the samples were diluted 1:200 with MeCN, for HPLC analysis 1:20.



Scheme 31. Proposed cleavage mechanism and **TEMPO**-adduct formation for photolysis experiments with **TEMPO** and compound **27**

The GC-MS spectra of the drawn samples gave hardly any indication, that the supposed **TEMPO**-adducts had been formed. Column chromatography of the residual reaction solution was not successful, probably due to destruction of the compounds on the silica gel.

In the GC-MS spectrum the **TEMPO** peak could be seen at 3.75 min, at 9.90 min was the peak for the internal standard, eicosane. No peak of the monomer, compound **27**, could be identified. Presumably, the polymerization of monomer **27** was significantly faster than the formation of the **TEMPO**-adduct. The largest of the new generated peaks was at 5.99 min. The corresponding MS spectrum showed a fragmentation pattern from an ethene-**TEMPO** adduct as presented in Scheme 32. Presumably the carboxyl radical of compound **27** decarboxylated and by transformation gave an acetylene radical, which was stable enough for binding to **TEMPO**. It had the mass of [181].



Scheme 32. Proposed fragmentation mechanism for the carboxyl radical of compound **27**.

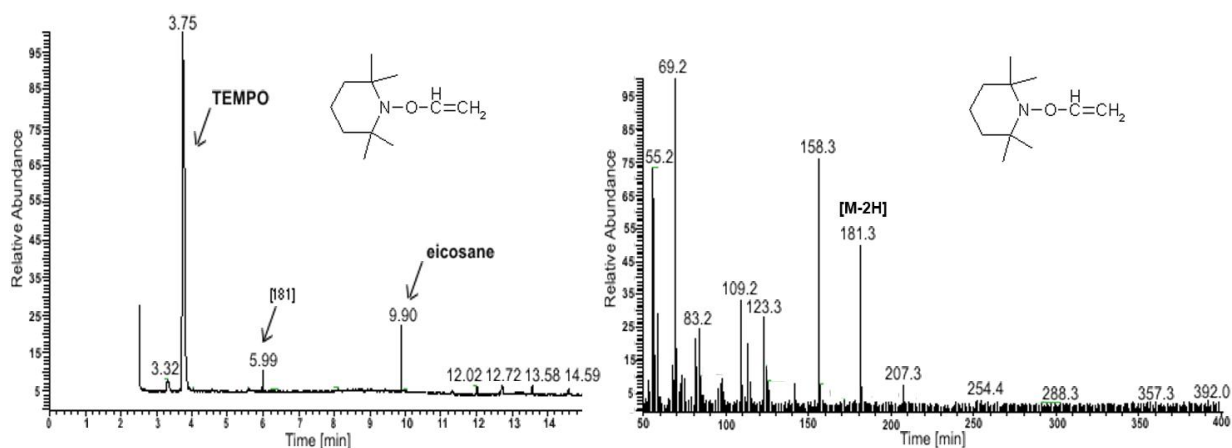
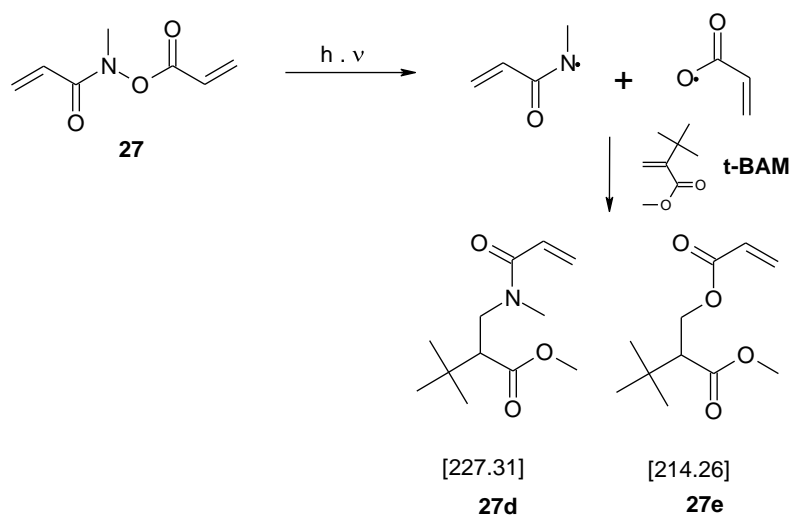


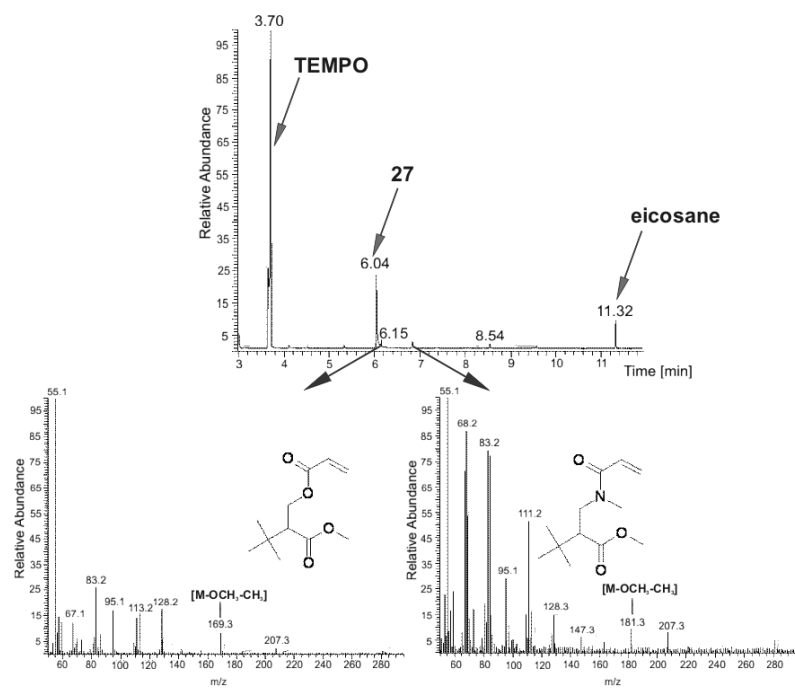
Figure 59. GC-MS spectrum for the supposed **TEMPO**-adduct **27c** of compound **27**

As the **TEMPO** experiments did not give a reliable picture of the cleavage mechanism for the hydroxylamine-based self initiating monomers, presumably due to the instability of the photoproducts, another method was chosen. Therefore, **t-BAM**, a non-polymerizable monomer as presented in Scheme 33, was used as radical trap for the irradiation experiment.

The photolysis experiment was carried out in MeCN under nitrogen atmosphere with 4 equivalents of **t-BAM**. 4 mL of photolysis solution containing 0.53 mmol of **27** and 2.25 mmol of **t-BAM** were irradiated at 250-450 nm for 30 min. At different times samples for GC-MS and HPLC analysis were drawn. For GC-MS analysis the samples were diluted 1:200 with MeCN, for HPLC analysis 1:20. In the GC-MS spectrum the peak for **t-BAM** occurred at 3.70 min [$M^+ = 142$], the internal standard, eicosane, at 11.32 min [$M^- = 281.2$]. The remaining monomer **27** showed a peak at 6.04 min [$M^+ = 155.2$]. Surprisingly, much of the monomer was still left, even after 5 min of irradiation time. Nevertheless, some smaller peaks occurred at 6.15 min, 6.83 min and 8.54 min. Investigation of the corresponding mass spectra led to the presumption, that the peak at 6.15 min resulted from the formation of the acryl ester adduct with **t-BAM**, according to Figure 60, whereas the peak at 6.83 could be derived from the acrylamide adduct with **t-BAM**.



Scheme 33. Proposed cleavage mechanism and **t-BAM**-adduct formation for photolysis experiments of compound **27**



4. Monomers for Biomedical Applications

The development of biocompatible polymers has been a fundamental topic for many years in biomedical sciences – and still is. Non-toxic, biodegradable synthetic materials are used to fabricate – in a more general sense – suitable replacement parts for human and animal bodies. Apart from biocompatibility, such polymers should also feature good mechanical properties and also high affinity to cells, as for example osteoblasts in case of bone replacement materials. The latter is crucial for the cell organization on the surface of the scaffold material, as it will direct the re-growth of the desired tissue. In the most ideal case, the polymer will be replaced by new, aboriginal tissue and the degradation products of the scaffold will be resorbed by the body.

Among biopolymers used currently in clinical practice, polyester-based materials such as poly(lactides) and-(glycolides), poly(lactones) and poly(lactames) maintain almost absolute dominance. Major drawback of these materials are their low mechanical stability due to lack of crosslinks and their uncontrolled decomposition by a bulk erosion mechanism.^{169,170} Therefore, crosslinkable co-polymers with, for example, fumaric acid were developed.^{171,172} Besides, the introduction of acrylate endgroups delivered improvement on manufacturing time in the precise case of poly(caprolactones).¹⁷³ However, it was discovered, that the use of acrylates in biopolymers had a negative effect on the biocompatibility of these materials. During decomposition of the polymer poly(acrylic acid) and residual monomer are released, which harm the surrounding cells – leading them to apoptosis – and impair the attachment of new cells to the surface of the scaffold. The toxicity of acrylates is based on Michael addition of the double bond to amino or mercapto-groups of biomolecules such as proteins or DNA, thus producing irreparable damages in the cell.^{170,174} Compared to poly(acrylates), methacrylates-containing polymers were identified to be less harmful,^{175,176} as they are less susceptible to Michael addition reactions, probably due to sterical hindrance and electron donating effect of the methyl group.¹⁷⁷ Additionally, methylmethacrylate esters have been identified as metabolism products in the human body and are considered therefore less toxic.¹⁷⁸ Based on these features, poly(methacrylates) find wide spread use as bone cement,¹⁷⁹ drug delivery devices,¹⁸⁰ artificial skin¹⁸¹ and for dental applications.¹⁸²

Recently, also vinyl esters or vinyl carbonates and -carbamates of alcohols, respectively amines, have proven to deliver biocompatible, photopolymerizable monomers, as the poly(vinyl alcohol) backbone of the polymer provides non-toxic degradation products.¹⁷⁰ Therefore, it was one of the concepts of this study to prepare monomers, which form a poly(vinyl alcohol) polymer backbone, bearing a self-initiating moiety, as the use of PIs in medical applications presents some disadvantages due production of toxic photoproducts, which might migrate out of the cured material. Two different concepts for self-initiating monomer structures were developed: they should consist of either an acylated N-O bond, which is already known to be photocleavable from the first two parts of this PhD thesis, or an acylated P(V) moiety, as the PI activity of phosphoacyl oxides, e.g. Lucirin TPO®BASF or Irgacure 819®Ciba, is well established.

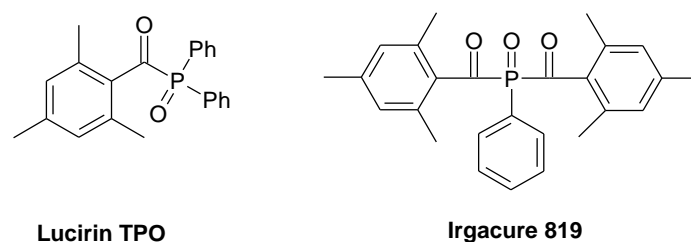


Figure 61. Structures of commercially available acylphosphine oxide PIs

Apart from the self-initiating properties, also low toxicity of the monomers was a key feature of this study. To further improve the biocompatibility of the phosphorus-containing monomers, which might be more suitable as bone replacement materials due to their constitution than the hydroxylamine-based carbamates, the acyl group should be exchanged by a simple alkoxy moiety, which might lead to loss of the self-initiating ability, but also imply lower toxicity. Target structures are shown in Figure 62.

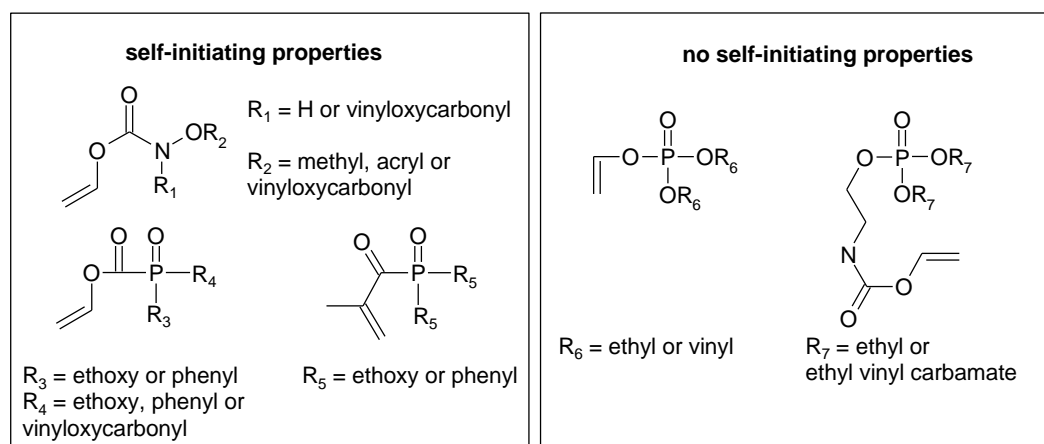


Figure 62. Target structures for biocompatible monomers with/without self-initiation

Basically, examination of the photochemical properties of the synthesized vinyl esters and vinylcarbamates should be performed by UV-Vis spectroscopy, ATR-IR spectroscopy and Photo-DSC. For the most promising polymers characterization should include additional tests concerning cell toxicity, mechanical stability and hydrolytical degradation behaviour.

4.1. Hydroxylamine-based monomers

Recently, the self-initiating behaviour of diacrylamides had been shown by Karasu *et al.*⁵⁶ In this context, compound **34** should be prepared, resembling the structure of the highly reactive diacrylamide monomers.

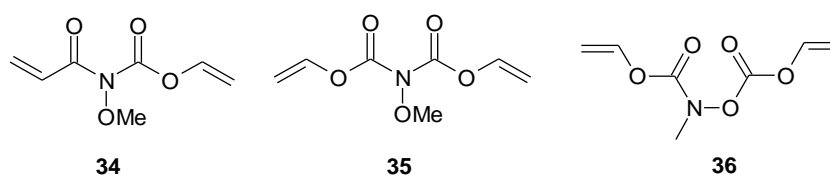


Figure 63. Structures of the synthesized vinylcarbamates

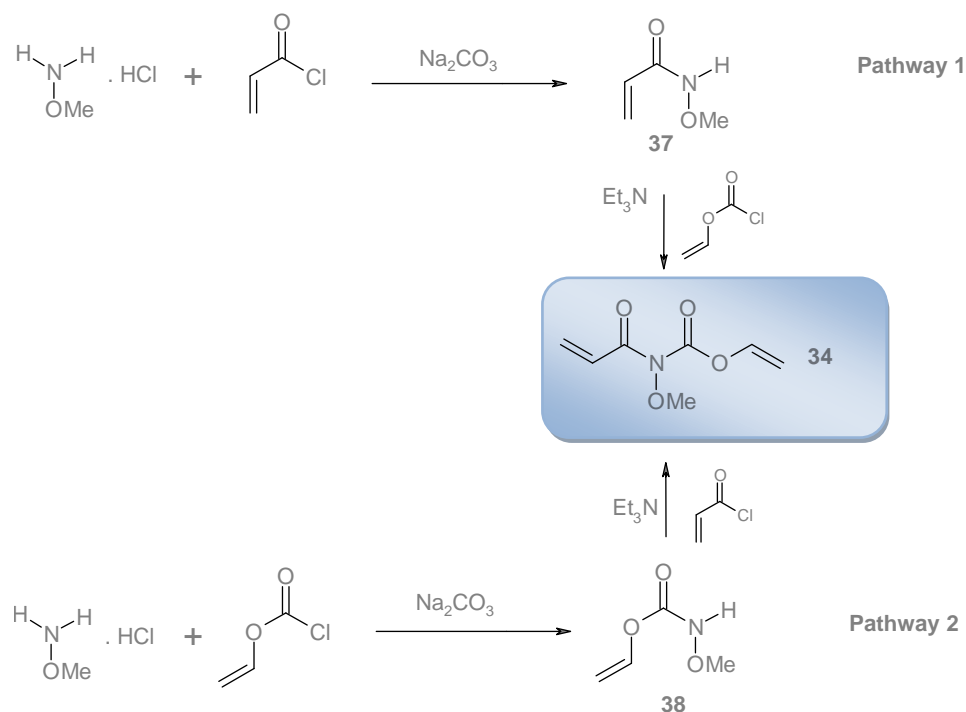
As the acrylic moiety in **34** might cause problems concerning its biocompatibility, also the corresponding divinylated monomer **35** was considered a potential target molecule. Another possibility to obtain self-initiating monomers might be compound **36**, where the vinyloxycarbonyl group is attached to the O-atom, displaying a similar assembling as the self-initiating diacrylated hydroxylamines from chapter 3.

O,N-bis(vinyloxycarbonyl)-*N*-methyl hydroxylamine (**36**) should be prepared to test it for self-initiation ability and biocompatibility. As low initiation potential might be expected for **29** due to weak conjugation of the chromophore, also a mixed structure containing one vinyl and one acryl functional group as for and *N*-(2-propenyl)-*N*-(vinyloxycarbonyl)-*O*-methyl hydroxylamine (**34**) should be synthesized.

4.1.1. Synthesis

4.1.1.1. *N*-(2-Propenyl)-*N*-(vinyloxycarbonyl)-*O*-methyl hydroxylamine (**34**)

Two possible reaction pathways were identified to prepare the vinyloxycarbonyl-acryloyl monomer **34**, depending on the nature of the polymerizable group, which was introduced to the *O*-methyl hydroxylamine moiety in the first step (Scheme 34).

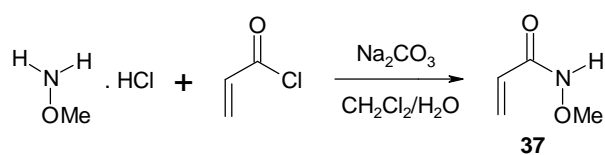


Scheme 34. Two possible reaction pathways for formation of compound **34**

Pathway 1 starts with the conversion of *O*-methyl hydroxylamine hydrochloride with one equivalent of acryloyl chloride to deliver the acryloyl hydroxylamine **37**, which subsequently would react with chlorovinyl formate to deliver target product **34**. Pathway 2 takes the other way round, starting with the addition of the chlorovinyl formate to obtain **38**, followed by reaction with acryloyl chloride to prepare desired product **34**.

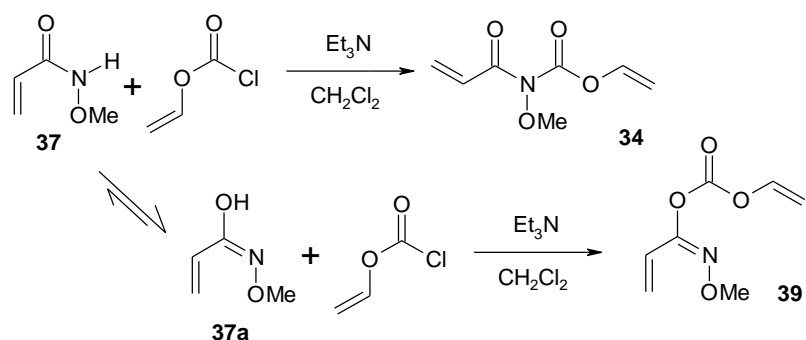
To avoid loss of the very expensive chlorovinyl formate by incomplete conversion in both reaction stages, pathway 1 was attempted first, where the reagent would be used in the final step.

Therefore, starting with pathway 1, the already known *N*-(2-propenyl)-*O*-methyl-hydroxylamine **37** was prepared under Schotten-Baumann conditions with equimolar amounts of acryloyl chloride and *O*-methyl hydroxylamine hydrochloride, as it had already been described by Kopeinig.¹⁵⁸



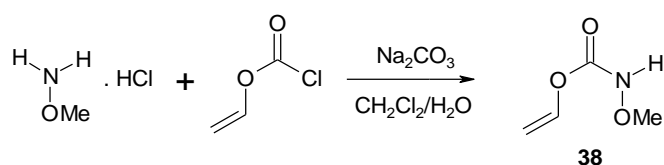
By this method **37** was obtained in 56% yield and it was used without further purification for the following reaction.

The next step was the conversion of monoacrylate **37** with one equivalent of chlorovinyl formate.



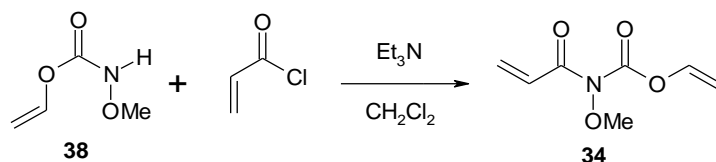
It had been discovered during the synthesis of triacrylate **32**, that the use of sodium bicarbonate as base in a two phase system, water/dichloromethane, had been unfavorably, as the nucleophilicity of the hydroxamic acid was much lower than that of water. Hence, it was obligatory to use an organic solvent and also an amino compound as base. Unfortunately, it was recognized, that chlorovinyl formate formed undesired adducts with the triethylamine. As a remedy to this problem, a sterical hindered base was employed, such as 1,8-diazabicyclo[5.4.0] undec-7-ene, instead of triethylamine. Nevertheless, the formation of adducts with the base could not be avoided neither this way. A second problem was the preferred formation of the tautomer **37a** of **37**. It resulted in the generation of the imino by-product **39**. The yield of the desired product **34** was only 18%.

Considering all those side reactions and the poor yield from pathway 1, the second pathway was chosen, starting from chloro vinylformate, using the aqueous solvent system and Na_2CO_3 as base to obtain *N*-vinylloxycarbonyl-*O*-methyl hydroxylamine (**38**).



Thus, almost pure **38** could be obtained. Only small traces of the divinylated product were detected, that were separated by column chromatography.

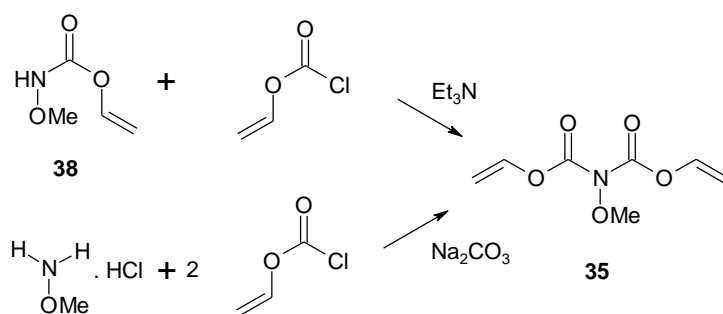
From intermediate product **38**, the next reaction step included the acylation with acryloyl chloride to obtain the target compound **34**.



Under already discussed water-free Schotten-Baumann conditions, using triethylamine as base, the N-atom of compound **38** was acylated and *N*-(2-propenyl)-*N*-(vinylloxycarbonyl)-*O*-methyl hydroxylamine was obtained in 56% yield after purification by column chromatography. ¹H-NMR analysis confirmed, that no monovinyl oxime tautomer was present – this phenomenon obviously arose only with the monoacrylic compound **37** from pathway 1.

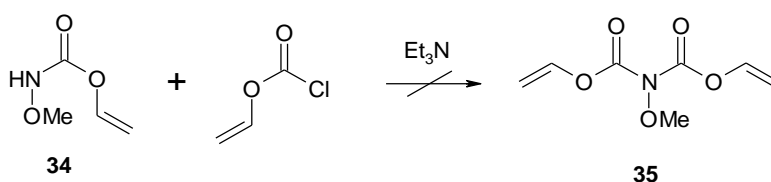
4.1.1.2. Attempted synthesis of *N,N*-bis(vinylloxycarbonyl)-*N*-methoxy hydroxylamine(**35**)

There are two possibilities to obtain divinyl compound **35** as presented in Scheme 35. Starting from intermediate **38**, the divinyl compound **35** should be obtained by addition of a second chlorovinyl formate group. The second pathway started from *O*-methyl hydroxylamine hydrochloride in a one pot synthesis with two equivalents of chlorovinyl formate.

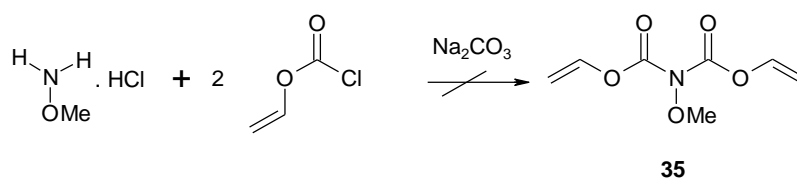


Scheme 35. Possible synthetic pathways leading to **35**

Therefore, **38** was reacted with one equivalent of chlorovinyl formate and triethylamine as acid scavenger. As described for the synthesis of **34** adducts of chlorovinyl formate with triethylamine were formed to a great extent, as the nucleophilicity of the nitrogen atom was strongly reduced for the second acylation reaction.

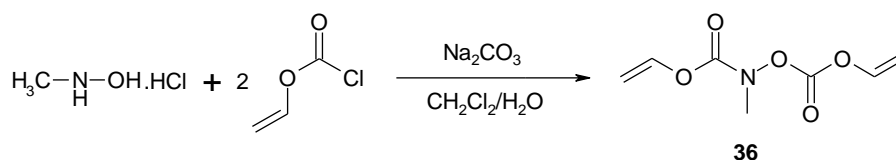


Due to very poor yields this reaction pathway was abandoned in preference of the second method, thus avoiding the use of triethylamine. However, also the aqueous reaction system using sodium carbonate as base did not work. Mostly monovinyl compound **38** and only traces of **35** could be obtained, as the nucleophilicity of the nitrogen atom was obviously too weak for the second acylation with chlorovinyl formate



4.1.1.3. *O,N*-Bis(vinyloxycarbonyl)-*N*-methyl hydroxylamine (**36**)

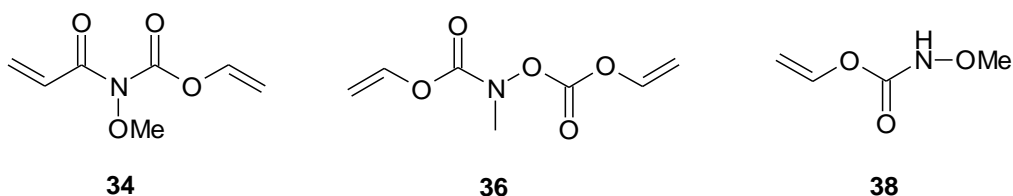
Generally, formates are well-known as protecting groups for the amino or hydroxyl moiety. The reaction between the chloroformate and the amine, respectively alcohol proceeds easily in the presence of a base as acid scavenger according to Schotten-Baumann conditions.¹⁸³



Hence, *O,N*-bis(vinyloxycarbonyl)-*N*-methyl hydroxylamine, **36**, was prepared from hydroxylamine hydrochloride and chlorovinyl formate. The reaction went smoothly and pure **36** was obtained in 81% yield.

4.1.2. Analyses

Hydroxylamine-based vinyl carbamates **34** and **36** and also intermediate **38**, the monofunctional vinyl carbamate, should be characterized by UV-Vis analysis and photo-DSC experiments. Concerning biocompatibility also conduction of toxicity tests on osteoblast cells were planned.



4.1.2.1. UV-Vis spectroscopy

UV-Vis spectra of all synthesized vinyl hydroxylamine compounds were carried out to investigate their absorption behaviour. As reference materials *N*-propyl acrylamide (**PAA**) and *N,N*-dimethyl acryl amide (**DMAA**) were used. All spectra were measured in MeOH at concentrations of $1 \times 10^{-2} \text{ mol L}^{-1}$ to $1 \times 10^{-5} \text{ mol L}^{-1}$.

The results from the UV-Vis measurements are shown in Figure 64 and Table 17.

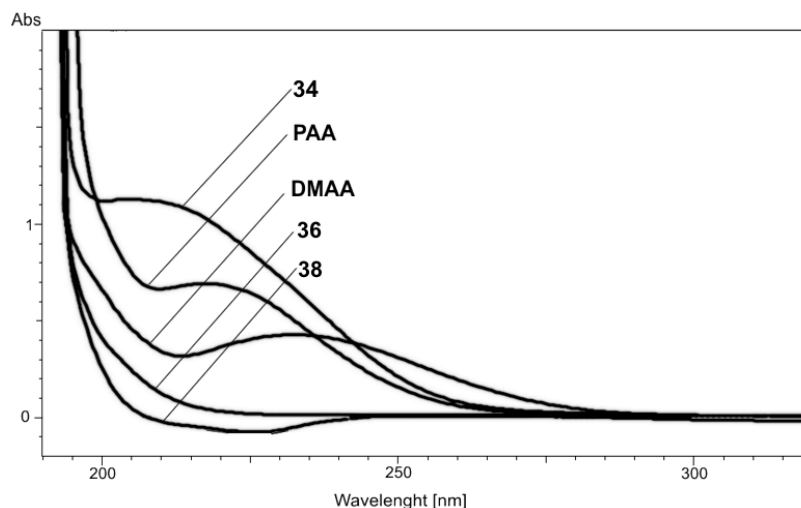


Figure 64 UV spectra of compounds **26**, **27** and **28** in comparison with **PAA** and **DMAA** in $1 \times 10^{-4} \text{ mol L}^{-1}$ acetonitrile

Table 17. UV-Vis data for vinylcarbamates **34**, **36** and **38** as well as references **DMAA** and **PAA**

Compound	λ_{max} [nm]	$\epsilon \times 10^{-2}$ [$\text{L mol}^{-1} \text{ cm}^{-1}$]
34	212	112.5
36	-	-
38	-	-
DMAA	238	42.3
PAA	226	52.5

Whereas compounds **38** and **36** showed no absorption, even at higher concentrations due to the absence of any longer conjugated system, compound **34** displayed an intensive maximum in the region for $\pi-\pi^*$ transitions of the chromophore, at 231 nm. Compared to the reference substances **DMAA** and **PAA**, the absorption of **34** showed a higher extinction coefficient, probably due to the higher electron density at the nitrogen atom caused by the methoxy group. The stronger red-shift of the absorption maxima of the references **PAA** and **DMAA** was found with increasing amount of alkyl groups attached to the nitrogen atom.

4.1.2.2. ATR-IR – Analysis

IR spectra were measured from the monomer compounds **34**, **36** and **38** and also for their corresponding polymers after UV curing in the photo-DSC experiments to determine the DBC and the $\Delta H_{0,P}$ for the new compounds by peak deconvolution, as already described in chapter 3.2.2.

Table 18. Calculated DBC and theoretical polymerization heat values for compounds **34**, **36** and **38** with PI (Darocur 1173, 2wt%)

Compound	DBC [%] by ATR-IR	H _p [J g ⁻¹] by Photo-DSC	$\Delta H_{0,P}$ [J mol ⁻¹]
34	82	495	103300
36	70	624	142700
38	81	517	74700

As shown in Table 18 DBC values for all three monomers were quite high (70-82%). However, in case of hybrid-compound **34**, there are different functionalities (acrylate, vinylcarbamate) present in the monomer. It is well-known, that the polymerization speed is significantly higher in acrylates than in vinyl esters and carbamates. Additionally it was not possible to distinguish both types of double bonds clearly in the IR spectra, therefore, it makes only sense to give the $\Delta H_{0,P}$ of the monomer and not for each double bond. The difference is also reflected in the values for the theoretical polymerization heat $\Delta H_{0,P}$. It was above the values for classical acrylates (70-80 kJ mol⁻¹), but lower than in the divinyl carbamate **36**, indicating different rates of conversion for the unequal polymerizable functionalities.

For compound **34** also PI-free samples were analysed. The DBC from these measurements was 66%, the theoretical polymerization heat was found to be in good accordance with the photo-DSC experiments, where a PI had been added ($\Delta H_{0,P} = 102000 \text{ J mol}^{-1}$).

4.1.2.3. Photo-DSC

Investigations aimed on the one hand at self-initiating ability in aspects of the previously synthesized acrylic hydroxylamine compounds and on the other hand at the monomer reactivity of the vinyl compared to the acrylic compounds. Therefore experiments with and without additional PI (Darocur 1173; 99 mmol L⁻¹) were conducted. As reference materials commercially available mono- and diacrylates

(lauryl acrylate; **LA** and hexane-1,6-diol diacrylate; **HDDA**) as well as mono- and divinyl esters (decanoic acid vinyl ester; **DVE** and divinyl adipate; **DVA**) were used.

4.1.2.3.1. PI-free photopolymerization

All three vinyl containing hydroxylamine compounds, **34**, **36** and **38** were tested for self initiating ability, as all were containing the UV cleavable N-O bond.⁹² As reference materials self-initiating di- and triacrylates **27** and **32** were used.

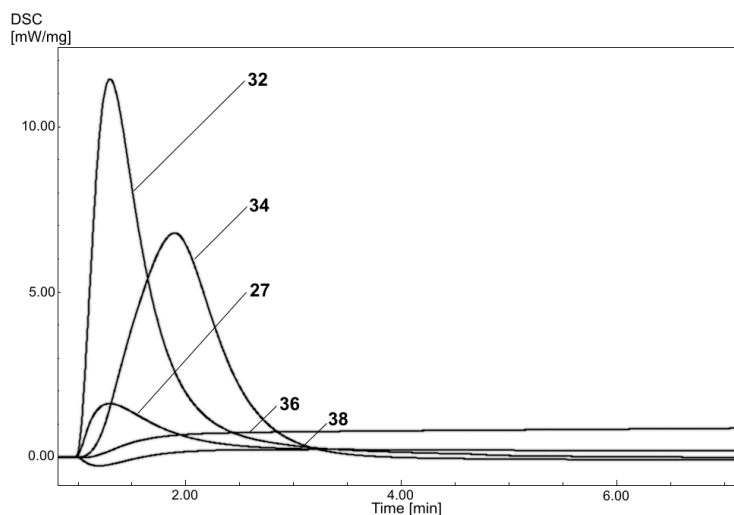


Figure 65: Photo-DSC Plots for PI-free measurements of vinyl compounds **34**, **36** and **38** in comparison with diacryloylated compound **27** and triacryloylated compound **32**

Table 19. Photo-DSC data for monomers **34**, **36** and **38** in comparison to acrylates **27** and **32** without PI

Compound	t_{\max} [s]	DBC [%]	$R_p \times 10^3$ [mol L ⁻¹ s ⁻¹]
34	56	66	751
36	-	-	-
38	-	-	-
27	30	24	111
32	20	43	629

As one can see from Figure 65, vinyl-acryl compound **34** showed better self-initiation activity than diacryl compound **27**, although the efficiency of triacrylate **32** could not be reached. Only t_{\max} , was increased for **34**, but this was acceptable for vinyl monomers compared to the considerably faster polymerizing acrylates. Surprisingly, the vinyl carbamate monomers **38** and **36** displayed no self-initiating ability. Obviously, the scission of the N-O bond cannot take place to a sufficient extent due to the less conjugated system. Furthermore, the difference in reactivity of the radicals

formed by UV-curing and the reactivity of the monomer double bond might play a role. Although vinyl radicals are highly reactive, vinyl monomers are significantly unreactive compared to monomers bearing an acrylic double bond. Probably, the vinyl radicals would rather terminate by proton abstraction, than adding to another vinylic C=C bond. Therefore, only compound **34**, which also contains an acrylic C=C bond was able to form a solid polymer upon irradiation with UV light.

4.1.2.3.2. Monomer reactivity with a Type I PI

By photo-DSC experiments monomer reactivity of **38**, **36** and **34** should be investigated and compared to self-initiating monomers **27** and **32**, as well as to standard acrylates and vinyl esters as lauryl acrylate (**LA**), hexane-1,6-diole diacrylate (**HDDA**), decanoic acid vinyl ester (**DVE**) and divinyladipate (**DVA**). Therefore, also experiments with the monomers and 2wt% PI (Darocur 1173) were carried out as outlined in Figure 66.

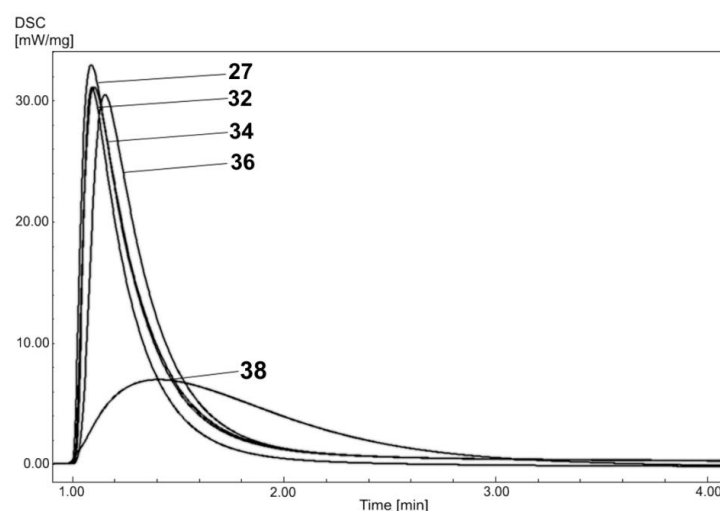


Figure 66: Plots for Photo-DSC experiments of compounds **34**, **36** and **38** in comparison to **27** and **32** with 2wt% PI (Darocur 1173)

Table 20. Photo-DSC data for monomers **34**, **36**, **38** in comparison to **LA**, **DVE** and **DVA** as well as **HDDA** and **DVA** (with 2wt% Darocur 1173 as PI)

Compound	t_{\max} [s]	DBC [%]	$R_p \times 10^3$ [mol L ⁻¹ s ⁻¹]
34	6.4	82	301
36	10.2	70	182
38	30.6	81	73
27	6.6	62	269
32	7.2	79	176
LA	4.0	91	359
DVE	7.8	88	99.4
HDDA	2.3	83	578
DVA	12.4	90	299

As shown in Table 20 diacrylate reference **HDDA** was the most reactive compound due to its high crosslinking ability and acrylate nature. Divinyl reference **DVA** displayed lower reactivity, but a slightly better DBC than the diacrylate. The monofunctional references **LA** and **DVE** displayed a lower polymerization rate than the difunctional references due to the lack of crosslinking reactions. Again the acrylate **LA** was more reactive than the vinyl ester **DVE**. Unexpectedly, the monovinyl ester **DVE** reached t_{\max} faster than the divinyl ester **DVA**. Assumedly, in the case of **DVA**, the rapid formation of crosslinks was outbalanced by the lower monomer reactivity. The hydroxylamine-based di- and triacrylates **27** and **32** were significantly less reactive than the commercially available acrylate references, as already discussed in chapter 3.

Due to minor reactivity of vinyl monomers, t_{\max} of divinyl carbamate **36** was significantly increased compared to the diacrylates **HDDA** and **27**. As expected, compound **38** displayed the lowest reactivity due to its monovinyl nature. Compared to the photo-DSC data for the reference monomers in Table 20, the reactivity of **34** ranged between monoacrylates and monovinyl esters according to its bivalent nature. However, these data should be considered carefully, as it is not possible to allocate specific features exactly to one of the two polymerizable groups. It can be assumed, that the good reactivity originated mainly from the acrylate double bond.

4.1.2.4. Toxicology Tests

With respect to possible application as biomaterials, a first evaluation concerning toxicology of the monomers should be performed with osteoblast cells. One important parameter to be determined is the interpolated concentration, where one half of the cells survived after a determined time span (5 days) in comparison to a control group, the so-called “In-vitro LC₅₀” value.

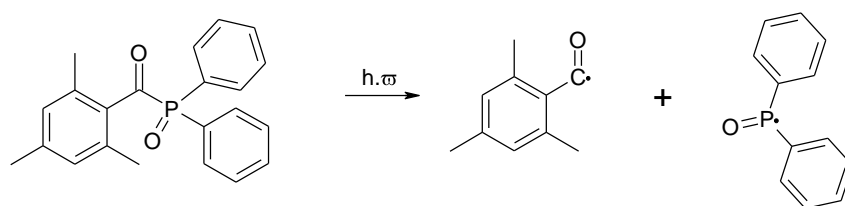
Table 21. In-Vitro LC50 data for vinylcarbamates **38**, **36** and **34** in comparison to acrylate **HDDA**

Compound	LC ₅₀ [mol L ⁻¹]
38	>100
34	<0.1
36	>100
HDDA	<0.1

The data in Table 21 shows, that the vinyl ester monomers **38** and **36** were at least three orders of magnitude less toxic than the reference acrylate **HDDA**. Only compound **34** displayed an equally toxic behaviour as the reference monomer due to its own acrylate group. Nevertheless, it could be considered a valuable tool for biomedical applications, at least due to its good reactivity and self-initiating properties. An imaginable application could be as co-polymerizing photoinitiator for biopolymers. The only limitation for its use might be the total removal of residual monomer from the cured material, by evaporation or several extraction steps.

4.2. Phosphorus-containing vinyl esters and vinyl carbamates

Generally, acylphosphine oxides have an important function as acylating agents in organic synthesis for nucleophiles like alcohols and amines. The mono- and bisacylphosphine oxides also serve as photocleavable initiators for radical polymerizations. Many studies have aimed at the generation of the reactive phosphorous radicals as well as their structural characterization. The mechanism for the α -cleavage of (2,4,6-trimethylbenzoyl)diphenylphosphine oxide from a triplet excited state to give the 2,4,6-trimethylbenzoyl and the diphenylphosphinoyl radicals as presented in Scheme 36, is well known.^{184,185,186}



Scheme 36. Formation of the diphenylphosphinoyl radical

Their use as self-initiating monomers has not been recorded in literature so far to the best knowledge of the author. Cho *et al.*¹⁸⁷ described photolysis experiments of alkenyl acylphosphonates to obtain radical cyclization adducts by intramolecular acylation. In their paper they reported a photochemical induced cleavage of alkenylacyl phosphine oxides with two phenyl rings attached to the phosphorus-atom. In contrast to that, they demonstrated, that no radicals were formed, if the phenyl groups were replaced by two ethoxy moieties (Figure 68).

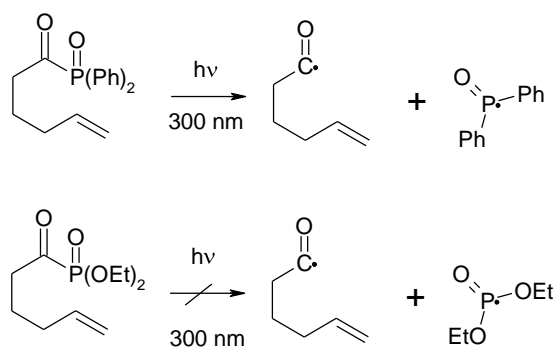


Figure 67. Cleavage mechanism for alkenyl acyl phosphine oxides proposed by Cho *et al.*

Nonetheless, the first representatives of acylphosphine PIs were dialkyl esters of acylphosphonic acids such as **DEBPO** as shown in Figure 69.

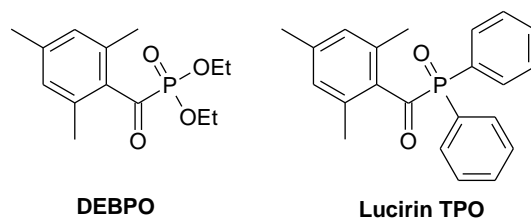


Figure 68. Structures of the first acylphosphine PIs

As their reactivity was low compared to common PIs, the alkoxy groups were exchanged by aryl moieties as in Lucirin TPO, thus delivering PIs with excellent reactivity.¹⁸⁸

These experiences from literature suggested the use of phenyl substituents for the targeted phosphorus-based self-initiating monomers. However, considering better biocompatibility also monomers with ethoxy substituents should be prepared. The nature of the polymerizable moiety should match the demands for biocompatibility, therefore the vinyloxycarbonyl and the methacrylate groups were chosen (Figure 70).

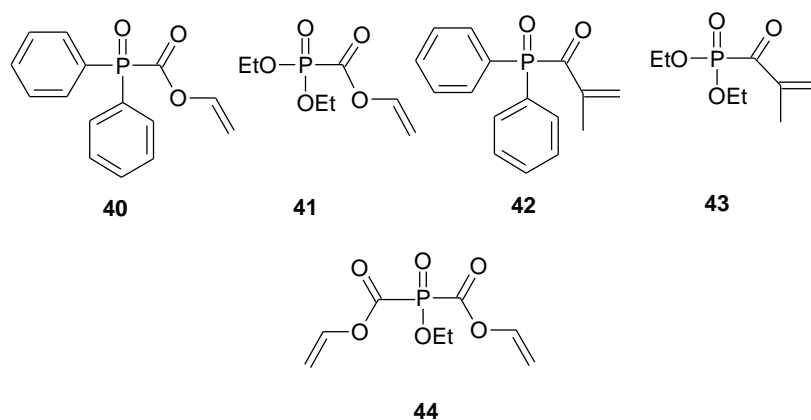


Figure 69. Structures of target phosphomonomers with assumed self-initiating properties

As already discussed in the general introduction to chapter 4, during this study also phosphate-based, degradable monomers without self-initiation, but enhanced biocompatibility and resemblance with bone structure, should be designed.

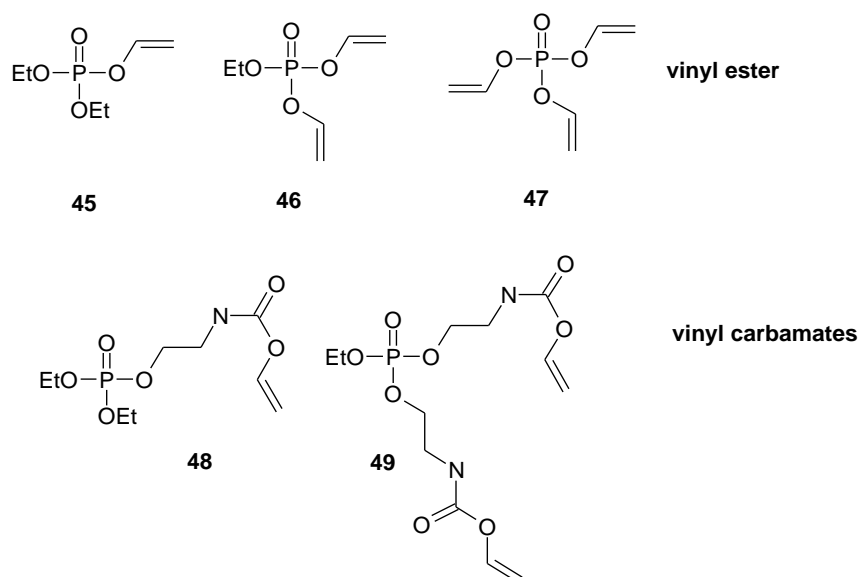


Figure 70. Structures of target phosphomonomers without self-initiation

Basically, vinyl esters of phosphoric acid similar to target molecules **45** and **46**, own a broad application spectrum as insecticides¹⁸⁹ and in pharmaceutical industry,¹⁹⁰ but they can also form polymers by radical polymerization, which are mainly in use in flame-retardant materials.¹⁹¹ According to Hayashi¹⁹² monovinyl and divinyl phosphates provide linear, respectively cross-linked polymers, that are able to undergo hydrolyzation. Inspired by the studies of Hayashi, biocompatible polymers should be obtained, that deliver only polyvinylalcohol and phosphates after degradation. Thus, non-toxic poly(vinyl alcohol) would be formed by hydrolytic decomposition, in contrast to scaffolds based on polyacrylates proved to be harmful due to residual monomer and degradation products, which have an adverse effect on the cells already adhered to the scaffold's surface and inhibit further cell adhesion by Michael addition to amino or thiol containing groups in proteins or DNA.^{170,174} Recently, the use of phosphoric acid esters containing polymerizable groups for hydrogels based on poly(ethylene glycol) and polyphosphoesters were reported by Du and co-workers.¹⁹³ Hydrogels act as drug and gene delivery matrices,¹⁹⁴ but also as scaffolds for tissue engineering¹⁶⁹ due to their good biocompatibility. Especially hydrogels which are formed in situ of the critical defect at physiologic conditions by photo-cross linking, are very common. Another point of interest is the biodegradability of polymers, which in the most ideal case leads to decomposition of the scaffold completely after the new tissue was formed. Well-known biodegradable polymers are based on poly(ethylene glycol), in addition to oligomers of polyesters such as

poly(caprolactone) and poly(lactide) containing acrylate groups.¹⁹³

Hence, considering toxicity and biocompatibility as well as biodegradability, also monomers for phosphate-based polymers containing a polymerizable vinyl ester group separated by a C2 linker as in **48** and **49**, should be developed. For both monomers, 2-hydroxyethyl vinyl carbamate was considered as an appropriate spacer, as it was easily accessible for synthesis and had already been cited in literature as suitable contact lens material.¹⁹⁵

Summarizing, the purpose of this study was the development of biocompatible polymers, which might display self-initiating properties in case of the acylated phosphine oxides. With respect to the mono- and trivinyl esters of phosphoric acid, which were already reported by Gefter and Kabachnik,¹⁹⁶ these concepts were not yet found in literature to the best knowledge of the author.

Radical polymerization experiments by photo-DSC should be carried out, followed by the calculation of the double bond conversion (DBC) and the theoretical heat of polymerization, $\Delta H_{0,P}$, using ATR-IR spectroscopy and peak deconvolution (PeakFit V4.12, SSI).

To gain insight into the biological compatibility of compounds resulting from unpolymerized monomers or products from the degradation process, the influence of the monomers on cell multiplication, viability and the expression of alkaline phosphatase (ALP) activity of osteoblasts should be investigated. Studies on mechanical stability can be performed by nano-indentation. Degradation behaviour of the crosslinked polymers should be monitored by weight loss of the samples under alkaline and acidic conditions.

4.2.1. Synthesis of phosphonates and phosphoformates

The syntheses of the monoacylphosphates and the phosphoformates **40-43** can be conducted according to the Michaelis Arbusov reaction.

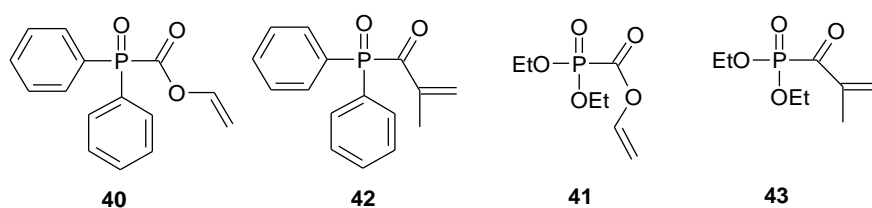
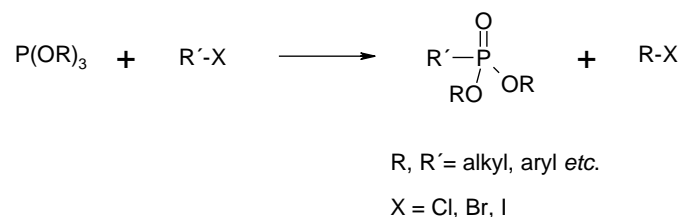


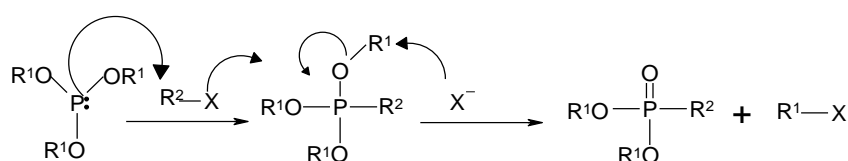
Figure 71. Structures of target phosphonates and phosphoformates

This reaction type was firstly described by August Michaelis in 1898¹⁹⁷ and further investigated by Aleksandr Arbuzov.¹⁹⁸ Herein, a phosphonate is formed from a trialkyl phosphite and an alkyl halide (Scheme 37).



Scheme 37. General reaction equation for the Michaelis-Arbuzov Reaction

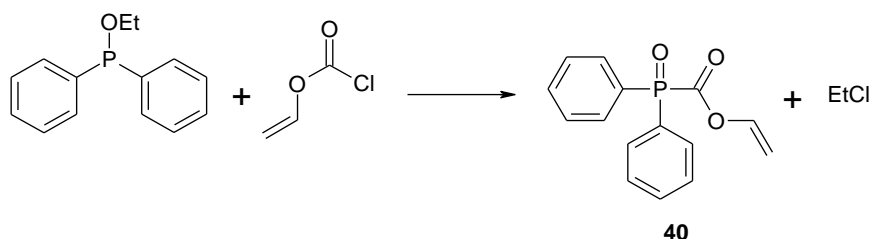
It has proved to be a convenient method to obtain many different phosphonates, phosphinates and phosphineoxides for organic synthesis. The mechanism is presented in Scheme 38. It consists of two nucleophilic substitution reactions of the type S_N2. Firstly, the free electron pair on the phosphorous atom in the nucleophilic phosphite (I) attacks the electrophilic alkyl halide in an S_N2-reaction. Therein a phosphonium intermediate is formed, which is transformed into the appropriate phosphonate by another S_N2-reaction, where the free halide takes one alkyl residue of the alkoxy group attached to the phosphonium molecule. Triarylphosphites are not able to perform the second step in the Michaelis Arbuzov reaction and form stable phosphonium salts.¹⁹⁹



Scheme 38. Mechanism of the Michaelis Arbuzov reaction

4.2.1.1. Diphenyl vinyloxycarbonyl phosphineoxide (**40**)

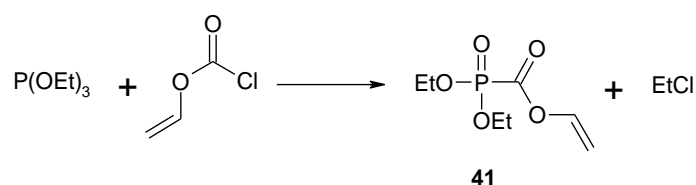
Diphenyl vinyloxycarbonyl phosphineoxide (**40**) was prepared according to Michaelis-Arbuzov conditions.



The ethyldiphenyl phosphinite was reacted with an equimolar amount of chlorovinylformate. After removal of all volatile compounds by distillation the pure product was obtained without further purification. ^{31}P and ^1H -NMR spectra showed only signals of the desired product. Purity was confirmed by GC-MS analysis. Product **40** was yielded in 98% as a white solid.

4.2.1.2. Diethyl vinyl phosphoformate (**41**)

Diethyl vinyl phosphoformate (**41**) was prepared analogue to diphenyl phosphineoxide **40** by adding chlorovinylformate at to triethyl phosphate without using any solvent.



The reaction went smoothly, without by-products. From ^{31}P -NMR analysis of the crude product no impurities containing phosphorous were visible. In ^1H -NMR residues of ethylchloride and vinyl ethanoate were detectable. Therefore, a purification by vacuum distillation was performed to obtain pure compound **41** in 83% yield.

4.2.1.3. Attempted synthesis of ethyl divinyl phosphobisformate (**44**)

Although the Michaelis Arbusov reaction is an excellent method to introduce one acyl group directly to the phosphorous atom, it would not be possible to obtain di- or trifunctional monomers by this method, which would also be an interesting aspect to this study.

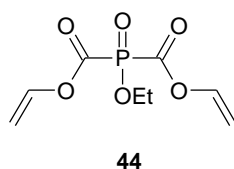


Figure 72. Structure of target phosphobis formate **44** analogous to monovinyl monomer **41**

An appropriate method to obtain **44** would be the formation of bisacylphosphine oxides from bistrimethylsilylhypophosphite (**50**) - accessible by reaction of trimethylsilyl silazane with ammonium hypophosphite as described by Isleib *et al.*²⁰⁰ Conversion of **50** with 1 equ. of chloroformate, would deliver the bistrimethylsilylacyl-

phosphonate or formylphosphonate. By reaction with another equivalent of the chloroformate, the bisacylphosphine oxide **51** could be obtained via a Michaelis-Arbuzov reaction, eliminating trimethylsilyl chloride. The final step should consist of ethanolysis of the trimethylsilyl group to obtain **44**.

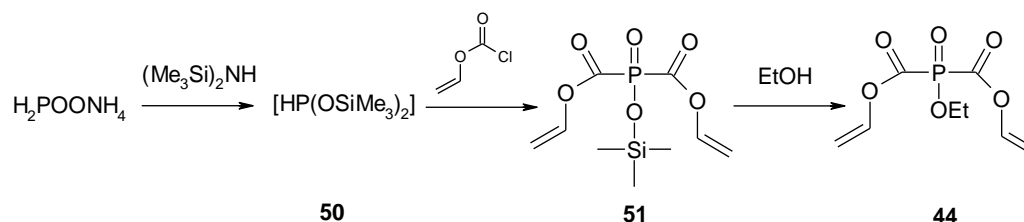
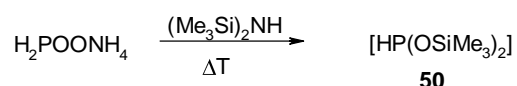


Figure 73. Proposed synthesis pathway to obtain divinyl monomer **44**

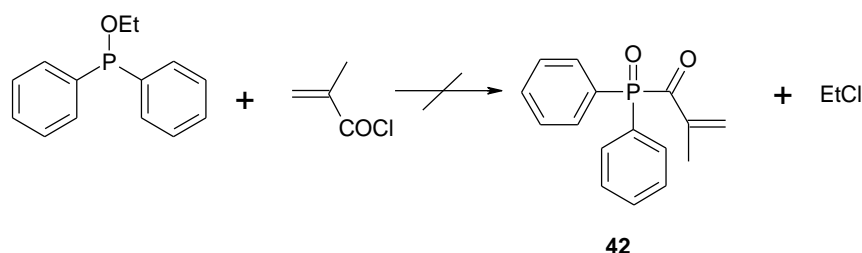
This reaction seemed a convenient way to get the desired phosphobisformate **44**. Therefore, according to the procedure described by Issleib *et al.*²⁰⁰ **50** was obtained from ammoniumhypophosphite and hexamethyldisilazane by mixing equimolar amounts of both compounds together under an inert and water-free atmosphere and heating the mixture up to 100°C.



After the evolution of ammonia had stopped, the raw product of **50** should be isolated by vacuum distillation. The reaction was cancelled at this stage, as the intermediate turned out to be highly flammable at simple traces of air. Due to these extremely dangerous reaction conditions and the lack of suitable laboratory equipment for safe handling of these compounds, no further experiments were performed on this route.

4.1.2.4. Diphenyl methacryloyl phosphineoxide (**42**)

As precursor for the Michaelis-Arbuzov reaction ethyldiphenylphosphinite was used.



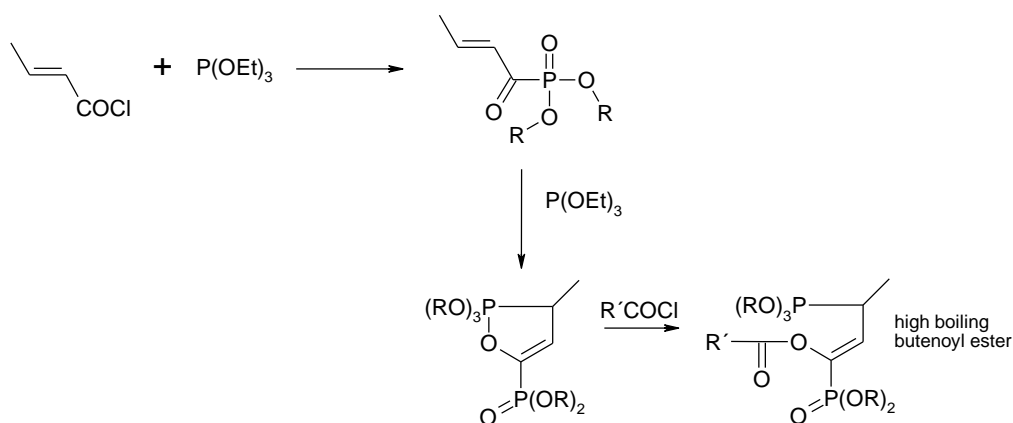
An equimolar amount of phosphinite and methacryloyl chloride were mixed and stirred at room temperature for 10 h. ³¹P-NMR analysis during the reaction already showed numerous by-products. Interestingly, when the product mixture was

investigated by TLC analysis, one spot could be seen under the UV-lamp at 366 nm, whereas at least 6 products were visible at 245 nm. The spot, which was visible at the higher UV-wavelength vanished after some time of irradiation. This observation led to the assumption, that the desired photo-reactive product **42** had been formed during the reaction and its radical decomposition was visible under irradiation with UV-light. Finally, **42** was located by a GC-MS analysis of the reaction mixture. Unfortunately, a separation from the various by-products was not possible due to rapid decomposition and transformation to diphosphoesters, as reported by Lindner *et al.*,²⁰¹ who already had tried to synthesize compound **42**. They discovered, that this Arbuzov reaction was not possible with acryloyl and methacryloyl chlorides, as the desired acylphosphineoxides were immediately transformed to an instable enolether and under cleavage of ethylchloride to the resulting phosphodiester.

4.2.1.5. Diethyl methacryloyl phosphonate (**43**)

No evidence for the successful synthesis of methacryloyl derivative **43** has been reported in literature yet.

Szpala *et al.*²⁰² indicated in their paper from 1989, that the formation of dimethyl-*trans*-but-2-enoylphosphonate could be obtained by slow addition of trimethylphosphite to a three-fold excess of *trans*-but-2-enoyl chloride at room temperature (Scheme 39).

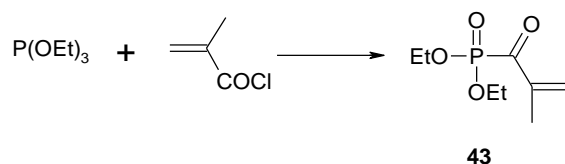


Scheme 39. Mechanistic pathway leading to the high boiling butenoyl ester

If the reaction was carried out with equimolar ratio of both reactants, then a high boiling oil was obtained, which they identified to be an ester containing two phosphorous atoms.

Szpala and co-workers postulated further, that also methacryloyl chloride reacted with the α -ketophosphonate more slowly and therefore the ketophosphonate was the major product, whereas the acryloyl chloride reacted much faster with the α -ketophosphonate even at a large excess of the acid chloride.

Therefore, with respect to the experiences from literature, the triethylphosphite was converted with a three-fold excess of methacryloyl chloride.



After the reaction was completed, the desired product **43**, could be isolated directly by high vacuum distillation in 21% yield. It was also tried to purify the crude product by column chromatography, but this method delivered product which was still impure and a following high vacuum distillation was necessary. Nevertheless, also traces of an butenoyl ester, similar to the one described in the paper of Szpala²⁰² could be identified in the ³¹P-NMR spectrum of the raw product ($\delta = 11.1$ ppm and 30.9 ppm) with chemical shifts of both phosphorus atoms comparable to the ones presented by Szpala and co-workers.²⁰²

4.2.2. Synthesis of vinyl esters of phosphoric acid

There are several synthetic pathways cited in literature to obtain vinyl phosphate esters, such as the Perkow reaction,²⁰³ dehydrochlorination of corresponding 2-chloroethylesters,²⁰⁴ use of mercurials,²⁰⁵ or chloroacetaldehyde.²⁰⁶

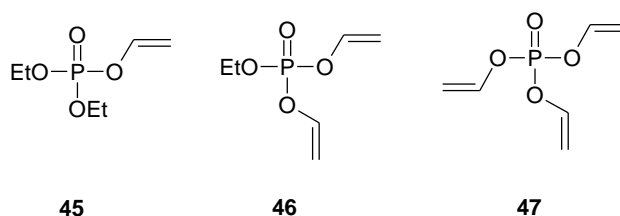


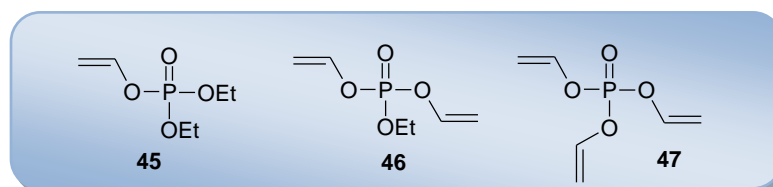
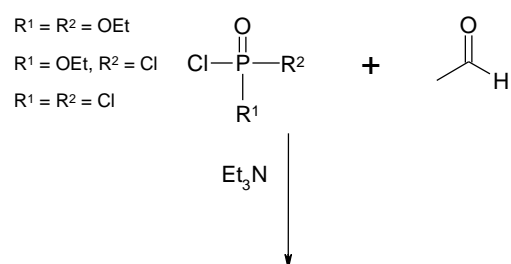
Figure 74. Structures of target vinyl esters of phosphoric acid

Most of these reactions contain undesirable or hazardous reagents. For example, in the Perkow reaction a trivalent phosphor with at least one alkoxy group is added to an α -haloketone. The vinyl group is introduced via anhydrous chloroacetaldehyde, which is uneasy to handle and not readily available. It can be generated in situ from

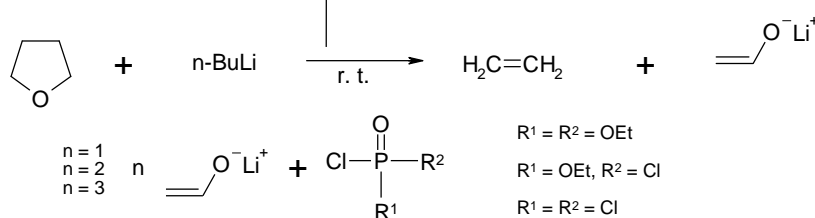
chloroethylene carbonate and catalytic amounts of triethylamine. Another possibility is the use of mercury salts, but this method definitely is expensive and leads to environmental problems.

Basically, two possible reaction pathways were chosen as shown in Scheme 40. On the one hand, the method of Gefter and Kabachnik could be applied, converting acid chlorides of phosphoric acid with acetaldehyde and triethylamine into the corresponding vinyl esters. On the other hand, the lithium enolate of acetaldehyde can be obtained by cycloreversion of tetrahydrofuran,¹¹¹ followed by reaction with the appropriate acid chloride of phosphoric acid.

pathway 1



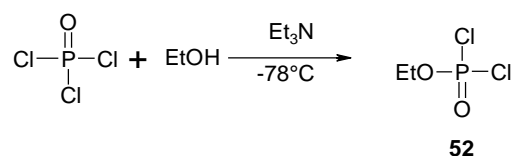
pathway 2



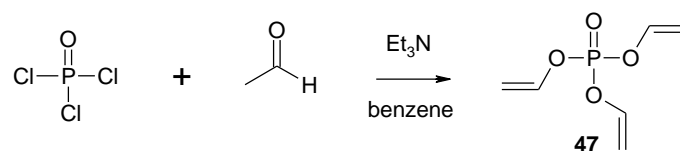
Scheme 40. Pathway 1: Using acetaldehyde and triethylamine according to Gefter *et al.* Pathway 2: Reaction mechanism for the cycloreversion of tetrahydrofuran, followed by reaction with mono-, di- and trichlorophosphates

In any case, appropriate phosphate precursors are required. While diethylchlorophosphate and phosphoryl chloride were purchased from Aldrich, the precursor for the divinylated phosphate, dichloroethylphosphate (**52**), was prepared easily from phosphoryl chloride and ethanol at low temperature according to Jones *et al.*²⁰⁷ After purification by vacuum distillation the product was obtained in 81% yield

as colourless liquid.



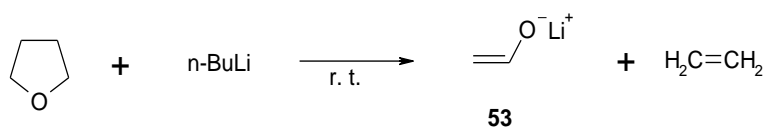
In a first attempt, the trivinylated phosphate should be prepared by a modified method of Gefer and Kabachnik,¹⁹⁶ who reported the formation of the trivinylated compound based on the formation of 1-chloroalkyl esters of trivalent phosphorous from phosphorous chlorides and aldehydes, which yielded the vinyl ester by addition of a base due to dehydrohalogenation.



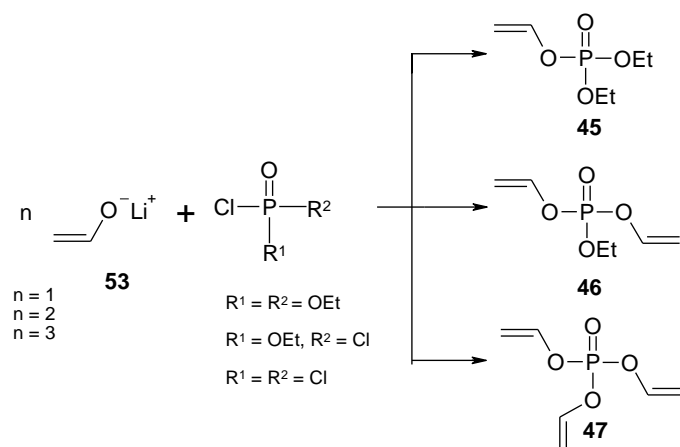
Therefore, phosphoryl chloride was treated with a three-fold excess of acetaldehyde and triethylamine under cooling and stirring in benzene. According to literature, the reaction took several days in the refrigerator, but even after 14 days at 4°C ¹³P- and ¹H-NMR did not show signals for the desired product. When the reaction mixture finally was distilled under reduced pressure, only triethylamine could be obtained. Probably the product already had polycondensated in the residue, which was a dark red highly viscous oil.

Searching for a more convenient procedure, the formation of the lithium enolate of acetaldehyde *via* the cycloreversion of tetrahydrofuran seemed a very good alternative to above mentioned methods. The reaction mechanism was reported by Bates *et al.*¹¹¹ and has already found broad application.^{189,190,208,}

Accordingly, n-butyllithium (2.1 M solution in THF) was added to THF at 0°C. This mixture was stirred at room temperature for 16 h to obtain the lithium enolate of acetaldehyde, which is formed preferably at higher temperatures.



This solution was added to the corresponding phosphohalide and again stirred at room temperature for 16 h.



Good yields of the corresponding mono- and divinyl phosphates were obtained (50-60%), only for the trivinylated compound **47** yield was lower with 26%. Product might be lost on the one hand by formation of a by-product, which is generated from the reaction of the *n*-butyllithium with the chlorophosphate.²⁰⁷ Purification of the crude products was carried out by column chromatography, using petrolether and ethylacetate of various ratios as eluent. Also purification by high vacuum distillation was tried, but in this case degradation of the product due to thermal instability and partly polymerization reactions reduced the yields by far. Especially the trivinyl compound **47** seemed to be very sensitive to heating.

4.2.3. Synthesis of phosphovinyl carbamates

Phosphovinyl carbamates **48** and **49** as shown in Figure 76, should be synthesized from the corresponding mono- and dichlorides of phosphoric acid and a vinyl carbamate containing an hydroxyethyl group.

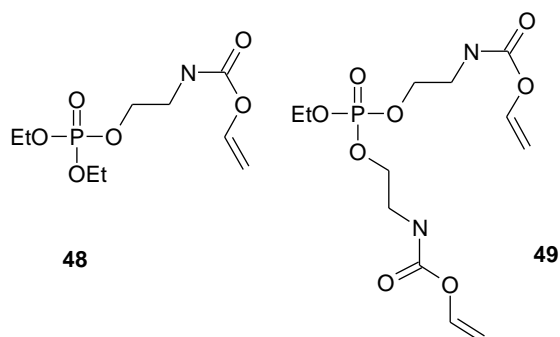
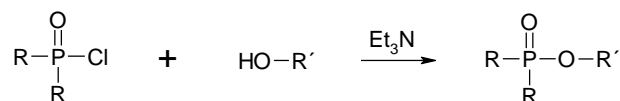
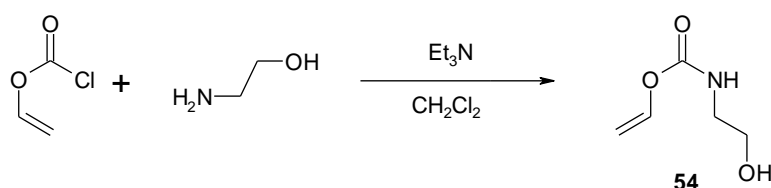


Figure 75. Structures of the target vinyl carbamates

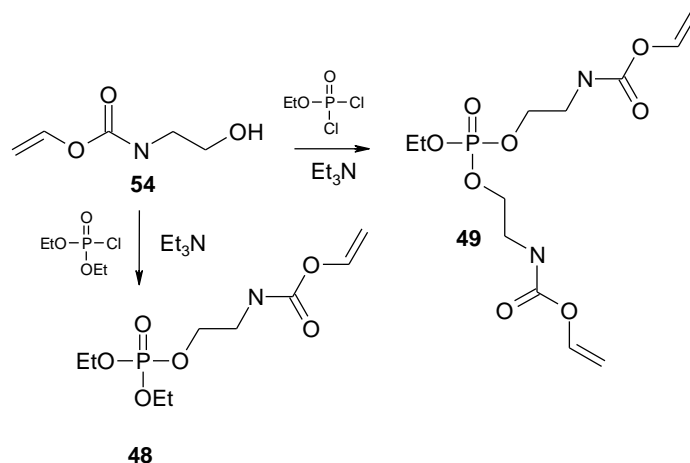
A convenient method to prepare esters of phosphoric acids is to convert phosphohalides, especially chlorides, with nucleophiles, such as alcohols or primary amines, to the corresponding phosphates using triethylamine as HCl scavenger.^{209,210,211}



As precursor-alcohol, 2-hydroxy-*N*-(vinyloxy) ethylamine (**54**) was prepared by adding the chlorovinyl formate to a two-fold excess of ethanolamine. The reaction went smoothly and after purification by high vacuum distillation the product was obtained in 75% yield.¹⁹⁵



The next step was the addition of the 2-hydroxy-*N*-(vinyloxy) ethylamine to diethylchlorophosphate and dichloroethylphosphate, respectively. A similar reaction was described by Liang *et al.*¹⁹¹ who used hydroxyethylacrylate as polymerizable residue.



The reaction was carried out using triethylamine as acid scavenger. After purification by column chromatography, the 2-(diethyl phospholoyloxy) ethyl vinylcarbamate (**48**) was obtained in 25% yield.

In the same way the divinylated compound, bis-(2,2'-(ethoxyphospholoyloxy) ethyl vinyl carbamate (**49**) was prepared. After 12 h stirring at room temperature still a

large amount of starting material was detected by TLC. To accelerate the reaction, the mixture was heated to 40-50°C for about 4 h. By TLC analysis it could be seen, that the amount of starting material was decreasing, but did not vanish. To avoid side reactions, e.g. addition at NH instead of OH, the reaction was stopped, even though still some starting material could be seen on the TLC plate. No extractive work up was performed to avoid loss of product in the aqueous layer.

After purification by column chromatography compound **40** was obtained in 43% yield.

4.2.4. Analyses

Successfully synthesized phosphorus containing vinyl esters and carbamates should be characterized by UV-Vis analysis and photo-DSC experiments, the later with respect to self-initiating behaviour and/or monomer reactivity. Concerning biocompatibility also toxicity tests on osteoblast cells can be conducted.

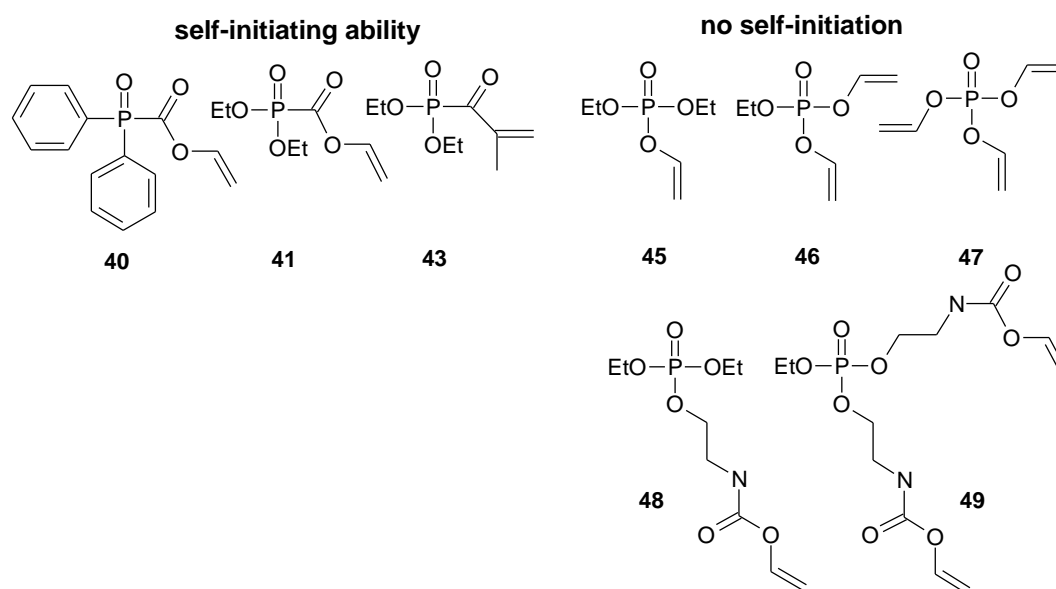


Figure 76. Structures of the investigated phosphorus-containing monomers

4.2.4.1. UV-Vis spectroscopy

UV-Vis spectroscopy of the phosphorous compounds containing an acyl residue should be carried out to investigate the existence of spin forbidden $n-\pi^*$ transitions (~360-450 nm), that would indicate the ability of these molecules to undergo α -cleavage and generate phosphoryl radicals upon irradiation with UV light and furthermore to act as self-initiating monomers as well. As reference materials a known monophosphineoxide PI, Lucirin TPO, and a simple vinyl ester, decanoic acid

vinyl ester (**DVE**), were used. All measurements were performed in acetonitrile solutions of 1×10^{-2} to 1×10^{-5} mol L⁻¹ concentrations.



Figure 77. Structures of references for UV-Vis spectroscopy, **DVE** and Lucirin TPO

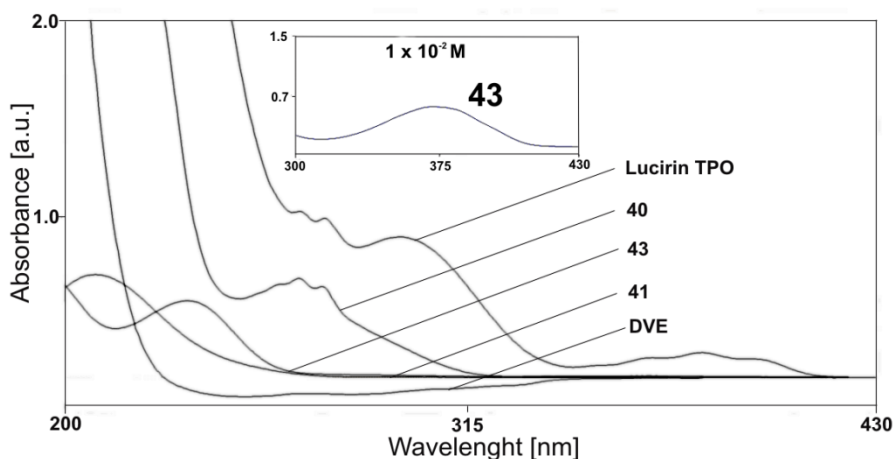


Figure 78: UV-spectrum of monoacylated compounds **40**, **41** and **43** in MeCN (1×10^{-4} , respectively 1×10^{-2} mol L⁻¹ for the insert of **43**) in comparison to phosphine oxide PI, Lucirin TPO and commercially available vinyl ester decanoic acid vinyl ester (**DVE**)

Table 22. UV-Vis data for compounds **40**, **41**, **43** and references **DVE** and Lucirin TPO

PI	$\pi-\pi^*$ transition		$n-\pi^*$ transition	
	λ_{\max} [nm]	$\epsilon_{\max} \times 10^{-2}$ [L mol ⁻¹ cm ⁻¹]	λ_{\max} [nm]	$\epsilon_{\max} \times 10^{-2}$ [L mol ⁻¹ cm ⁻¹]
40	266	55.7	-	-
41	208	57.7	-	-
43	234	43.0	372	0.47
Lucirin TPO	273	89.2	380	14.0
	295	78.7		
DVE	-	-	-	-

The data outlined in Table 22 demonstrated, that commercially available reference PI, Lucirin TPO, displayed maxima for the $\pi-\pi^*$ transitions at 273 and 295 nm. Its $n-\pi^*$ transition was located at 380 nm. As expected, the vinyl ester, **DVE**, displayed no significant absorption maxima at all.

UV-Vis spectra of the monomers showed for **40** a peak with maximum at 266 nm, which tailed out at 315 nm related to a $\pi-\pi^*$ transition. The vinyl ester **41** displayed a maximum for the $\pi-\pi^*$ transition at 208 nm with lower ϵ due to the absence of any aryl group. The $\pi-\pi^*$ transition of methacryloyl phosphineoxide **43** had a bathochromic shift of 26 nm compared to **41** due to an elongated conjugated system. At higher concentrations **43** showed also a maximum (372 nm), tailing out at 432 nm, which might belong to a $n-\pi^*$ transition. During this analysis only for the methacrylated compound **43** the $n-\pi^*$ transition with an apex at 372 nm could be seen in the very concentrated sample solution (1×10^{-2} mol L⁻¹), whereas the phosphoformate **41** showed only the normal $\pi-\pi^*$ transition at 208 nm.

Vinyl esters and vinylcarbamates **45–49** were not examined by UV-Vis analysis as for them no photoinitiating properties were expected.

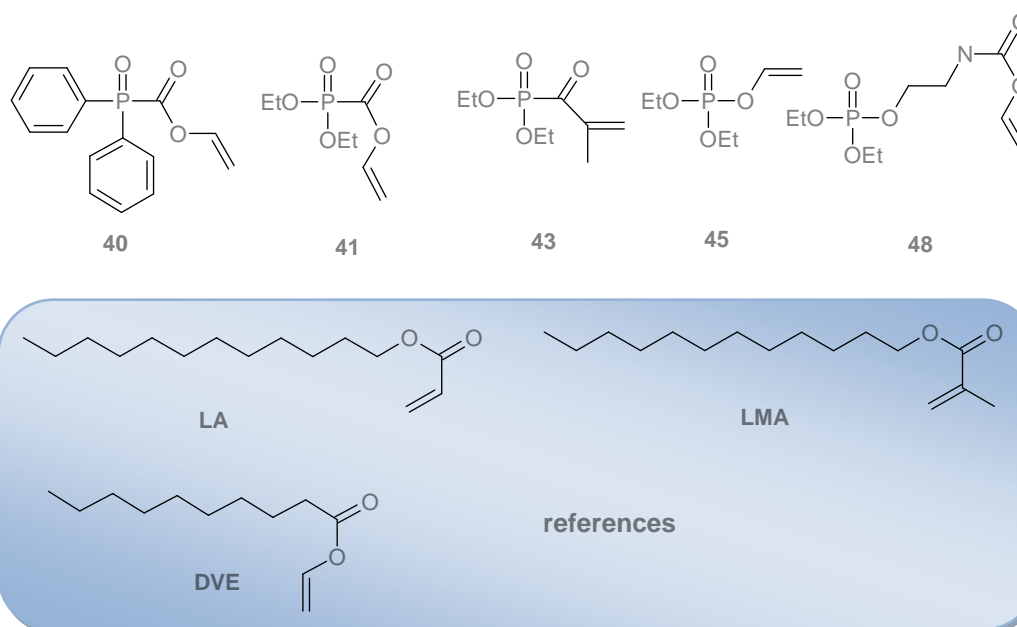
4.2.4.2. ATR-IR analysis

ATR-IR analysis of the phosphorous monomers should be performed to determine their photoreactivity. The DBC obtained from the comparison of the monomer IR spectra and the polymer IR-spectra should be used to calculate the theoretical polymerization heat $\Delta H_{0,P}$ in combination with the actual heat of polymerization from the photo-DSC experiments.

As described for the hydroxylamine-based monomers in chapter 3.2.2., the peak areas for the C=C bonds in the monomer and the polymer ATR-IR spectra were compared using peak deconvolution (PeakFit V4.12, SSI).

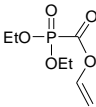
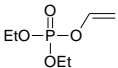
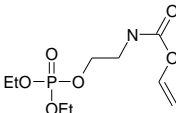
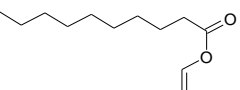
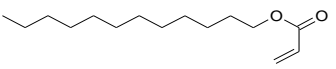
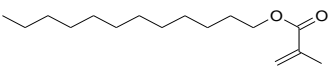
4.2.4.2.1. Monovinylated phosphorus containing monomers

The monomer reactivity of monophosphoformate **41**, monophosphovinyl ester **45** and monofunctional vinyl carbamate **48** was compared to a commercially available monovinyl ester, acryloyl ester and methacrylate ester as follows: decanoic acid vinyl ester (**DVE**), lauryl acrylate (**LA**) and laurylmethacrylate (**LMA**).



Of all examined compounds, polymer lenses were prepared by photo-DSC, which were investigated by the ATR-IR method to obtain the DBC. The C=O bonds at 1730 cm^{-1} in the ATR-IR spectra were considered as the internal reference, whereas the C=C bonds at 1645 and 890 cm^{-1} were investigated for the double bond conversion. In case of compound **45** the P=O bond at 1280 cm^{-1} in the ATR-IR spectra was considered as the internal reference, whereas the C=C bond at 1640 cm^{-1} were investigated for the double bond conversion. According equation 2 the DBC was calculated, which was used to calculate the theoretical polymerization heat, $\Delta H_{0,P}$. The values obtained for DBC and $\Delta H_{0,P}$ are shown in Table 23.

Table 23: Calculated DBC and theoretical polymerization heat values for compounds **41**, **45**, **48**, **DVE**, **LA** and **LMA** (2wt% Darocur 1173)

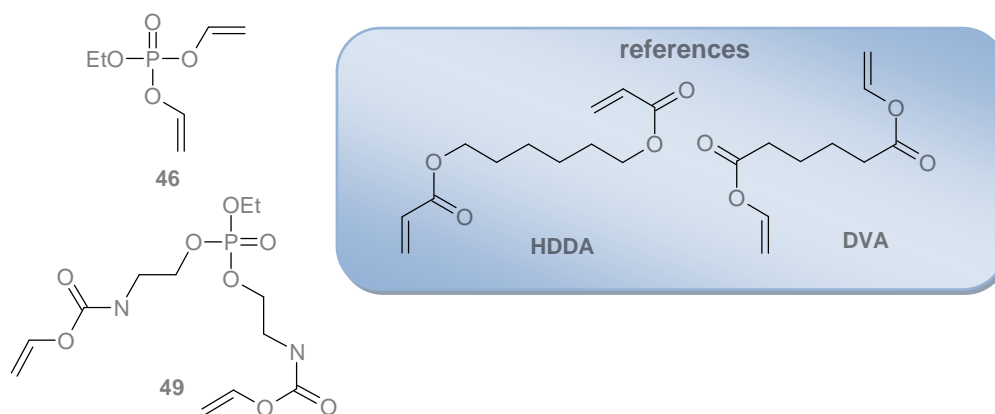
Compound	Structure	DBC [%] by ATR-IR	H _P [J g ⁻¹] by Photo-DSC	ΔH _{0,P} [J mol ⁻¹]
41		95	458	95900
45		90	417	83500
48		70	230	87800
DVE		88	362	81600
LA		91	293	77600
LMA		86	541	66900

The diphenyl derivative **40** could not be investigated as it was a solid. Nevertheless, it might have interesting co-polymerization properties.

For all compounds good DBC values between 70% and 95% could be obtained. ΔH_{0,P} values for the monovinyl esters compound **41** and **DVE** are in good accordance. Generally, the vinyl esters and vinylcarbamates had a higher theoretical polymerization heat than the reference acrylate **LA** and methacrylate **LMA**. No photoreactivity could be seen for the methacrylic phosphor compound **43**. There was no hardening of the sample for the photo-DSC experiments without nor with PI (2wt% Darocur 1173). The reason for the lack of self-initiation of **43** could be the formation of a stable phosphoryl radical. The inactivity of the monomer in presence of a PI could not be explained yet.

4.2.4.2.2. Divinylated phosphorus containing monomers

The monomer reactivity of the difunctional vinyl esters of **46** and **49** was investigated and compared to commercially available divinyl esters, as divinyl adipate (**DVA**), diacrylates, hexane-diol-1,6-diacrylate (**HDDA**).



Polymer lenses of all compounds were prepared by photo-DSC, which were examined by the ATR-IR method. In case of compound **46** the P=O bond at 1280 cm^{-1} in the ATR-IR spectra was considered as the internal reference, whereas the C=C bond at 1640 cm^{-1} were investigated for the double bond conversion. According equation 2 the DBC was calculated, which was used to calculate the theoretical polymerization heat, $\Delta H_{0,P}$. The values determined for DBC and $\Delta H_{0,P}$ are shown in Table 24.

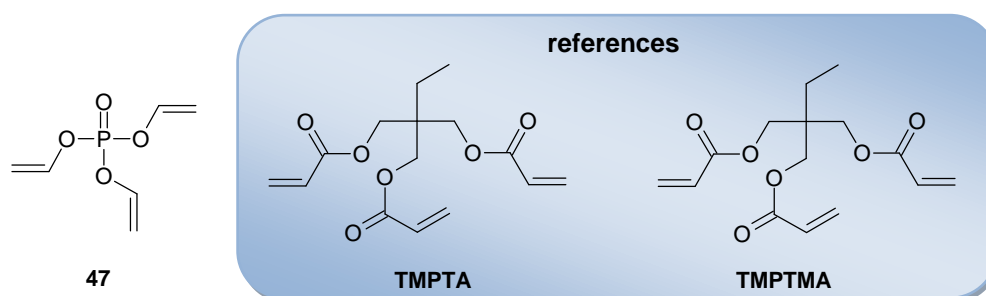
Table 24: Calculated DBC and theoretical polymerization heat values for compounds **46**, **49**, **DVA** and **HDDA** (2wt% Darocur 1173)

Compound	Structure	DBC [%] by ATR-IR	H_p [J g^{-1}] by Photo-DSC	$\Delta H_{0,P}$ [J mol^{-1}]
46		89	847	169600
49		59	291	173700
DVA		90	763	168100
HDDA		83	541	147600

The DBC value for **46** was rather high, considering the high crosslinking ability of difunctional monomers. For vinylcarbamate **49** the DBC was significantly lower, probably due to limited mobility of the molecule combined with lower monomer reactivity. The $\Delta H_{0,P}$ value for compound **46** was in perfect accordance with its monovinylated counterpart **45**, the same consistency could also be found for **49** and **48**. Also in these experiments the general trend of higher $\Delta H_{0,P}$ for vinyl monomers compared to acrylates could be confirmed.

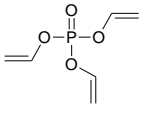
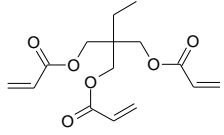
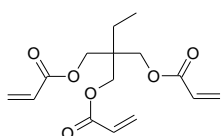
4.2.4.2.3. Trivinylated phosphorus containing monomers

Photoreactivity of the trivinylated phosphate ester was examined and compared to commercially available trivalent acrylic and methacrylic monomers, as follows: 1,1,1-trimethylolpropyltriacyrylate (**TMPTA**) and 1,1,1-trimethylolpropyl trimethacrylate (**TMPTMA**).



The P=O bond at 1250 cm^{-1} in the ATR-IR spectra was considered as the internal reference, whereas the C=C bonds at 1645 and 870 cm^{-1} were investigated for the double bond conversion. According equation 2 the DBC was calculated, which was used to calculate the theoretical polymerization heat, $\Delta H_{0,P}$. The values obtained for DBC and $\Delta H_{0,P}$ are shown in Table 25.

Table 25: Calculated DBC and theoretical polymerization heat values for compounds **47**, **TMPTA** and **TMPTMA** (2wt% Darocur 1173)

Compound	Structure	DBC [%] by ATR-IR	H_p [$J g^{-1}$] by Photo-DSC	$\Delta H_{0,P}$ [$J mol^{-1}$]
47		75	1141	267900
TMPTA		55	440	237400
TMPTMA		41	250	206300

The theoretical polymerization heat of compound **47** was again in good accordance to its structure analogues **45** and **46**. Surprisingly, also a very high DBC of 75% was reached for the trivinyl ester **47**. This extraordinary good double bond conversion for a trifunctional monomer compared to the trifunctional references could be explained by the smallness of the molecule compared to the rather bulky acrylate/methacrylate. The small molecule **47** could move through the viscous mass of polymerizing material much easier than the others, although also a high rate of crosslinking must be considered.

4.2.4.3. Photo-DSC

By photo-DSC experiments the photoreactivity of the phosphorous compounds should be investigated. It was the aim to determine the polymerization characteristics such as t_{max} , R_{Pmax} and the actual polymerization heat H_P for each compound.

For all experiments a Type I photoinitiator, Darocur 1173 should be used. Only for compounds **40**, **41** and **43** self-initiating ability was expected. Therefore also measurements under PI-free conditions should be performed. Additionally, their suitability as PI for standard acrylates like **HDDA** should be examined.

4.2.4.3.1. Monovinylated phosphorus containing monomers

Photo-DSC measurements of compounds **41**, **43**, **45** and **48** were carried out with Darocur 1173 as PI ($121 \mu\text{mol g}^{-1}$). Diphenyl phosphoformate **40** was not investigated in this series as it was a solid. As reference monomer systems **DVE**, **LA** and **LMA** were used. The plots in Figure 80 demonstrate, that the reactivity of all compounds but **43**, expressed by t_{max} , was surpassed the methacrylate, **LMA**. The plot for **43** is not shown, as no exotherm was detected.

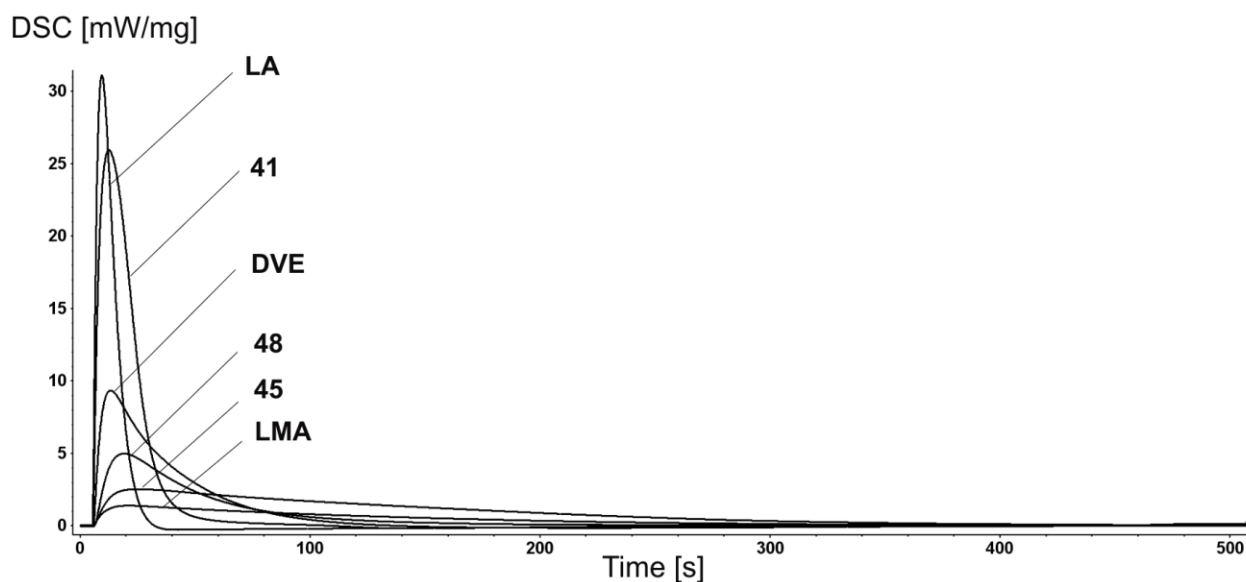
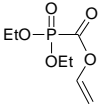
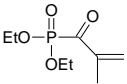
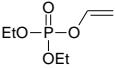
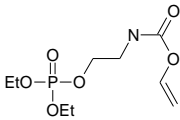
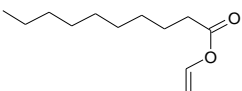
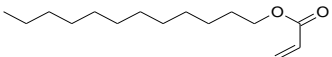
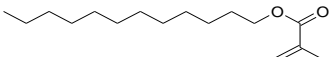


Figure 79: PDSC plots for monofunctional compounds **41**, **45** and **48** and the reference monomers **LA**, **LMA** and **DVE**

Table 26. Photo-DSC data for monomers **41**, **45**, **48**, **DVE**, **LA** and **LMA** with Darocur 1173 as PI (2 wt%)

Compound	Structure	t_{\max} [s]	DBC [%]	$R_{P\max} \times 10^3$ [mol L ⁻¹ s ⁻¹]
31		11.4	95	247
32		-	-	-
34		19.5	90	32.8
39		13.7	70	60.1
DVE		7.8	76	85.7
LA		4.0	99	290
LMA		15.8	86	18.6

Amazingly, the performance of **41** was significantly better than for the commercially available monovinyl ester **DVE** and only the acrylate, **LA**, superseded phosphoformate **41** only marginally with respect to $R_{P\max}$. The time to reach maximum polymerization heat, t_{\max} , was shorter for references **LA** and **DVE** than for **41**, which nonetheless beat the methacrylate, **LMA**. Reactivity of compounds **45** and **48** was not as good as for compound **41**. Whereas **39** exhibited comparable behaviour to **DVE**, the performance of **45** was considerably lower although a high DBC was reached (Table 26).

4.2.4.3.2. PI activity of monoacyl phosphineoxides **40**, **41** and **43**

The radical forming ability of monoacyl and diacyl phosphineoxides is well known from literature.^{184,185} Photo-DSC experiments with methacryloyl phosphineoxide compound **43** and the phosphoformates **40** and **41** should therefore elucidate their self-initiation ability and PI reactivity in a standard formulation with **HDDA**.

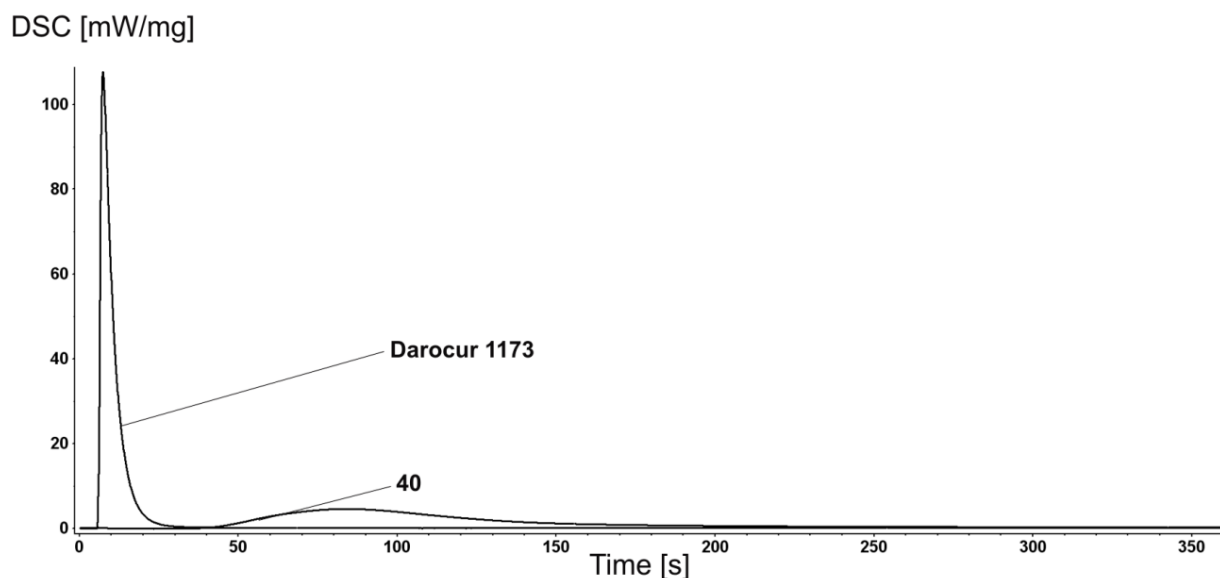


Figure 80. Photo-DSC plots for **HDDA** with 2wt% of compound **40** as PI compared to commercial available PI Darocur 1173

Diphenyl phosphoformate **40** as a solid could not be tested for its monomer, but its initiation ability. An acrylate formulation containing **HDDA** and 2wt% **40** as photoinitiator was investigated by photo-DSC. Surprisingly, compound **40** could act as PI due to its two phenyl substituents attached to the phosphorus atom as in well known PI, Lucirin TPO. The poor performance of **40** compared to industrially applied PI Darocur 1173 might be caused by the delocalization of the radical by the vinyl ester moiety. Unfortunately, for **41** and **43** no self-initiating ability could be detected in PI-free measurements. Also when compounds **41** and **43** were used as PI in **HDDA** (2 wt%) no initiation activity was detected. The inactivity of **41** might result from the lack of the phenyl groups, that are necessary for the radical formation process as it could be deflected from compound **40**. The structure of **43** might indicate better self-initiating ability than the vinyl esters as the radical cannot be delocalized efficiently by the methacrylate moiety. However, the presence of the two ethoxy groups might impair the radical generation. The ideal structure for the self-initiating monomer would be compound **42**, where the two ethoxy substituents were exchanged by two phenyl groups. Unfortunately, the isolation of **42** after synthesis had not been possible due to the hydrolytic instability of this compound.

4.2.4.3.3. Divinylated phosphorus containing monomers

Photo-DSC measurements of compounds **46** and **49** were carried out with Darocur 1173 as PI ($12.1 \mu\text{mol g}^{-1}$). As reference monomer systems commercially available vinyl ester **DVA** and acrylate **HDDA** were used.

DSC [mW/mg]

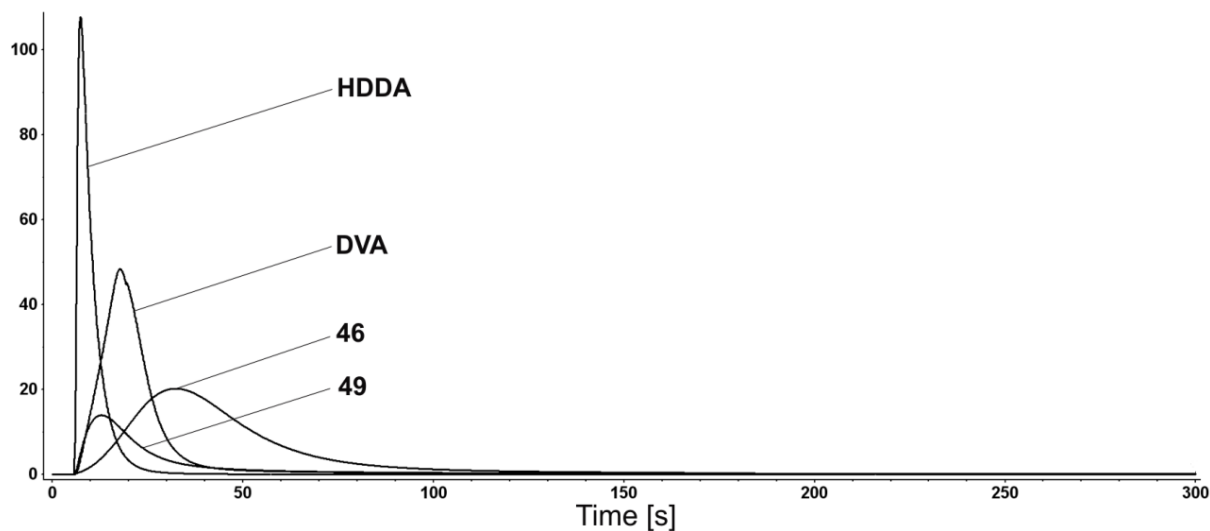


Figure 81 : PDSC plots for difunctional compounds **46** and **49** compared to diacrylate **HDDA** and divinyl ester **DVA**

Table 27. Photo-DSC data for monomers **46**, **49**, **DVA** and **HDDA** with Darocur 1173 as PI (2 wt%)

Compound	Structure	t_{max} [s]	DBC [%]	$R_{\text{Pmax}} \times 10^3$ [mol L ⁻¹ s ⁻¹]
46		27.0	89	127
49		7.3	59	68.2
DVA		12.4	90	299
HDDA		2.3	83	578

Divinyl phosphate **46** and vinyl ester reference **DVA** displayed very good double bond conversions, better than for reference acrylate **HDDA**, whereas reactivity expressed by t_{\max} and $R_{P\max}$ was significantly decreased for the vinyl compounds, probably due to lower resonance stabilization in vinyl radicals. Compared to monovinyl ester **45** the difunctional analogue **46** displayed better performance expressed by almost four times higher polymerization rate, although t_{\max} of **45** is slightly lower than of **46** due to its contorted peak form.

It is generally known, that increased molecular weight of the monomer decreases the polymerization rate of vinyl esters. This concept might also hold true for vinylcarbamates and might therefore explain the low $R_{P\max}$ and DBC values of **49**, which are in good accordance with the values for its monovinylated analogue **48**.

4.2.4.3.4. Trivinylated phosphorus containing monomers

Photoreactivity of trivinylated compound **47** and the reference triacrylate and trimethacrylate, **TMPTA** and **TMPTMA**, was investigated using Darocur 1173 as PI ($12.1 \mu\text{mol g}^{-1}$). Plots are shown in Figure 83.

DSC [mW/mg]

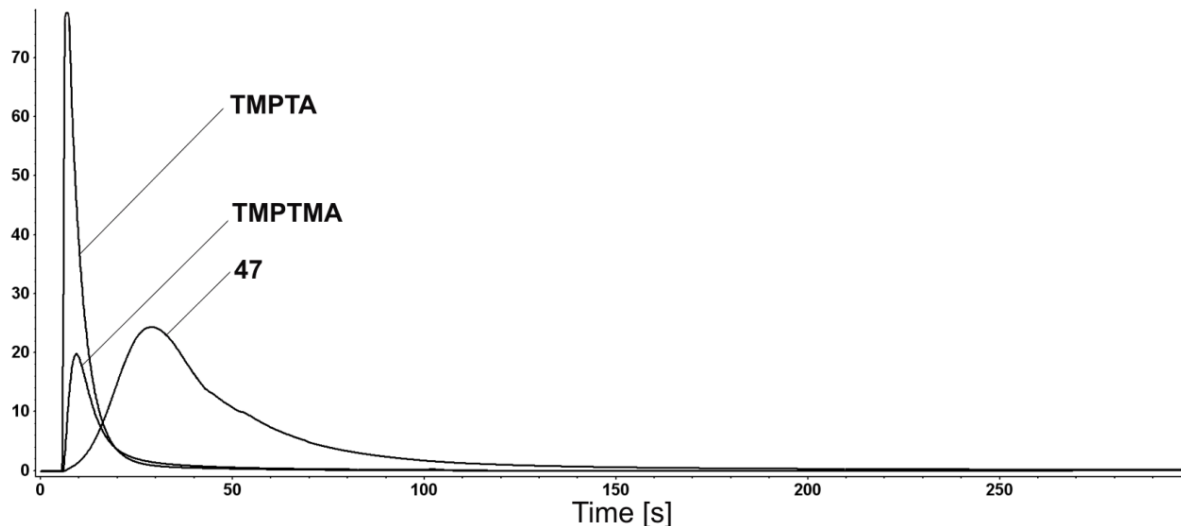
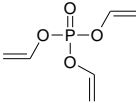
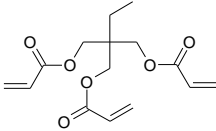
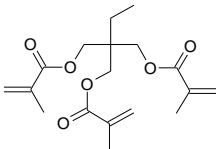


Figure 82: PDSC Plot for compound **47**, **TMPTA** and **TMPTMA** with Darocur 1173 (2wt%) as PI

Table 28. Photo-DSC data for monomers **47** and references, **TMPTA** and **TMPTMA** with Darocur 1173 as PI (2 wt%)

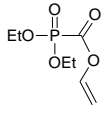
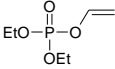
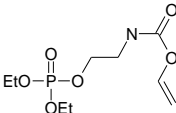
Compound	Structure	t_{\max} [s]	DBC [%]	$R_{P_{\max}} \times 10^3$ [mol L ⁻¹ s ⁻¹]
47		23.3	75	101
TMPTA		1.9	55	330
TMPTMA		3.5	41	102

As presented in Table 28, reactivity of **37** expressed by t_{\max} was relatively low for a trivalent monomer compared to the references **TMPTA** and **TMPTMA**. On the other hand, the double bond conversion superseded the value of the model compounds considerably. This might result also from the smallness of the molecule and therefore the ability to move within the gelating mass more quickly for an extended time than the more bulky molecules of **TMPTA** and **TMPTMA**. Compared to its difunctional analogue **46**, reactivity of **47** was in good accordance concerning the polymerization rate $R_{P_{\max}}$. The DBC differed only 10 % lower for the trifunctional monomer than for the difunctional compound, assumedly to the reasons already stated above in the comparison with the references **TMPTA** and **TMPTMA**.

4.2.4.4. GPC analysis

The monofunctional polymers were also subjected to GPC measurements in THF to determine the number average molecular weight, M_N , of the linear polymers. The results are shown in Table 29. Surprisingly, compound **41** superseded the other monofunctional monomers by one order of magnitude and proved its excellent monomer properties once more.

Table 29: M_N values and polymerization grade n for the linear polymers from compounds **41**, **45** and **48**, determined by GPC

Compound	Structure	M_N	n
41		37100	178
45		4900	27.2
48		3800	14.2

The low molecular weight of vinyl ester **45** and vinylcarbamate **48** might be caused by stronger influence of chain transfer reactions, which could also have contributed to the lower monomer reactivity, that was found for these two compounds in the photo-DSC experiments.

4.2.4.5. Toxicology and cell compatibility tests

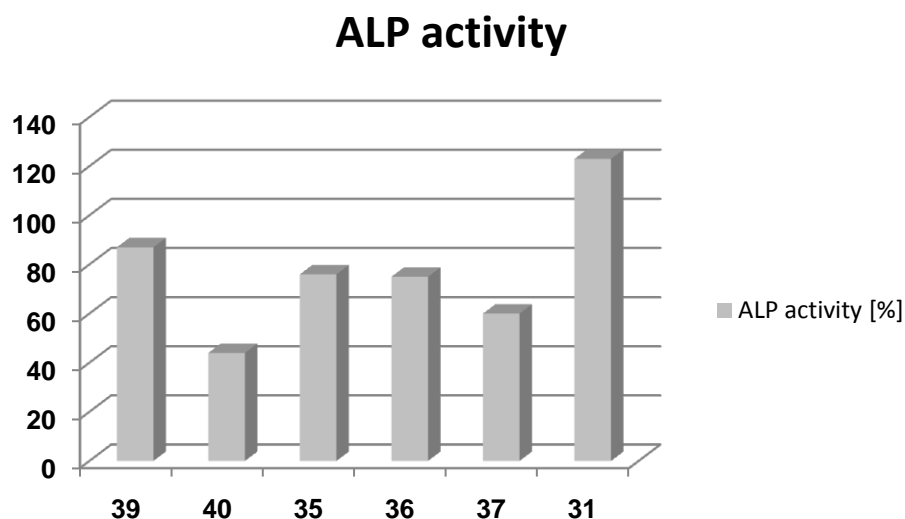
Cell viability and multiplication as well as ALP-activity of osteoblasts are sensitive indicators of any substance displaying its compatibility with the biological tasks of the cells. Especially the ALP-activity is an important indicator whether osteoblasts proceed in their differentiation process or are blocked by a reagent.²¹²

With respect to an onward application of the new phosphorus-containing monomers in the biomedical field, especially in osteosurgery, the monomers (excluding **43**, as it displayed no reactivity in the preceded experiments) should be tested for these parameters.

Therefore, MC3T3-E1 osteoblast cells were treated with monomers solutions of decreasing concentrations (0.1 M, 0.05 M, 0.025 M and 0.0125 M). In Table 30 the concentration in [mM] is given, where the half-maximal value of viability or DNA-content compared to control was found. The ALP-activity was the maximum value that was found at the investigated concentrations in % of the control (controls: cell cultures on a standard culture dish).

Table 30. Influence of the phosphorus-containing monomers on cell multiplication and viability

	40	41	45	46	47	48	49
Viability [mM]	3	12	6	5	3	8	5
Cell number [mM]	6	16	7	6	5	14	8

**Figure 83.** ALP activity on osteoblasts for the investigated phosphorus containing monomers

Although, some differences between cell viability and cell number were found, both parameters were comparable for all investigated monomers. In this match vinylcarbamate 48 and vinyl ester 41 had the least influence on cell multiplication. 48 had only marginal effect on ALP-activity (-13%) while 41 even increased (+23%) the activity of the osteoblastic enzyme indicating a stimulatory effect on osteoblast differentiation. All other monomers down regulated the ALP-activity indicating some influence on the osteoblastic differentiation process.

4.2.4.6. Mechanical properties

Nanoindentation should be applied to study the mechanical properties of polymers containing **41** with variable amounts of **46** as crosslinker, as well as polymers of **47** and **49** alone. By this method parameters like Young's Modulus (YM) and hardness (H) are easily accessible.

Thus, polymer disks were prepared by UV-curing of a sample of **47**, respectively **49** alone or of **41** with varying amounts of **46**. 2wt% of a photoinitiator (Irgacure 819)

was added to all formulations. The samples were immersed for 3 days in EtOH to extract residual monomer, equilibrated for 3 days in deionized water and dried in vacuo at 40°C for 12 h.

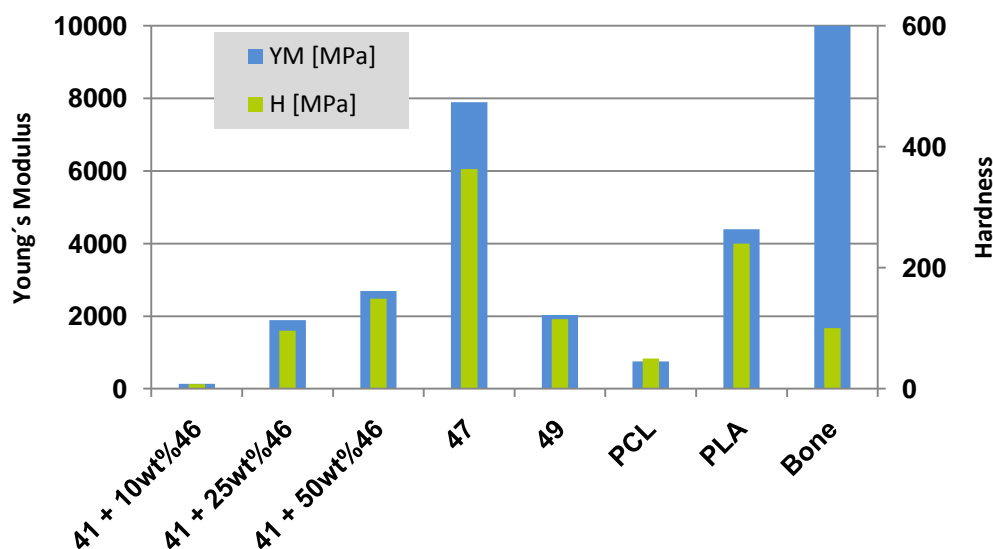


Figure 84. Young's Modulus (Y_{IT}) and hardness (H_{IT}) values for copolymers of **41** containing various amounts of **46** as crosslinker, **47** and **49** in comparison to poly(caprolactone), **PCL**, polylactide, **PLA** and human bone.

As shown in Figure 85, the mechanical properties of **41** with 25% **46** as crosslinker and **41** with 50% **46** as crosslinker and of **47** and **49** alone superseded the reference material poly(caprolactone), **PCL**, which is used as biodegradable polymer for various biomedical applications, e.g. bone replacement or tissue engineering.²¹³ Increasing amount of **46** led to polymers, that were too brittle to be examined by this method, therefore no data for mixtures of **41** with higher amounts of **46** or **46** alone are available.

Astonishingly, the polymer of **47** displayed even better YM and hardness values than the reference **PLA**, which finds also wide-spread application as biodegradable material.²¹⁴ Moreover, its Young's Modulus almost reached the league of human bone.

4.2.4.7. Degradation behaviour

Poly(vinylalcohol) (**PVA**) is a water-soluble, biocompatible polymer and therefore finds broad applications in the medical field.^{215,216} The introduction of phosphate containing side chains at the backbone of the **PVA** might favour biodegradability and biocompatibility of the crosslinked polymers **46** and **47**. Hayashi¹⁹² had already

reported degradation studies of poly(vinyl phosphates) resembling **46** and **47** in alkaline ethanol. He described the nature of the degradation products, which he identified by IR-spectroscopy of the solutions as presented in Figure 86.

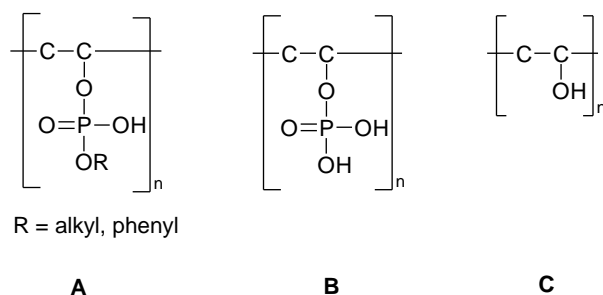


Figure 85. Degradation products of poly(phosphovinyl esters) described by Hayashi

The results of Hayashi's studies and also more recent degradation studies of polyphosphoesters,²¹⁷ which confirmed this degradation mechanism and its products, opened good prospects to obtain biocompatible and degradable polymers from the phosphate-based monomers, as the degradation products consist of (partially) hydrolyzed phosphates and non-toxic poly(vinyl alcohol), which might be harmless to the human body. Furthermore, degradation of polymers from **49** might lead to modified poly(vinyl alcohol) chains with a 2-hydroxyethyl carbamate residue, which is also used for contact lens materials.¹⁹⁵

Therefore, in accordance with literature,²¹⁸ to gain a first estimation of the degradation behaviour of the crosslinked polymers, hydrolysis experiments in NaOH solution with pH 12.0 at 37°C, as well as in HCl solution with pH 1.0 at 37°C and 65°C should be performed, as the degradation under simulated physiological conditions proceeded very slow.

Polymer disks (about 5 x 1 mm) were prepared, immersed for 3 d in EtOH to extract residual monomer and equilibrated for 3 d in distilled water. Weight loss was measured by the gravimetric method.²¹⁵ The initial weight, W_0 , of the samples was determined after drying for 8 h at 40°C in vacuo. For measurement of the weight W_t after defined degradation times, the solution was removed, the polymer disk was washed thoroughly with distilled water and dried for 10 h at 70°C in vacuo. The weight loss was calculated according to equation 4.

$$WL[\%] = \frac{W_0 - W_t}{W_0} \times 100 \quad \text{Equation 3}$$

4.2.4.7.1. Alkaline hydrolysis

Hydrolysis of the polymers obtained from **46**, **47** and **49** was studied in a pH 12.0 NaOH solution. The weight loss (%) and degradation rate profiles of the **PVA**-based polymers are shown in Figure 87.

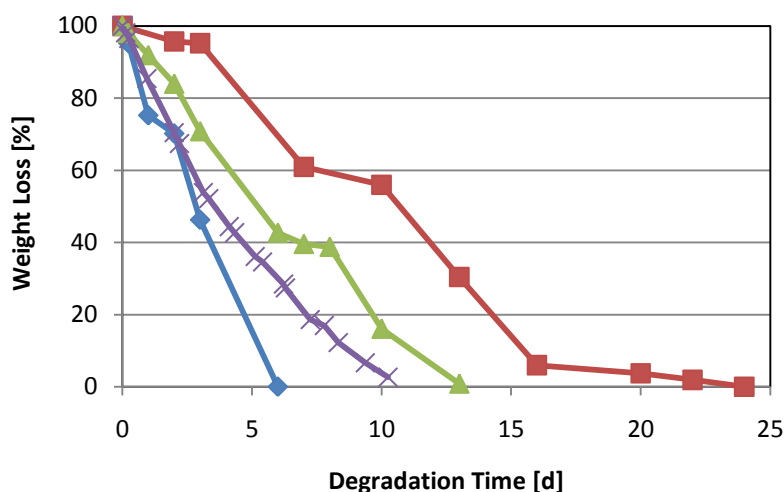


Figure 86. Weight loss of the modified PVAs of compound **46**, **47** and **49** compared to **PLA** after degradation at pH 12.0; **◆** **46**; **■** **47**; **▲** **49**; **×** **PLA**

After 24 days full degradation of all three compounds could be detected. The polymer of the trifunctional compound **47** had decomposed fastest compared to very similar polymer of compound **46**. This might be explained by different grades of double bond conversion for the di- and trifunctional monomers. Higher DBC provided a denser polymer network in compound **46** and less free groups, that could be cleaved under hydrolysis conditions. Therefore, trifunctional monomer **47**, with the lowest DBC, degraded fastest. Vinylcarbamate **49** displayed also a high DBC, but it built a much wider network by the ethanolamine spacer groups, resulting in faster decomposition than **46**. The reference material **PLA** showed slower degradation under these conditions than **47**, but was faster consumed than **46** and **49**.

4.2.4.7.2. Acidic hydrolysis

Hydrolysis of the polymers obtained from **46**, **47** and **49** was studied in a pH 1.0 HCl solution. As degradation at lower temperature (37°C) was considered quite slow, also a second experiment series was conducted at 65°C.

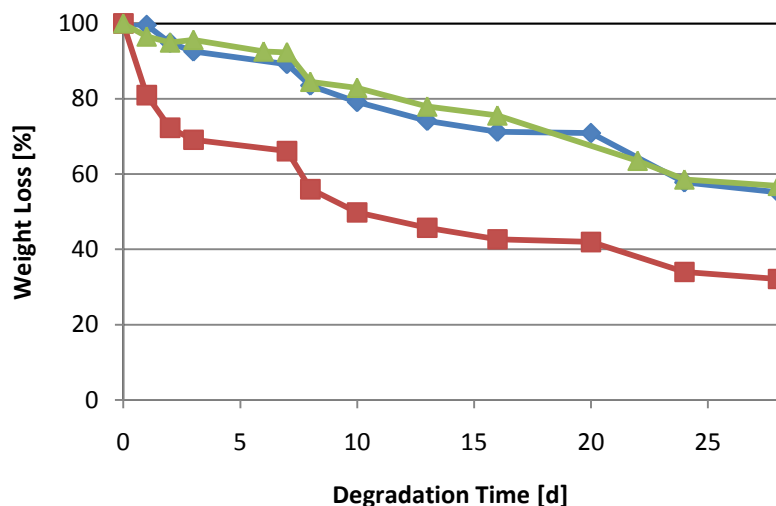


Figure 87. Weight loss of the modified PVAs of compound **46**, **47** and **49** by degradation at pH 1.0 at 37°C; -◇- **46**; -■- **47**; -▲- **49**

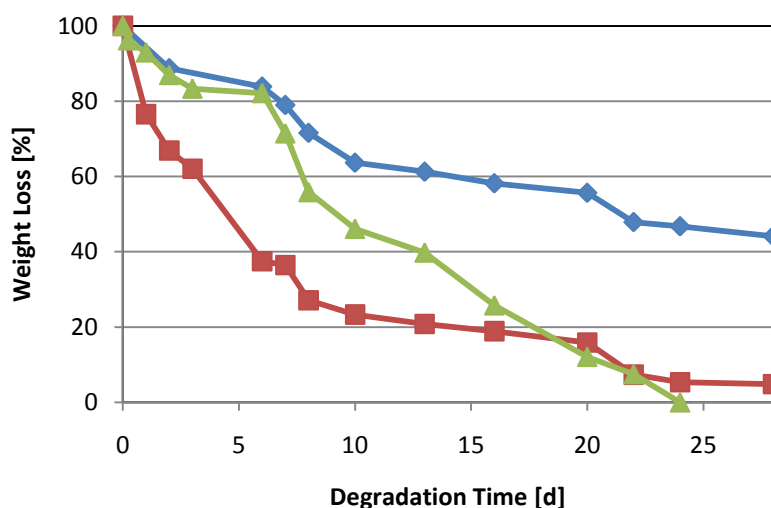


Figure 88. Weight loss of the modified PVAs of compound **36**, **37** and **40** by degradation at pH 1.0 at 65°C; -◇- **46**; -■- **47**; -▲- **49**

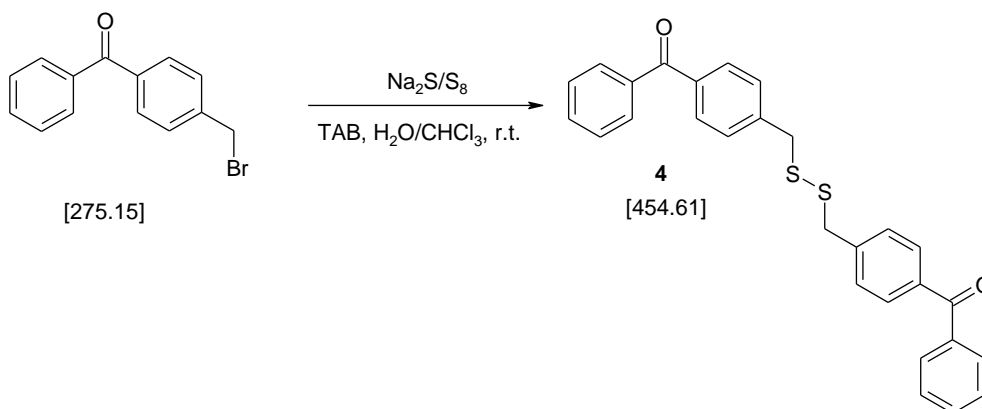
For the highly crosslinked polymer of trifunctional compound **47** acidic hydrolysis seemed to be less crucial than in alkaline medium. Acid hydrolysis was also more or less temperature-independent. Less crosslinked polymer of **49** showed similar acidic degradation as **47** at lower temperatures, but at higher temperature it degrades rather fast. The polymer of compound **46** showed much higher affinity to acidic hydrolysis than in the alkaline medium. These differences in hydrolysis behaviour especially of compound **46** and **47** might result from variable basicity of the leaving group (polyvinylalcohol vs. ethanol) and different network density in the polymers.

EXPERIMENTAL PART

1. Novel Photoinitiators bearing the Benzophenone Moiety

1.1. Synthesis

1.1.1. Bis-[(4-methyl)-benzophenone]-disulfane (4)



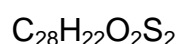
Materials:	1.00 g	(3.6 mmol)	(4-bromomethyl)-benzophenone
	0.06 g	(1.8 mmol)	sulfur
	0.87 g	(3.6 mmol)	sodium sulfide
	0.05 g	(0.2 mmol)	tetrabutyl ammonium bromide
	20.00 mL		chloroform
	20.00 mL		distilled water

Preparation:

0.06 g of sulfur and 0.87 g of sodium sulfide were weighed into a 100 mL round bottomed flask. 20 mL of distilled water were added. The mixture was heated to 50°C until all solid had dissolved (about 1 h). Then the yellow solution was cooled to room temperature and a solution of (4-bromomethyl)-benzophenone in 20 mL of chloroform was added. The reaction mixture was stirred at room temperature for 4 h. Reaction progress was monitored by TLC. When the reaction was finished, the aqueous layer was extracted with 3 x 20 mL of chloroform. The combined organic layers were washed with 1 x 20 mL of water and 1 x 10 mL of brine. After drying over sodium

sulfate and filtration of the drying agent, the solvent was removed by distillation under reduced pressure. The brown oily residue was purified by column chromatography (CH_2Cl_2). 0.43 g of product were obtained as orange-pink solid. $^1\text{H-NMR}$ -analysis showed, that the product still contained 16% impurities, presumably bis-[(4-bromo-4-methyl)-benzophenone]-disulfane due to contamination of starting material with (4,4-dibromomethyl)-benzophenone, which could be fully separated from the monobromide.

Yield: 0.43 g (26% calculated yield) of an orange-pink solid



$R_f = 0.15$ (CH_2Cl_2)

Mp: 88-92°C

$^1\text{H-NMR}$ (CDCl_3) δ (ppm) = 7.76-7.81 (ddd, 8H, $J_1 = 8.61$ Hz, $J_2 = 2.38$ Hz, $J_3 = 1.59$ Hz, ar-H2+H3+H5+H6), 7.35-7.64 (m, 10H, ar-H2'+H3'+H5'+H6'+H4), 3.71 (s, 4H, $\text{CH}_2\text{-S}$).

$^{13}\text{C-NMR}$ (CDCl_3) δ (ppm) = 196.3 (C=O), 142.2 (ar-C- $\text{CH}_2\text{-S}$), 137.7 (ar-C1'), 136.8 (ar-C4), 132.6 (ar-C4'), 130.5 (ar-C2'+C6'), 130.1 (ar-C3+C5), 129.4 (ar-C2+C6), 128.5 (ar-C3'+C5'), 43.0 (CH_2S).

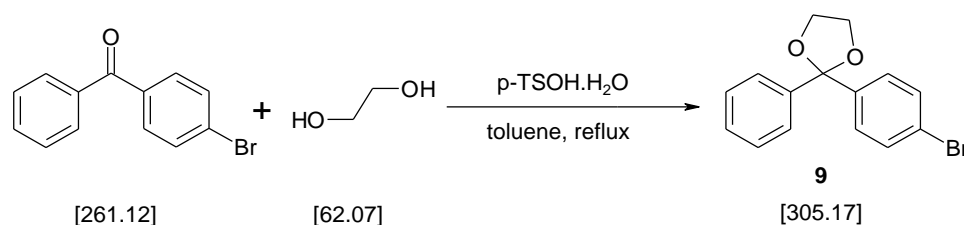
IR (AT-IR, thin film, cm^{-1}): 1652 (C=O), 1416 (S- CH_2)

MS (m/z): calcd. 454.61, found: 229.99 [$\text{BPCH}_2\text{S} + 2\text{H}$] $^+$

No elemental analysis was performed due to impurities, which could not be removed by column chromatography or recrystallization.

1.1.2. Attempted synthesis of 4,4'-(dibenzoyl)-bis(dithiocarbonylphenyl) disulfide (5)

1.1.2.1. 2-Phenyl-2-(4-bromophenyl)-1,3-dioxalane (9)¹⁰¹



Materials:	5.00 g	(19.0 mmol)	4-bromobenzophenone
	2.38 g	(38.0 mmol)	ethylene glycol
	0.10 g	(1.0 mmol)	toluene-4-sulfonic acid monohydrate
	10 mL		toluene

Preparation:

5.0 g of 4-bromobenzophenone were weighed into a 25 mL roundflask adapted with a Dean and Stark condenser. It was dissolved in 10 mL of toluene and 0.10 g of toluene-4-sulfonic acid monohydrate were added. Ethylene glycol was added by a syringe. Then the reaction mixture was heated to reflux for 48 h. The organic layer was washed with saturated NaHCO₃ solution (1 x 10 mL) and with distilled water (2 x 10 mL). Finally the organic layer was dried over sodium sulfate and after filtration of the drying agent the solvent was distilled off. After purification by column chromatography on silica gel (PE : CH₂Cl₂ = 2:1) 4.3 g of white solid were obtained.

Yield: 4.3 g (75% yield, 100% literature yield) of a white solid

C₁₅H₁₃BrO₂

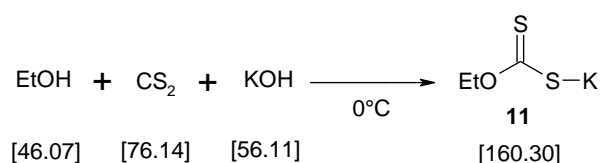
R_f = 0.35 (PE : CH₂Cl₂ = 2:1)

Mp: 54.0-55.1 °C (Lit.: 55.0-55.7 °C)¹⁰¹

¹H-NMR (CDCl₃) δ (ppm) = 7.27-7.54 (m, 9H, ar-H), 4.04-4.10 (t, 4H, 2 x CH₂)

¹³C-NMR (CDCl₃) δ (ppm) = 141.5 (O-C-O) 131.2 (ar-C3+C5), 128.15 (ar-C2+C6), 127.9 (ar-C3'+C5'), 127.8 (ar-C2'+C6'), 125.9 (ar-C4') 108.9 (ar-C-Br), 64.8 (CH₂)

MS (*m/z*): calcd.: 305.2, found: 304.0 [M-H]⁻

1.1.3. Synthesis of dithiocarbonates 6 and 7**1.1.3.1. Potassium dithiocarbonyl O-ethyl ester (11)¹⁰⁶**

Materials: 4.60 g (99.8 mmol) dry ethanol
7.60 g (99.8 mmol) carbon disulfide
5.59 g (99.8 mmol) potassium hydroxide

Preparation:

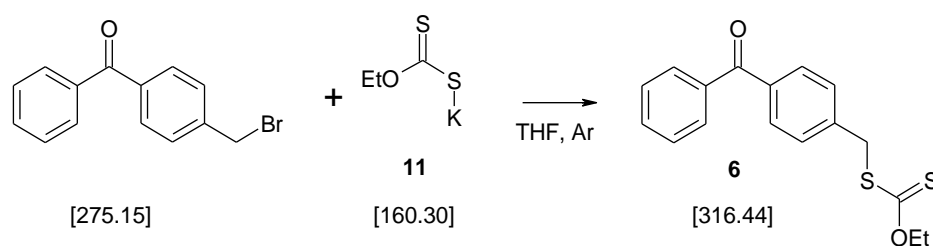
In a round bottomed 2-necked flask with attached cooler 5.59 g fine powdered sodium hydroxide were dissolved in 4.60 g of dry ethanol under vigorous stirring and heating to reflux for 2 h. By this procedure the solution turned red. After dissolution was finished, the reaction mixture was cooled to 0°C with an ice bath. Then 7.60 g of carbon disulfide were added dropwise, keeping the temperature at about 0°C. During the addition a yellow solid precipitated. After warming to room temperature and 30 min stirring, 30 mL of diethylether were added to accomplish the precipitation. The yellow-brownish solid was filtered off and washed with several portions of cold diethyl ether. 14.3 g of crude product **11** were obtained. It was dried in a vacuum exsiccator for 48 h over P₂O₅ and was used without further purification.

Yield: 14.3 g (89% calculated yield) of a yellow-brown solid
C₃H₅KOS₂

Mp: > 215°C decomposition [$>210^{\circ}\text{C}$ decomposition]²¹⁹

¹H-NMR (D₂O) δ (ppm) = 4.40 - 4.51 (q, 2H, J = 7.2 Hz, OCH₂), 1.29 - 1.37 (t, 3H, J = 7.1 Hz, CH₃).

¹³C-NMR (D₂O) δ (ppm) = 70.2 (CH₂), 13.5 (CH₃).

1.1.3.2 S-(4-Benzoyl)-benzyl O-ethyl dithiocarbonate (6)

Materials: 2.00 g (7.3 mmol) (4-bromomethyl)-benzophenone
1.16 g (7.3 mmol) potassium dithiocarbonyl O-ethyl ester (**11**)
30.00 mL dry THF

Preparation:

1.16 g of potassium dithiocarbonyl *O*-ethyl ester (**11**) were dispersed in 15 mL of dry THF. Then a solution of 2 g of (4-bromomethyl)-benzophenone in 15 mL of dry THF was added dropwise under Ar-atmosphere. The reaction mixture was stirred for 20 h at room temperature. When the reaction was finished according to TLC analysis, the white precipitate (KBr) was filtered off and the THF was distilled off. To the orange residue were added 20 mL of diethylether and the organic layer was washed with 2 x 20 mL of distilled water. After drying over sodium sulfate and removal of the drying agent, the organic solvent was distilled off under reduced pressure. The raw product was obtained as orange oil and was purified by column chromatography on silica gel (PE : EE = 20 : 1) to deliver 0.74 g (32% of calculated yield) of a highly viscous, slightly yellow coloured oil. ¹H-NMR analysis of the purified product showed still traces of the dibrominated educt, which could not be separated from the desired xanthogenate **6**.

Yield: 0.74 g (32% calculated yield) of a viscous slightly yellow oil

$C_{17}H_{16}O_2S_2$

$R_f = 0.26$ (PE : EE = 20 : 1)

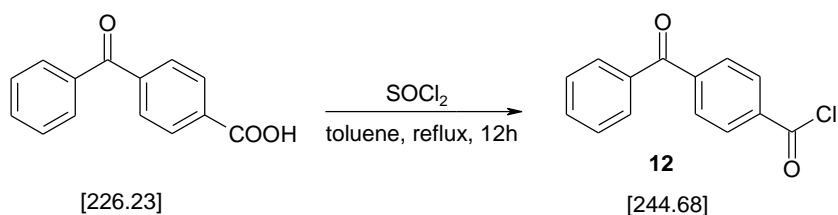
¹H-NMR (CDCl₃) δ (ppm) = 7.71-7.82 (m, 4H, ar-H), 7.53-7.63 (m, 1H, ar-H4'), 7.41-7.52 (m, 4H, ar-H), 4.60-4.71 (q, 2H, $J = 7.4$ Hz, OCH₂), 4.42 (s, 2H, SCH₂), 1.38-1.45 (t, 3H, $J = 7.4$ Hz, CH₃).

¹³C-NMR (CDCl₃) δ (ppm) = 213.4 (C=S), 140.8 (C=O), 139.5 (ar-C1), 137.5 (ar-C1'), 136.7 (ar-C4), 132.5 (ar-C2'+C6'), 130.4 (ar-C3+C5), 129.0 (ar-C2+C6), 128.3 (ar-C3'+C5'), 70.4 (CH₂S), 39.9 (CH₂O), 13.8 (CH₃).

IR (AT-IR, thin film, cm⁻¹): 1657 (C=O), 1277 (S-CH₂), 1044 (C=S)

MS (m/z): calcd. 454.61, found: 281.10 [M-CS]⁻

Elem. Anal. Calcd. for $C_{17}H_{16}O_2S_2$: C: 64.53%, H: 5.10%, S: 20.27%, found: C: 64.11%, H: 5.04%, S: 19.86%

1.1.3.3. 4-Benzoyl benzoic acid chloride (**12**)¹⁰⁹

Materials: 3.00 g (13.3 mmol) 4-benzoyl benzoic acid
7.89 g (66.3 mmol) thionyl chloride
40 mL toluene

Preparation:

3.0 g 4-benzoyl benzoic acid were weighed into a 100 mL round bottomed flask and dispersed in 40 mL of dry toluene. Under Ar-atmosphere 7.89 g of thionyl chloride were added and the reaction mixture is heated to 75°C for 12 h. Finally, solvent and excess of thionyl chloride were removed by distillation under reduced pressure. To enhance the removal of thionyl chloride, the residue was dissolved in 20 mL toluene, followed by removal of the solvent on the rotary evaporator. This procedure was repeated three times. 3.2 g of crude product were obtained as light brown solid. It was used for further reactions without purification. For determination of the melting point an analytical sample was recrystallized from toluene : PE = 1 : 4. The product **12** was obtained as white needles.

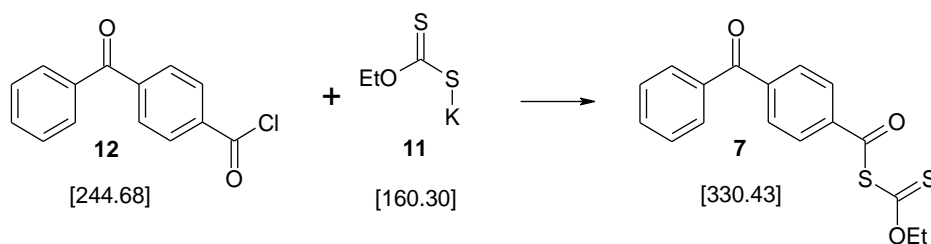
Yield: 3.2 g (98% of calculated yield) of light brown solid

C₁₄H₉ClO₂

Mp: 82-85°C [Lit. 86-89°C, recrystallized from toluene : petrolether = 1 : 4]¹⁰⁹

¹H-NMR (CDCl₃) δ (ppm) = 7.79-7.92 (m, 2H, ar-H₂+H₆), 7.61-7.70 (m, 4H, ar-H₃+H₅+H₂' +H₆'), 7.61-7.69 (m, 1H, ar-H₄'), 7.48-7.57 (m, 2H, ar-H₃' +H₅').

¹³C-NMR (CDCl₃) δ (ppm) = 195.5 (Ph₂C=O), 168.06 (ClC=O), 143.4 (ar-C₁), 136.5 (ar-C₄), 133.5 (ar-C₂+C₆), 131.3 (ar-C₃+C₅), 130.1 (ar-C₄'), 130.0 (ar-C₁'), 129.1 (ar-C₂' +C₆'), 128.6 (ar-C₃' +C₅').

1.1.3.4. *S*-(4-Benzoyl)-benzoyl *O*-ethyl dithiocarbonate (**7**)

Materials: 2.00 g (8.17 mmol) (4-benzoyl) benzoyl chloride (**12**)
1.30 g (8.17 mmol) potassium dithiocarbonyl *O*-ethyl ester (**11**)
30.00 mL dry dichloromethane

Preparation:

1.30 g of potassium dithiocarbonate *O*-ethyl ester was (**11**) dispersed in 15 mL of dry dichloromethane. Then a solution of 2 g of (4-benzoyl)-benzoyl chloride (**12**) in 15 mL of dry dichloromethane was added dropwise under Ar-atmosphere at -20°C. The reaction mixture was stirred at -20°C for 1 h, then it was warmed to room temperature. When the reaction was finished according to TLC analysis, the organic layer was washed with 2 x 20 mL of distilled water and then dried over sodium sulfate. After removal of the drying agent, the organic solvent was distilled off under reduced pressure. The raw product of **7** was obtained as brown oil, which solidified after cooling. **7** was purified by recrystallization from ethanol to yield 1.34 g of yellow solid.

Yield: 1.34 g (49% calculated yield) of yellow solid

$C_{17}H_{14}O_3S_2$

$R_f = 0.44$ (PE : EE = 8 : 1)

Mp: 57-61 °C

1H -NMR ($CDCl_3$) δ (ppm) = 7.96-8.04 (dd, 2H, $J_1 = 8.55$ Hz, $J_2 = 1.67$ Hz, ar-H2+H6), 7.75-7.91 (m, 4H, ar-H3+H5+H2'+H6'), 7.58-7.69 (m, 1H, ar-H4'), 7.45-7.56 (m, 2H, ar-H3'+H5'), 4.69-4.80 (q, 2H, $J = 7.2$ Hz, OCH_2), 1.47-1.54 (t, 3H, $J = 7.2$ Hz, CH_3).

^{13}C -NMR ($CDCl_3$) δ (ppm) = 202.3 (C=S), 195.7 (C=O), 184.9 ($Ph_2-C=O$), 142.5 (ar-C1), 138.4 (ar-C1'), 136.6 (ar-C4), 133.2 (ar-C4'), 130.3 (ar-C3+C5), 130.1 (ar-

C2+C6), 128.6 (ar-C2'+C6'), 127.8 (ar-C3'+C5'), 71.39 (CH₂O), 13.5 (CH₃).

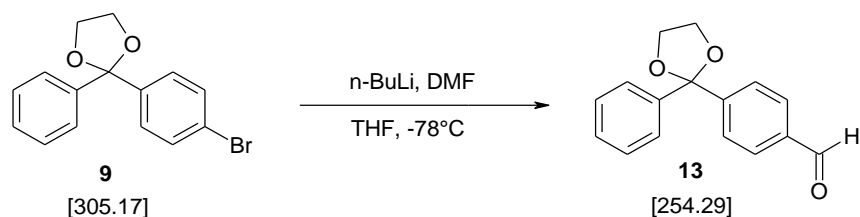
IR (AT-IR, thin film, cm⁻¹): 1696 (SC=O), 1251 (C-O), 1027 (C=S).

MS (*m/z*): calcd. 330.43, found: 281.22 [M – H₂S – CH₃]

Elem. Anal. Calcd. for C₁₇H₁₄O₃S₂: C: 61.80%, H: 4.27%, S: 19.36%, found: C: 62.13%, H: 4.31%, S: 18.67%

1.1.4. Attempted synthesis of *N*-(benzoyloxy)-(4-benzoyl) benzenemethanamine (**8**)

1.1.4.1. 2-Phenyl-2-(4-formylphenyl)-1,3-dioxalane (**13**)¹⁰¹



Materials: 5.00 g (3.0 mmol) 2-phenyl-2-(4-bromophenyl)-1,3-dioxalane (**9**)
8.86 mL (3.0 mmol) *n*-butyllithium solution (2.0 M in hexane)
1.28 g (4.0 mmol) *N,N*-dimethylformamide
50 mL dry THF

Preparation:

Under inert atmosphere 5 g of dioxolane **9** were dissolved in 20 mL of dry THF. Ar was bubbled through the solution for 10 minutes to remove all oxygen. Then the solution was cooled to -80°C by a MeOH/N₂ bath. Afterwards the *n*-butyllithium was added dropwise *via* a syringe. The deep blue solution was stirred at -80°C for 1 h, then DMF was added. After the addition was finished, the now slightly yellow reaction mixture was slowly warmed to room temperature. After further 2 h the reaction was worked up by addition of a saturated ammonium chloride solution, followed by extraction with 4 x 50 mL of diethylether. The organic layer was washed with 1 x 60 mL of water and 1 x 60 mL of brine. Then it was dried over sodium sulfate and after filtration of the drying agent, the solvent was distilled off under reduced pressure. Purification of the raw product was performed by column chromatography on silica gel (PE : CH₂Cl₂ = 2:1). 2.48 g of **13** as a white solid were obtained.

Yield: 2.48 g (60% calculated yield, 60% literature yield¹⁰¹) as white solid

$C_{16}H_{14}O_3$

$R_f = 0.37$ (PE : $CH_2Cl_2 = 2:1$)

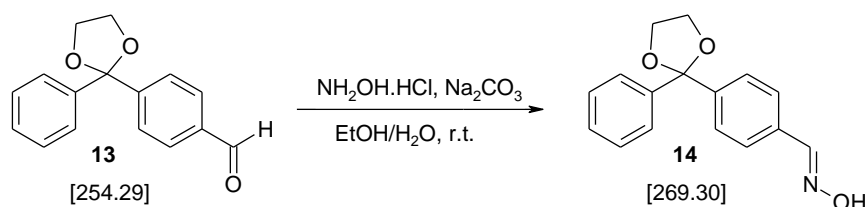
Mp: 71.3-75.0 °C (61.7-63.4 °C)¹⁰¹

1H -NMR ($CDCl_3$) δ (ppm) = 9.99 (s, 1H, CHO), 7.81-7.89 (dd, 2H, $J_1 = 6.47$ Hz, $J_2 = 1.56$ Hz, ar-H3+H5), 7.67-7.75 (dd, 2H, $J_1 = 6.47$ Hz, $J_2 = 1.56$ Hz, ar-H2+H6), 7.47-7.55 (m, 2H, ar-H2'+H6') 7.27-7.40 (m, 3H, ar-H4'+H3'+H5'), 4.06-4.10 (t, 4H, 2 x CH_2)

^{13}C -NMR ($CDCl_3$) δ (ppm) = 192.0 (CHO), 148.9 (ar-C-CHO) 141.5 (OCO), 136.1 (ar-C1+C1'), 129.5 (ar-C2+C6+C2'+C6'), 128.5 (ar-C3+C5), 126.9 (ar-C3'+C5'), 126.0 (ar-C4'), 65.1 (CH_2)

MS (m/z): calcd. 254.3, found: 254.0 [M]

1.1.4.2. (4-[[1,3]-Dioxolan-2-yl-2-phenyl])benzamidoxime (**14**)



Materials:	1.05 g	(4.1 mmol)	2-phenyl-2-(4-formylphenyl)-1,3-dioxalane (13)
	0.57 g	(8.3 mmol)	hydroxylamine hydrochloride
	0.48 g	(4.5 mmol)	sodium carbonate
	12 mL		distilled water
	60 mL		ethanol

Preparation:

In a 100 mL round flask 1.05 g of 2-phenyl-2-(4-formylphenyl)-1,3-dioxalane (**13**) were dissolved in 60 mL of ethanol. Under stirring a solution of 0.57 g of hydroxylamine hydrochloride in 9 mL of distilled water was added. Finally, a solution of 0.48 g sodium carbonate in 3 mL of distilled water was added dropwise. The reaction mixture was stirred at room temperature for 7 days. Reaction progress was

monitored by TLC analysis (CH_2Cl_2). When the reaction was finished, ethanol was distilled off. The residue was diluted with distilled water (approx. 40 mL). The white precipitate was filtered off. The aqueous layer was extracted with 2 x 15 mL of ethyl acetate. The organic layer was dried over sodium sulfate and after filtration of the drying agent, the solvent was removed by distillation under reduced pressure. The crude products were combined and purified by recrystallization from $\text{Et}_2\text{O}/\text{PE}$. 0.51 g of product **14** were obtained as white solid.

Yield: 0.51 g (46% calculated yield) as white solid

$\text{C}_{16}\text{H}_{15}\text{NO}_3$

$R_f = 0.87$ (CH_2Cl_2)

Mp: 102 - 105 °C

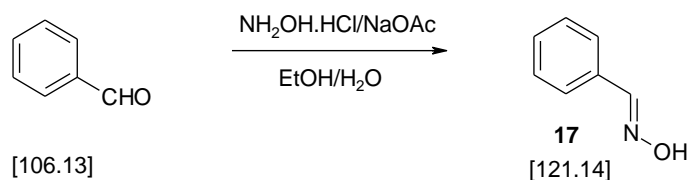
$^1\text{H-NMR}$ (CDCl_3) δ (ppm) = 8.13 (s, 1H, $\text{CH}=\text{N}$), 7.49-7.55 (m, 6H, OH; ar-H₂+H₃+H₄+H₅), 7.27-7.39 (m, 4H, ar-H_{2'}+H_{3'}+H_{5'}+H₆), 4.06-4.09 (t, 4H, 2 x CH_2).

$^{13}\text{C-NMR}$ (CDCl_3) δ (ppm) = 150.1 (C=N), 144.3 (ar-C-C=N), 141.8 (ar-C₄), 141.7 (ar-C_{1'}), 131.7 (OCO), 128.5 (ar-C_{4'}), 128.4 (ar-C₂+C₆), 127.1 (ar-C₃+C₅), 126.8 (ar-C_{2'}+C_{6'}), 126.1 (ar-C_{3'}+C_{5'}), 65.1 (CH_2).

IR (AT-IR, thin film, cm^{-1}): 3243 (assoc. N-OH), 1208 (C-O-C), 1655 (C=N), 1077 (C-O-C-O-C)

MS (m/z): calcd. 269.3, found: 267.8 [M-H]⁻

Elem. Anal. Calcd. for $\text{C}_{16}\text{H}_{15}\text{NO}_3$: C: 71.29%, H: 5.61%, N: 5.20%, found: C: 70.78%, H: 5.67%, N: 4.87%

1.1.4.3. Benzaldoxime (**17**)²²⁰

Materials: 4.55 g (42.8 mmol) benzaldehyde
5.00 g (72.5 mmol) hydroxylamine hydrochloride
5.00 g (60.9 mmol) sodium acetate
24 mL ethanol
30 mL distilled water

Preparation:

Benzaldehyde was dissolved in 30 mL of ethanol. Then hydroxylamine hydrochloride in 15 mL of distilled water and an aqueous solution of sodium acetate were added subsequently under stirring. The reaction mixture was stirred at room temperature for 24 h. After the reaction was finished, the ethanol was distilled off under reduced pressure. The aqueous residue was extracted with 3 x 10 mL of dichloromethane. The organic layer was washed with 3 x 10 mL of 5% sodium bicarbonate solution and with 10 mL of distilled water. Then it was dried over sodium sulphate. After filtration of the drying agent the solvent was distilled off under reduced pressure to yield 4.9 g of a clear solution, which solidified after cooling at 4°C.

Yield: 4.9 g (95% of calculated yield) of a clear solution

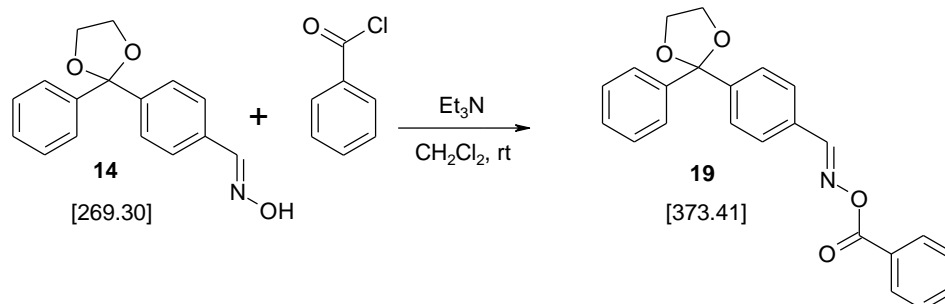
$\text{C}_7\text{H}_7\text{NO}$

Mp: 29-31 °C [Lit.: 28-29°C]²²⁰

$^1\text{H-NMR}$ (CDCl_3) δ (ppm) = 8.83 (bs, 1H, OH), 8.17 (s, 1H, CH=N), 7.32 – 7.65 (m, 5H, ar-H).

$^{13}\text{C-NMR}$ (CDCl_3) δ (ppm) = 150.4 ($\underline{\text{C}}=\text{N}$), 131.8 (ar-C1), 130.2 (ar-C4), 128.8 (ar-C3+C5), 127.1 (ar-C2+C6).

MS (m/z): calcd. 121.14, found: 121.07 [M]

1.1.4.4. (4-Phenyl)-O-phenylacetyl benzamidoxime (**20**)1.1.4.4.1. (4-[[1,3]-Dioxalan-2-yl-2-phenyl])-O-phenylacetyl benzamidoxime (**19**)

Materials: 0.15 g (0.56 mmol) (4-[[1,3]-dioxalan-2-yl-2-phenyl])
benzamidoxime (**14**)
0.09 g (0.67 mmol) benzoyl chloride
0.07 g (0.67 mmol) triethyl amine
7.00 mL dichloromethane

Preparation:

In a 25 mL 2-necked round bottomed flask with adapted cooler and septum 0.15 g of 4-[[1,3]-dioxalan-2-yl-2-phenyl])benzamidoxime (**14**) and 0.07 g of triethyl amine were dissolved in 5 ml of dichloromethane under Ar-atmosphere. This mixture was cooled with an ice-bath to 0°C and 0.09 g of benzoyl chloride were added dropwise with a syringe. After the addition was finished, the yellow solution was stirred for 30 min at 0°C and afterwards 4.5 h at room temperature. Reaction progress was monitored by TLC analysis (CH₂Cl₂). Finally, the organic layer was washed with 1 x 10 mL of distilled water and 1 x 10 mL of brine. Alkaline work up was avoided due to danger of hydrolysis of the product. Then the organic layer was dried over sodium sulphate. After filtration of the drying agent the solvent was removed by distillation under reduced pressure. A yellow-white solid was obtained as crude product of **19**, which was purified by column chromatography (CH₂Cl₂). 0.06 g of white solid were obtained.

Yield: 0.06 g (35% calculated yield) of a white solid

C₂₃H₁₉NO₄

R_f = 0.21 (CH₂Cl₂)

Mp: 188 – 190 °C

$^1\text{H-NMR}$ (CDCl_3) δ (ppm) = 8.54 (s, 1H, CH=N), 8.10-8.15 (ddd, 2H, $J_1 = 7.1$ Hz, $J_2 = 1.8$ Hz, $J_3 = 1.0$ Hz, ar-H₂+H₆), 7.76-7.80 (ddd, 2H, $J_1 = 8.3$ Hz, $J_2 = 2.3$ Hz, $J_3 = 1.9$ Hz, ar-H_{2''}+H_{6''}), 7.44-7.64 (m, 7H, ar-H), 7.31-7.35 (m, 3H, ar-H), 4.07-4.1 (t, 4H, 2 x CH₂).

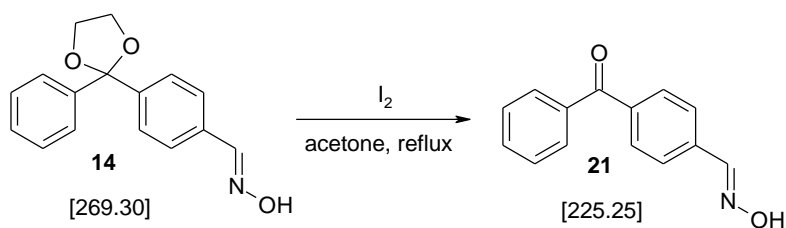
$^{13}\text{C-NMR}$ (CDCl_3) δ (ppm) = 164.1 (C=O), 156.5 (C=N), 147.1 (ar-C-C=N), 146.2 (ar-C₄), 141.7 (ar-C_{1'}), 133.7 (OCO), 129.9 (ar-C), 129.8 (ar-C), 128.7 (2 x ar-C), 128.6 (2 x ar-C), 128.5 (2 x ar-C), 128.4 (2 x ar-C), 128.3 (ar-C), 126.9 (2 x ar-C), 126.1 (2 x ar-C), 65.2 (CH₂).

IR (AT-IR, thin film, cm^{-1}): 1734 (C=O), 1257 (C-O), 1082 (C-O-C)

MS (m/z): calcd. 373.41, found: 277.0 [M-H₂O-phenyl]

Elem. Anal. Calcd. for C₂₃H₁₉NO₄: C: 73.98%, H: 5.13%, N: 3.75%, found: C: 73.90%, H: 5.18%, N 3.56%

1.1.4.5.2. (4-Phenyl)-benzamidoxime (**21**)



Materials: 0.51 g (1.9 mmol) (4-[[1,3]-dioxolan-2-yl-2-phenyl])
benzamidoxime (**14**)
0.05 g (0.2 mmol) iodine
5.00 mL acetone

Preparation:

In a 100 mL round bottomed flask 0.51 g of (4-[[1,3]-dioxolan-2-yl-2-phenyl]) benzamidoxime (**14**) were dissolved in 4 mL of acetone. Under stirring a solution of 0.048 g iodine in 1 mL of acetone was added dropwise. The reaction mixture was heated to reflux for 3 h. After 3 hours an additional portion of 10 mg iodine was added

and refluxing was continued for 1 h. Finally, the acetone was removed by distillation under reduced pressure. The brown oily residue was dissolved in 5 mL of dichloromethane and washed with 1 x 5 mL of 5% sodium thiosulfate solution, 1 x 5 mL of distilled water and 1 x 5 mL of brine. The organic layer was dried over sodium sulphate and after filtration of the drying agent, the solvent was distilled off. 0.45 g of crude **21** were obtained as light yellow oil. Several attempts to purify the product by recrystallization did not work. Column chromatography was not carried out due to instability of the product. Therefore it was used without further purification for the following reaction.

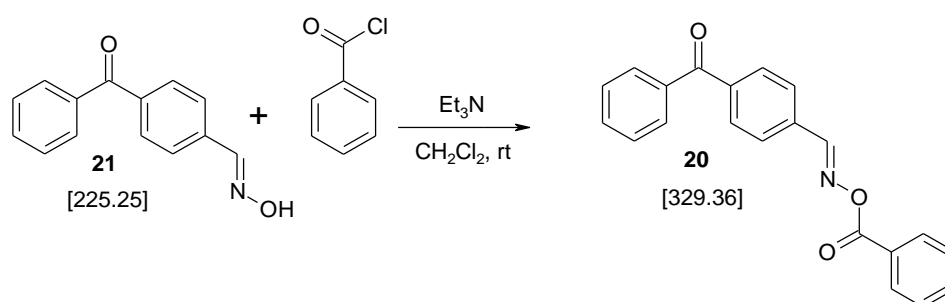
Yield: 0.45 g (72% calculated yield) of a light yellow oil

$C_{14}H_{11}NO_2$

1H -NMR ($CDCl_3$) δ (ppm) = 8.21 (s, 1H, CH=N), 7.45-8.03 (m, 10H, ar-H+OH). A small peak at 10.13 ppm indicated formation of aldehyde.

MS (m/z): calcd. 225.25, found: 225.05 [M]

1.1.4.5.3. (4-Phenyl)-O-phenylacetyl benzamidoxime (**20**)



Materials: 0.30 g (1.33 mmol) (4-phenyl) benzamidoxime (**21**)
0.22 g (1.60 mmol) benzoyl chloride
0.16 g (1.60 mmol) triethyl amine
5.00 mL dichloromethane

Preparation:

In a 25 mL 2-necked round bottomed flask with adapted cooler and septum 0.30 g of (4-phenyl)-benzamidoxime (**21**) and 0.16 g of triethyl amine were dissolved in 4 mL of dichloromethane under Ar-atmosphere. This mixture was cooled with an ice-bath to

0°C and 0.22 g of benzoyl chloride in 1 mL of dichloromethane was added dropwise with a syringe. After the addition was finished, the yellow solution was stirred for 30 min at 0°C and afterwards 4 h at room temperature. Reaction progress was monitored by TLC analysis (CH₂Cl₂). Finally, the organic layer was washed with 1 x 5 mL of distilled water and 1 x 5 mL of brine. Alkaline work up was avoided due to danger of hydrolysis of the product. Then the organic layer was dried over sodium sulfate. After filtration of the drying agent the solvent was removed by distillation under reduced pressure. A brown-white solid was obtained as crude product **21**, which was purified by column chromatography (CH₂Cl₂). 0.15 g of white solid were obtained.

Yield: 0.15 g (34% calculated yield) of white solid

C₂₁H₁₅NO₃

R_f = 0.09 (CH₂Cl₂)

Mp: 152-155°C

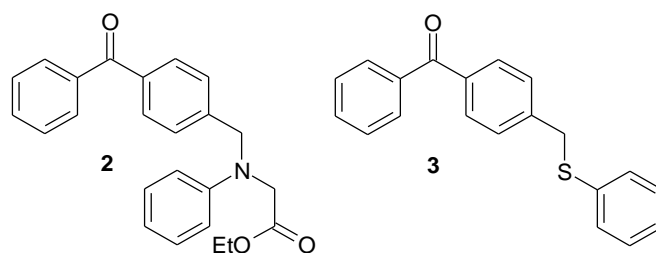
¹H-NMR (CDCl₃) δ (ppm) = 8.64 (s, 1H, CH=N), 8.12-8.17 (ddd, 2H, J₁ = 7.0 Hz, J₂ = 1.6 Hz, J₃ = 1.2 Hz, ar-H), 7.88-7.97 (ddd, 4H, J₁ = 6.4 Hz, J₂ = 2.4 Hz, J₃ = 2.2 Hz, ar-H), 7.79-7.84 (ddd, 2H, J₁ = 7.0 Hz, J₂ = 1.7 Hz, J₃ = 1.0 Hz, ar-H), 7.58-7.68 (m, 2H, ar-H), 7.46-7.55 (m, 4H, ar-H).

¹³C-NMR (CDCl₃) δ (ppm) = 196.0 (BP-C=O), 163.9 (Bz-C=O), 155.9 (C=N), 140.2 (ar-C4), 137.1 (ar-C1'), 133.7 (2 x ar-C), 132.9 (2 x ar-C), 130.5 (2 x ar-C), 130.1 (2 x ar-C), 129.9 (2 x ar-C), 128.7 (ar-C), 128.5 (2 x ar-C), 128.4 (3 x ar-C).

IR (AT-IR, thin film, cm⁻¹): 1731 (C=O), 1656 (C=N), 1254 (C-O).

MS (*m/z*): calcd. 329.36, found: 330.94 [M+H]⁺

Elem. Anal. Calcd. for C₂₃H₁₉NO₄: C: 76.58%, H: 4.59%, N: 4.25%, found: C: 76.03%, H: 4.63%, N: 4.22%

1.1.5. Reference compounds 2 and 3

Benzophenone-*N*-phenylglycine ethylester (**2**) was purified by column chromatography (PE : EE = 5 : 1), followed by 3 times recrystallization from diethyl ether/*n*-hexane (1 : 15).

$^1\text{H-NMR}$ (CDCl_3) δ (ppm) = 7.84 – 7.80 (m, 4H, ar-H₂+H₃+H₅+H₆), 7.65 – 7.40 (m, 5H, ar-H₂' + H₃' + H₄' + H₅' + H₆'), 7.29 – 7.16 (m, 2H, ar-H₃'' + H₅''), 6.88 – 6.70 (m, 3H, ar-H₂'' + H₆'' + H₄''), 4.27 (s, 2H, EtOCOCH₂), 4.28 - 4.10 (m, 4H, OCH₂, ar-C-CH₂-N), 1.31-1.21 (t, 3H, CH₃).

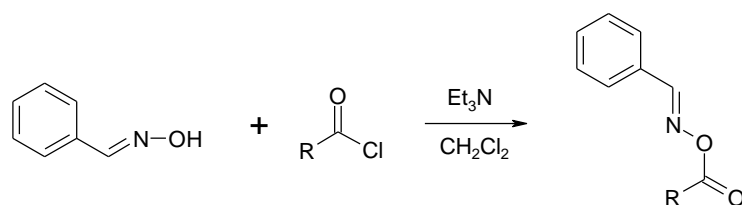
Phenyl-(4-phenylsulfanylmethyl-phenyl)-methanone (**3**) was purified by two times recrystallization from petrolether.

$^1\text{H-NMR}$ (CDCl_3) δ (ppm) = 7.84-7.65 (m, 5H, ar-H₂+H₃+H₅+H₆+H₄'), 7.64-7.14 (m, 9H, ar-H₂'' + H₃'' + H₄'' + H₅'' + H₆'' + H₂' + H₃' + H₅' + H₆'), 4.16 (s, 2H, CH₂).

2. Alternative Co-Initiators for Type II PIs

2.1. Synthesis

2.1.1. Synthesis of benzaldoxime esters **22**, **23** and **24**



17
[121.14]

22 R = benzoyl [140.57]
23 R = acetyl [78.50]
24 R = methacryloyl [104.54]

22 R = benzoyl [225.25]
23 R = acetyl [163.18]
24 R = methacryloyl [189.22]

Materials:

Reagent	22	23	24
benzaldoxime (17)	3.00 g (24.8 mmol)	3.50 g (28.9 mmol)	3.00 g (24.8 mmol)
RCOCl	5.22 g (37.1 mmol)	3.40 g (43.3 mmol)	3.88 g (37.1 mmol)
triethylamine	3.76 g (37.1 mmol)	4.39 g (43.3 mmol)	3.76 g (37.1 mmol)
dry dichloromethane	40 mL	40 mL	40 mL

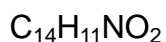
Preparation:

Benzaldoxime (**17**) were dissolved in 30 mL of dry dichloromethane. Then the acid chloride was added. The solution was cooled to 0°C and a mixture of triethylamine in 10 mL dry dichloromethane was added dropwise. The reaction was stirred for 30 min at 0°C, then 4 h at room temperature. The progress of the reaction was monitored by TLC analysis (dichloromethane). After the reaction was finished, the organic layer was washed with 2 x 20 mL of distilled water, 1 x 20 mL of 5% bicarbonate solution and 2 x 20 mL of saturated sodium chloride solution. After drying of the organic layer over sodium sulfate and filtration of the drying agent, the solvent was distilled off.

2.1.1.1. O-Benzoyl benzaldoxime ester (22)¹¹⁹

The crude product of **22** was purified by recrystallization from ethanol to yield 1.86 g of a white crystalline solid.

Yield: 1.86 g (33% calculated yield) of white crystalline solid



$R_f = 0.60$ (CH_2Cl_2)

Mp: 100 - 102 °C [Lit.: 99 – 101°C]¹¹⁹

¹H-NMR (CDCl_3) δ (ppm) = 8.57 (s, 1H, HC=N), 8.10 – 8.18 (m, 2H, ar-H2'+H6'), 7.77 – 7.86 (m, 2H, ar-H2+H6), 7.57 – 7.67 (m, 1H, ar-H4'), 7.40 – 7.56 (m, 5H, ar-H4+H3+H5+H3'+H5').

¹³C-NMR (CDCl_3) δ (ppm) = 164.0 (C=O), 156.8 (HC=N), 133.5 (ar-C4'), 131.8 (ar-C4), 130.2 (ar-C1+C1'), 129.8 (ar-C3+C5), 128.9 (ar-C2'+C6'), 128.6 (ar-C2+C6), 128.5 (ar-C3'+C5').

MS (m/z): calcd. 225.25, found: 226.41 [$\text{M}+\text{H}$]⁺

2.1.1.2. O-Methyl benzaldoxime ester (23)²²¹

The crude product was purified by column chromatography on silica gel (PE: EE = 6:1). Thus 2.2 g of **23** as a colorless liquid were obtained.

Yield: 2.2 g (47% calculated yield) of colorless liquid



$R_f = 0.35$ (PE : EE = 6:1)

¹H-NMR (CDCl_3) δ (ppm) = 8.35 (s, 1H, HC=N), 7.71 – 7.77 (m, 2H, ar-H2+H6), 7.37 – 7.52 (m, 3H, ar-H4+H3+H5), 2.23 (s, 3H, CH₃).

¹³C-NMR (CDCl_3) δ (ppm) = 168.8 (C=O), 156.0 (HC=N), 131.8 (ar-C4), 130.2 (ar-C1), 129.0 (ar-C3+C5), 128.5 (ar-C2+C6), 19.7 (CH₃)

MS (m/z): calcd. 163.18, found: 163.08 [M]

2.1.1.3. *O*-Methacryloyl benzaldoxime ester (**24**)

The crude product of **24** was purified by column chromatography on silica gel (PE : EE = 15:1).

Yield: 1.52 g (33% calculated yield) of a white solid

$C_{11}H_{11}NO_2$

$R_f = 0.31$ (PE : EE = 15:1)

Mp: 78.0 – 82.2°C

1H -NMR ($CDCl_3$) δ (ppm) = 8.44 (s, 1H, $\underline{H}C=N$), 7.73 – 7.81 (m, 2H, ar-H2+H6), 7.39 – 7.51 (m, 3H, ar-H4+H3+H5), 6.22-6.26 (dq, 1H, $J_1 = 2.1$ Hz, $J_2 = 1.0$ Hz, \underline{CH}_2 *trans* to CH_3), 5.67-5.71 (dq, 1H, $J_1 = 3.2$ Hz, $J_2 = 1.5$ Hz, \underline{CH}_2 *cis* to CH_3), 2.04-2.07 (dd, 3H, $J_1 = 1.5$ Hz, $J_2 = 1.1$ Hz, CH_3).

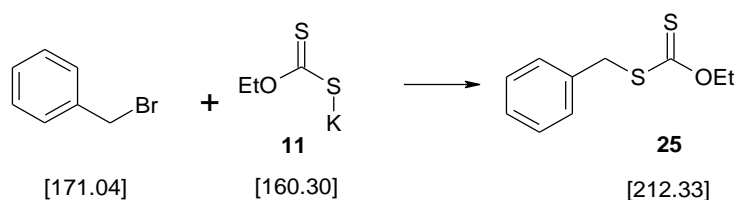
^{13}C -NMR ($CDCl_3$) δ (ppm) = 164.7 (C=O), 156.6 (HC=N), 135.0 (ar-C1), 131.8 (C4-arom), 130.3 ($\underline{C}CH_3$), 128.9 (ar-C3+C5), 128.5 (ar-C2+C6), 126.6 (CH_2), 18.6 (CH_3)

IR (AT-IR, thin film, cm^{-1}): 1736 (C=O), 1251 (C-O), 1119 (C-O).

MS (m/z): calcd. 189.22, found: 174.32 [$M - CH_3$]

Elem. Anal. Calcd. for $C_{11}H_{11}NO_2$: C: 69.83%, H: 5.86%, N: 7.40%, found: C: 69.40%, H: 5.88%, N: 7.38%

2.1.2. *S*-Benzyl *O*-ethyl dithiocarbonate (**25**)²²²



Materials: 4.00 g (23.4 mmol) benzylbromide
3.74 g (23.4 mmol) potassium dithiocarbonate *O*-ethyl ester (**11**)
60.00 mL dry tetrahydrofuran

Preparation:

The preparation was carried out according to the procedure for compound **11**. The orange colored crude product was purified by Kugelrohr distillation to deliver 2.41 g of **25** as a clear liquid.

Yield: 2.41 g (57% calculated yield) of a clear liquid

$C_{10}H_{12}OS_2$

$R_f = 0.86$ (CH_2Cl_2)

Bp: 110°C (0.03 mbar) [Lit.: 75°C, 10 torr]²²²

1H -NMR ($CDCl_3$) δ (ppm) = 7.27 – 7.40 (m, 5H, ar-H), 4.61 – 4.71 (q, 2H, $J = 7.1$ Hz, O- CH_2), 4.38 (s, 2H, S- CH_2), 1.39-1.46 (t, 3H, $J = 7.3$ Hz, CH_3).

^{13}C -NMR ($CDCl_3$) δ (ppm) = 214.0 (C=S), 135.6 (ar-C1), 129.1 (ar-C2+C6), 128.6 (ar-C3+C5), 127.6 (ar-C4), 70.1 (CH_2 -S), 40.4 (CH_2O), 13.8 (CH_3).

MS (m/z): calcd. 212.33, found: 212.05 [M]

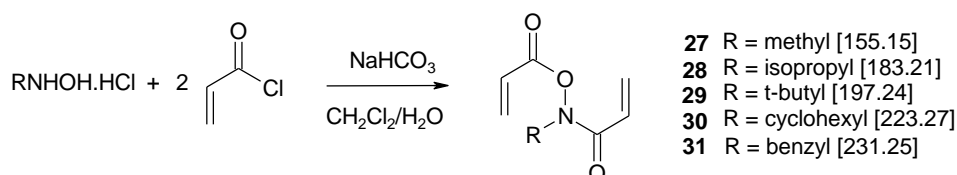
$^1\text{H-NMR}$ (CDCl_3) δ (ppm) = 9.99 (s, 1H, NH), 6.65 – 6.55 (dd, 1H, $J_1 = 17.2$ Hz, $J_2 = 1.4$ Hz, amide- $\text{CH}=\text{CH}_2$, *trans*), 6.50 – 6.41 (dd, 1H, $J_1 = 17.0$ Hz, $J_2 = 1.5$ Hz, acryl- $\text{CH}=\text{CH}_2$, *trans*), 6.32-6.15 (m, 2H, $\text{CH}=\text{CH}_2$), 6.06 – 6.00 (dd, 1H, $J_1 = 10.5$ Hz, $J_2 = 1.3$ Hz, amide- $\text{CH}=\text{CH}_2$, *cis*), 5.83-5.77 (dd, 1H, $J_1 = 10.3$ Hz, $J_2 = 1.6$ Hz, acryl- $\text{CH}=\text{CH}_2$, *cis*).

$^{13}\text{C-NMR}$ (CDCl_3) δ (ppm) = 164.0 (2 x C=O), 134.4 (amide- $\text{CH}=\text{CH}_2$), 129.5 (acryl- $\text{CH}=\text{CH}_2$), 126.0 (amide- $\text{CH}=\text{CH}_2$), 124.2 (acryl- $\text{CH}=\text{CH}_2$)

IR (AT-IR, thin film, cm^{-1}): 1775 (C=O), 1674 and 1630 (C=C), 1407 (N-O)

MS (m/z): calcd. 141.13, found: 142.20 [$\text{M}+\text{H}^+$]

3.1.2. *O,N*-Bis(1-oxo-2-propen-1-yl)-*N*-(alkyl)-hydroxylamines



Materials:

Reagent	27	28	29	30	31
RNHOH.HCl	1.50 g (18.0 mmol)	0.90 g (8.1 mmol)	1.50 g (11.9 mmol)	0.90 g (6.0 mmol)	0.90 g (5.7 mmol)
acryloyl chloride	3.58 g (39.5 mmol)	1.61 g (18.0 mmol)	2.38 g (26.0 mmol)	1.19 g (13.1 mmol)	1.13 g (12.4 mmol)
NaHCO ₃	6.64 g (79.0 mmol)	2.98 g (35.5 mmol)	4.41 g (52.5 mmol)	2.20 g (26.2 mmol)	2.10 g (24.9 mmol)
CH ₂ Cl ₂	100 mL	25 mL	70 mL	45 mL	45 mL
water	30.0 mL	5.0 mL	20.0 mL	10.0 mL	10.0 mL r

Preparation:

To a solution of *N*-alkyl hydroxylamine hydrochloride in water sodium bicarbonate and $\frac{2}{3}$ of the total amount of CH_2Cl_2 were added. The reaction mixture was stirred at 0°C and a solution of acryloyl chloride in CH_2Cl_2 was added dropwise over a period of 30 min. Then the reaction mixture was stirred at room temperature and progress was monitored by TLC. After 24 h in total the reaction was stopped and the aqueous phase was extracted with CH_2Cl_2 . The combined organic layers were washed with

5% sodium bicarbonate solution and with brine. The organic layer was dried over Na_2SO_4 and the solvent was distilled off.

3.1.2.1. *O,N-Bis(1-oxo-2-propen-1-yl)-N-(methyl)-hydroxylamine (27)*

The crude product was purified by column chromatography (PE : EE = 4:1) to yield 1.00 g of **27** as a colourless liquid.

Yield: 1.00 g (60% calculated yield) of a colourless liquid

$\text{C}_7\text{H}_9\text{NO}_3$

$R_f = 0.29$ (PE : EE = 4:1)

$^1\text{H-NMR}$ (CDCl_3) δ (ppm) = 6.66 – 6.57 (dd, 1H, $J_1 = 16.9$ Hz, $J_2 = 1.7$ Hz, amide- $\text{CH}=\text{CH}_2$, *trans*), 6.46-6.14 (m, 3H, amide- $\text{CH}=\text{CH}_2$, acryl- $\text{CH}=\text{CH}_2$, acryl- $\text{CH}=\text{CH}_2$ *trans*), 6.10 – 6.04 (dd, 1H, $J_1 = 10.6$ Hz, $J_2 = 1.6$ Hz, amide- $\text{CH}=\text{CH}_2$, *cis*), 5.75 – 5.69 (dd, 1H, $J_1 = 8.9$ Hz, $J_2 = 3.3$ Hz, acryl- $\text{CH}=\text{CH}_2$, *cis*) 3.35 (s, 3H, NCH_3).

$^{13}\text{C-NMR}$ (CDCl_3) δ (ppm) = 165.9 (amide- $\text{C}=\text{O}$), 163.7 (acryl- $\text{C}=\text{O}$), 134.9 (amide- CH_2), 130.1 (acryl- CH_2), 125.2 (amide- CH), 124.4 (acryl- CH), 35.8 (NCH_3).

IR (AT-IR, thin film, cm^{-1}): 1772 ($\text{C}=\text{O}$), 1666 and 1628 ($\text{C}=\text{C}$), 1408 (N-O)

MS (m/z): calcd. 155.15, found: 155.06

Elem. Anal. Calcd. for $\text{C}_7\text{H}_9\text{NO}_3$: C: 54.19%, H: 5.85%, N: 9.03%, found: C: 54.10%, H: 5.79%, N: 8.89%.

3.1.2.2. *O,N-Bis(1-oxo-2-propen-1-yl)-N-(isopropyl)-hydroxylamine (28)*

The crude product was purified by column chromatography (PE : EE = 5:1) to yield 0.86 g of **28** as a colourless liquid.

Yield: 0.86 g (58% calculated yield) of a colourless liquid

$\text{C}_9\text{H}_{13}\text{NO}_3$

$R_f = 0.40$ (PE : EE = 5:1)

$^1\text{H-NMR}$ (CDCl_3) δ (ppm) = 6.67 – 6.58 (dd, 1H, $J_1 = 17.2$ Hz, $J_2 = 1.5$ Hz, amide- $\text{CH}=\text{CH}_2$, *trans*), 6.46-6.18 (m, 3H, amide- $\text{CH}=\text{CH}_2$, acryl- $\text{CH}=\text{CH}_2$, acryl, $\text{CH}=\text{CH}_2$,

trans), 6.10 – 6.04 (dd, 1H, $J_1 = 10.6$ Hz, $J_2 = 1.5$ Hz, amide-CH=CH₂, *cis*), 5.73 – 5.67 (dd, 1H, $J_1 = 9.9$ Hz, $J_2 = 2.3$ Hz, acryl-CH=CH₂, *cis*), 4.89 – 4.69 (hep, 1H, $J = 6.6$ Hz, NCHCH₃CH₃), 1.19 – 1.16 (d, 6H, $J = 6.7$ Hz, NCHCH₃CH₃).

¹³C-NMR (CDCl₃) δ (ppm) = 165.6 (amide-C=O), 164.6 (acryl-C=O), 134.7 (amide-CH=CH₂), 129.8 (acryl-CH=CH₂), 126.2 (amide-CH=CH₂), 124.4 (acryl-CH=CH₂), 50.1 (NCHCH₃CH₃), 19.4 (NCHCH₃CH₃).

IR (AT-IR, thin film, cm⁻¹): 1776 (C=O), 1667 and 1626 (C=C), 1409 (N-O)

MS (*m/z*): calcd. 183.21, found: 183.06

Elem. Anal. Calcd. for C₉H₁₃NO₃: C: 59.00%, H: 7.15%, N: 7.65%, found: C: 59.17%, H: 7.26%, N: 7.46%.

3.1.2.3. *O,N-Bis(1-oxo-2-propen-1-yl)-N-(t-butyl)-hydroxylamine (29)*

The crude product was purified by column chromatography (PE : EE = 7:1) to yield 0.82 g of **29** as a colourless liquid.

Yield: 0.82 g (58% calculated yield) of a colourless liquid

C₁₀H₁₅NO₃

$R_f = 0.44$ (PE : EE = 7:1)

¹H-NMR (CDCl₃) δ (ppm) = 6.63 – 6.55 (dd, 1H, $J_1 = 16.9$ Hz, $J_2 = 1.6$ Hz, amide-CH=CH₂, *trans*), 6.27-6.06 (m, 4H, amide-CH=CH₂ *cis*, amide-CH=CH₂, acryl-CH=CH₂, acryl-CH=CH₂ *trans*), 5.61 – 5.55 (dd, 1H, $J_1 = 9.7$ Hz, $J_2 = 2.7$ Hz, acryl-CH=CH₂, *cis*), 1.42 (s, 9H, NCCH₃CH₃CH₃).

¹³C-NMR (CDCl₃) δ (ppm) = 166.7 (amide-C=O), 165.1 (acryl-C=O), 134.9 (amide-CH=CH₂), 128.8 (acryl-CH=CH₂), 127.9 (amide-CH=CH₂), 124.3 (acryl-CH=CH₂), 62.6 (C), 27.4 (NCCH₃CH₃CH₃).

IR (AT-IR, thin film, cm⁻¹): 1775 (C=O), 1668 and 1627 (C=C), 1406 (N-O)

MS (*m/z*): calcd. 197.24, found: 197.20

Elem. Anal. Calcd. for C₁₀H₁₅NO₃: C: 60.90%, H: 7.67%, N: 7.10%, found: C:

61.15%, H: 7.81%, N: 6.82%.

3.1.2.4. *O,N-Bis(1-oxo-2-propen-1-yl)-N-(cyclohexyl)-hydroxylamine (30)*

The crude product was purified by column chromatography (PE : EE = 6:1) to yield 1.06 g of **30** as a slightly yellow oil.

Yield: 1.06 g (80% calculated yield) of a slightly yellow oil

$C_{12}H_{17}NO_3$

$R_f = 0.36$ (PE : EE = 6:1)

1H -NMR ($CDCl_3$) δ (ppm) = 6.64 – 6.55 (dd, $J_1 = 17.0$ Hz, $J_2 = 1.4$ Hz, amide- $CH=CH_2$, *trans*, 1H), 6.29 – 6.16 (m, 3H, amide- $CH=CH_2$, acryl- $CH=CH_2$, acryl- $CH=CH_2$ *trans*), 6.07 – 6.01 (dd, 1H, $J_1 = 10.5$ Hz, $J_2 = 1.5$ Hz, amide- $CH=CH_2$, *cis*), 5.70 – 5.64 (dd, 1H, $J_1 = 9.8$ Hz, $J_2 = 2.4$ Hz, acryl- $CH=CH_2$, *cis*), 4.45 – 4.30 (m, 1H, N-CH), 1.85 – 1.00 (m, 10H, chxn- CH_2).

^{13}C -NMR ($CDCl_3$) δ (ppm) = 165.2 (amide-C=O), 164.6 (acryl-C=O), 134.7 (amide- $CH=CH_2$), 129.6 (acryl- $CH=CH_2$), 126.1 (amide- $CH=CH_2$), 124.4 (acryl- $CH=CH_2$), 57.5 (N-CH), 29.75 + 25.4 + 25.2 (chxn- CH_2).

IR (AT-IR, thin film, cm^{-1}): 1776 (C=O), 1667 and 1626 (C=C), 1409 (N-O)

MS (m/z): calcd. 223.27, found: 223.10

Elem. Anal. Calcd. for $C_{12}H_{17}NO_3$: C: 64.55%, H: 7.67%, N: 6.27%, found: C: 64.97%, H: 7.73%, N: 7.67%.

3.1.2.5. *O,N-Bis(1-oxo-2-propen-1-yl)-N-(benzyl)-hydroxylamine (31)*

The crude product was purified by column chromatography (PE : EE = 6:1) to yield 0.84 g of **31** as a colourless oil.

Yield: 0.84 g (65% calculated yield) of a colourless oil

$C_{13}H_{13}NO_3$

$R_f = 0.38$ (PE : EE = 6:1)

1H -NMR ($CDCl_3$) δ (ppm) = 7.36 – 7.26 (m, 5H, ar-H), 6.59 – 6.46 (m, 2H, amide-

Yield: 0.39 g (28% calculated yield) of a colourless liquid

$C_9H_9NO_3$

$R_f = 0.28$ (PE : EE = 8:1)

1H -NMR ($CDCl_3$) δ (ppm) = 6.92 – 6.78 (dd, 2H, $J_1 = 16.9$ Hz, $J_2 = 10.1$ Hz, amide- $\underline{C}H=CH_2$,), 6.75-6.66 (dd, 1H, $J_1 = 17.1$ Hz, $J_2 = 1.4$ Hz, acryl- $\underline{C}H=CH_2$, *trans*), 6.60 – 6.51 (dd, 2H, $J_1 = 17.1$ Hz, $J_2 = 1.6$ Hz, amide- $\underline{C}H=CH_2$, *trans*), 6.41– 6.27 (dd, 1H, $J_1 = 17.3$ Hz, $J_2 = 10.5$ Hz, acryl- $\underline{C}H=CH_2$), 6.18 – 6.12 (dd, 1H, $J_1 = 10.3$ Hz, $J_2 = 1.6$ Hz, acryl- $\underline{C}H=CH_2$, *cis*), 5.95 – 5.89 (dd, 2H, $J_1 = 10.7$ Hz, $J_2 = 1.4$ Hz, amide- $\underline{C}H=CH_2$, *cis*).

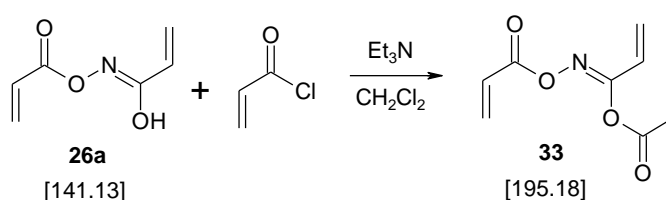
^{13}C -NMR ($CDCl_3$) δ (ppm) = 163.7 (acryl- $C=O$), 162.9 (amide- $C=O$), 136.0 (acryl- $\underline{C}H=CH_2$), 133.0 (amide- $\underline{C}H=CH_2$), 127.6 (amide- $\underline{C}H=CH_2$), 123.7 (acryl- $\underline{C}H=CH_2$).

IR (AT-IR, thin film, cm^{-1}): 1782 ($C=O$), 1707 + 1620 ($C=C$), 1402 ($N-O$)

MS (m/z): calcd. 195.18, found: 195.20

Elem. Anal. Calcd. for $C_9H_9NO_3$: C: 55.39%, H: 4.65%, N: 7.18%, found: C: 55.52%, H: 4.79%, N: 7.13%.

As by-product of this reaction 2-propenoyl acid-1-(2-propenoyl oximino) propenoate (**33**) was identified after column chromatography.



Yield: 0.22 g (16% calculated yield) as colorless liquid

$R_f = 0.19$ (PE : EE = 8:1)

1H -NMR ($CDCl_3$) δ (ppm) = 6.71 – 6.61 (dd, 1H, $J_1 = 16.8$ Hz, $J_2 = 1.5$ Hz, acryl- $\underline{C}H=CH_2$ *trans*), 6.56-6.43 (m, 2H), 6.36 – 6.05 (m, 3H), 5.96– 5.87 (m, 2H), 5.80 – 5.74 (dd, 1H, $J_1 = 10.9$ Hz, $J_2 = 0.6$ Hz).

MS (m/z): calcd. 195.18, found: 195.16

3.2.4. Steady state photolysis experiments with TEMPO and t-BAM

3.2.4.1. Compound **27** with **TEMPO**

Materials: 0.13 mol L⁻¹ of compound **27**
0.51 mol L⁻¹ **TEMPO**
4 mL acetonitrile

Preparation:

In a 25 mL 3-necked flask equipped with a magnetic stirrer a solution of **27** and **TEMPO** was prepared in water free MeCN and rinsed with Argon for 10 min. The solution was irradiated with light (EFOS, Novacure, 240-450 nm, 1000 mW/cm²) for 30 min under stirring. Samples for GC-MS and HPLC (~ 100 μ l) were taken at defined time intervals. Those samples were diluted 1:20 or 1:200 when applicable.

3.2.4.2. Compound **27** with **t-BAM**

Materials: 0.13 mol L⁻¹ **27**
0.57 mol L⁻¹ **t-BAM**
4 mL acetonitrile

Preparation:

In a 25 mL 3-necked flask equipped with a magnetic stirrer a solution of **27** and **t-BAM** was prepared in water free MeCN and rinsed with Argon for 10 min. The solution was irradiated with light (EFOS, Novacure, 240-450 nm, 1000 mW/cm²) for 30 min under stirring. Samples for GC-MS and HPLC (~ 100 μ l) were taken at defined time intervals. Those samples were diluted 1:20 or 1:200 when applicable.

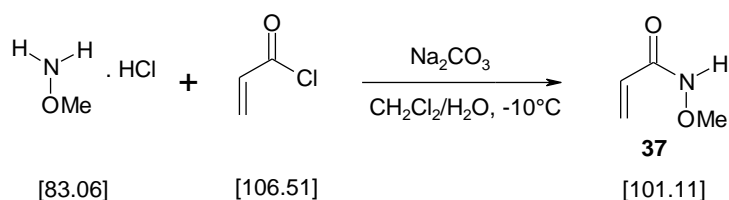
4. Monomers for Biomedical Applications

4.1. Hydroxylamine-based Monomers

4.1.1. Synthesis

4.1.1.1. *N*-(1-oxo-2-propen-1-yl)-*N*-(vinylloxycarbonyl)-*O*-methyl-hydroxylamine (**34**)

4.1.1.1.1. *N*-(1-oxo-2-propen-1-yl)-*O*-methyl-hydroxylamine (**37**)²²⁴



Materials: 0.50 g (6.0 mmol) *O*-methyl hydroxylamine hydrochloride
 0.54 g (5.1 mmol) acryloyl chloride
 0.95 g (8.5 mmol) sodium bicarbonate
 45 mL dichloromethane
 15 mL water

Preparation:

To a solution of *O*-methyl hydroxylamine hydrochloride in 15 mL of distilled water sodium bicarbonate and 45 mL of CH₂Cl₂ were added. The reaction mixture was stirred at 0°C and acryloyl chloride was added dropwise. Then the reaction mixture was stirred at room temperature. The progress of the reaction was monitored by TLC (ethyl acetate). After 2 h of reaction time the acryloyl chloride had been consumed and the reaction was stopped. The aqueous layer was separated and acidified with 0.1 M HCl, followed by extraction with 3 x CH₂Cl₂. The combined organic layers were dried over sodium sulfate and after filtration of the drying agent the solvent was distilled off. The crude product was used without further purification for the next reaction step. 0.25 g of **37** as a white solid were obtained.

Yield: 0.25 g (56% calculated yield, 80% literature yield) of a white solid

C₄H₇NO₂

R_f = 0.48 (ethyl acetate)

EXPERIMENTAL PART

^{13}C -NMR (CDCl_3) δ (ppm) = 154.3 (C=O), 141.2 ($\underline{\text{C}}\text{H}=\text{CH}_2$), 97.12 ($\text{CH}=\underline{\text{C}}\text{H}_2$), 64.79 (OCH_3)

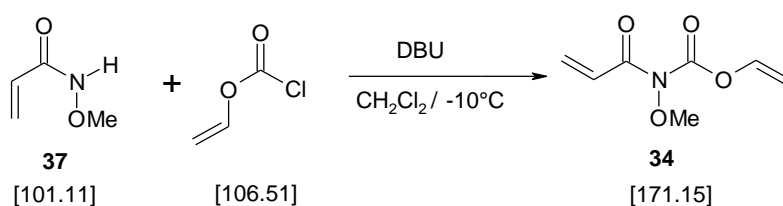
IR (AT-IR, thin film, cm^{-1}): 1736 (C=O), 1650 (C=C), 1357 (N-O)

MS (m/z): calcd. 117.11, found: 117.1

Elem. Anal. Calcd. for $\text{C}_4\text{H}_7\text{NO}_3 \times 1/6 \text{H}_2\text{O}$ [120.11 g/mol]: C: 39.96%, H: 6.10%, N: 11.65%, found: C: 39.93%, H: 5.94%, N: 11.74%.

4.1.1.1.3. *N*-(1-oxo-2-propen-1-yl)-*N*-(vinylloxycarbonyl)-*O*-methyl-hydroxylamine (**34**)

Pathway 1: Via *N*-(1-ox-2-propen-1-yl)-*O*-methyl-hydroxylamine (**37**)



Materials: 0.24 g (2.4 mmol) *N*-(1-oxo-2-propen-1-yl)-*O*-methyl-hydroxylamine (**37**)
0.25 g (2.4 mmol) chlorovinyl formate
0.54 g (3.6 mmol) 1,8-diazabicyclo[5.4.0]undec-7-ene (**DBU**)
20 mL dichloromethane

Preparation:

To a solution of *N*-(1-oxo-2-propen-1-yl)-*O*-methyl-hydroxylamine (**37**) in 20 mL of dry CH_2Cl_2 **DBU** was added. The reaction mixture was stirred at 0°C and chlorovinyl formate was added dropwise over a period of 10 min. Then the reaction mixture was stirred at room temperature and progress was monitored by TLC. After 5 h reaction time in total the reaction was completed. The organic layer was washed with 0.1 M HCl (3 x 10 mL). Then the organic layer was dried over Na_2SO_4 and the solvent was distilled off. The crude product was purified by column chromatography (petrolether : ethylacetate = 8:1) to yield 0.04 g of **34** as a colourless liquid.

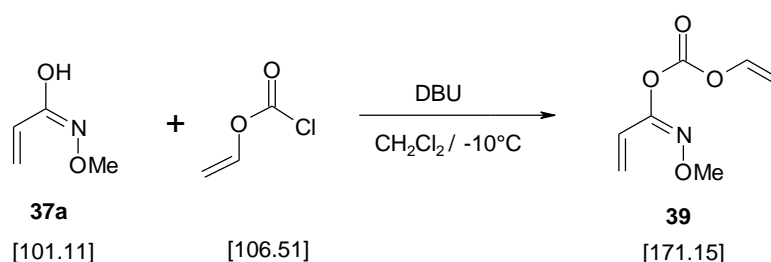
Yield: 0.04 g (9% calculated yield) of a colourless liquid

$\text{C}_7\text{H}_9\text{NO}_4$

$R_f = 0.29$ (PE : EE = 8:1)

$^1\text{H-NMR}$ (CDCl_3) δ (ppm) = 7.25 – 7.16 (dd, 1H, $J_1 = 13.8$ Hz, $J_2 = 6.1$ Hz, carbamate- $\text{CH}=\text{CH}_2$), 7.08 – 6.95 (dd, 1H, $J_1 = 16.8$ Hz, $J_2 = 10.5$ Hz, amide- $\text{CH}=\text{CH}_2$), 6.60 – 6.50 (dd, 1H, $J_1 = 17.1$ Hz, $J_2 = 1.6$ Hz, amide- $\text{CH}=\text{CH}_2$, *trans*), 5.92 – 5.59 (dd, 1H, $J_1 = 10.6$ Hz, $J_2 = 1.9$ Hz, amide- $\text{CH}=\text{CH}_2$, *cis*), 5.12 – 5.04 (dd, 1H, $J_1 = 13.9$ Hz, $J_2 = 2.2$ Hz, carbamate- $\text{CH}=\text{CH}_2$, *trans*), 4.78 – 4.73 (dd, 1H, $J_1 = 6.3$ Hz, $J_2 = 2.1$ Hz, carbamate- $\text{CH}=\text{CH}_2$, *cis*), 3.88 (s, 3H, OCH_3).

The imine tautomer of compound **37** formed a by-product, *N*-methoxy-2-propenecarboximidic acid vinyl carbonate anhydride (**39**), which was isolated by column chromatography to yield 0.08 g of a colourless liquid.



Yield: 0.08 g (18% of calculated) of a colourless liquid

$\text{C}_7\text{H}_9\text{NO}_4$

$R_f = 0.57$ (PE : EE = 8:1)

$^1\text{H-NMR}$ (CDCl_3) δ (ppm) = 7.12 – 7.02 (dd, 1H, $J_1 = 13.8$ Hz, $J_2 = 6.3$ Hz, carbamate- $\text{CH}=\text{CH}_2$), 6.29 – 6.21 (dd, 1H, $J_1 = 17.5$ Hz, $J_2 = 11.0$ Hz, imine- $\text{CH}=\text{CH}_2$), 5.80 – 5.71 (dd, 1H, $J_1 = 17.5$ Hz, $J_2 = 0.5$ Hz, imine- $\text{CH}=\text{CH}_2$, *trans*), 5.58 – 5.25 (dd, 1H, $J_1 = 11.3$ Hz, $J_2 = 0.5$ Hz, imine- $\text{CH}=\text{CH}_2$, *cis*), 5.07 – 4.99 (dd, 1H, $J_1 = 13.7$ Hz, $J_2 = 2.3$ Hz, carbamate- $\text{CH}=\text{CH}_2$, *trans*), 4.71 – 4.67 (dd, 1H, $J_1 = 6.1$ Hz, $J_2 = 2.3$ Hz, carbamate- $\text{CH}=\text{CH}_2$, *cis*), 3.90 (s, 3H, OCH_3).

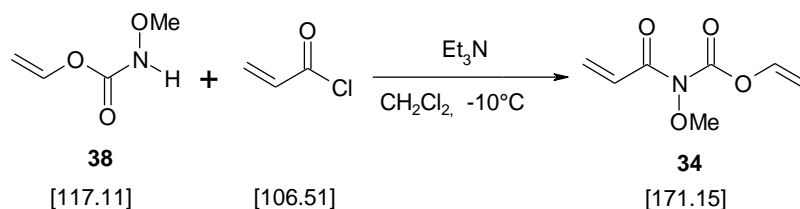
$^{13}\text{C-NMR}$ (CDCl_3) δ (ppm) = 147.71 (C=O), 146.77 (C=N), 142.50 (carbamate- $\text{CH}=\text{CH}_2$), 125.47 (imine- $\text{CH}=\text{CH}_2$), 121.63 (imine- $\text{CH}=\text{CH}_2$), 99.24 (carbamate- $\text{CH}=\text{CH}_2$), 63.12 (O-CH_3)

IR (AT-IR, thin film, cm^{-1}): 1751 (C=O), 1709 (C=O), 1651 (C=C vinyl), 1621 (C=C acryl), 1285 (N-O)

MS (m/z): calcd. 171.15, found: 171.2

Elem. Anal. Calcd. for $C_7H_9NO_4$: C: 49.12%, H: 5.30%, N: 8.18%, found: C: 50.25%, H: 5.43%, N: 7.78%.

Pathway 2: Via *N*-(vinylloxycarbonyl)-*O*-methyl hydroxylamine (**38**)



Materials: 0.60 g (5.1 mmol) *N*-(vinylloxycarbonyl)-*O*-methyl hydroxylamine (**38**)
 0.46 g (5.1 mmol) acryloyl chloride
 0.78 g (7.7 mmol) triethylamine
 30 mL dichloromethane

Preparation:

To a solution of *N*-(vinylloxycarbonyl)-*O*-methyl-hydroxylamine (**38**) in 25 mL of distilled CH_2Cl_2 triethylamine was added. The reaction mixture was stirred at 0°C and a solution of acryloyl chloride in 5 mL of CH_2Cl_2 was added dropwise over a period of 15 min. Then the reaction mixture was stirred at room temperature and progress was monitored by TLC. After 2.5 h reaction time in total the reaction had finished. The organic layer was washed with 0.1 M HCl (4 x 20 mL). Then the organic layer was dried over Na_2SO_4 and the solvent was distilled off. The crude product was purified by column chromatography (PE : EE = 9:1) to yield 0.50 g of **34** as a colourless liquid.

Yield: 0.50 g (56% calculated yield) of a colourless liquid

$C_7H_9NO_4$

$R_f = 0.34$ (PE : EE= 9:1)

$^1\text{H-NMR}$ (CDCl_3) δ (ppm) = 7.25 – 7.16 (dd, 1H, $J_1 = 13.8$ Hz, $J_2 = 6.1$ Hz, carbamate- $\text{CH}=\text{CH}_2$), 7.08 – 6.95 (dd, 1H, $J_1 = 16.8$ Hz, $J_2 = 10.5$ Hz, amide- $\text{CH}=\text{CH}_2$), 6.60 – 6.50 (dd, 1H, $J_1 = 17.1$ Hz, $J_2 = 1.6$ Hz, amide- $\text{CH}=\text{CH}_2$, *trans*),

Na₂SO₄ and the solvent was distilled off after filtration of the drying agent. 0.91 g of **36** were obtained as colourless liquid. According to ¹H-NMR and GC-MS analysis no further purification of the crude product was necessary.

Yield: 0.91 g (81% calculated yield) of a colorless liquid

C₇H₉NO₅

R_f = 0.36 (PE : EE = 6:1)

¹H-NMR (CDCl₃) δ (ppm) = 7.17 – 7.00 (m, 2H, CH=CH₂ for carbamate and carbonate), 5.09 – 5.1 (dd, 1H, J₁ = 13.7 Hz, J₂ = 2.4 Hz, carbamate-CH=CH₂, *trans*), 4.94 – 4.86 (dd, J₁ = 13.9 Hz, J₂ = 2.0 Hz, carbonate-CH=CH₂, *trans*, 1H), 4.75 – 4.71 (dd, 1H, J₁ = 6.07 Hz, J₂ = 2.6 Hz, carbamate-CH=CH₂, *cis*), 4.62– 4.58 (dd, 1H, J₁ = 6.2 Hz, J₂ = 2.1 Hz, carbonate-CH=CH₂, *cis*), 3.75 (s, 3H, NCH₃).

¹³C-NMR (CDCl₃) δ (ppm) = 152.9 (carbamate-C=O), 151.7 (carbonate-C=O), 142.2 (carbamate-CH=CH₂), 141.6 (carbonate-CH=CH₂), 99.87 (carbamate-CH=CH₂), 98.0 (carbonate-CH=CH₂), 37.6 (N-CH₃)

IR (ATR-IR, thin film, cm⁻¹): 1745 (C=O), 1652 (C=C), 1349 (N-O)

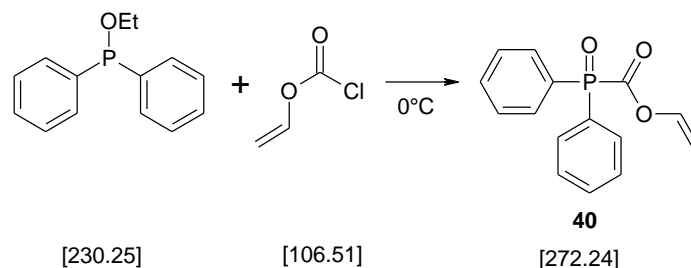
MS (*m/z*): calcd. 187.15, found: 187.1

Elem. Anal. Calcd. for C₇H₉NO₅: C: 44.92, H: 4.85, N: 7.48, found: C: 45.77, H: 4.91, N: 7.34.

4.2. Phosphorus containing vinyl esters and vinyl carbamates

4.2.1. Synthesis of acylphosphoxides & phosphoformates

4.2.1.1. Diphenyl vinyloxycarbonyl phosphin oxide (**40**)



Materials: 1.00 g (4.3 mmol) ethyldiphenylphosphinite
 0.69 g (6.5 mmol) chlorovinyl formate

Preparation:

1.0 g ethyldiphenylphosphinite was added dropwise at 0°C over a period of 15 min to 0.69 g chlorovinyl formate. After the addition was finished, the reaction mixture was stirred at room temperature for additional 3 h. To remove the evolving ethylchloride, the solution was distilled under reduced pressure.

The crude product was obtained as white solid. After drying in high vacuum the product needed no further purification. 1.1 g were obtained of **40** as a white solid.

Yield: 1.1 g (99% calculated yield) of white solid

$\text{C}_{15}\text{H}_{13}\text{O}_3\text{P}$

Mp: 61.0 – 63.8°C

$^1\text{H-NMR}$ (CDCl_3) δ (ppm) = 7.81-7.95 (m, 4H ar-H₂+H₆), 7.47-7.67 (m, 6H, ar-H₃+H₄+H₅), 7.33-7.41 (dd, 1H, $J_1 = 14.0$ Hz, $J_2 = 6.3$ Hz, $\text{CH}_2=\text{CH}-\text{O}$), 5.09-5.19 (m, 1H, $J_1 = 13.9$ Hz, $J_2 = 1.7$ Hz, $\text{CH}_2=\text{CH}-\text{O}$, *trans*), 4.75-4.82 (m, 1H, $J_1 = 6.1$ Hz, $J_2 = 2.0$ Hz, $\text{CH}_2=\text{CH}-\text{O}$, *cis*).

$^{13}\text{C-NMR}$ (CDCl_3) δ (ppm) = 166.9 (C=O, $J_{\text{P-C}} = 140.1$ Hz), 140.3 ($\text{OCH}=\text{CH}_2$, $J_{\text{P-C}} = 4.3$ Hz), 133.2 (ar-C₄, $J_{\text{P-C}} = 2.9$ Hz), 131.9 (ar-C₂+C₆, $J_{\text{P-C}} = 10.9$ Hz), 127.0 (ar-C₁, $J_{\text{P-C}} = 105.2$ Hz), 126.6 (ar-C₃+C₅, $J_{\text{P-C}} = 11.9$ Hz), 101.2 ($\text{OCH}=\text{CH}_2$)

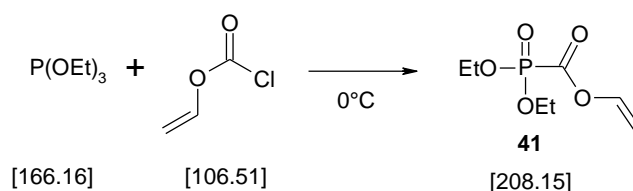
^{31}P -NMR (CDCl_3) δ (ppm) = 18.0

IR (AT-IR, thin film, cm^{-1}): 1720 (C=O), 1647 (C=C), 1216 (P=O), 1163 (P-O)

MS (m/z): calcd. 272.24, found: 273.3 $[\text{M}+\text{H}]^+$

Elem. Anal. Calcd. for $\text{C}_{15}\text{H}_{13}\text{O}_3\text{P} \times \frac{1}{6} \text{H}_2\text{O}$ [275.24 g/mol]: C: 65.39%, H: 4.78%, P: 11.26%, found: C: 65.55%, H: 4.53%, P: 11.46%.

4.2.1.2. Diethyl vinyl phosphoformate (**41**)



Materials: 3.13 g (18.8 mmol) triethylphosphite
 2.00 g (18.8 mmol) chlorovinyl formate

Preparation:

3.13 g of triethylphosphite were added dropwise at 0°C over a period of 15 min to the chlorovinyl formate. After the addition was finished, the reaction mixture was stirred at room temperature for additional 2 h. To remove the evolving ethylchloride, the solution is heated gently to 40°C for 30 min.

The slightly yellow crude product of **41** was purified by vacuum distillation ($125\text{-}128^\circ\text{C}$ at 8 mbar) to yield 3.3 g of a colourless liquid.

Yield: 3.3 g (83% calculated yield) of a colourless liquid

$\text{C}_7\text{H}_{13}\text{O}_5\text{P}$

^1H -NMR (CDCl_3) δ (ppm) = 7.01 - 6.99 (dd, 1H, $J_1 = 6.3$ Hz, $J_2 = 0.7$ Hz, $\text{OCH}=\text{CH}_2$), 4.79 - 4.88 (2dd, 1H, $\text{OCH}=\text{CH}_2$, *trans*), 4.48 - 4.55 (2dd, 1H, $\text{OCH}=\text{CH}_2$, *cis*), 3.97 - 4.12 (2q, 4H, OCH_2CH_3), 1.09-1.17 (2t, 6H, OCH_2CH_3).

^{13}C -NMR (CDCl_3) δ (ppm) = 161.2 (C=O, $J_{(\text{P}-\text{C})} = 273.6$ Hz), 139.9 ($\text{OCH}=\text{CH}_2$, $J_{(\text{P}-\text{C})} = 6.8$ Hz), 100.8 ($\text{OCH}=\text{CH}_2$ Hz), 64.8 (OCH_2CH_3 , $J_{(\text{P}-\text{C})} = 6.2$ Hz), 16.2 (OCH_2CH_3 , $J_{(\text{P}-\text{C})} = 5.8$ Hz).

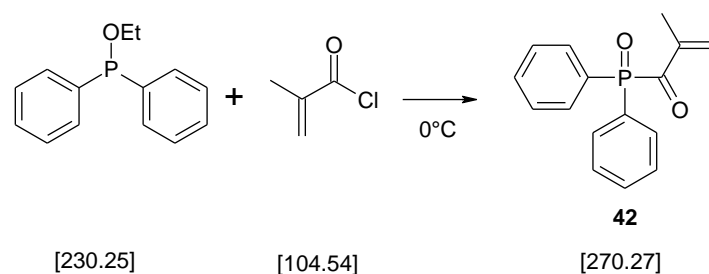
^{31}P -NMR (CDCl_3) δ (ppm) = - 4.2

IR (ATR-IR, thin film, cm^{-1}): 1729 (C=O), 1645 (C=C), 1273 (P=O), 1011 (P-O-C)

MS (m/z): calcd. 208.15, found: 209.2 $[\text{M}+\text{H}]^+$

Elem. Anal. Calcd. for $\text{C}_7\text{H}_{13}\text{O}_5\text{P}$: C: 40.39%, H: 6.30%, P: 14.88%, found: C: 40.09%, H: 6.14%, P: 14.47%.

4.2.1.4. Diphenyl methacryloyl phosphin oxide (**42**)



Materials: 1.20 g (5.0 mmol) ethyldiphenylphosphinite
0.45 g (4.0 mmol) methacryloyl chloride

Preparation:

1.20 g ethyldiphenylphosphinite were added dropwise to 0.45 g methacryloyl chloride under vigorous stirring at 0°C in a round bottomed flask with applied drying tube. After the addition was finished, the reaction solution had turned yellow. It was left stirring at room temperature for 12 h.

A ^{31}P -NMR of the reaction mixture showed many by-products. This was also seen in a TLC analysis, nevertheless, the single dot on the TLC plate, which absorbed at 355 nm under the UV-lamp was considered as the desired product.

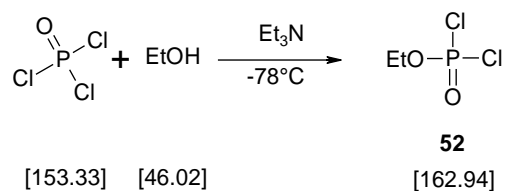
However, isolation of the product was not possible due to fast degradation in air. The existence of compound **42** could only be confirmed by GC-MS analysis.

$R_f = 0.19$ (PE : EE = 1:3)

MS (m/z): calcd. 270.27, found: 271.3 $[\text{M}+\text{H}]^+$

4.2.2. Synthesis of vinyl esters of phosphoric acid

4.2.2.1. Ethyl dichlorophosphate (**52**)



Materials: 9.97 g (65.0 mmol) phosphorylchloride
 6.57 g (65.0 mmol) triethylamine
 2.99 g (65.0 mmol) ethanol
 200 mL diethylether

Preparation:

In a flame-dried 250 mL 3-necked round flask 9.97 g of phosphoryl chloride were dissolved in 100 mL of dry diethylether. Under Ar-atmosphere a mixture of ethanol and triethylamine in 100 mL of dry diethylether is added dropwise at -78°C . After the addition is finished, the reaction mixture is stirred at room temperature for 20 h. Then the precipitate of triethylamine hydrochloride is filtered off and the solvent is removed under reduced pressure. The crude product of **52** was purified by vacuum distillation to yield 8.5 g of a colorless oil.

Yield: 8.5 g (81% calculated yield) of a colorless oil

$\text{C}_2\text{H}_5\text{Cl}_2\text{O}_2\text{P}$

Bp: $52\text{-}53^\circ\text{C}$ at 10 mbar (Lit. 117°C at 760 mmHg)²²⁵

$R_f = 0.48$ (PE : EE = 1:1)

$^1\text{H-NMR}$ (CDCl_3) δ (ppm) = 4.23-4.45 (q, 2H, POCH_2CH_3), 1.29-1.51 (t, 3H, POCH_2CH_3).

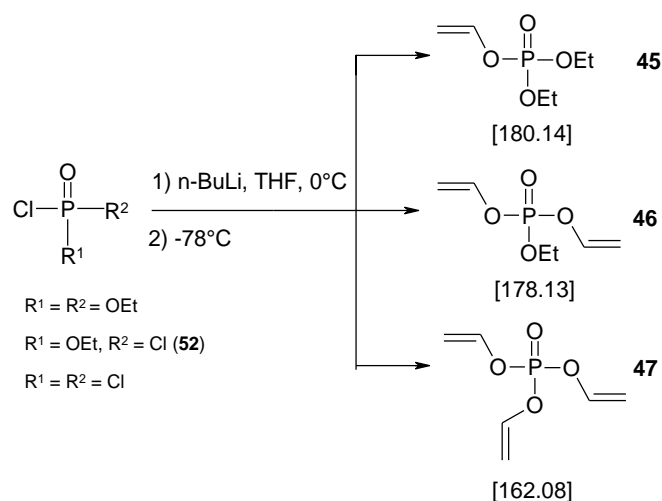
$^{13}\text{C-NMR}$ (CDCl_3) δ (ppm) = 68.8 ($\text{CH}_3\text{-}\underline{\text{C}}\text{H}_2\text{O}$, $J_{(\text{P-C})} = 9.0$ Hz), 15.7 ($\underline{\text{C}}\text{H}_3\text{-CH}_2\text{O}$, $J_{(\text{P-C})} = 9.1$ Hz).

$^{31}\text{P-NMR}$ (CDCl_3) δ (ppm) = 7.9

IR (AT-IR, thin film, cm^{-1}): 1292 (P=O), 1007 (P-O-C), 773 (P-Cl)

MS (m/z): calcd. 162.94, found: 147.0 $[M-CH_3]^-$

4.2.2.2. Vinyl esters of phosphoric acid **45**, **46** and **47**



Materials:

Reagent	45	46	47
	4.31 g (25.0 mmol) diethyl chloro- phosphite	2.57 g (15.7 mmol) ethyl dichloro phosphate (52)	1.61 g (11 mmol) phosphoryl chloride
THF	11.0 g (152.5 mmol)	44.45 g (61.6 mmol)	44.45 g (616 mmol)
<i>n</i> -butyllithium (2.1 M in hexane)	14.43 g (25.0 mmol)	15.00 g (31.5 mmol)	21.65 g (32.0 mmol)

Preparation:

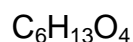
N-butyl lithium solution (2.1 M in hexane) was added dropwise to THF under Ar-atmosphere at 0°C. Then the solution was stirred 30 min at 0°C and for 16 h at room temperature. This reaction mixture was added to the corresponding phosphohalide at -76°C. After the addition was finished, the mixture was stirred 1 h with cooling, then 16 h at room temperature. Finally, the white precipitate was filtered off and the solvent was removed by distillation under reduced pressure.

4.2.2.2.1. Diethyl vinyl phosphate (**45**)

The slightly yellow crude product of **45** was purified by vacuum distillation to yield 0.20 g of a yellow oil. This kind of purification showed to be inadequate as it could not fully separate the product from the butyl by product and also decreased the yield because of thermal instability of the product, it was also tried to purify the

phosphovinyl ester by column chromatography (PE : EE = 1:1) which delivered 3.0 g of product.

Yield: 0.2 g (4% calculated yield) by distillation; 3.0 g (60% calculated yield) of a yellow oil by column chromatography



Bp: 91-93°C at 10 mbar (Lit. 94-95°C at 11 mmHg)²⁰⁸

$R_f = 0.48$ (PE : EE = 1:1)

$^1\text{H-NMR}$ (CDCl_3) δ (ppm) = 6.51-6.61 (dd, 1H, $J_1 = 12.6$ Hz, $J_2 = 6.3$ Hz, $\text{CH}_2=\text{CH-O}$), 4.85-4.91 (dd, 1H, $J_1 = 12.6$ Hz, $J_2 = 1.2$ Hz, $\text{CH}_2=\text{CH-O trans}$), 4.53-4.57 (dd, 1H, $J_1 = 6.3$ Hz, $J_2 = 1.2$ Hz, $\text{CH}_2=\text{CH-O cis}$), 4.09-4.21 (m, 4H, POCH_2CH_3), 1.29-1.37 (m, 6H, POCH_2CH_3).

$^{13}\text{C-NMR}$ (CDCl_3) δ (ppm) = 142.0 ($\text{CH}_2=\text{CHO}$, $J_{\text{(P-C)}} = 6.2$ Hz), 99.5 ($\text{CH}_2=\text{CH-O}$, $J_{\text{(P-C)}} = 11.1$ Hz), 64.2 (POCH_2CH_3 , $J_{\text{(P-C)}} = 6.5$ Hz), 15.8 (POCH_2CH_3 , $J_{\text{(P-C)}} = 7.2$ Hz).

$^{31}\text{P-NMR}$ (CDCl_3) δ (ppm) = -3.5

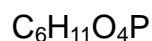
IR (AT-IR, thin film, cm^{-1}): 1645 (C=C), 1271 (P=O), 1012 (P-O-C), 820 (C=C)

MS (m/z): calcd. 180.14, found: 181.3 $[\text{M}+\text{H}]^+$

4.2.2.2. Ethyl divinyl phosphate (**46**)

The slightly yellow crude product was purified column chromatography (PE : EE = 3:1) to yield 1.0 g of **46** as a slightly yellow liquid.

Yield: 1.0 g (36% of calculated yield) of a slightly yellow liquid



$R_f = 0.42$ (PE : EE = 3:1)

$^1\text{H-NMR}$ (CDCl_3) δ (ppm) = 6.48-6.65 (dd, 1H, $J_1 = 6.6$ Hz, $J_2 = 1.4$ Hz, $\text{CH}_2=\text{CH-O}$), 4.87-5.01 (dd, 1H, $J_1 = 13.5$ Hz, $J_2 = 1.1$ Hz, $\text{CH}_2=\text{CH-O trans}$), 4.57-4.68 (m, 1H, $\text{CH}_2=\text{CH-O cis}$), 4.14-4.32 (m, 4H, POCH_2CH_3), 1.30-1.45 (m, 6H, POCH_2CH_3).

^{13}C -NMR (CDCl_3) δ (ppm) = 141.9 ($\text{CH}_2=\underline{\text{C}}\text{HO}$, $J_{(\text{P-C})} = 7.4$ Hz), 100.8 ($\underline{\text{C}}\text{H}_2=\text{CHO}$, $J_{(\text{P-C})} = 10.8$ Hz), 65.4 ($\text{PO}\underline{\text{C}}\text{H}_2\text{CH}_3$, $J_{(\text{P-C})} = 5.9$ Hz), 16.1 ($\text{POCH}_2\underline{\text{C}}\text{H}_3$, $J_{(\text{P-C})} = 7.4$ Hz).

^{31}P -NMR (CDCl_3) δ (ppm) = -7.7

IR (AT-IR, thin film, cm^{-1}): 1644 (C=C), 1279 (P=O), 1011 (P-O-C), 820 (C=C)

MS (m/z): calcd. 178.1, found: 179.2 $[\text{M}+\text{H}]^+$

Elem. Anal. Calcd. for $\text{C}_6\text{H}_{11}\text{O}_4\text{P}$: C: 40.46%, H: 6.22%, found: C: 40.68%, H: 6.11%.

4.2.2.2.3. Trivinyl phosphate (**47**)

The yellow crude product was purified by column chromatography (PE : EE = 5:1) to yield 0.48 g of **47** as a yellow oil.

Yield: 0.48 g (26% of calculated yield) of a yellow oil

$\text{C}_6\text{H}_9\text{O}_4\text{P}$

$R_f = 0.43$ (PE : EE = 5:1)

^1H -NMR (CDCl_3) δ (ppm) = 6.46-6.66 (m, 1H, $\text{CH}_2=\underline{\text{C}}\text{H-O}$), 4.86-5.09 (m, 1H, $\underline{\text{C}}\text{H}_2=\text{CH-O trans}$), 4.57-4.77 (m, 1H, $\underline{\text{C}}\text{H}_2=\text{CH-O cis}$).

^{13}C -NMR (CDCl_3) δ (ppm) = 141.3 ($\text{CH}_2=\underline{\text{C}}\text{HO}$, $J_{(\text{P-C})} = 6.6$ Hz), 101.6 ($\underline{\text{C}}\text{H}_2=\text{CHO}$, $J_{(\text{P-C})} = 11.9$ Hz).

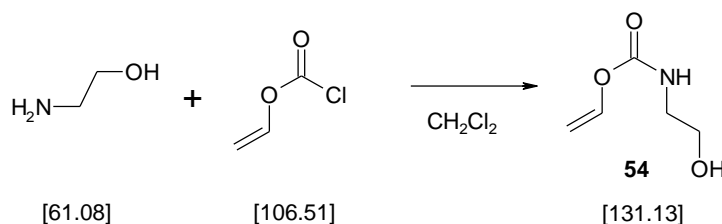
^{31}P -NMR (CDCl_3) δ (ppm) = -12.2

IR (AT-IR, thin film, cm^{-1}): 1643 (C=C), 1286 (P=O), 1017 (P-O-C)

MS (m/z): calcd. 176.11, found: 175.1 $[\text{M}-\text{H}]^-$

4.2.3. Synthesis of phosphovinyl carbamates

4.2.3.1. 2-Hydroxyethyl vinyl carbamate (**54**)¹⁹⁵



Materials: 4.00 g (65.5 mmol) ethanolamine
 3.49 g (32.7 mmol) chlorovinyl formate
 20 mL dichloromethane

Preparation

4.00 g of ethanolamine were mixed with 15 mL of dichloromethane in a 50 mL 2-necked flask. Under Ar-atmosphere 3.49 g of vinylchloroformate were added dropwise with a syringe during a 20 min period. After the addition was finished, the reaction mixture was stirred at room temperature for 16 h.

Then the white solid (ethanolamine hydrochloride) was filtered off and after drying over sodium sulfate and filtering, the solvent was removed under reduced pressure. The crude product was purified by high vacuum distillation to yield 3.21 g of **54** as a colourless liquid.

Yield: 3.21 g (75% calculated yield; 76% literature yield) as colorless liquid

$\text{C}_5\text{H}_9\text{NO}_3$

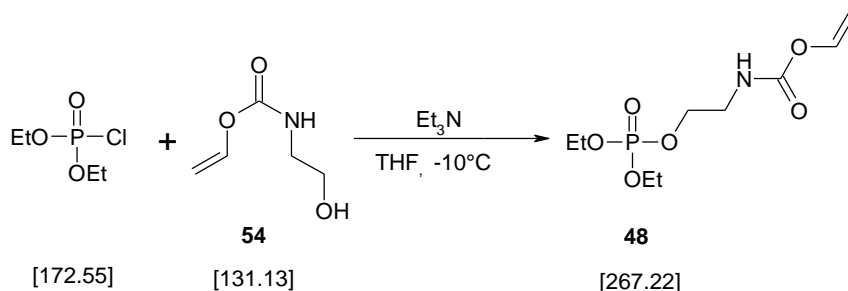
Bp: 86-88°C at 7.8×10^{-2} mbar (Lit.: 125°C at 8.9×10^{-1} Torr)¹⁹⁵

$^1\text{H-NMR}$ (CDCl_3) δ (ppm) = 7.05-7.14 (dd, 1H, $J_1 = 14.1$ Hz, $J_2 = 5.9$ Hz, $\text{CH}_2=\text{CH}-\text{O}$), 5.82 (s, 1H, NH), 4.64-4.71 (dd, 1H, $J_1 = 13.8$ Hz, $J_2 = 1.4$ Hz, $\text{CH}_2=\text{CH}-\text{O}$ *trans*), 4.36-4.39 (dd, 1H, $J_1 = 6.4$ Hz, $J_2 = 1.5$ Hz, $\text{CH}_2=\text{CH}-\text{O}$ *cis*), 3.62-3.66 (t, 2H, $\text{HOCH}_2\text{CH}_2\text{NH}$), 3.48 (s, 1H, OH), 3.25-3.32 (t, 2H, $\text{HOCH}_2\text{CH}_2\text{NH}$).

$^{13}\text{C-NMR}$ (CDCl_3) δ (ppm) = 151.8 (C=O), 141.9 ($\text{CH}_2=\text{CHO}$), 95.4 ($\text{CH}_2=\text{CHO}$), 64.2 (HOCH_2), 43.2 (2HNCH_2).

IR (AT-IR, thin film, cm^{-1}): 3328 (O-H), 1708 (C=O), 1651 (C=C), 1526 (C-N), 862 (C=C)

4.2.3.2. 2-(Diethyl phospholoyloxy) ethyl vinyl carbamate (**48**)



Materials: 1.00 g (5.8 mmol) diethylchlorophosphate
 0.76 g (5.8 mmol) 2-hydroxyethyl vinyl carbamate (**54**)
 0.59 g (5.8 mmol) triethylamine
 14 mL dry tetrahydrofurane

Preparation:

0.76 g of 2-hydroxyethyl vinyl carbamate (**54**) and 0.59 g of triethylamine were mixed together in 10 mL of dry THF. The reaction flask was cooled in an ice-bath and 1.00 g of diethylchlorophosphate in 4 mL of dry THF was added dropwise over a period of 30 min. After the addition was finished, the reaction mixture was stirred at room temperature for 12 h. On the following day, the white precipitate (triethylamine hydrochloride) was filtered off and the solvent was removed under reduced pressure. The slightly yellow oily residue was dissolved in 10 mL of distilled dichloromethane and washed with 1 x 10 mL of 5% sodium bicarbonate solution. Then the organic layer was dried over sodium sulfate and after filtration of the drying agent, the solvent was distilled off under reduced pressure. The crude product was purified by column chromatography (PE : EE = 1 : 5) to yield 0.39 g of **48** as a transparent oil.

Yield: 0.39 g (25% of calculated yield) of a transparent oil

$\text{C}_9\text{H}_{18}\text{NO}_6\text{P}$

$R_f = 0.28$ (PE : EE = 1 : 5)

$^1\text{H-NMR}$ (CDCl_3) δ (ppm) = 7.11-7.19 (dd, 1H, $J_1 = 14.0$ Hz, $J_2 = 6.4$ Hz, $\text{CH}_2=\text{CH-O}$), 5.69 (s, 1H, NH), 4.68-4.74 (dd, 1H, $J_1 = 14.0$ Hz, $J_2 = 1.3$ Hz, $\text{CH}_2=\text{CH-O trans}$),

4.39-4.42 (dd, 1H, $J_1 = 6.3$ Hz, $J_2 = 1.2$ Hz, $\text{CH}_2=\text{CH-O}$ *cis*), 4.04-4.16 (m, 6H, POCH_2CH_3 , $\text{HOCH}_2\text{CH}_2\text{NH}$), 3.45-3.51 (m, 2H, $\text{HOCH}_2\text{CH}_2\text{NH}$), 1.29-1.35 (m, 6H, POCH_2CH_3).

$^{13}\text{C-NMR}$ (CDCl_3) δ (ppm) = 186.5 (C=O), 141.9 ($\text{CH}_2=\text{CHO}$), 95.3 ($\text{CH}_2=\text{CH-O}$), 66.2 (OCH_2CH_2 , $J_{\text{(P-C)}} = 5.6$ Hz), 64.1 (POCH_2CH_3 , $J_{\text{(P-C)}} = 6.4$ Hz), 41.3 (HNCH_2CH_2 , $J_{\text{(P-C)}} = 5.6$ Hz), 16.0 (POCH_2CH_3 , $J_{\text{(P-C)}} = 6.8$ Hz).

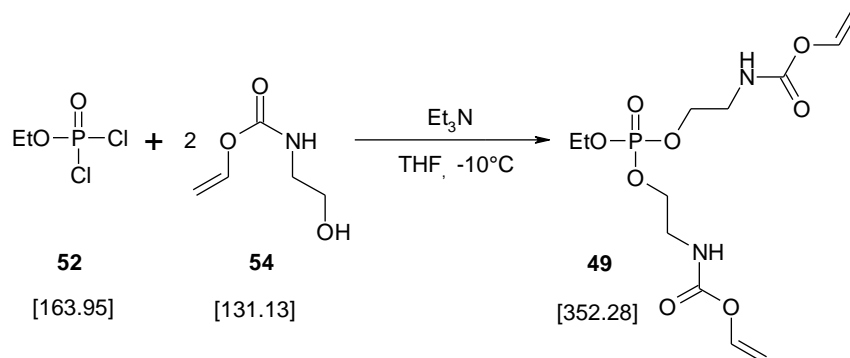
$^{31}\text{P-NMR}$ (CDCl_3) δ (ppm) = 0.76

IR (AT-IR, thin film, cm^{-1}): 3277 (N-H), 1740 (C=O), 1650 (C=C), 1531 (C-N), 1248 (P=O), 1020 (P-O-C), 864 (C=C)

MS (m/z): calcd. 267.22, found: 224.2 [M-OCH=CH_2]⁻

Elem. Anal. Calcd. for $\text{C}_9\text{H}_{18}\text{NO}_6\text{P} \times \frac{1}{3} \text{H}_2\text{O}$ [273.22 g/mol]: C: 39.52%, H: 6.71%, N: 5.12%, found: C: 39.26%, H: 6.61%, N: 4.79%

4.2.3.3. Bis-(2,2'-(ethoxyphospholoyloxy))ethyl vinyl carbamate (**49**)



Materials: 1.50 g (9.2 mmol) ethyldichlorophosphate (**52**)
 2.41 g (18.4 mmol) 2-hydroxyethyl vinyl carbamate (**54**)
 1.86 g (18.4 mmol) triethylamine
 15 mL dry tetrahydrofurane

Preparation:

The preparation was carried out according to the procedure for compound **48**. The yellow-orange oily crude product was purified by column chromatography (PE : EE = 1:5) to yield 1.05 g of a slightly yellow coloured highly viscous oil.

Yield: 1.05 g (43% calculated yield) of a slightly yellow coloured highly viscous oil
 $C_{12}H_{21}N_2O_8P$

$R_f = 0.23$ (PE : EE = 1:5)

1H -NMR ($CDCl_3$) δ (ppm) = 7.11-7.21 (dd, 2H, $J_1 = 14.3$ Hz, $J_2 = 6.3$ Hz, $CH_2=CH-O$), 5.76 (s, 2H, NH), 4.69-4.76 (dd, 2H, $J_1 = 14.1$ Hz, $J_2 = 1.4$ Hz, $CH_2=CH-O$ *trans*), 4.40-4.44 (dd, 2H, $J_1 = 6.3$ Hz, $J_2 = 1.6$ Hz, $CH_2=CH-O$ *cis*), 4.04-4.19 (m, 6H, $POCH_2CH_3$, $HOCH_2CH_2NH$), 3.44-3.51 (m, 4H, $HOCH_2CH_2NH$), 1.26-1.35 (m, 3H, $POCH_2CH_3$).

^{13}C -NMR ($CDCl_3$) δ (ppm) = 186.5 (C=O), 141.8 ($CH_2=CH-O$), 95.5 ($CH_2=CH-O$), 66.5 (OCH_2CH_2 , $J_{(P-C)} = 5.6$ Hz), 64.5 ($POCH_2CH_3$, $J_{(P-C)} = 6.4$ Hz), 41.3 ($HNCH_2CH_2$, $J_{(P-C)} = 5.6$ Hz), 16.1 ($POCH_2CH_3$, $J_{(P-C)} = 6.8$ Hz).

^{31}P -NMR ($CDCl_3$) δ (ppm) = 0.69 and -11.11 (from the *N*-phosphorylated by-product)

IR (AT-IR, thin film, cm^{-1}): 3319 (N-H), 1721 (C=O), 1652 (C=C), 1528 (C-N), 1242 (P=O), 1022 (P-O-C), 865 (C=C)

MS (m/z): calcd. 352.3, found: 355.3 $[M+3H]^+$

Elem. Anal. Calcd. for $C_{12}H_{21}N_2O_8P$: C: 40.91%, H: 6.01% found: C: 40.33%, H: 5.70%

MATERIALS, TECHNICAL EQUIPMENT AND CHARACTERIZATION METHODS

Materials

All reagents of standard synthetic quality were used without further purification except stated in a different way. The solvents were dried and purified by standard laboratory methods. Column chromatography was performed on VWR silica gel 60 (0.040 – 0.063 mm). The monomer hexan-1,6-diol dicrylate (**HDDA**) was provided by IVOCLAR Vivadent.

Determination of the molarity of n-butyllithium in THF

The molarity of commercially available n-butyllithium solutions had to be determined before use by titration with *N*-benzylbenzamide as indicator.

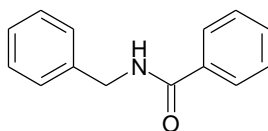


Figure 89. Structure of *N*-benzylbenzamide

Approximately 0.2 g of the amide were weighed exactly into a 10 ml round-bottomed flask and dissolved in 4 mL of dry THF. The solution was degassed with N_2 for 10 min, followed by cooling to -40°C in a MeOH- N_2 bath. The n-BuLi solution was added dropwise to the cooled THF mixture by a 1 mL syringe. Each drop resulted in a short blue coloration of the titrate ($< 1\text{s}$). As soon as a stable blue color was observed, the residual volume of the n-BuLi solution, respectively weight was recorded. The addition of a further drop n-BuLi solution caused a deep blue stain of the mixture. The concentration of the n-butyllithium solution was calculated from the mmol of amide, that had been weighed into the flask, and the consumed amount of n-BuLi solution.

Techniquel Equipment & Characterization Methods

Thin Layer Chromatography

Thin layer chromatography analysis was performed on silica gel 60 F₂₅₄ aluminium sheets from Merck.

Melting Points

Melting points were determined with a “Zeiss Axioskop” microscope equipped with a heating device from Leitz. Melting points are not corrected.

NMR Spectroscopy

¹H and ¹³C NMR spectra were recorded on a Bruker AC-200 FT-NMR spectrometer with CDCl₃ as solvent.

³¹P NMR spectra were measured on a Bruker AVANCE 300 (121.49 MHz, H₃³¹PO₄ = 0 ppm) with a 5 mm broad-invers sample probe and z-gradient.

IR Spectroscopy

ATR-FTIR measurements were carried out on a Biorad FTS 135 spectrophotometer with a Golden Gate MkII diamond ATR equipment (L.O.T.).

GC-MS

Gas chromatography/mass spectrometry was performed on a Hewlett Packard 5890/5970 B system using a fused silica capillary column (SPB-5, 60 m x 0.25 mm). MS spectra were recorded using EI ionistaion (70 eV) and a quadrupole analyzer.

Elemental Analyses

Elemental Analyses were performed at the microanalytic lab of the Department of Physical Chemistry of the University of Vienna under the supervision of Mag. J. Theiner.

UV-Vis Spectroscopy

UV-Vis absorption was measured using a Hitachi U-2001 spectrometer with spectrophotometric grade acetonitrile (MeCN) and methanol (MeOH) as solvent. The parameters are listed below:

Layer thickness: 1 cm

Wavelength Range: 600 – 200 nm

Scan Speed: 200 nm s⁻¹

Lamp Change: 350 nm

HPLC

HPLC measurements were carried out on a reversed-phase HP-1100 HPLC system with a DAD-detector. All separations were carried out on a Waters Xterra MS C₁₈ column, particle size 5 μm, 150 x 3.9 mm² ID. A linear gradient with flow 0.8 mL/min was formed from 97% water to 97% acetonitrile (MeCN) over a period of 30 min.

GPC

GPC measurements were carried out on a Viscothek GPCmax VE2001 GPC Solvent Sample Module, equipped with two Ultrahydrogel columns (250 and 1000) and a Viscothek VE3580 RI detector. Measurements were performed with a pump speed of 0.6 ml min⁻¹ at 40°C column temperature.

Photo-DSC

Photo-DSC analyses of compounds in Chapter 3 and 4.1 were conducted with a modified Shimadzu DSC 50, equipped with a home-made aluminium cylinder.²²⁶ The compounds were irradiated with filtered UV-light (250 – 450 nm) by a light guide (EXFO-Omniculture 2000) attached to the top of the cylinder. The light intensity at the surface level of the cured samples was measured with an EIT Uvicure[®] high energy integrating radiometer. The default light intensity at the tip of the light guide was 1000 mW/cm². The measurements were carried out in an isocratic mode at room temperature under a nitrogen atmosphere. To permit an oxygen free irradiation of the samples a nitrogen purge (~ 50 mL min⁻¹) was used for at least 5 min prior to the measurements.

Photo-DSC analyses of compounds in Chapter 1, 2 and 4.2 were conducted with a Netzsch DSC 204 F1 Phoenix equipped with an autosampler. The compounds were irradiated with filtered UV-light (280 – 500 nm) by a double light guide (EXFO Omniculture 2001) attached to the top of the DSC unit. The default light intensity at the tip of the light guide was 3000 mW/cm². All measurements were carried out in an

isocratic mode at 25°C under a nitrogen atmosphere. To permit an oxygen free irradiation of the samples a nitrogen purge (~ 20 mL/min) was used for at least 5 min prior to the measurements.

Principle

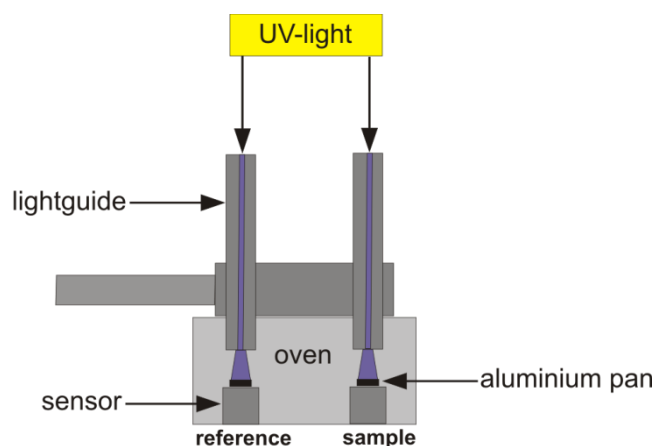


Figure 90. Principle assembly for photo-DSC measurements

By this method it is possible to simulate industrially applied UV-curing processes in small-scale experiments. Generally, the temperature difference between a sample and a reference sample, is monitored with differential scanning calorimetry. The reference can be either an aluminium pan with an already cured sample of the formulation or an empty pan, depending on the mode of evaluation. If both pans are irradiated with UV-light by one in a single oven cell, respectively two wave guides in separated oven cells, the pan containing the uncured formulation will heat up to a greater extent than the pan without or with the already cured sample due to the polymerization process, causing a temperature difference between the reference and sample sensor. After the polymerization is finished, the temperatures on the two sensors will align again. The difference in temperature is proportional to the difference of the heat flow, which is accessible by calibration of the DSC unit.

The reactivity can be derived from 3 parameters, which are given by the photo-DSC plot: the time, which is needed to reach the maximum polymerization heat (t_{max} ; s), the peak height (h ; mW mg^{-1}) and the area under the trace (H_p ; J g^{-1}).

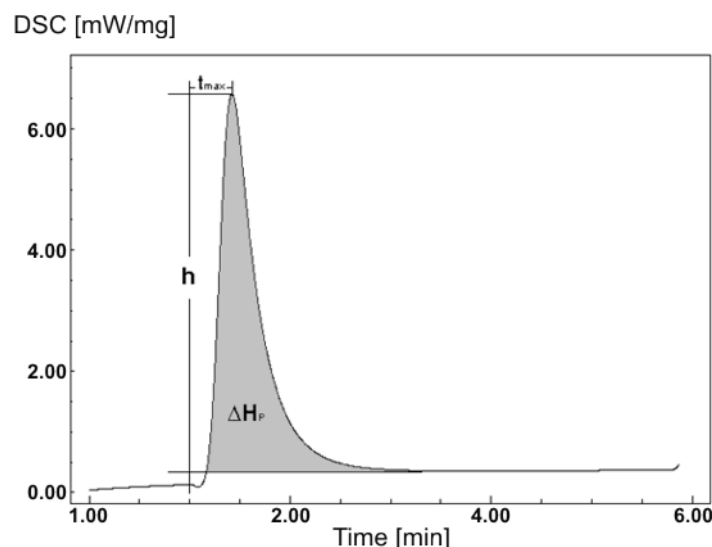


Figure 91. Parameters derived from photo-DSC experiments

The DBC and the initial rate of polymerization (R_{pmax} , mol L⁻¹ s⁻¹) give additional information on the performance of a system. DBC of the different formulations can be calculated following eq 1 with known $\Delta H_{0,P}$ of a monomer according to equation 4.

$$DBC = \frac{\Delta H_P \times M_M}{\Delta H_{0,P}} \times 100 \quad \text{Equation 4}$$

ΔH_P polymerization heat [J g⁻¹], area under the trace of the photo-DSC plot

M_M molecular weight of the monomer [g mol⁻¹]

$\Delta H_{0,P}$ theoretocal polymerization heat of the monomer [J mol⁻¹]

R_{Pmax} can be calculated from the height of the maximum (h ; mW/mg), and the density of the monomers (ρ ; g L⁻¹) following eq. 5.

$$R_{Pmax} = \frac{h \times \rho}{\Delta H_{0,P}} \quad \text{Equation 5}$$

Photo-CIDNP

¹H NMR and CIDNP spectra were recorded on a 200 MHz Bruker Avance DPX spectrometer. Irradiation source was a Hamamatsu L8235 Hg/Xe lamp, which emitted a broad UV light spectrum. Experiments were performed under Ar-atmpshere with samples of 10⁻⁵ M concentration in deuterated acetonitrile.

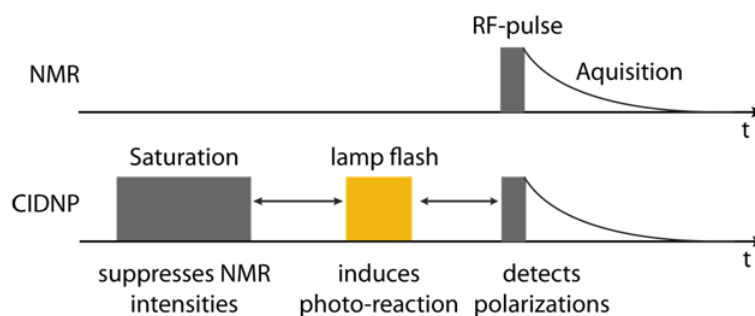


Figure 92. Experimental setup for the photo-CIDNP experiments

The following pulse sequence led to the recorded ^1H -CIDNP spectra:

Saturation (waltz 16) – Light pulse (300 ms) – 30° Radio Frequency Pulse ($2.25\mu\text{s}$) – Aquisition

Saturation was not completely effective due to the long lamp flash. The actual CIDNP spectra were derived as a difference between a CIDNP and a corresponding ^1H -NMR spectrum. Additionally, a continuous irradiation for ~ 1.5 min was performed, where spectra were recorded, which helped to identify some photoproducts, even if they had been invisible in the CIDNP experiment.

Nanoindentation

Nanoindentation experiments were carried out on a Nanoindenter XP from MTS Systems. The sample disks were fixed on an aluminium cylinder with a two-component stick. Furthermore, the samples were bared and polished with sandpaper of different grain size to obtain a smooth surface. The indentation experiment was performed with a diamant pyramide according to Berkovich. The penetration depth was $2\ \mu\text{m}$ with a penetration velocity of $0.1\ \mu\text{m s}^{-1}$. After a hold time of 30 s with maximum charge, the sample disk was discharged.

Principle

Nanoindentation testing is generally applied to determine the mechanical properties of different materials. High accuracy and precision of modern nanoindenter machines made it possible to record fractional signals to calculate the specific mechanical values from the load and displacement data. With the possibility to apply small tip sizes and loads nanoindentation provides the advantage of needing only small specimens for the testing compared to conventional methods for indentation. During the experiments parameters like load and depth of penetration can be measured.

These values are plotted on a graph, creating a load-displacement curve, from which mechanical properties as Young's Modulus and hardness can be derived.

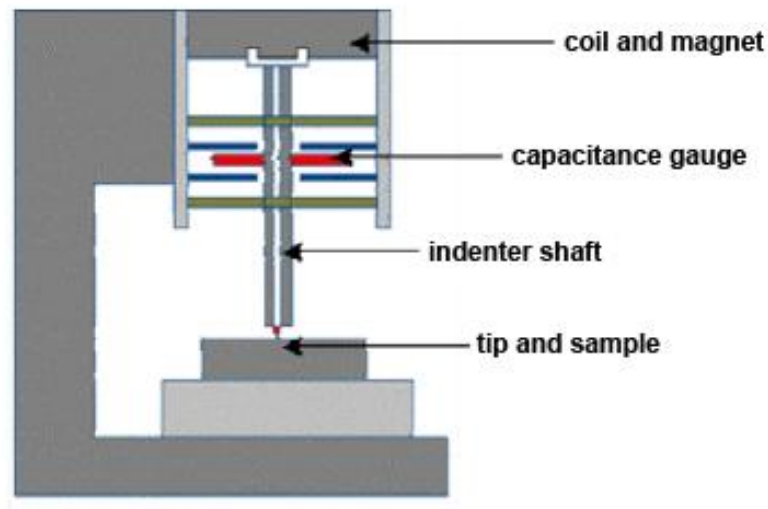


Figure 93. Model of a nanoindenter

The pyramidal tip penetrates the sample with a defined velocity and load. Thereby the load-displacement curve can be recorded.

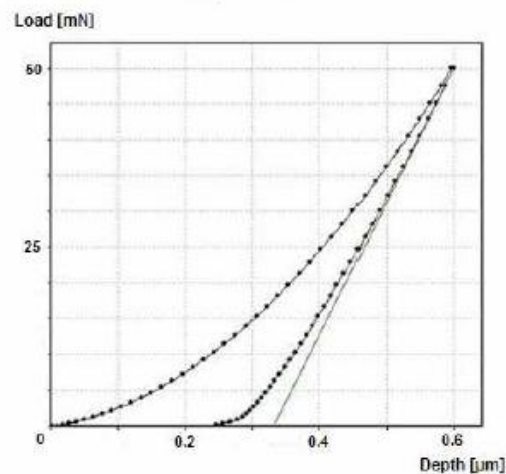


Figure 94. Example for a Load-Displacement curve obtained from nanoindentation experiments

From the tangential gradient of the discharging curve the indentation Young's Modulus (YM_{IT}) can be calculated according to equation 5 and equation 6.²²⁷

$$YM_{IT} = \frac{1-(\nu_s)^2}{\frac{1}{YM_r} - \frac{1-(\nu_i)^2}{YM_i}} \quad \text{Equation 6}$$

$\nu_{s,i}$ Poisson relation of sample and indenter (0.35)

YM_i modulus of the indenter [MPa]

YM_r reduced modulus of indentation contact [MPa]

The reduced Young`s Modulus can be calculated according to equation 6.

$$YM_r = \frac{\sqrt{\pi} \times s}{2 \times \sqrt{A_p}} \quad \text{Equation 7}$$

s contact strenght

A_p projected contact area [m²]

The contact strength is defined as the resistance of two particles against their mutual displacement.

Following Oliver *et al.*²²⁸, H_{IT} can be calculated from the maximum force F_{max} according to equation 7.

$$H_{IT} = \frac{F_{max}}{24.5 \times h_c^2} \quad \text{Equation 8}$$

$$h_c = h_{max} - \varepsilon(h_{max} - h_r)$$

h_{max} penetration depth at F_{max} [m]

h_r intercept point of discharging tangential at maximum force with x-axis

ε indentation constant

Cell Multiplication (DNA Amount) and Alkaline Phosphatase Activity

MC3T3-E1 osteoblast-like cells were seeded in culture dishes at a density of 20,000/cm² and grown in α MEM (α -minimum essential medium; Biochrom) containing 5% fetal calf serum (FCS; Biochrom), supplemented with 4.5 g/l L-glucose, 50 μ g/ml ascorbic acid (Sigma) and

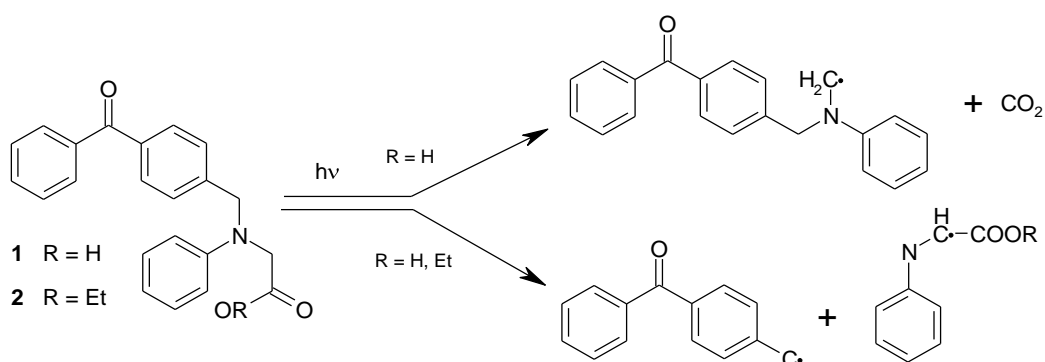
10 μ g mL⁻¹ gentamycin (Sigma). On the next day, the medium was changed and the cells were treated with decreasing concentrations of the monomers (0.1, 0.05, 0.025 and 0.0125 M) for 5 days and compared to untreated cells. Thereafter, cell viability was addressed by incubation of the cultures with a colorimetric growth indicator based on the detection of cellular metabolic activity (EZ4U, Biomedica, Austria). Furthermore, amount of DNA of the cultures were measured by fluorescence with Hoechst 33258 dye as a surrogate of the cell number. Alkaline phosphatase activity

was measured in the same cultures by means of p-nitrophenyl-phosphate and normalized to the DNA-amount (Varga *et al.*).²¹²

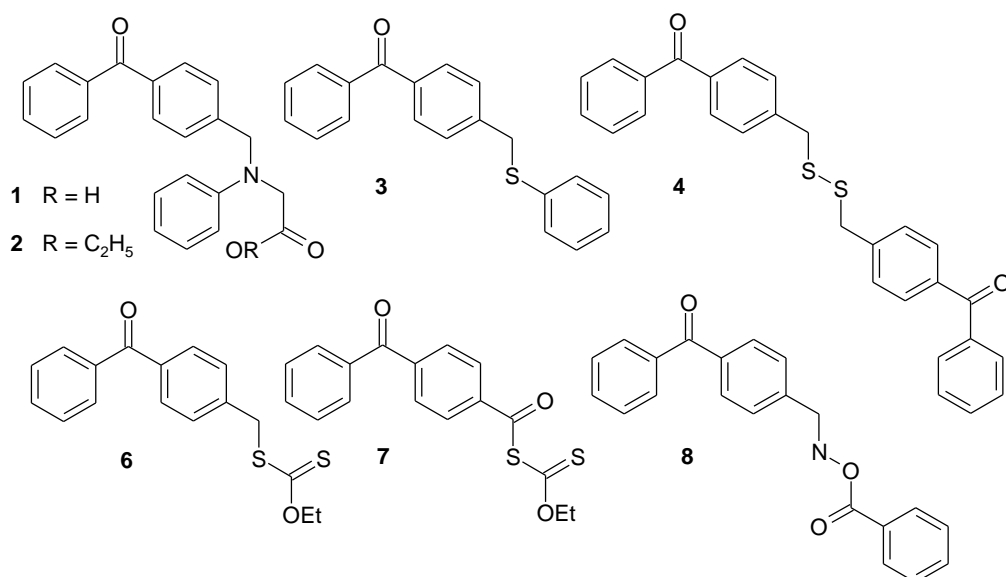
The preparation and analysis of the photosensitive compounds and mixtures was conducted in a **yellow light lab**. This laboratory was placed in a window-less room to avoid admittance of day light. Adhesive foils of the company IFOHA (article nr. 11356, melon yellow) were used to cover fluorescent lamps.

SUMMARY

During the last decades photopolymerization has found numerous new applications due to its versatility. This has evoked much attention on the development of systems with better performance and/or lower adverse impact on the environment. In this context it was the aim of this PhD-thesis to improve the performance of bimolecular type II PIs containing the **BP** moiety. The novel concept arose from the use of *N*-phenyl glycine as coinitiator, thus avoiding the back electron transfer process by spontaneous decarboxylation after electron transfer to the excited ketone. By linking the **NPG** group covalently via a methylene spacer to the **BP** chromophore as in **1** and also **2**, the efficiency of this type of PI was increased dramatically, presumably due to an additional β -phenylogous cleavage.

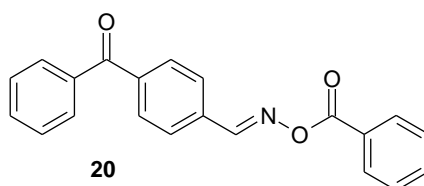


To develop the concept of the β -phenylogous cleavage mechanism further, new heteroatom moieties were introduced to benzophenone via a methylene linker. The heteroatom group should consist either of sulfur or the N-O group.



The use of sulfur-containing photoinitiators with the benzophenone chromophore as in compounds **4**, **6** and **7** are an interesting concept concerning the β -phenylogous cleavage mechanism. Yamaji and co-workers had reported this type of radical formation in an earlier study for reference compound **3**, which contains a thiophenyl moiety. For the PIs bearing a thio-moiety apart from good reactivity, even comparable to industrially used Type I PI Darocur 1173 in the case of dithiocarbonate **6**, also molecular weight regulating features were detected in analogy to so-called photoiniferters. Significant molecular weight reduction by the use of dithiocarbonate **6** as PI was detected by GPC analysis of the polymer samples from the photo-DSC experiments.

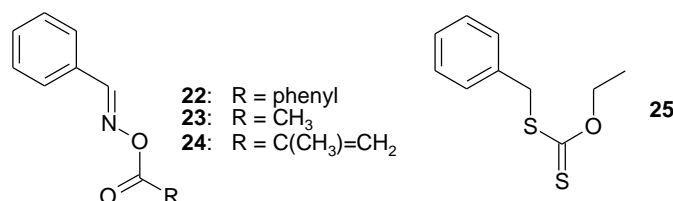
The N-O group, linked by a methylene group to the benzophenone chromophore as in **8**, was chosen as second heteroatom system to induce β -phenylogous cleavage. Unfortunately, it was not possible to receive target molecule **8** by common synthetic pathways, but oxime **20**, obtained as intermediate during the synthesis of **8**, promised interesting PI features as well.



The unexpected extraordinary high photoreactivity of oxime **20** implicated further investigations of the photochemical and photophysical processes leading to such

reactivity. Hence, photo-CIDNP experiments for characterization of the generated radicals during irradiation with UV-light were performed, confirming the formation of an imino radical of **20**, accompanied by decarboxylation of the benzoyloxy radical.

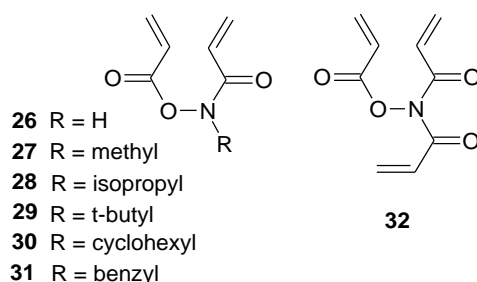
The excellent properties of dithiocarbonate **6** and oxime **20** gave rise to further examination of their photochemical behaviour, using physical mixtures of 4-methyl benzophenone with structural analoga bearing a phenyl residue instead of the **BP**-chromophore.



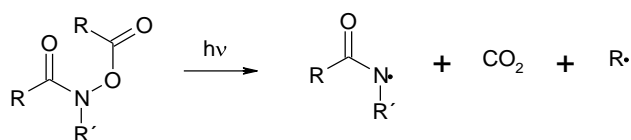
Accordingly, dithiocarbonate **25**, the benzyl derivative of **6**, was tested as co-initiator in a physical mixture with 4-methyl benzophenone. Also here a very good initiation activity was observed, combined with surprisingly good molecular weight regulating properties. Additionally, **25** alone exhibited a remarkable PI reactivity comparable to **BP**/amine systems.

Physical mixtures of **22**, the benzaloxime derivative of **20**, with 4-methyl benzophenone were used as PI for standard diacrylate monomer hexane-1,6-diol diacrylate and surprisingly also here an outstanding reactivity was found. Further investigations on the variation of the O-oxime ester group and the nature of the residue attached to the carbon atom of the oxime, confirmed, that only oxime esters based on benzaloxime were suitable co-initiators for the benzophenone chromophore with considerably better performance than industrially applied **BP**/amine systems, coming up to well-known Type I PIs like Darocur 1173.

These tremendous positive experiences with the high photoreactivity of the N-O bond, directed the focus of this work onto new concepts for photoinitiating systems. The need for migrationstable PIs, which are incorporated into the polymer network is high, not least to recent incidents concerning contamination of food by photoproducts of commonly used PIs. Hydroxylamines, where polymerizable acryl groups could be attached easily onto the N or O atom as in **26-32**, might be advantageous in this context.



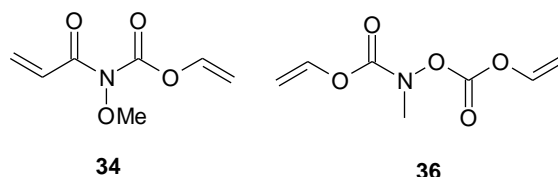
Their photochemical behaviour was investigated by UV-spectroscopy and photo-DSC experiments. Additionally, a method to derive the DBC from comparison of ATR-IR spectra both of monomers and UV cured polymer samples was applied and furthermore it was possible to calculate the theoretical heat of polymerization for the new monomers. As expected, the hydroxylamine-based monomers showed the ability to self-initiate radical polymerization upon exposure to UV light. Generally, the photoinitiation activity of the triacrylate **32** in **HDDA** exceeded the difunctional acrylates by far and was also comparable to well-known Type II PI system **BP/TEA**, although only a fraction of the light can be consumed – as shown by UV-Vis analysis. Concerning monomer reactivity with an additional PI such as Darocur 1173, also the triacrylated hydroxylamine showed the best performance. Here some of the hydroxylamine based diacrylates gave good results as well. Finally, the ability to self-initiate radical polymerization in bulk was not comparable to common formulations of monomers and PIs, but nevertheless, they might be a model system for a new generation of PIs, that are copolymerizable parts of the polymer network. In accordance to literature, the surprising behaviour of self initiation is related to the N-O bond cleavage, as shown in Scheme 41.



Scheme 41. UV-induced N-O bond cleavage in acylated hydroxylamines

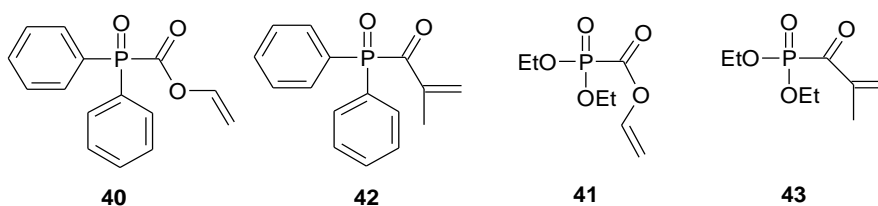
Resuming these prospective results, the last part of this PhD thesis was dedicated to special applications for such self-initiating monomers. Renouncement of PIs and their potentially harmful photoproducts is definitely of interest for biomedical applications. Therefore, monomers with self-initiating features and good biocompatibility should be prepared and characterized. Hence, hydroxylamine-based vinylcarbamates were

prepared, trying to extend the concept of self-initiating monomers from rather irritant and toxic acrylates to non-toxic vinyl carbamates as in **36**.

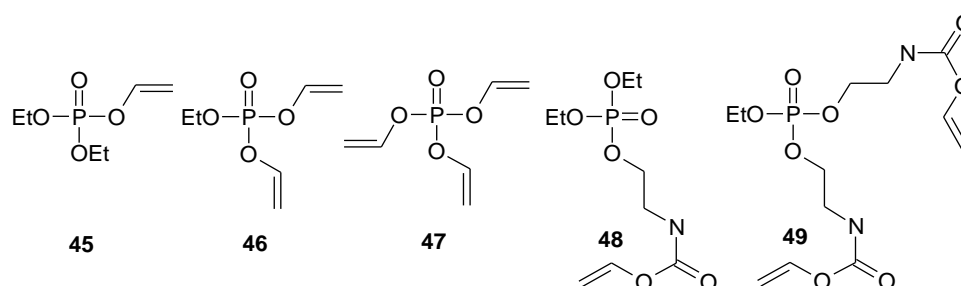


Indeed, in the case of **34**, self-initiation was observed, but unfortunately, it turned out that **36** was not able to form reactive radicals under irradiation with UV-light, probably due to the loss of a conjugated acrylamide chromophore.

Another concept is based on the photocleavage of well known acyl phosphine oxides, that have been modified with polymerizable methacrylate or vinyl groups as in **40-43**.



However, only the diphenyl phosphine oxide vinyl ester **40** was able to induce photopolymerization in a standard acrylate like **HDDA**. Nevertheless, focusing also on the design of biocompatible monomers for medical applications as e.g. bone replacement surgery, other types of phosphorus-containing monomers were prepared. The most outstanding feature of these compounds is the formation of a poly(vinyl alcohol) backbone, which represents a milestone compared to the toxicity of acrylic resins. Thus, only harmless poly(vinyl alcohol) and phosphates are generated during the biodegradation process in the mammalian body.



The synthesis and photopolymerization behaviour of these monomers based on vinyl esters and vinylcarbamates with mono- di- and trivalent polymerizable groups was

investigated. All monomers, except **40** – which was a solid – and **43** – which showed no photoreactivity at all - were polymerizable with a type I PI, Darocur 1173, under irradiation with UV light.

Surprisingly, the diethyl phosphonovinyl ester **41** turned out to be the most reactive monomer exhibiting very high DBC and rate of polymerization. Also the other monofunctional vinyl ester **45** and vinylcarbamate **48** performed better than the reference, lauryl methacrylate. For the strongly crosslinking trifunctional vinyl ester **47** a very high DBC was achieved in contrast to the references, trimethylol propane triacrylate and -methacrylate. Degradation behaviour of the polymers from the di- and trifunctional monomers was quite fast in alkaline medium and much slower under acidic conditions. Cell viability and measurements on the development of ALP-activity of the osteoblast-like cells MC3T3-E1 showed low cytotoxicity for all phosphorus-based monomers. Especially **48** did not significantly influence the differentiation of the preostoblastic cell line while **41** appeared even to increase the differentiation process.

Mechanical properties of **47** (YM = 7900 MPa) almost resembled human bone (YM = 10000 MPa). Also **41** with varying amounts of **45** as crosslinker showed remarkable hardness, already superseding poly(caprolactone), which is commonly used in tissue engineering. Its non-toxic properties might furthermore contribute to its suitability as biocompatible material for osteo surgery in the future.

ABBREVIATIONS

A	absorbancy
ATR-IR	attenuated total reflectance infrared spectroscopy
ATRP	atom transfer radical polymerization
BET	back electron transfer
Bp	boiling point
BP	benzophenone
BuLi	n-buthyl lithium
c	concentration
CA	molecular weight control agent
CH ₂ Cl ₂	dichloromethane
CDCl ₃	deuterated chloroform
CHCl ₃	chloroform
CIDNP	chemically induced dynamic nuclear polarization
CQ	camphorquinone
CS ₂	carbon disulfide
d	doublet
dd	doublet of doublets
DBA	dibutyl anthracene
DBC	double bond conversion
DBDS	dibenzyl disulfide
DBODS	dibenzoyl disulfide
DBU	1,8-diazabicyclo[5.4.0.] undec-7-ene
DC1173	Darocur 1173@Ciba
DEXDS	O,O-diethyl xanthogen disulfide
DMAA	<i>N,N</i> -dimethyl acrylamide
DMAB	4-dimethylamino benzoic acid ethyl ester
DMF	dimethylformamide
DMSO	dimethylsulfoxide
DSC	differential scanning calorimetry/differential scanning calorimeter
DVA	divinyl adipate

ABBREVIATIONS

DVE	decanoic acid vinyl ester
ε	extinction coefficient
EE	ethyl ethanoate
EEEE	2-(2-ethoxy ethoxy) ethyl acrylate
ESR	electron spin resonance
E_T	triplet energy
Et ₂ O	diethylether
EtOH	ethanol
GC-MS	gas chromatography coupled with mass spectrometry
GPC	gel permeation chromatography
H	hardness
h	peak height (DSC)
HCN	hydrogen cyanide
HDDA	hexane-1,6-diol diacrylate
H _P	actual polymerization heat; area under the trace (DSC)
$\Delta H_{0,P}$	theoretical polymerization heat
HPLC	high pressure liquid chromatography
IR	infrared spectroscopy
λ_{\max}	wavelength of the absorption maximum
LA	lauryl acrylate
LFP	laser flash photolysis
LMA	lauryl methacrylate
LRP	living radical polymerization
ITX	2-isopropyl thioxanthone
MAP	4-methoxy acetophenone
MAX	S-methacryloyl O-ethyl xanthate
MBp	4-methyl benzophenone
MeCN	acetonitril
MeOH	methanol
MS	mass spectrometry
M _p	melting point
MW	molecular weight
M _w	weight average molecular weight

ABBREVIATIONS

M_n	number average molecular weight
NAM	<i>N</i> -acryloyl morpholine
NMP	nitroxide mediated polymerizations
NMR	nuclear magnetic resonance spectroscopy
<i>p</i> -TSOH	<i>p</i> -toluene sulfonic acid
PAA	<i>N</i> -propyl acrylamide
PADS	phenyl acetyl disulfide
PCL	poly(caprolactone)
PE	petrolether
PI	photoinitiator
PLA	poly(lactide)
PS	photosensitizer
PTC	phase transfer catalysis
PVA	poly(vinyl alcohol)
Qu	quartet
RAFT	reversible addition fragmentation chain transfer polymerization
R_f	retention factor (TLC)
r.t.	room temperature
R_{Pmax}	polymerization rate when the maximum polymerization heat is reached
s	singlet
SSP	steady state photolysis
t	time
TAB	tetrabutyl ammonium bromide
t-BAM	methyl-3,3-dimethyl-2-methylene butanoate
TBDTS	<i>N,N,N',N'</i> -tetrabutyl dithiocarbamate disulfide
TEA	triethanol amine
TEMPO	2,2,6,6-tetramethyl-piperidine-1-yloxy radical
THF	tetrahydrofuran
TLC	thin layer chromatography
t_{max}	time until maximum polymerization heat is reached (DSC)
TMPTA	trimethylol propane triacrylate
TMPTMA	trimethylol propane trimethacrylate

ABBREVIATIONS

UV-Vis	ultraviolet-visible light
w%	weight percent
YM	Young's Modulus

REFERENCES

- ¹ Source: http://www.mageist.net/Images/lascaux_horse.jpg
- ² Brock, T.; Groteklaes, M.; Mischke, P. in *European Coatings Handbook*, (Ed. U. Zorll); Vincentz Verlag Hannover, Germany, 2000; p. 313.
- ³ Source: <http://www.paint.org/industry/history.cfm>
- ⁴ Myers, R.R.; "*History of coatings science and technology.*" *Journal of Macromolecular Science Part A*; 1981; **15**(6); 1133-1149
- ⁵ Rehse, G.; "*Development of inks*"; *Farbe und Lack*; 1970; **76**(12); 1222-1225.
- ⁶ Herz, C. P.; Eichler, J.; Neisius, K. H.; Ohngemach, J.; "*UV radiation curing, Part 2*"; *Kontakte*; 1980; **3**; 15-20.
- ⁷ Bett, S. J.; Dworjany, P. A.; Garnett, J. L.; "*UV and EB [electron beam] curing*"; *Journal of the Oil Colour Chemical Association*; 1990; **73**; 446-453.
- ⁸ Allen, N. S.; Edge, M.; "*UV and electron beam curing*"; *Journal of the Oil Colour Chemical Association*; 1990; **73**(11); 438 – 445.
- ⁹ Senich, G. A.; Florin, R. E.; "*Radiation curing of coatings*"; *JMS-Rev. Macromolecular Chemistry and Physics Part C*; 1983; **24**(2); 239-324.
- ¹⁰ Kirchmayr, R.; Berner, G.; Rist, G.; "*Photoinitiators for UV curing of paints*"; *Farbe und Lack*; 1980; **86**(3); 224 – 230.
- ¹¹ Fouassier, J. P. in *Photoinitiation, Photopolymerization and Photocuring. Fundamentals and Applications*; Hanser: Munich, Vienna, 1995, p 2.
- ¹² Fouassier, J. P.; "*Photochemistry and UV-curing: a brief survey of the latest trends.*"; in *Photochemistry and UV Curing: New Trends 2006*; Research Signpost, Kerula, India; 2006; 1-8.
- ¹³ Shahidi, I. K.; Powanda, T. M.; "*Ultraviolet curing. Review of the technology.*"; *American Ink Maker*; 1975; **53**(1); 20-26.
- ¹⁴ Fouassier, J. P. in *Photoinitiation, photopolymerization and photocuring.*

Fundamentals and applications; Hanser: Munich, Vienna; 1995; p 11.

- ¹⁵ Knistle, J. F.; "Polymerization by UV radiation. II. Free radical homopolymerization in liquid systems"; Journal of Radiation Curing; 1974; **1**; 2.
- ¹⁶ Osborn C. L.; „Photoinitiation systems and their role in UV-curable coatings and inks“; Journal of Radiation Curing; 1976; **3**; 3.
- ¹⁷ Davidson R. S.; Orton S. P.; "Photo-induced electron-transfer reactions. Fragmentation of 2-aminoethanols"; Journal of the Chemical Society Chemical Communications; 1974; 6; 209-210.
- ¹⁸ Crivello, J. V.; Dietliker, K.; "Photoinitiators for free radical cationic and anionic photopolymerization. Chemistry & Technology of UV & EB Formulations for coatings, inks & paints"; (Ed. G. Bradley); 2nd ed.; SITA Technology Ltd., 1991; **Vol. III.**; p 20-21.
- ¹⁹ Source: <http://web.uvic.ca/ail/techniques/Jablonski.jpg>
- ²⁰ Bonamy, A.; Fouassier, J. P.; Lougnot, D. J.; Green, P. N.; "Novel and efficient water-soluble photoinitiators for polymerisation"; Journal of Polymer Science: Polymer Letters; 1982; **20**; 315-320.
- ²¹ Fouassier, J. P.; "Radiation curing in polymer science and technology"; in Elsevier Applied Science Vol.II: Photoinitiating Systems, 1993, 717 pp
- ²² Yamaji, M.; Suzuki, A.; Ito, F.; Tero-Kubota, S.; Tobita, S.; Marciniak, B.; "A new-type photoreaction of a carbonyl compound Part 2. Photoinduced ω -bond dissociation in *p*-halomethylbenzophenone studied by time-resolved EPR technique and laser flash photolysis"; Journal of Photochemistry and Photobiology A: Chemistry; 2005, **170**; 253-259.
- ²³ Yamaji, M.; Inomata, S.; Nakajima, S.; Akiyama, K.; Tero-Kubota, S.; Tobita, S.; Marciniak, B.; "Time resolved EPR and laser photolysis investigations of photoinduced ω -bond dissociation in an aromatic carbonyl compound having triplet π, π^* character."; Chemical Physics Letters; 2006; **417**, 211-216:

- ²⁴ Cai, X.; Sakamoto, M.; Hara, M.; Inomata, S.; Yamaji, M.; Tojo, S.; Kawai, K.; Endo, M.; Fujisuka, M.; Majima, T.; "Homolytic cleavage of C-Si bond of *p*-trimethylsilylmethylacetophenone upon stepwise two-photon excitation using two-color two-laser flash photolysis"; Chemical Physics Letters 2005; **407**; 402-406.
- ²⁵ Shah, B.; Neckers, D.C.; "Triplet energy distribution in photoinitiators containing two dissociable groups."; Journal of Organic Chemistry; 2002; **67**;6117-6123:
- ²⁶ Cai, X.; Sakamoto, M.; Yamaji, M.; Fujisuka, M.; Majima, T.; "C-O-bond cleavage of benzophenone substituted by 4-CH₂OR (R=C₆H₅ and CH₃) with stepwise Two-Photon Excitation"; Journal of Physical Chemistry Part A ; 2005; **109**; 5989-5994.
- ²⁷ Yamaji, M.; Inomata, S.; Nakajima, S.; Akiyama, K.; Tobita, S.; Marciniak, B.; "Photoinduced ω -bond dissociation in the higher excited singlet (S₂) and lowest triplet (T₁) states of a benzophenone derivative in solution"; Journal of Physical Chemistry Part A; 2005; **109**; 3843-3848.
- ²⁸ Chen, Y. C.; Ferracane, J. L.; Prahl, S. A.; "Quantum yield of conversion of the photoinitiator camphorquinone"; Dental Materials; 2007, **23**; 655-664.
- ²⁹ Andrzejewska, E.; Zych-Tomkowiak, D.; Andrzejewski, M.; Hug, G. L.; Marciniak, B.; "Heteroaromatic thiols as co-initiators for Type II photoinitiating systems based on camphorquinone and isopropylthioxanthone."; Macromolecules; 2006; **39**(11); 3777-3785.
- ³⁰ Becker, H. G. O. in „Einführung in die Photochemie“; DVW, 1991, p 358.
- ³¹ Cohen, S. G.; Parola, A.; Parsons Jr., G. H.; "Photoreduction by Amines"; Chemical Reviews; 1973; **73**(2); 141-161.
- ³² Paczkowski, J.; "Electron-transfer photoinitiators of free radical polymerization. The effect of co-initiator structure on photoinitiation ability"; in Photochemistry and UV Curing: New Trends 2006; (Ed. J.P. Fouassier); Research Signpost, Kerula, India; 2006; 101-115.
- ³³ Peters, K. S.; Kim, G.; "Characterization of solvent and deuterium isotope effects on nonadiabatic proton transfer in the benzophenone/*N,N*-dimethylaniline contact radical ion pair "; Journal of Physical Chemistry Part A; 2004; **108**(14); 2598-2606.

- ³⁴ Brimage, D. R. G.; Davidson, R. S.; "*Photoreactions of polycyclic aromatic hydrocarbons with N-aryl-glycines*"; Journal of the Chemical Society Perkin Transactions 1: Organic and Bio-Organic Chemistry; 1973; **5**; 496-499.
- ³⁵ Hageman, H. J.; "*Photoinitiators and photoinitiation. Part 12. The aromatic ketone/tert-amine type-II photoinitiation system. Identification of the initiating species*"; Macromolecular Rapid Communications; 1997; **18**(5); 443 – 449.
- ³⁶ Clarke, S. R.; Shanks, R. A.; "*Factors affecting the ultraviolet-initiated polymerization of vinyl monomers*"; Journal of Macromolecular Science Part A; 1982; **17**(1); 77 – 85.
- ³⁷ Crivello, J. V.; Dietliker, K.; "*Photoinitiators for free radical cationic and anionic photopolymerization. Chemistry & Technology of UV & EB Formulations for coatings, inks & paints*"; (Ed. G. Bradley); 2nd ed.; SITA Technology Ltd., 1991; **Vol. III.**; 71-82.
- ³⁸ Fouassier, J. P. in Photoinitiation, Photopolymerization and Photocuring: Fundamentals and Applications; Hanser: Munich, Vienna, 1995, pp 1 – 7, p 174.
- ³⁹ Wei, H.; Lee, T. Y.; Miao, W.; Fortenberry, R.; Magers, D. H.; Hait S.; Guymon, A. C.; Jonsson, S. E.; Hoyle, C. E.; "*Characterization and photopolymerization of divinyl fumarate*"; Macromolecules; 2007; **40**; 6172 – 6180.
- ⁴⁰ Kilambi, H.; Reddy, S. K.; Schneidewind, L.; Lee, T. Y.; Stansbury, J. W.; Bowman, C. N.; "*Design, development, and evaluation of monovinyl acrylates characterized by secondary functionalities as reactive diluents to diacrylates.*"; Macromolecules; 2007; **40**; 6112 – 6118.
- ⁴¹ Gruber, H.F.; "*Photoinitiators for free radical polymerization*"; Progress in Polymer Science; 1992; **17**; 953.
- ⁴² Jonsson, E. S., Hoyle, C. E.; "*Monomeric photoinitiators*" in Photochemistry and UV-Curing: New trends, 2006, (Ed. J.P. Fouassier); Research Signpost: Trivandrum, India; 2006; 165-175.
- ⁴³ Source: <http://www.european-coatings.com/blog/index.cfm?mode=entry&entry=C380D505-BF00-E8F3-59DD4C6D3BE40FF4>

- ⁴⁴ <http://www.foodprocessing-technology.com/features/feature51361/>
- ⁴⁵ Sandholzer, M.; Schuster, M.; Varga, F.; Liska, R.; Slugovc, C.; “*ROMP based photoinitiator - coinitiator systems with improved migration stability*”; Journal of Polymer Science Part A: Polymer Chemistry 2008; **46**(11); 3648-3661.
- ⁴⁶ Catalina, F.; Peinado, C.; Allen, N.S.; “*Spectroscopic and photoreduction study of 2-acryloxy-thioxanthone: photoinitiation activity of methyl methacrylate polymerization.*”; Journal of Photochemistry and Photobiology A: Chemistry; 1992; **67**(2); 255-263.
- ⁴⁷ Visconti, M.; “*Difunctional photoinitiators*”; in Photochemistry and UV-Curing: New trends, 2006, (Ed. J.P. Fouassier); Research Signpost: Trivandrum, India; 2006; 153-163.
- ⁴⁸ Wei, J.; Wang, H.; Jiang, X.; Yin, J.; “*Novel photosensitive thio-containing polyurethane as macrophotoinitiator comprising side-chain benzophenone and co-initiator amine for photopolymerization*”; Macromolecules; 2007; **40**(7); 2344-2351.
- ⁴⁹ Angiolini, L.; Caretti, D.; Salatelli, E.; “*Synthesis and photoinitiation activity of radical polymeric photoinitiators bearing side-chain camphorquinone moieties*”; Macromolecular Chemistry and Physics; 2000; **201**(18); 2646-2653.
- ⁵⁰ Hoyle, C. E.; Miller, C. W.; Jonsson, E. S. “*Photochemistry and photopolymerization of maleimides*”; Trends in Photochemistry & Photobiology 1999, **5**; 149-167.
- ⁵¹ Morel, F., Decker, C., Jonsson, S., Clark, S.C., Hoyle, C.E., “*Kinetic study of the photo-induced copolymerization of N-substituted maleimides with electron donor monomers.*”; Polymer; 1999; **40**; 2447-2454.
- ⁵² Von Sonntag, J.; Knolle, W.; “*Maleimides as electron-transfer photoinitiators: quantum yields of triplet states and radical-ion formation*”; Photochemistry and Photobiology Part A; 2000; **136**; 133-139.
- ⁵³ Dietliker K. in “*A compilation of photoinitiators commercially available for UV today.*”; SITA Technology Limited; Edinburgh, London, 2002, 216-217.

-
- ⁵⁴ Fukuda, W.; Nakao, M.; Okumura, K.; Kakiuchi, H.; "Polymerization of vinyl methacrylate and vinyl acrylate"; Journal of Polymer Science Part A; 1972; **10**; 237-250.
- ⁵⁵ Lee, Y. L.; Roper, T. M.; Jonsson, S.; Guymon, C. A.; Hoyle, C.E.; "Thiol-ene photopolymerization kinetics of vinyl acrylate/multifunctional thiol mixtures."; Macromolecules; 2004; **37**; 3606-3613.
- ⁵⁶ Karasu, F.; Dworak, C.; Kopeinig, S.; Hummer, E.; Arsu, N.; Liska, R.; "Photoinitiating monomers based on diacrylamides."; Macromolecules; 2008; **41**(21); 7953-7958.
- ⁵⁷ Decker, C.; Bianchi, C.; Jonsson, S.; "Light induced crosslinking polymerization of a novel N-substituted bis-maleimide monomer"; Polymer ;2004; **45**(17); 5803-5811.
- ⁵⁸ Lee, T. Y.; Roper, T. M.; Jonsson, S. E.; Kudyakov, I.; Viswanathan, K.; Nason, C.; Guymon, C. A.; Hoyle, C. E.; "The kinetics of vinyl acrylate photopolymerization"; Polymer; 2003; **44**; 2859-2865.
- ⁵⁹ Lee, T. Y.; Guymon, C. A.; Jonsson, E. S.; Hait, S.; Hoyle, C. E.; "Synthesis, initiation and polymerization of photoinitiating monomers"; Macromolecules; 2005; **38** (18); 7529-7531.
- ⁶⁰ Fouassier, J. P., in Photoinitiation, photopolymerization and photocuring: Fundamentals and applications; Hanser: New York 1995, p 152.
- ⁶¹ Andrzejewska, E.; "Thiols in photopolymerization." in Photochemistry and UV-Curing: New trends, 2006, (Ed. J. P: Fouassier); Research Signpost: Trivandrum, India; 2006; 127-140.
- ⁶² Brandrup, J., Immergut, E. H., in Polymer Handbook 3rd ed., Wiley, New York 1989.
- ⁶³ Maillard, B.; Ingold, K. U.; Scaiano, J. C.; "Rate constants for the reactions of free radicals with oxygen in solution."; Journal of the American Chemical Society; 1983; **105**(15); 5095 – 5099.

- ⁶⁴ Decker, C.; Jenkins, A. D.; "*Kinetic Approach of O₂ Inhibition in Ultraviolet- and Laser-Induced Polymerizations.*"; *Macromolecules*; 1985; **18**; 1241-1244.
- ⁶⁵ Crivello, J. V.; Dietliker, K.; in *Photoinitiators for free radical cationic and anionic photopolymerization. Chemistry & Technology of UV & EB Formulations for coatings, inks & paints.*; (Ed. G. Bradley); 2nd ed.; SITA Technology Ltd., 1991; **Vol. III.**; 83-86
- ⁶⁶ Bradley, G.; Davidson, R. S.; "Some aspects of the role of amines in the photoinitiated polymerization of acrylates in the presence and absence of oxygen." *Recueil des Travaux Chimiques des Pays-Bas*; 1995; **114**(11/12); 528-533.
- ⁶⁷ Kucybala, Z.; Pietrzak, M.; Paczkowski, J.; "*Kinetic studies of a new photoinitiator hybrid system based on camphorquinone-N-phenylglycine derivatives for laser polymerization of dental restorative and stereolithographic (3D) formulations*"; *Polymer*; 1996; **37**(20); 4585-4591.
- ⁶⁸ Hug, G. L.; Bonifai, M.; Asmus, K.-D.; Armstrong, D. A.; "*Fast decarboxylation of aliphatic amino acids induced by 4-carboxybenzophenone triplets in aqueous solutions. A nanosecond laser flash photolysis study.*"; *Journal of Physical Chemistry Part B*; 2000, **104**(28); 6674 – 6682.
- ⁶⁹ Su, Z.; Mariano, P. S.; Falvey, D. E.; Yoon, U. C.; Oh, S. W.; "*Dynamics of anilinium radical α -heterolytic fragmentation process. Electrofugal group, substituent, and medium effects on desilylation, decarboxylation, and retro-aldol cleavage pathways*"; *Journal of the American Chemical Society*; 1998; **120**; 10676-10686.
- ⁷⁰ Davidson, R. S.; Steiner, P. R.; "*Photosensitized decarboxylation of carboxylic acids by benzophenone and quinones*"; *Journal of the Chemical Society Section C: Organic*; 1971; **9**; 1682-1689.
- ⁷¹ Jauk, S.; Liska, R.; "*Photoinitiators with functional groups VIII: Benzophenone with covalently bound phenylglycine*"; *Macromolecular Rapid Communications*; 2005; **26**(21); 1687-1692.

- ⁷² Jauk, S.; Liska, R.; “*Photoinitiators with functional groups IX: New derivatives of covalently linked benzophenone-amine based photoinitiators*”; Journal of Macromolecular Science Part A: Pure and Applied Chemistry; 2008; **45**(10); 804-810.
- ⁷³ Anderson, R.W. Jr.; Hochstrasser, R.M.; Lutz, H.; Scott, G.W.; “*Direct measurements of energy transfer between triplet states of molecules in liquids using picoseconds pulses.*”; Journal of Chemical Physics; 1974; **61**(7); 2500-2506.
- ⁷⁴ Damschen, D.E.; Merritt, Ch.; Perry, D.L.; Scott, G.W.; Talley, L.D.; “*Intersystem Crossing Kinetics of Aromatic Ketones in the Condensed Phase.*”; Journal of Physical Chemistry; 1978; **82**(21); 2268-2272.
- ⁷⁵ Jauk, S. “*Kovalent verbundene Typ II Photoinitiatoren für die Radikalische Photopolymerisation*”; PhD-Thesis; Institute of Applied Synthetic Chemistry; Vienna University of Technology; Vienna, Austria 2008.
- ⁷⁶ Byers, G.W.; Gruen, H.; Giles, H.G.; Schott, H.N.; Kampsmeier, J.A.; “*Photochemistry of disulfides I. Carbon-sulfur cleavage in the photosensitized decomposition of simple disulfides.*”; Journal of the American Chemical Society; 1972; **93**(3); 1016-1018.
- ⁷⁷ Rosenfeld, S.M.; Lawler, R.G.; Ward, H.R.; “*Photo-CIDNP from carbon-sulfur cleavage of alkyl disulfides.*”; Journal of the American Chemical Society; 1972; **94**(26); 9255-9256.
- ⁷⁸ Lalevée, J.; Zadoina, L.; Allonas, X.; Fouassier, J.P.; “*New sulfur-centered radicals as photopolymerization initiating species.*”; Journal of Polymer Science Part A: Polymer Chemistry; 2007; **45**; 2494-2502.
- ⁷⁹ Jun, N.; Zhi-ying, C.; Hong-mei, C.; Miao-zhen, L.; Er-jian, W.; „*Reinvestigation of photoinitiator mechanism and kinetics of aryl disulfides.*“; Journal of Photopolymer Science & Technology; 1995; **8**(1); 155-162.

- ⁸⁰ Niwa, M.; Matsumotu, T.; Izumi, H.; „*Kinetics of the photopolymerization of vinyl monomers by bis(Isopropylxanthogen) disulfide. Design of block copolymers.*”; Journal of Macromolecular Science: Pure and Applied Chemistry; 1987; **24**(5); 567-585.
- ⁸¹ Otsu, T.; Nayatani, K.; Muto, I.; Imai, M.; “*Vinyl polymerization XXVII. Organic polysulfides as polymerization initiators*”; Die Makromolekulare Chemie; 1958; **27**; 142-148
- ⁸² Lavalée, J.; El-Roz, M.; Allonas, X.; Fouassier, J.P.; “*Controlled photopolymerization reactions: the reactivity of new photoiniferters.*”; Journal of Polymer Science Part A: Polymer Chemistry; 2007; **45**; 2436-2442.
- ⁸³ Stenzel, M.H.; Cummins, L.; Roberts, G.E.; Davis, T.P.; Vana, P.; Berner-Kowollik, C.; “*Xanthate mediated living polymerization of vinyl acetate: a systematic variation in MADIX/RAFT agent structure.*”; Macromolecular Chemistry and Physics; 2003; **204**; 1160-1168.
- ⁸⁴ Lalevée, J.; Allonas, X.; Fouassier, J.P.; “*A new efficient photoiniferter for living radical photopolymerization.*”; Macromolecules; 2006; **39** (24); 8216-8216.
- ⁸⁵ Moad, G.; Rizzardo, E.; Thang, S.H.; “*Radical addition-fragmentation chemistry in polymer synthesis.*”; Polymer; 2008; **49**; 1079-1131.
- ⁸⁶ Ajayaghosh, A.; Francis, R.; “*Narrow polydispersed reactive polymers by a photoinitiated free radical polymerization approach. Controlled polymerization of methyl methacrylate.*”; Macromolecules; 1998; **31**; 1436-1438.
- ⁸⁷ Francis, R.; Ajayaghosh, A.; “*Minimization of homopolymer formation and control of dispersity in free radical induced graft polymerization using xanthate derived macro-photoinitiators*”; Macromolecules; 2000; **33**; 4699-4704.
- ⁸⁸ Lalevée, J.; Blanchard, N.; El-Roz, M.; Allonas, X.; Fouassier, J. P.; “*New photoiniferters: repective role of the initiating and persistent radicals.*”; Macromolecules; 2008; **41**; 2347-2352.
- ⁸⁹ Hawker, C.; Bosman, A.W.; Harth, E.; “*New polymer synthesis by nitroxide mediated living radical polymerizations.*”; Chemical Reviews; 2001; **101**; 3661-3688.

- ⁹⁰ Haddleton, D.M.; Crossman, M.C.; Dana, B.H.; Duncalf, D.J.; Heming, A.M.; Kukulj, D.; Shooter, A.J.; “*Atom Transfer Polymerization of methyl methacrylate mediated by alkylpyridylmethanimine type ligands, copper(I) bromide, and alkyl halides in hydrocarbon solution.*”; *Macromolecules*; 1999; **32**; 2110-2119.
- ⁹¹ Wang, J.S., Matyjaszewski, K., “*Controlled/Living Radical Polymerization. Atom Transfer Radical Polymerization in the Presence of Transition metal complexes*”; *Journal of the American Chemical Society*; 1995; **117**; 5614-5615.
- ⁹² Stermitz, F. R.; Neiswander, D. W.; “*Diacylamino and diacyl nitroxide radicals from triacylhydroxylamine photolyses.*”; *Journal of the American Chemical Society*; 1973; **95** (8); 2630-2634.
- ⁹³ Liu, K.T.; Tong, Y.C.; “*Oxidation with supported oxidants III. A facile conversion of thiols to disulfides.*”; *Synthesis*; 1978; **9**; 669-70.
- ⁹⁴ Fries, K.; Koch, H.; Stukenbrock, H.; “*Thianthrene. III.*”; *Justus Liebigs Annalen der Chemie*; 1929; **468**; 162-201.
- ⁹⁵ Drabowicz, J.; Mikolajczyk, M.; “*A simple procedure for the oxidation of thiols to disulfides by means of bromine/aqueous potassium hydrogen carbonate in a two-phase system.*”; *Synthesis*; 1980; **1**; 32-34.
- ⁹⁶ Rheinboldt, H.; Mott, F.; Motzkus, E.; “*Tertiary butyl mercaptan.*”; *Journal fuer Praktische Chemie (Leipzig)*; 1932; **134**; 257-281.
- ⁹⁷ Onufrowicz, S.; “*Sulphides of β -naphthol.*”; *Berichte der Deutschen Chemischen Gesellschaft* **23**, 3355-3373.
- ⁹⁸ Sonavane, S.U.; Chidambaram, M.; Almog, J.; Sasson, Y.; “*Rapid and efficient synthesis of symmetrical alkyl disulfides under phase transfer conditions.*”; *Tetrahedron Letters*; 2007; **48**; 6048-6050.
- ⁹⁹ Jauk, S. “*Kovalent verbundene Typ II Photoinitiatoren für die Radikalische Photopolymerisation*”; PhD-Thesis; Institute of Applied Synthetic Chemistry; Vienna University of Technology; Vienna, Austria 2008, p.69.
- ¹⁰⁰ Kocienski P., in *Protecting Groups* 3rd ed., Thieme Stuttgart, New York, 2005, p 50-110.

- ¹⁰¹ Matsuda, K.; Ulrich, G.; Iwamura, H.; “*Design and synthesis of diphenyldiazomethanes possessing stable aminoxyl radicals: photolytic generation or quartet species and their reaction with C₆₀*.”; Journal of the Chemical Society Perkin Transactions 2: Physical Organic Chemistry; 1998; **7**; 1581-1588.
- ¹⁰² Chun, J.; Yin, Y.I.; Yang, G.; Tarassishin, L.; Li, Y.-M.; “*Stereoselective synthesis of photoreactive peptidomimetic γ -secretase inhibitors*”; Journal of Organic Chemistry; 2004; **69**; 7344-7347.
- ¹⁰³ Sprong, E.; De Wet-Roos, D.; Tonge, M.P.; Sanderson, R.D.; “*Characterization and Rheological properties of model-alkali-soluble modifiers synthesized by reversible addition-fragmentation chain transfer polymerization*”; Journal of Polymer Science Part A: Polymer Chemistry; 2003; **41**; 223-235.
- ¹⁰⁴ Benaglia, M.; Rizzardo, E.; Alberti, A.; Guerra, M.; “*Searching for more effective agents and conditions for the RAFT polymerization of MMA: Influence of dithioester substituents, solvent and temperature*”; Macromolecules; 2005; **38**(8); 3129-3140.
- ¹⁰⁵ Aycock, D.F.; Jurch, G.R.; “*Synthesis of alkyl trithioesters (alkyl thiocarbonyl disulfides)*.”; Journal of Organic Chemistry; 1979; **44**(4); 569-572.
- ¹⁰⁶ Kraatz, U.; “*Dithiokohlensäure-Derivate*“ in Methoden der Organischen Chemie (Ed. K.H. Büchel), E4, Vol 2, G. Thieme, Stuttgart; 1966; 426-427.
- ¹⁰⁷ Ladavière, C.; Dörr, N.; Claverie, J.P.; “*Controlled radical polymerization of acrylic acid in protic media*.”; Macromolecules; 2001; **34**; 5370-5372.
- ¹⁰⁸ Hua, D.; Xiao, J.; Bai, R.; Lu, W.; Pan, C.; “*Xanthate-mediated controlled/living free-radical polymerization under ⁶⁰Co γ -Ray irradiation: structure effect of O-group*.”; Macromolecular Chemistry and Physics; 2004; **205**; 1793-1799.
- ¹⁰⁹ Wheeler, P. A.; Wang, J.; Baker, J.; Mathias, L.J.; “*Synthesis and characterization of covalently functionalized Laponite clay*”; Chemistry of Materials; 2005; **17**(11); 3012-3018.

- ¹¹⁰ Ajayaghosh, A.; Das, S.; Serong, V.; "S-Benzoyl-O-ethyl xanthate as new Photoinitiator: Photopolymerization and Laser Flash Photolysis Studies."; Journal of Polymer Science Part A: Polymer Chemistry; 1993; **31**; 653-659.
- ¹¹¹ Bates, R.B.; Kroposki, L.M.; Potter, D.E.; "Cycloreversion of anions from tetrahydrofurans. A convenient synthesis of lithium enolates of aldehydes."; Journal of Organic Chemistry; 1972; **37**, 560-562.
- ¹¹² Irgartinger, H.; Weber, A.; Escher, T.; "Photooxidation and intramolecular reaction of the anthryl moiety in [60]fullerene derivatives."; European Journal of Organic Chemistry; 2000; 1647-1651.
- ¹¹³ Salama, T.; Lackner, B.; Falk, H.; "An efficient synthesis of O-methyl protected Emodin aldehyde and Emodin nitrile."; Monatshefte fuer Chemie; 2003; **134**, 1113-1119.
- ¹¹⁴ Shchekotikhin, A.E.; Lusikov, Y.N.; Buyanov, V.N.; Preobrazhnskaya, M.N.; "Heterocyclic analogs of 5,12 naphthacenequinone 6. * synthesis of 4,11-dimethoxy derivatives of anthra-[2,3-b]thiophene-5,10-dione and anthra[2,3-d]isothiazole-5,10-dione."; Chemistry of Heterocyclic Compounds; 2007; **43**(4); 439-444.
- ¹¹⁵ Borch, R.F.; Bernstein, M.D.; Dupont Durst, H.; "The cyanohydrin borate anion as a selective reducing agent."; Journal of the American Chemical Society; 1971; **93**(12); 2897-2904.
- ¹¹⁶ Maskill, H.; Jencks, W.P.; "Solvolysis of benzyl azoxytosylate and the effect of added bases and nucleophiles in aqueous trifluoroethanol and aqueous acetonitrile."; Journal of the American Chemical Society; 1987; **109** (7); 2062-2070.
- ¹¹⁷ Fang, L.; Chan, W.-H.; He, Y.-B.; "Selective complexation of metals with isoxazolidine-containing fluorophores."; Tetrahedron Letters; 2005; **46**; 173-176.
- ¹¹⁸ Kelly, D.R.; Simon, C.B.; King, D.S.; deSilva, D.S.; Lord, G.; Taylor, J.P.; "Studies of nitrile oxide cycloadditions, and the phenolic oxidative coupling of vanillin aldoxime by *Geobacillus* sp. DDS012 from Italian rye grass silage."; Organic and Biomolecular Chemistry; 2008; **6**; 787-796.

- ¹¹⁹ Ritson, D.J.; Cox, R.J.; Berge, J.; "Sodium mediated allylation of glyoxylate oxime ethers, esters and cyanoformates."; *Organic and Biomolecular Chemistry*; 2004; **2**; 1921-1933.
- ¹²⁰ Jeong, T. S.; Kim, M. J.; Yu, H.; Kim, K. S.; Choi, J. K.; Kim, S. S.; Lee, W. S.; "(E)-phenyl- and heteroaryl-substituted O-benzoyl- (or acyl)oximes as lipoprotein-associated phospholipase A₂ inhibitors."; *Bioorganic & Medical Chemistry Letters*; 2005; **15**; 1525-1527.
- ¹²¹ Jeong, H. J.; Park, Y.-D.; Park, H.-Y.; Jeong, I.Y.; Jeong, T.-S.; Lee, W.S.; "Potent inhibitors of lipoprotein-associated phospholipase A₂: Benzaldehyde O-heterocycle-4-carbonyloxime."; *Bioorganic & Medical Chemistry Letters*; 2006; **16**; 5576-5579.
- ¹²² Borrelly, S.; Paquette, L.A.; "Studies directed to the synthesis of the unusual cardiotoxic agent Kalmanol. Enantioselective construction of the advanced tetracyclic 7-oxy-5,6-dideoxy congener."; *Journal of the American Chemical Society*; 1996, **118**(4); 727-740.
- ¹²³ Toshima, K.; Jyojima, T.; Yamaguchi, H.; Noguchi, Y.; Yoshida, T.; Murase, H.; Nakata, M.; Matsumura, S.; "Total synthesis of Bafilomycin A1."; *Journal of Organic Chemistry*; 1997; **62**(10); 3271-3284.
- ¹²⁴ Sun, J.; Dong, Y.; Cao, L.; Wang, X.; Wang, S.; Hu, Y.; "Highly efficient chemoselective deprotection of O,O-aetals and O,O-ketals catalyzed by molecular iodine in acetone."; *Journal of Organic Chemistry*; 2004; **69**; 8932-8934.
- ¹²⁵ Kawase, M.; Kikugawa, Y.; "Chemistry of amine boranes. Part 5. Reduction of oximes, O-acyloximes and O-alkyl oximes with pyridine-borane in acid."; *Journal of the Chemical Society (1972-1999)*; 1979; **3**; 643-645.
- ¹²⁶ Groenenboom, C.J.; Hageman, H.J.; Oosterhoff, O. T.; Verbeek, J.; "Photoinitiators and photoinitiation Part XI. The photodecomposition of some O-acyl 2-oximinoketones."; *Journal of Photochemistry and Photobiology Part A: Chemistry*; 1997; **107**; 261-269.

- ¹²⁷ Suyama, K.; Shirai, M.; "Photobase generators: recent progress and application trend in polymer systems."; Progress in Polymer Science; 2009; **34**; 194-209.
- ¹²⁸ Gaertzen, O.; Buchwald, S. L.; "Palladium-catalyzed intramolecular α -arylation of α -amino acid esters."; Journal of Organic Chemistry; 2002; **67**; 465-475.
- ¹²⁹ Jauk, S.; "Kovalent verbundene Typ II Photoinitiatoren für die Radikalische Photopolymerisation." PhD-Thesis, Institute of Applied Synthetic Chemistry, Vienna Technical University, Vienna, Austria 2008, p.91.
- ¹³⁰ Lalevée, J.; Allonas, X.; Fouassier, J.P.; Tachi, H.; Izumitani, A.; Shirai, M.; Tsunooka, M.; "Investigation of the photochemical properties of an important class of photobase generators: the O-acyloximes."; Journal of Photochemistry and Photobiology Part A: Chemistry; 2002; **151**; 27-37.
- ¹³¹ Fouassier, J.P.; in Photoinitiation, photopolymerization and photocuring. Fundamentals and application; Hanser Munich Vienna, New York; 1995; p 17-19.
- ¹³² Sayamol, K.; Knight, A.R.; "Reactions of thiyl radicals. III. Photochemical equilibrium in the photolysis of liquid disulfide mixtures."; Canadian Journal of Chemistry; 1968; **46**; 999-1003.
- ¹³³ Aloïse, S.; Ruckebusch, C.; Blanchet, L.; Réhault, J.; Buntinx, G.; Huvenne, J.P.; "The benzophenone $S_1(n, \pi^*) \rightarrow T_1(n, \pi^*)$ states intersystem crossing reinvestigated by ultrafast absorption spectroscopy and multivariate curve resolution."; Journal of Physical Chemistry A; 2008; **112**; 224-231.
- ¹³⁴ Guthrie, J.; Jeganathan, M.B.; Otterburn, M.S.; Woods, J.; "Light Screening effects of Photoinitiators in UV-curable systems."; Polymer Bulletin; 1986; **15**; 51-58.
- ¹³⁵ Sitzman, E.; Fuchs, A.; Wostratzky, D.; "Photoinitiators: Their mechanisms, use and applications"; in Handbook of Coating Additives, (Ed. Florio, J.J; Miller, D.J.), CRC 2004; 77-78.
- ¹³⁶ Hwang, H.; Jang, D.J.; Chae, K.H.; "Photolysis reaction mechanism of dibenzophenoneoxime hexamethylenediurethane: A new type of photobase generator."; Journal of Photochemistry and Photobiology Part A; 1999; **126**, 37.

- ¹³⁷ Fouassier, J.P.; Ruhlmann, D.; Graff, B.; Morlet-Savary, F.; Wieder, F.; *“Excited state processes in polymerization photoinitiators.”*; Progress in Organic Coatings; 1995; **25**; 235-271.
- ¹³⁸ Fouassier, J.P.; in Photoinitiation, photopolymerization and photocuring. Fundamentals and applications; Hanser Munich Vienna, New York 1995; 32-35.
- ¹³⁹ Valderas, C.; Bertolotti, S.; Previtali, C.M.; Encinas, M.V., *“Influence of the amine structure on the polymerization of methyl methacrylate photoinitiated by aromatic ketone/amine.”* Journal of Polymer Science Part A: Polymer Chemistry; 2002; **40**; 2888-2893.
- ¹⁴⁰ McCarroll, A.J.; Walton, J.C.; *“Enhanced radical delivery from aldoxime esters for EPR and ring closure applications.”*; Chemical Communications; 2000; 351-352.
- ¹⁴¹ McCarroll, A.J.; Walton, J.C., *“Exploitation of aldoxime esters as radical precursors in preparative and EPR spectroscopic roles.”*; Journal of the Chemical Society: Perkin Transactions 2; 2000; 2399-2409.
- ¹⁴² Yoshida, M.; Sakuragi, H.; Nishimura, T.; Ishikawa, S.; Tokumaru, K.; *“Nature of the excited triplet states in the photolysis of O-acyloximes.”*; Chemistry Letters; 1975; 1125-1130.
- ¹⁴³ Hong, S.I.; Kurosaki, T.; Okawara, M.; *“Photopolymerizations initiated by oxime derivatives”*; Journal of Polymer Science; 1974; **12**; 2553-2566.
- ¹⁴⁴ Gan, L.M.; Chew, C.H.; *“Vulcanization of butyl rubber by p-quinone dioxime dibenzoate”*; Journal of Applied Polymer Science; 1979; **24**; 371-383.
- ¹⁴⁵ $E_T(p)$ values from *“Handbook of photochemistry”* Murov, S.L.; Carmichael, I.; Hug, G.L.; Dekker New York, Basel, Hong Kong 1993; p 66 and p 84
- ¹⁴⁶ Okawara, M.; Nakai, T.; Otsuji, Y.; Imoto, E.; *“Photochemical behaviour of O-ethyl S-benzyl xanthate as a model compound for a photosensitive resin”*; Journal of Organic Chemistry; 1965; **30**(6); 2025-2029.
- ¹⁴⁷ Ajayaghosh, A., Francis, R.; *“A xanthate-derived photoinitiator that recognizes and controls the free radical polymerization pathways of methyl methacrylate and styrene”*; Journal of the American Chemical Society; 1999; **121**; 6599-6606.

- ¹⁴⁸ Dworak, C.; Kopeinig, S.; Hoffmann, H.; Liska, R.; “*Photoinitiating Monomers based on di- and triacryloylated hydroxylamine derivatives*”; Journal of Polymer Science Part A: Polymer Chemistry; 2009; **47**; 392-403.
- ¹⁴⁹ Kopeinig, S.; “*Synthese und Untersuchung photopolymerisierbarer Gruppen für Silikonbeschichtungen.*”; PhD Thesis, Institute of Applied Chemistry, Vienna Technical University, Vienna, Austria 2007; p 142-158.
- ¹⁵⁰ Roper, T. M.; Hoyle, C. E., Magers, D. H; “*Reaction enthalpies of monomers involved in photopolymerization*” in Photochemistry and UV-Curing New Trends 2006; (Ed. J.P. Fouassier); Research Signpost, Kerala, India, 2006; 253-264.
- ¹⁵¹ Henecka, H.; Kurtz, P.; „*Sauerstoffverbindungen III*“; in Houben-Weyl Methoden der Organ. Chemie VIII; (Ed. K.H. Büchel); Georg Thieme Verlag, Stuttgart 1952; pp 684.
- ¹⁵² Metzger, H.; „*Stickstoffverbindungen*“; in Houben-Weyl Methoden der Organ. Chemie X/4; (Ed. K.H Büchel); Georg Thieme Verlag, Stuttgart 1968; p 193.
- ¹⁵³ Exner, O.; Horák, M.; “*Derivatives of oximes. V. Determination of the constitution of hydroxylamine acyl derivatives by infrared spectroscopy.*”; Collection of Czechoslovakian Chemical Communications; 1959; **24**; 2992-3001.
- ¹⁵⁴ Kliegel, W.; Nanninga, D.; “*Boron chelates of N-substituted hydroxamic acids.*“; Chemische Berichte; 1983; **116**; 2616-2629.
- ¹⁵⁵ Prabhakar, S.; Lobo, A. M.; Santos, A.; „*A convenient method for the synthesis of N-hydroxythiobenzamides (C-arylthiohydroxamic acids)*“; Synthesis; 1984; **10**; 829-831.
- ¹⁵⁶ Hoffmann, R. V.; Nayyar, N. K.; “*A facile preparation of N-(Isopropoxyalkyl) amides by generation and trapping of N-acyliminium ions from ionization-rearrangement reactions of N-triflyloxy amides.*“; Journal of Organic Chemistry; 1994; **59**; 3530-3539.
- ¹⁵⁷ Miyata, O.; Namba, M.; Ueda, M.; Naito, T.; “*A novel synthesis of amino-1,2-oxazinones as a versatile synthon for β -amino acid derivatives.*“; Journal of Organic and Biomolecular Chemistry; 2004; **2**; 1274–1276.

- ¹⁵⁸ Kopeinig, S.; “*Synthese und Untersuchung photopolymerisierbarer Gruppen für Silikonbeschichtungen.*”; PhD Thesis, Institute of Applied Chemistry, Vienna Technical University, Vienna, Austria 2007; p 240 – 241.
- ¹⁵⁹ Zinner, G., Hitze, M. “*N,O-bis(carbamoyl)-hydroxylamine. 35. Hydroxylamine-derivatives.*” Archiv der Pharmazie; 1969; **10**; 788 – 795.
- ¹⁶⁰ Bauer, L., Exner, O., „*Chemistry of hydroxamic acids and N-hydroxyimides.*“, Angewandte Chemie; 1974; **12**; 419 – 458.
- ¹⁶¹ Yale, H. L., “*The hydroxamic acids.*” Chemical Reviews; 1943; **33**; 209 – 256.
- ¹⁶² Banwell, C.N.; in Fundamentals of Molecular Spectroscopy, McGraw Hill, London 1966.
- ¹⁶³ An approximate value ($71.6 \text{ kJ mol}^{-1} \text{ DB}^{-1}$) was also found in literature. Scoconi, M., Rossetti, S., Leonardi, M. in “*Photoinduced free radical polymerisation of unsaturated polyesters in presence of multiacrylate reacting diluents*”, RTE Conference papers archive 2003.
- ¹⁶⁴ Smith, T. J.; Shemper, B. S.; Nobles, J. S.; Casanova, A. M.; Ott, C.; Mathias, L. J.; “*Crosslinking kinetics of methyl and ethyl (α -hydroxymethyl)acrylates: effect of crosslinker type and functionality.*”; Polymer; 2003; **44**(20); 6211-6216.
- ¹⁶⁵ McCormick, C. L.; Zhang, Z. B.; Anderson, K. W.; “*Cyclopolymerization and cyclocopolymerization of N,N-diacryloylmetribuzin.*”; Polymer Preprints (American Chemical Society, Division of Polymer Chemistry); 1983; **24**(2), 364-5.
- ¹⁶⁶ Hagemann, H.J, Overeem, T.; “*Photoinitiators and photoinitiation. 4. Trapping of primary radicals from photoinitiators by 2,2,6,6-tetramethylpiperidinoxyl.*”, Macromolecular Chemistry Rapid Communications; 1981; **2**(12); 719-724.
- ¹⁶⁷ a) Desobry, V., Dietliker, K., Huesler, R., Rutsch, W., Loeliger, H.; “*New developments in radical and cationic photopolymerization*”; Polymers and Paint Colour Journal; 1988; **178**; 913-921.
- b) Desobry, V., Dietliker K., Huesler, R., Rutsch, W.; Loeliger, H.; “*New developments in radical and cationic photopolymerization. Part I. Radical photopolxmerization*”; Polymer and Paint Colour Journal (Suppl.); 1988; 125-138.

-
- ¹⁶⁸ Wang, D.; Wu, Z.; “*Facile synthesis of new unimolecular initiators for living radical polymerizations.*”; *Macromolecules*; 1998; **31**; 6727 – 6729.
- ¹⁶⁹ Drury, J.L.; Mooney, D.J.; “*Hydrogels for tissue engineering: scaffold design variables and applications*”; *Biomaterials*; 2003; **24**; 4337-4351.
- ¹⁷⁰ Liska, R.; Stampfl, J.; Varga, F.; Gruber, H.; Baudis, S.; Heller, C.; Schuster, M.; Bergmeister, H.; Weigel, G.; Dworak, C.; “*Composition that can be cured by polymerization for the production of biodegradable, biocompatible, cross-linkable polymers on the basis of polyvinyl alcohol.*”; *PCT Int. Appl.*; 2009; 78 pp.
- ¹⁷¹ Matsuda, T.; Mizutani, M.; Arnold, S.; “*Molecular design of photocurable liquid biodegradable copolymers 1. Synthesis and photocuring characteristics.*” *Macromolecules*; 2000; **33**, 795-800.
- ¹⁷² Jansen, J.; Melchels, F. P. W.; Grijpma, D. W.; Feijen, J.; “*Fumaric acid monoethyl ester-functionalized poly(D,L-lactide)/N-vinyl-2-pyrrolidone resins for the preparation of tissue engineering scaffolds by stereolithography.*”; *Biomacromolecules*; 2009; **10**(2); 214-220.
- ¹⁷³ Tokuda, K.; Naitou, M.; Mizutani, G.; Kobayashi, D.; “*UV-curable resin composition and cured product thereof.*”; *PCT Int. Appl.*; 2007; 32 pp.
- ¹⁷⁴ McCarthy, T. J., Hayes, E. P., Schwartz, S., Witz, G.; “*The reactivity of selected acrylate esters toward glutathione and deoxyribonucleosides in vitro: Structure-activity relationships*”; *Fundamental and Applied Toxicology*; 1994; **22**; 543-548.
- ¹⁷⁵ Pfluger, C. A.; Carrier, R. L.; Sun, B.; Ziemer, K. S.; Burkey, D. D.; “*Cross-linking and degradation properties of plasma enhanced chemical vapor deposited poly(2-hydroxyethyl methacrylate).*”; *Macromolecular Rapid Communications*; 2009; **30**(2); 126-132.
- ¹⁷⁶ Your, J.; “*Polymeric materials suitable for ophthalmic devices and methods of manufacture.*”; *PCT Int. Appl.*; 2009; 20pp.
- ¹⁷⁷ Zhang, J.; Yu, J.; Guo, Z.X.; “*Modification of nano-alumina surface by Michael Addition reaction*”; *Chinese Chemical Letters*; 2006; **17**; 251-252.

- ¹⁷⁸ Sundstrom S.; Scolnick, B.; Sullivan. J.B.; “*Acrylates, Methacrylates and Cyanoacrylates*” in *Clinical Environmental Health & Toxic Exposures*, (Ed. J.B. Sullivan; G. R. Krieger); 2nd ed; Lippincott, Williams & Wilkins, Philadelphia, USA; 2001; p 999.
- ¹⁷⁹ Singh, M. K.; Shokuhfar, T.; De Almeida, J.G.; Mendes de Sousa, A. C.; Fereira, J. M.; Garmestani, H.; Ahzi, S.; “*Hydroxyapatite modified with carbon-nanotube-reinforced poly(methyl methacrylate)*: a nanocomposite material for biomedical applications.”; *Advanced Functional Materials*; 2008; **18**(5); 694-700.
- ¹⁸⁰ Sivakumar, M.; Rao, K. P.; “*Synthesis, characterization, and in vitro release of ibuprofen from poly(MMA-HEMA) copolymeric core-shell hydrogel microspheres for biomedical applications.*”; *Journal of Applied Polymer Science*; 2002; **83**(14); 3045-3054.
- ¹⁸¹ Young C D; Wu J R; Tsou T L.; “*High-strength, ultra-thin and fiber-reinforced pHEMA artificial skin.*”; *Biomaterials* 1998; **19**(19); 1745-52.
- ¹⁸² Pienkowski, D. A.; Andrews, R. J.; “*Poly(methylmethacrylate) augmented with carbon nanotubes for dental or medicinal use.*”; U.S. Pat. Appl. Publ.; 2002; 7 pp.
- ¹⁸³ Kocienski P., in *Protecting Groups*; 3rd ed., Thieme Stuttgart, New York; 2005; p 503.
- ¹⁸⁴ Kajiwara, A.; Konishi, Y.; Morishima, Y.; Schnabel, W.; Kuwata, K.; Kamachi, M.; “*Time-resolved electron spin resonance study on radical polymerization with (2,4,6-trimethylbenzoyl)diphenylphosphine oxide. Direct estimation of rate constants for addition reactions of diphenylphosphonyl radicals to vinyl monomers.*” *Macromolecules*; 1993; **26**; 1656-1658.
- ¹⁸⁵ Jokusch, S.; Koptuyug, I. V.; McGarry, P. F.; Sluggett, G. W.; Turro, N., J.; Watkins, D. M.; “*A steady-state and picosecond pump-probe investigation of the photophysics of an acyl and a bis(acyl)phosphine oxide.*”; *Journal of the American Chemical Society*; 1997; **119**; 11495-11501.

- ¹⁸⁶ Baxter, J. E.; Davidson, R. S.; Hageman, H. J.; Overeem, T.; “*Photoinitiators and photoinitiation. 8. The photoinduced α -cleavage of acylphosphine oxides: identification of the initiating radicals using a model substrate.*”; Die Makromolekulare Chemie; 1988; **189**(12); 2769-2780.
- ¹⁸⁷ Cho, C. H., Kim, S., Yamane, M., Miyauchi, H., Narasaka, K.; “*Radical cyclizations of alkenyl acylphosphonate derivatives under thermal and photochemical conditions.*”; Bulletin of the Chemical Society of Japan; 2005; **78**; 1665-1672.
- ¹⁸⁸ Crivello, J.V.; Dietliker, K.; in “*Photoinitiators for free radical cationic and anionic photopolymerization. Volume III.*”(Ed. G. Bradley); 2nd ed.; John Wiley and Sons, London; 1998; 168-169.
- ¹⁸⁹ Zhang, N., Casida, J.E., “*Convenient syntheses of biologically relevant vinyl and divinyl phosphates by selective dealkylation of the corresponding phosphites.*”; Synthesis; 2000; **10**; 454-458.
- ¹⁹⁰ Kumpulainen, H.; Järvinen, T.; Saari, R.; Lehtonen, M.; Vepsäläinen, J.; “*An efficient strategy for the synthesis of 1-chloroethyl phosphates and phosphoramidates.*”; Journal of Organic Chemistry; 2005; **70**(22); 9056-9058.
- ¹⁹¹ Liang, H.; Shi, W., “*Thermal behaviour and degradation mechanism of phosphate di/triacrylate used for UV curable flame-retardant coatings.*”; Polymer Degradation & Stability; 2004; **84**; 525-532.
- ¹⁹² Hayashi, K.; “*Radical Polymerization and Co-polymerization of some vinylphosphates*”; Die Makromolekulare Chemie; 1978; **179**(7); 1753-1763.
- ¹⁹³ Du, J. Z.; Sun, T. M.; Weng, S. Qu.; Chen, X. S.; Wang, J.; “*Synthesis and characterization of photo-cross-linked hydrogels based on biodegradable polyphosphoesters and poly(ethylene glycol) copolymers.*”; Biomacromolecules; 2007; **8**; 3375-3381.
- ¹⁹⁴ Jeong, B.; Bae, Y. H.; Lee, D. S.; Kim, S. W.; “*Biodegradable block copolymers as injectable drug-delivery systems*”; Nature; 1997; **388** (6645); 860-862.
- ¹⁹⁵ Bambury, R. E.; Seelye, D. E.; “*Preparation of vinyl carbonate and vinyl carbamate copolymers for contact lenses.*”; Eur. Pat. Appl.; 1990; 36 pp.

- ¹⁹⁶ Gefter, E. L.; Kabachnik, M. I.; "Synthesis and study of some vinyl esters of acids of phosphorus" Doklady Akademii Nauk SSSR; 1957; **114**; 541-544.
- ¹⁹⁷ Michaelis, A.; Kaehne, R. "On the behavior of the iodine alkyls against so-called phosphorous acid ester or O-phosphines."; Berichte der Deutschen Chemischen Gesellschaft; 1898; **31**; 1048-1055.
- ¹⁹⁸ Arbuzov, B. A.; "Michaelis- Arbuzov and Perkov reactions." Pure and Applied Chemistry; 1964; **9**(2); 307-335.
- ¹⁹⁹ Landauer, S. R.; Rydon, H. N.; "The organic chemistry of phosphorus. I. Some new methods for the preparation of alkyl halides."; Journal of the Chemical Society; 1953; 2224-2234.
- ²⁰⁰ Issleib, K.; Mögelin, W.; Balszuweit, A.; "Bis(trimethylsilyl)-hypophosphit und Alkoxy-carbonylphosphonigsäure-bis(trimethylsilyl)ester als Schlüsselsubstanzen für die Synthese von Organophosphoverbindungen."; Zeitschrift für anorganische und allgemeine Chemie; 1985; **530**, 16-28.
- ²⁰¹ Lindner, E.; Tamoutsidis, E.; "Reactive behavior of methyl-substituted propenoyldiphenylphosphines and their oxides."; Chemische Berichte; 1983; **116**(9); 3141-3150.
- ²⁰² Szpala, A.; Tebby, J. C.; Griffiths, D. V.; "Reaction of phosphites with unsaturated acid chlorides: synthesis and reactions of dimethyl but-2-enoylphosphonate."; Journal of the Chemical Society, Perkin Transactions 1: Organic and Bio-Organic Chemistry (1972-1999); 1981; **5**; 1363-1366.
- ²⁰³ Lichtenthaler, Frieder W.; "Chemistry and properties of enol phosphates."; Chemical Reviews; 1961; **61**; 607-649.
- ²⁰⁴ Upson, R. W.; "Diethyl vinyl phosphate, divinyl benzenephosphonate, and their polymers."; Journal of the American Chemical Society; 1953; **75**; 1763-1764.
- ²⁰⁵ Magee, P. S.; "New reversible synthesis of vinyl phosphates from mercurials."; Tetrahedron Letters; 1965; **45**; 3995-3998.
- ²⁰⁶ Allen, J. F.; Johnson, O. H.; "The synthesis of monovinyl esters of phosphorus(V) acids."; Journal of the American Chemical Society; 1955; **77**; 2871-2875.

- ²⁰⁷ Jones, S.; Selitsianos, D.; “*Stereochemical consequences of the use of chiral N-phosphoryl oxazolidinones in the attempted kinetic resolution of bromomagnesium alkoxides.*”; *Tetrahedron: Asymmetry*; 2005; **16**(18); 3128-3138.
- ²⁰⁸ Johnston, K. F.; Padias, A. B.; Hall, H. K.; “*Synthesis of vinyloxy phosphorus monomers from the enolate of acetaldehyde.*”; *Polymer Bulletin*; 2000; **45**(4-5); 359-364.
- ²⁰⁹ Rosenzweig, B. A.; Ross, N. T.; Tagore, D. M.; Jayawickramarajah, J.; Saraogi, I.; Hamilton, A. D.; “*Multivalent protein binding and precipitation by self-assembling molecules on DNA pentaplex scaffold.*”; *Journal of the American Chemical Society*; 2009; **131**(4); 5020-5021.
- ²¹⁰ White, M. A.; Johnson, J. A.; Koberstein, J. T.; Turro, N. J.; “*Toward the syntheses of universal ligands for metal oxide surfaces: controlling surface functionality through click chemistry*”; *Journal of the American Chemical Society*; 2006; **128**(35); 11356-11357.
- ²¹¹ Zalan, Z.; Martinek, T.A.; Lazar, L.; Sillanpaa, R.; Fuleop, F.; “*Synthesis and conformational analysis of tetrahydroisoquinoline- and piperidine-fused 1,3,4,2-oxadiazaphosphinanes, new ring systems*”; *Tetrahedron*; 2006; **62**(12); 2883-2891.
- ²¹² Varga, F.; Rumpler, M.; Luegmayer, E.; Fratzi-Zelman, N.; Glantschnig, H.; Klaushofer, K.; “*Triiodothyronine, a regulator of osteoblastic differentiation: depression of histone H4, attenuation of c-fos/c-jun and induction of osteocalcin expression*”; *Calcification Tissue International*; 1997; **61**; 404-411.
- ²¹³ Dhanaraju, M. D.; Vema, K.; Jayakumar, R.; Vamsadhara, C.; “*Preparation and Characterization of injectable microspheres of contraceptive hormones*”; *International Journal of Pharmaceutics*, 2003; **268**, 23-29.
- ²¹⁴ Shalaby, W. S.; Burg, K. J.; “*Absorbable and Biodegradable Polymers*”; in *Advances in Polymeric Biomaterials Series*; CRC Press, Boca Raton; 2004; p 6.
- ²¹⁵ Xiao, C.; Zhou, G.; “*Synthesis and properties of degradable poly(vinyl alcohol) hydrogel*”; *Polymer Degradation and Stability*; 2003; **81**; 297-301.

- ²¹⁶ Matsumura, S.; Tomizawa, N.; Toki, A.; Nishikawa, K.; Toshima, K.; “*Novel poly(vinyl alcohol)-degrading enzyme and the degradation mechanism.*”; *Macromolecules*; 1999; **32**; 7753-7761.
- ²¹⁷ Nair, L.S.; Laurencin, C.T.; “*Biodegradable polymers as biomaterials*”; *Progress in Polymer Science*; 2007; **32**; 762-798.
- ²¹⁸ Zhang, H.; He, Y.; Li, S.; Liu, X.; “*Synthesis and hydrolytic degradation of aliphatic polyesteramides branched by glycerol*”; *Polymer Degradation and Stability*; 2005; **88**; 309-316.
- ²¹⁹ Data provided for SciFinder by Syracuse Research Corp., New York
- ²²⁰ Haney, W. G.; Brown, R. G.; Isaacson, E. I.; Delgado, J. N.; “*Synthesis and structure-activity relationships of selected isomeric oxime O-ethers as anticholinergic agents.*”; *Journal of Pharmaceutical Sciences*; 1977; **66**; 1602-1606.
- ²²¹ Oka, H.; Kunimoto, K.; Kura, H.; Ohwa, M.; Tanabe, J.; “*Light-sensitive photoresist composition containing oxime esters as polymerization initiator in fabrication of optical filters in optical imaging devices.*”; *Fr. Demande*; 2001; 110 pp.
- ²²² Degani, I.; Fochi, R.; “*The phase-transfer synthesis of O,S-dialkyl dithiocarbonates from alkyl halides and alkyl methanesulfonates.*”; *Synthesis*; 1978; **5**; 365-368.
- ²²³ Kopeinig, S.; “*Synthese und Untersuchung photopolymerisierbarer Gruppen für Silikonbeschichtungen.*”; PhD Thesis, Institute of Applied Chemistry, Vienna Technical University, Vienna, Austria 2007; p 240.
- ²²⁴ Kopeinig, S.; “*Synthese und Untersuchung photopolymerisierbarer Gruppen für Silikonbeschichtungen.*”; PhD Thesis, Institute of Applied Chemistry, Vienna Technical University, Vienna, Austria 2007; p 232.
- ²²⁵ Hall, C.R., Inch, T.D., Pottage, C.; “*The effect of added lithium cations on the stereochemistry of nucleophilic displacement reactions at phosphorus.*”; *Phosphorous, Sulfur, and Silicone and the Related Elements*; 1981; **10**; 229-232.

- ²²⁶ Liska, R.; Herzog, D.; “*New photocleavable structures II. A-cleavable photoinitiators based on pyridines.*”; *Journal of Polymer Science Part A: Polymer Chemistry*; 2004; **42**; 752 – 764.
- ²²⁷ Oliver, W.C.; Pharr, G. M.; “*An improved technique for determining hardness and elastic modulus using load and displacement sensing indentation experiments.*”; *Journal of Materials Research*; 1992; **7**; 1564-1583.
- ²²⁸ Oliver, W.C.; Pharr, G.M.; “*Measurement of hardness and elastic modulus by instrumented indentation: Advances in understanding and refinements to methodology.*”; *Journal of Material Research*; 2004; **19**; 3-20.